

Terrestrial ecosystems on a Greenhouse Earth: Climate
and vegetation in the high southern latitudes during the early Paleogene

Dissertation
for attaining the PhD degree
of Natural Sciences

Submitted to the Faculty of Geosciences and Geography
of the Johann Wolfgang Goethe University
Frankfurt am Main

By Lineth Contreras Arias
from Bogotá (Colombia)

Frankfurt am Main
2014



accepted by the faculty of Geosciences and Geography
of the Johann Wolfgang Goethe University as a dissertation

Dean: Prof. Dr. Ulrich Achatz

Expert assessors: Prof. Dr. Jörg Pross
Prof. Dr. Henk Brinkhuis
Prof. Dr. Silke Voigt

Examination board: Prof. Dr. Jörg Pross
Prof. Dr. Silke Voigt
Prof. Dr. Jens Herrle
Prof. Dr. Eberhard Gischler

Date of the disputation: April 24, 2015

Table of contents

Table of contents	3
List of figures	5
List of tables	7
Abstract	8
Chapter 1. Introduction	9
1.1 Early Paleogene Greenhouse Earth	10
1.2 Vegetation during the early Paleogene: A focus on the southern high latitudes.....	12
1.3 Focus of this research.....	16
1.4 Terrestrial ecosystems from marine pollen records at the Australo-Antarctic region.....	16
1.5 Proxy for reconstructing vegetation: Pollen and spores.....	18
1.6 Quantitative methods for inferences of diversity and composition of the vegetation.....	20
1.7 Paleoclimatic estimations based on pollen and spores.....	21
1.8 Comparison with organic proxies	23
1.9 Framework of this thesis	24
Chapter 2. Persistent near-tropical warmth on the Antarctic continent during the early Eocene epoch	27
Abstract	27
2.1 Introduction	28
2.2 Results and Discussion.....	29
2.3 Methods summary	34
2.4 Supplementary Information for Chapter 2	35
Chapter 3. Early to Middle Eocene vegetation dynamics at the Wilkes Land Margin (Antarctica)	61
Abstract	61
3.1 Introduction.....	62
3.2 Study site.....	63
3.3 Methods.....	65
3.4 Results.....	69
3.5 Discussion	74
3.6 Conclusions	80
Chapter 4. Terrestrial climate dynamics in the Tasmanian sector of the Southwest Pacific Ocean during the Paleocene-Eocene deduced from a marine pollen record (ODP Site 1172, East Tasman Plateau)	81
Abstract	81
4.1 Introduction	82
4.2 Material and methods	85

4.3	Results	92
4.4	Interpretation	96
4.5	Conclusions	107
4.6	Supplementary Information for Chapter 4	108
Chapter 5. Conclusions and Outlook		117
6.1	Conclusions	117
6.2	Outlook.....	119
Acknowledgements		121
References		123
Zusammenfassung		148
Appendices		153
	Appendix 1 Taxonomy Site U1356.....	153
	Appendix 2 Taxonomy Site 1172.....	170
Declaration of contribution		186
Curriculum Vitae		189

List of figures

Figure 1.1 Cenozoic atmospheric CO ₂ and deep-sea temperatures	10
Figure 1.2 Modelled and estimated SSTs of the early Eocene.....	12
Figure 1.3 Modern and Eocene extent of vegetation types	13
Figure 1.4 Middle Paleocene to middle Eocene vegetation - Southern high latitudes.....	15
Figure 1.5 Australo-Antarctic region during the early Paleocene and middle Eocene	17
Figure 1.6 Steps of the palynological laboratory processing	19
Figure 1.7 Temperature profiles of informative taxa.	22
Figure 2.1 Location of Site U1356 and Antarctica at early Eocene times.	29
Figure 2.2 Sporomorphs record of Site U1356 (selected taxa)	30
Figure 2.3 Paleoclimatic reconstructions of Site U1356.....	32
Supplementary Figure S2.1 Age model of Site U1356	37
Supplementary Figure S2.2 NMDS results of Site U1356.....	40
Supplementary Figure S2.3 Rarefaction results of Site U1356	41
Supplementary Figure S2.4 Temperature reconstructions of Site U1356.....	45
Supplementary Figure S2.5 Precipitation reconstructions of Site U1356.....	46
Supplementary Figure S2.6 Neodymium isotopic compositions	52
Supplementary Figure S2.7 Photomicrographs of key taxa of Site U1356.....	60
Figure 3.1 Present-day and Eocene configuration of Oceania and Antarctica.....	68
Figure 3.2 Range chart of sporomorphs of Site U1356.....	70
Figure 3.3 Diversity and DCA results of Site U1356.....	73
Figure 3.4 Species accumulation curves of Site U1356 and Holocene records.....	78
Figure 4.1 Location of Site 1172 and SW Pacific Ocean at early Eocene times.....	84
Figure 4.2 Sporomorphs record of Site 1172 (selected taxa).	93

Figure 4.3 Comparison of the DCA sample scores.97

Figure 4.4 Terrestrial and marine paleoclimatic estimates of Site 117298

List of tables

Supplementary Table S2.1. NLRs and climatological databases – Site U1356.....	43
Table 3.1 Climatic conditions of Site U1356, Plum Swamp and Wallaceville Swamp.....	76
Table 3.2 Summary of the quantitative sporomorph results of Site U1356.	79
Table 4.1 Sporomorph datasets from Southeast Australia and New Zealand.	87
Table 4.2 NLRs and climatological databases – Site 1172.	88
Table 4.3 Climate estimates from Southeast Australia, New Zealand and Site 1172	96

Abstract

Terrestrial climate and ecosystem evolution during ‘Greenhouse Earth’ phases of the early Paleogene remain incompletely known. Particularly, paleobotanical records from high southern latitudes are giving only limited insights into the Paleocene and early Eocene vegetation of the region. Hence, data from continuous well-calibrated sequences are required to make progress with the reconstruction of terrestrial climate and ecosystem dynamics from the southern latitudes during the early Paleogene.

In order to elucidate the terrestrial conditions from the high southern latitudes during the early Paleogene, terrestrial palynology was applied in the present study to two well-dated deep-marine sediment cores located at the Australo-Antarctic region: (i) IODP Site U1356 (Wilkes Land margin, East Antarctica) and (ii) ODP Site 1172 (East Tasman Plateau, southwest Pacific Ocean). The studied sequence from IODP Site U1356 comprises mid-shelfal sediments from the early to middle Eocene (53.9 – 46 million years ago [Ma]). For the ODP Site 1172, the studied succession is characterized by sediments deposited in shallow marine environments of the middle Paleocene to the early Eocene (60.7 – 54.2 Ma).

Based on the obtained pollen and spores (sporomorphs) results from the studied sequences of Site U1356 and Site 1172, this study aims to: (1) decipher the terrestrial climate conditions along the Australo-Antarctic region from the middle Paleocene to the middle Eocene; (2) evaluate the structure, diversity and compositional patterns of forests that thrived in the Australo-Antarctic region during the early Paleogene; (3) understand the response of forests from the high southern latitudes to the climate dynamics from the early Paleogene; (4) establish a connection between the generated terrestrial palynomorph data and published Sea Surface Temperatures (SSTs) from the same cores.

To decipher the terrestrial climatic conditions on the Australo-Antarctic region, this study relies on the nearest living relative (NLR) concept that assumes that fossil taxa have similar climate requirements as their modern counterparts. This approach was applied to the sporomorph results of Site U1356 and Site 1172, following mainly the bioclimatic analysis. With regard to the structure and diversity patterns of the vegetation from the same region, the present study presents combined qualitative (i.e., reconstruction of the vegetation based mainly on the habitats of the known living relatives) and quantitative (i.e., application of ordination techniques, rarefaction and diversity indices) analyses of the fossil sporomorph results.

The overall results from the paleoclimatic and vegetation reconstruction approaches applied in the present study, indicate that temperate and paratropical forests during the early Paleogene thrived under different climatic conditions on the Wilkes Land margin and on Tasmania, at paleolatitudes of ~70°S and ~65°S, respectively.

Specifically, the sporomorph results from Site U1356, suggest that a highly diverse forest similar to present-day forests from New Caledonia was thriving on Antarctica during the early Eocene (53.9 – 51.9 Ma). These forests were characterized by the presence of termophilous taxa that are restricted today to tropical and subtropical settings, notably Bombacoideae, *Strasburgeria*, *Beauprea*, *Spathiphyllum*, *Anacolosa* and *Lygodium*. In combination with MBT/CBT paleotemperature results, they provide strong evidence for

near-tropical warmth at least in the coastal lowlands along the Wilkes Land margin. The coeval presence of frost tolerant taxa such as *Nothofagus*, Araucariaceae and Podocarpaceae during the early Eocene on the same record suggests that paratropical forests were thriving along the Wilkes Land margin. Due to the presence of this kind of vegetation, it is possible to suggest that forests in this region were subject to a climatic gradient related to differences in elevation and/or the proximity to the coastline.

By the middle Eocene, the paratropical forests that characterized the vegetation of the early Eocene on the Wilkes Land margin were replaced by low diversity temperate forests dominated by *Nothofagus*, and similar to present-day cool-temperate forests from New Zealand. The dominance of these forests and the absence of thermophilous elements together with the lower temperatures suggested by the MBT/CBT and the sporomorph-based temperatures indicate consistently cooler conditions during this time interval.

With regard to the sporomorph results of Site 1172, this study suggests that three vegetation types were thriving on Tasmania from the middle Paleocene to the early Eocene under different climatic conditions. During the middle to late Paleocene, warm-temperate forests dominated by Podocarpaceae and Araucariaceae were the prevailing vegetation on Tasmania. The dominance of these forests was interrupted by the transient predominance of cool-temperate forests dominated by *Nothofagus* and Araucariaceae across the middle/late Paleocene transition interval (~59.5 to ~59.0 Ma). This cool-temperate forest was characterized by a lack of frost-sensitive elements (i.e., palms and cycads) indicating cooler conditions with harsher winters on Tasmania during this time interval. By the early Eocene, and linked with the Paleocene Eocene Thermal Maximum (PETM), Paleocene temperate forests dominated by gymnosperms were replaced by paratropical rainforests with the remarkable presence of the tropical mangrove palm *Nypa* during the PETM and the earliest Eocene. The overall results from Site U1356 and Site 1172, provide a new assessment of the terrestrial climatic conditions in the Australo-Antarctic region for validating climate models and understanding the response of high-latitude terrestrial ecosystems to the climate dynamics of the early Paleogene on southern latitudes.

The climatic conditions in the higher latitudes during the early Paleogene were further unravelled by comparing the obtained terrestrial and marine results. The integration of the obtained sporomorph data with previously published TEX₈₆-based SSTs from Site 1172 documents that the vegetation dynamics were closely linked with the temperature evolution from the Australo-Antarctic region. Moreover, the comparison of TEX₈₆-based SSTs and sporomorph-based climatic estimations from Site 1172 suggests a warm-season bias of both calibrations of TEX₈₆ (i.e., TEX₈₆^H and TEX₈₆^H), when this proxy is applied to high southern latitudes records of the early Paleogene.

Chapter 1. Introduction

1.1 Early Paleogene Greenhouse Earth

Globally warm intervals without major icecaps represent close to 75% of the past 540 million years (Crowley, 2000; see Fig. 1.1). In particular, the early Paleogene has long been known to be the most recent period of extreme global warmth and is characterized by levels of CO₂ that may have been above 1,000 ppm (e.g., Pearson and Palmer, 2000; Beerling and Royer, 2011; see Fig. 1.1). The extreme case is the early Eocene that is distinct by deep sea temperatures of ~10°C higher than modern values (Miller et al., 1987; Lear, 2000; Zachos et al., 2001), higher concentrations of CO₂ with peak values above 2,000 ppm (Pearson and Palmer, 2000; Beerling and Royer, 2011; Huber and Caballero, 2011) and extremely reduced latitudinal temperature gradients that are characterized by extremely warm extratropical and above freezing mean temperatures (Barron, 1987; Greenwood and Wing, 1995; Bijl et al., 2009; Huber and Caballero, 2011). Only since 34 million years ago Earth has been characterized by lower concentrations of CO₂, cooler conditions and a glaciated South Pole (e.g., Zachos et al., 2008; see Fig. 1.1).

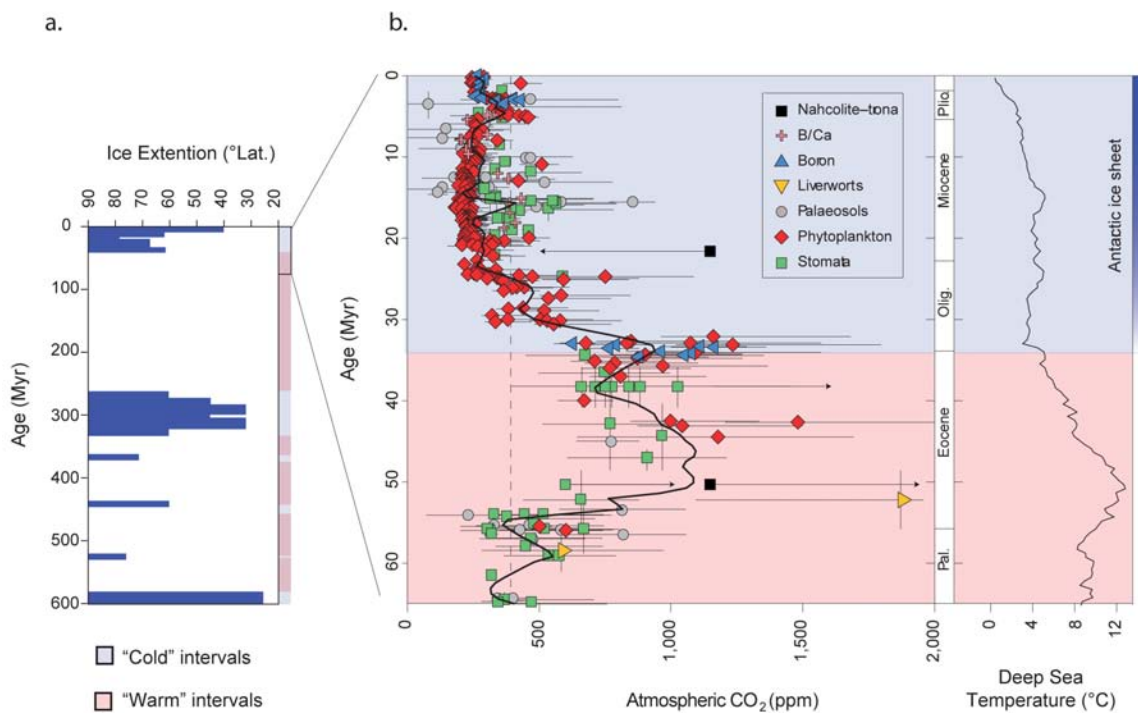


Figure 1.1. a) Glaciological evidence for continental-scale glaciation of the last 600 Ma from a compilation of Crowley (2000). b) Earth's Cenozoic atmospheric CO₂ reconstructed by marine and continental proxies and global average of deep-sea temperatures after Beerling and Royer (2011). Symbols with arrow indicate either upper or lower limits. The vertical dashed line indicates the present-day atmospheric CO₂ concentration (390 ppm).

On a shorter time scale, hyperthermal events have been recognized superimposed on the climate trends during the early Paleogene (e.g., Zachos et al., 2008). The best understood warming event is the Paleocene Eocene Thermal Maximum (PETM) that occurred at ~56 Ma (using the timescale of Gradstein et al. 2012) and lasted for ~170 kyr (Röhl et al.,

2007). This event was caused by the release of a large quantity of carbon into the atmosphere and ocean over about 10 kyr (Dickens et al., 1995; Cui et al., 2011) that was accompanied by an increase of temperature of 4 to 8°C (e.g., Zachos et al., 2003; Sluijs et al., 2006; Cui et al., 2011). Even though the average of temperature change during the onset of the PETM ($\sim 0.05^\circ\text{C}/\text{century}$; assuming warming of 5°C in 10 kyr) was 20 – 50 times slower than projected anthropogenic warming in the next centuries (IPCC, 2007), the PETM is considered as the closest analogue for our likely future (e.g., Norris et al., 2013).

Caldeira and Wicket (2003) predict that by the year 2400 humans will have released 5000 gigatonnes of carbon and that as a consequence the partial pressure of CO₂ will rise to at least 1800 ppm (Zachos et al., 2008). The uncertainties in the climatic response of a man-made increase in atmospheric $p\text{CO}_2$, have led to an increased interest in past episodes with high CO₂ concentrations, particularly those in which the partial pressure of CO₂ was much higher than today, such as the early Paleogene and particularly the PETM. The recent development of different paleoclimatic proxies, sophistication of climatic modelling, improvements of the timing and pace of past climatic fluctuations together with the new geologic data from different regions have opened new insights into the understanding of early Paleogene greenhouse conditions from long to short term climate trends. Particularly, the higher southern latitudes has garnered special attention during the last decade due to the fact that this region is important to understand the overturning circulation, which has significant effects on the redistribution of heat and nutrients in the global ocean (Thomas et al., 2003; Norris et al., 2013).

Most of the recent marine temperature approaches of the early Paleogene from the higher southern latitudes are based on organic compounds proxies (notably Tex_{86} ; Bijl et al., 2009; 2011; 2013a; Hollis et al., 2009; 2012). Sea Surface Temperatures (SSTs) trends derived from different calibration of TEX_{86} , reveal extremely warm conditions during the early Eocene and the Paleocene Eocene Thermal Maximum (PETM) in the southwest Pacific Ocean on the order of 26 – 28°C (Hollis et al., 2012) and 30° – 35°C (Bijl et al., 2009; Hollis et al., 2009). Coeval records from the tropical region reveal surface marine and terrestrial mean temperatures on the order of 30°C (see Jaramillo and Cárdenas, 2013 and references therein). The above-mentioned highly similar temperatures from the tropics and high latitudes suggest an extremely low latitudinal temperature gradient during the early Paleogene (see Fig. 1.2 for comparison of Eocene records). However, the comparison of SSTs derived from climate models and marine temperature proxies (TEX_{86} , $\delta^{18}\text{O}$ and Mg/Ca; Fig. 1.2), suggests that the estimated SSTs of the higher southern latitudes are in general untenably warm and can not be reconciled with current climate models (Huber and Caballero, 2011; Hollis et al., 2012).

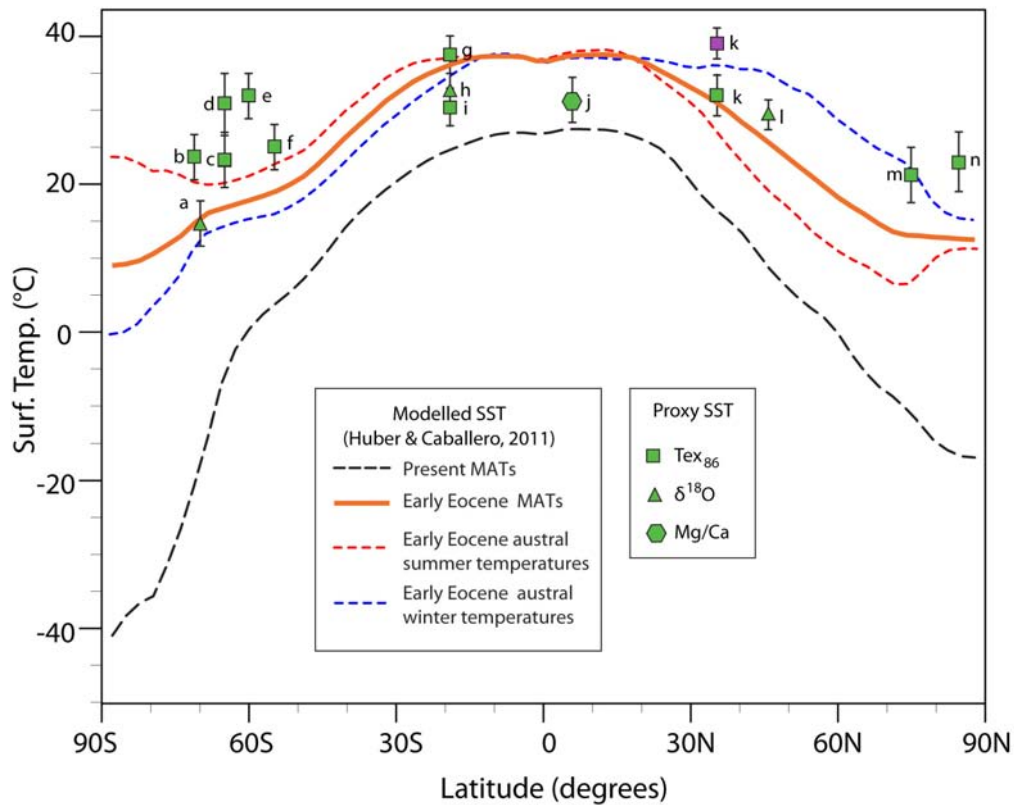


Figure 1.2. Comparison of modelled Sea Surface Temperatures (SSTs) under 4480 ppmv CO₂ (Huber and Caballero, 2011) and SST estimates derived from proxies from the early Eocene. Data are from: (a) Seymour Island (Ivany et al., 2008); (b) Integrated Ocean Drilling Project (IODP) Site U1356 (Tex₈₆^L; Bijl et al., 2013a); (c) Ocean Drilling Project (ODP) 1172 (Tex₈₆^L; Hollis et al., 2012); (d) ODP 1172 (Tex₈₆; Bijl et al., 2009); (e) Deep Sea Drilling Project (DSDP) Site 277 (Liu et al., 2009); (f) Mid-Waipara sections (Tex₈₆^L; Hollis et al., 2009); (g, h) Tanzania (Tex₈₆; Pearson et al., 2007); (i) Tanzania (1/Tex₈₆; Pearson et al., 2007; Hollis et al., 2012); (j) ODP 865 (Tripathi et al., 2003); (k) New Jersey (Tex₈₆; Sluijs et al., 2007); purple square represents peak PETM SSTs; (l) Belgian Basin (Vanhove et al., 2011); (m) IODP Site 302-4A, Arctic Basin (Tex₈₆^L; Sluijs et al., 2009; Hollis et al., 2012); (n) IODP Site M0004, PETM data (Sluijs et al., 2008b). Error bars indicate the range of variation. Compilation after Bijl et al. (2009) and Huber and Caballero (2011).

The recent SSTs trends from the higher southern latitudes outlined above have become available over the last decade based on continuous, chronostratigraphically well-calibrated records (Bijl et al., 2009; 2011; 2013a; Hollis et al., 2009; 2012; 2014). Considering the potential warm bias on those marine temperature estimations, the use of other proxies appears indispensable to unravel the actual climatic conditions on the high southern latitudes of the early Paleogene. Hence, the documentation of the terrestrial ecosystems responses and the estimation of terrestrial temperatures along high southern latitudes may create a solid benchmark for our understanding of the climate evolution of the greenhouse conditions of the early Paleogene.

1.2 Vegetation during the early Paleogene: A focus on the southern high latitudes

The warmer conditions during the early Paleogene, particularly during the early Eocene, facilitated the expansion of tropical to subtropical forest belts to higher latitudes (see Fig. 1.3). Hence, taxa with a mainly tropical distribution such as *Nypa*, other members of Arecaceae (palms) and Bombacoideae have been documented in fossil records from higher latitudes (see Fig. 1.3b). On the polar latitudes, paleobotanical records from the early Paleogene reveal that temperate rainforests dominated by *Nothofagus* and Podocarpaceae

were prevailing on Antarctica (e.g., Askin, 1990; Poole et al., 2001; Truswell and Macphail, 2009; see Fig. 1.3b). Such forests are restricted today to the southern part of Australia, Tasmania, New Zealand and South America (Kershaw, 1988; see Fig. 1.3a). Similarly, macrofloral remains indicate that swamp-cypress and broad floodplain vegetation similar to present-day vegetation from southeastern North America was the dominant ecosystem during the Eocene in the Arctic (Eberle and Greenwood, 2011).

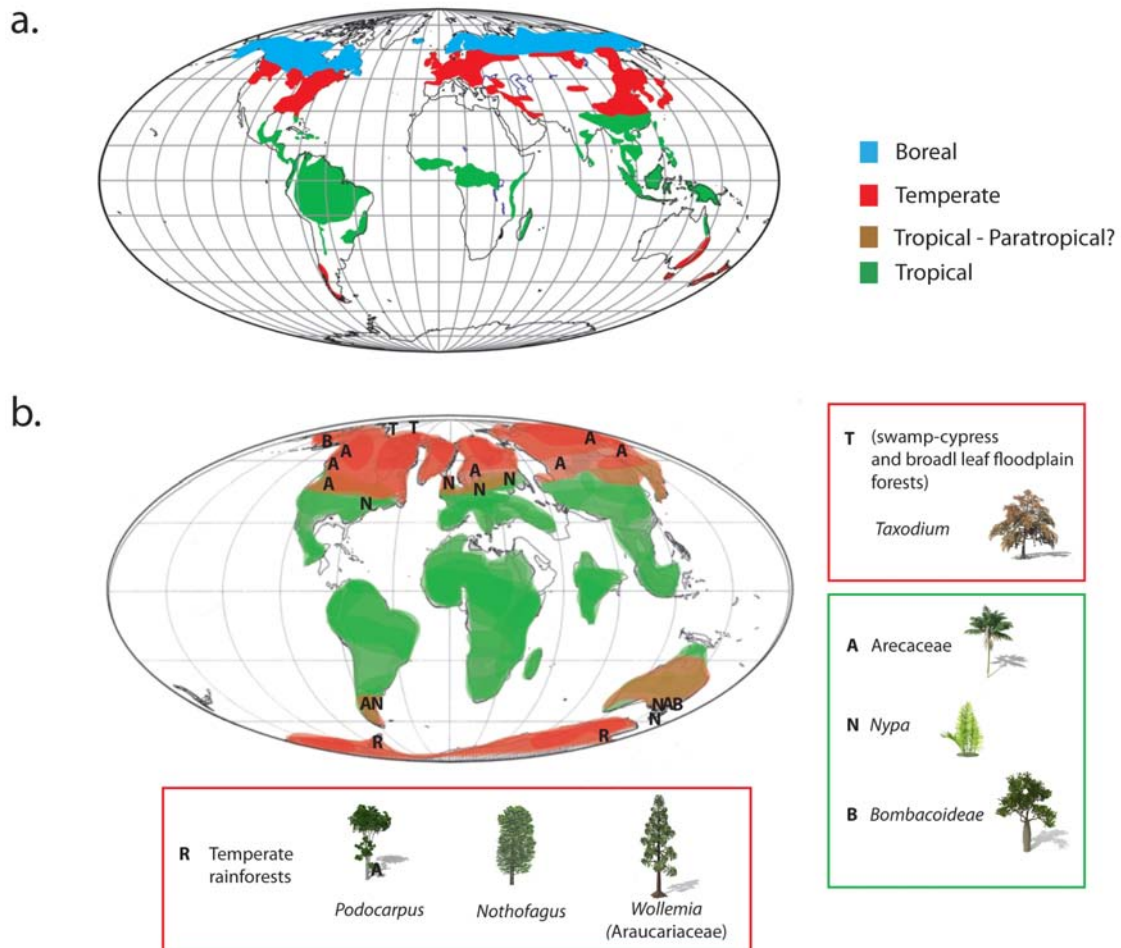


Figure 1.3. (a) Modern extent of vegetation types and (b) interpretation of Eocene vegetation types distribution after Fine and Ree (2006). Records of Arecaceae (palms) and the mangrove palm *Nypa* are derived from the paleomap project (<http://www.scotese.com>), including *Nypa* from Patagonia (Palazzesi and Barreda, 2007) and England (Collinson, 2000). Bombacoideae records are based on sporomorph records from southeast Australia (Stover and Partridge, 1973) and Alaska (Frederiksen et al., 2002). Presence of swamp cypress and broad leaf floodplain forests on the Arctic is derived from Eberle and Greenwood (2011). Temperate rainforest on Antarctica during the middle and late Eocene records are based on Truswell and Macphail (2009) and Poole et al. (2001).

Particularly, paleobotanical records from the high southern latitudes reflect the recurrence of temperate and tropical rainforests through the early Paleogene (e.g., Morley, 2000; see Fig. 1.4). For the Paleocene, paleobotanical records indicate that temperate, gymnosperm-rich forests dominated by podocarps were thriving on Southeast Australia (e.g., Macphail et al., 1994; Greenwood et al., 2003; Greenwood and Christophel, 2005), Seymour Island (Antarctica [early Paleocene]; Askin, 1990) and New Zealand (Mildenhall, 1980; Raine et

al., 2009). In Argentina, forests rich in gymnosperms (Araucariaceae and Podocarpaceae) and angiosperms (e.g., Proteaceae, Areaceae) were the prevailing vegetation in southern Patagonia (Palazzesi and Barreda, 2007).

The extreme warm and wet climate during the Eocene, facilitated the presence of paratropical vegetation on Australia and New Zealand; remarkably mangrove swamps characterized by the *Nypa* palm extended as far south as paleolatitude of 65°S on Tasmania (Pocknall, 1990; Macphail et al., 1994; Pole and Macphail, 1996; Morley, 2000; Greenwood et al., 2003; Carpenter et al., 2012). On Chile and Argentina, forests called “Mixed Paleoflora”, which were a blend of taxa with Australo-Antarctic and Neotropical affinities, were the prevailing vegetation on this region (e.g., Wilf et al., 2003; Gayó et al., 2005; Hinojosa and Villagrán, 2005).

By the middle to late Eocene, mixed forests (i.e., paratropical forests) from the early Eocene were replaced by temperate forests dominated by *Nothofagus* on Australia, Chile, Argentina and New Zealand (e.g., Macphail et al., 1994; Hinojosa and Villagrán, 1997; Greenwood et al., 2003; Barreda and Palazzesi, 2007). Similar vegetation dominated by *Nothofagus* forests with Araucariaceae and Podocarpaceae as prominent components were recorded on Antarctica (e.g., Pole et al., 2000; Macphail and Truswell, 2004; Truswell and Macphail, 2009; Warny and Askin, 2011). Towards the Oligocene, the cooler conditions resulted in an herb-moss tundra vegetation on Antarctica that was fully developed by Miocene times (Askin and Raine, 2000; Anderson et al., 2011).

The pronounced recurrence of tropical and temperate forests on the high southern latitudes summarized above, suggests a noticeable, climatically driven change in terrestrial environments during the early Paleogene. However, the above-mentioned studies only give a general picture of the vegetation dynamics during this time interval. This is due to the fact that paleobotanical studies are mainly based on discontinuous outcrops (Greenwood et al., 2003) and that sporomorph studies have been predominantly focussed on the generation of biostratigraphic schemes (e.g., Stover and Evans, 1973; Stover and Partridge, 1973; Truswell, 1997; MacPhail, 1999). Hence, the timing and nature of the transition between tropical and temperate forests during the early Paleogene and their connection with the climate dynamics from the high southern latitudes during this time interval have remained poorly understood.

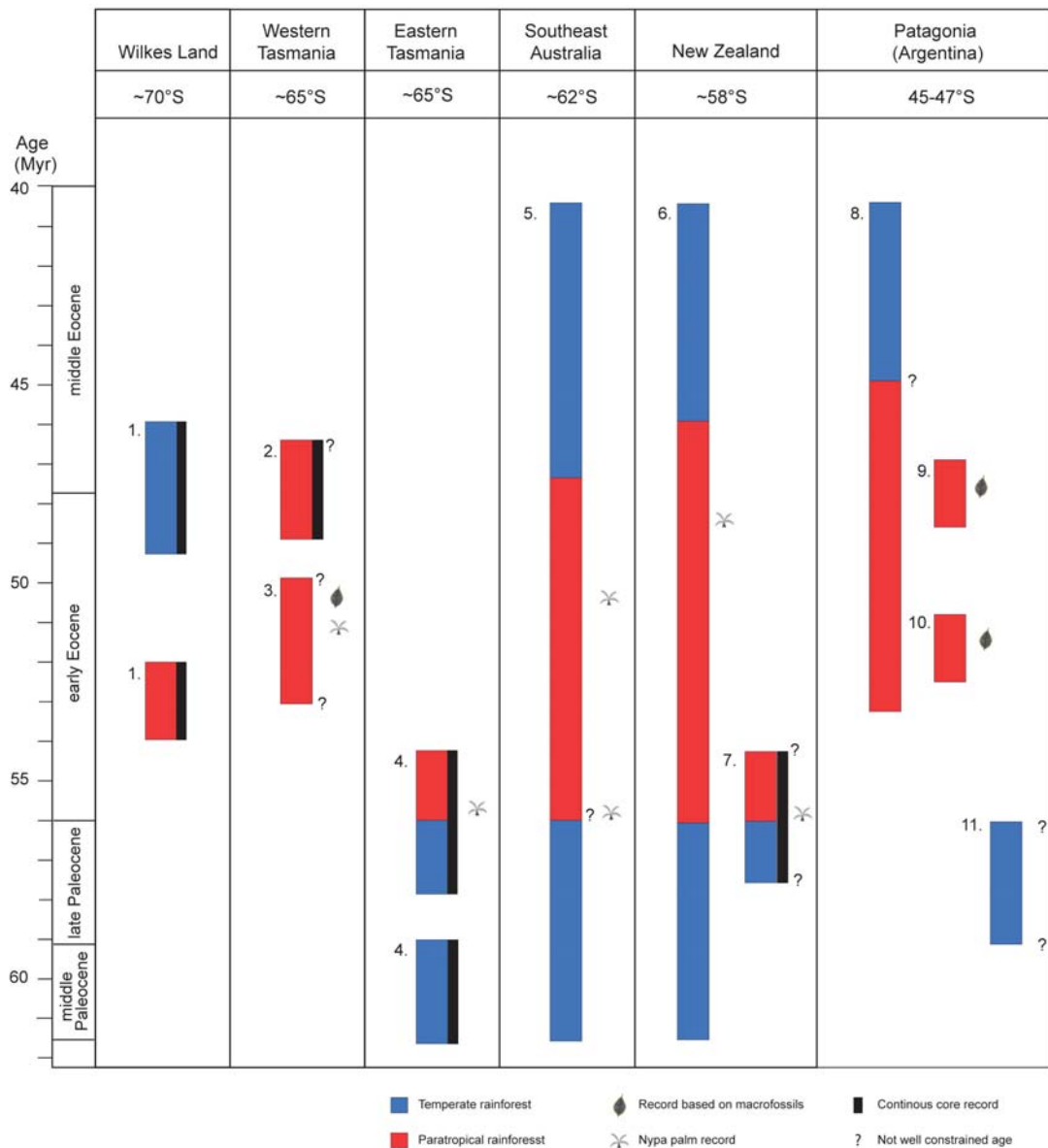


Figure 1.4 Comparison of the middle Paleocene to middle Eocene vegetation between different localities at southern high latitudes. 1. IODP site U1356 (Chapter 2 and 3); 2. Gravity core S36-22/SL (Truswell, 1997; data based on 4 samples); 3. Lowana Road fossil site (Carpenter et al., 2012); 4. ODP Site 1172 (Chapter 4); 5. Gippsland and Bass basins (Stover and Evans, 1973; Partridge et al., 2003; Partridge, 2006; composite data from different exploration wells); 6. Tui-1 exploration well (Raine et al., 2009; data from drill cutting material); 7. Kumara-2 core from New Zealand (Handley et al., 2011); 8. Nahuel Haupí Este and Confluencia localities of Huitrera Formation (Melendi et al., 2003); 9. Río Pichileufú outcrop sections (Wilf et al., 2005); 10. Laguna del Hunco outcrop sections (Wilf et al., 2005); 11. Río Chubut outcrop sections (Palazzesi and Barreda, 2007; Quatroccio et al., 2011). Paleolatitudes based on the Eocene paleogeographic maps of Cande and Stock (2004) and Wilf et al. (2005). The presence of temperate rainforests during the middle Eocene in New Zealand is based on an increase of pollen derived from *Nothofagidites* spp. (*fusca* type) and the absence of *Nypa* palm. Paratropical rainforests in Argentina is better referred as: “Mixed Paleoflora”.

1.3 Focus of this research

As outlined above, paleobotanical records from high southern latitudes are giving only limited insights into the early Paleogene vegetation of the region. Particularly, Antarctica has remained as *terra incognita* for the early Eocene and only sparse macrofloral remains and terrestrial palynological records are accessible for the early Paleocene, middle and late Eocene terrestrial ecosystems (e.g., Truswell and Drewry, 1984; Askin, 1989; 1990; Li, 1992; Raine and Askin, 2001; Francis and Poole, 2002; Poole et al., 2005; Truswell and Macphail, 2009). Clearly, data from longer sequences with high-quality age control are required to make a step forward to reconstruct the terrestrial conditions of high southern latitudes during the early Paleogene. Moreover, these data sets may allow a direct comparison with current marine temperature estimations derived from the same cores (Bijl et al., 2009; 2013a; 2013b; Hollis et al., 2012; 2014). Based on this notion, this study aims at reconstructing terrestrial climate and ecosystem dynamics from the higher southern latitudes during the early Paleogene, based on continuous, chronostratigraphically well-calibrated records from the Australo-Antarctic region (see below Section 1.4).

Considering the above, this research mainly focuses on the following major questions:

- (i) What were the terrestrial climate conditions along the Australo-Antarctic region from the middle Paleocene to the middle Eocene?
- (ii) How did the forests that prevailed on the Australo-Antarctic region respond to the climate dynamics of the early Paleogene?
- (iii) What were the structure, diversity and compositional patterns of the vegetation along the Australo-Antarctic region during the early Paleogene?
- (iv) What is the connection between the generated terrestrial palynomorph data and the SSTs derived from organic proxies (i.e., Tex_{86})?

1.4 Terrestrial ecosystems from marine pollen records at the Australo-Antarctic region

As outlined above, a promising avenue towards a better understanding of early Paleogene climate dynamics on high southern latitudes is the generation of continuous terrestrial climate and ecosystem records in well-dated, deep-marine sediment cores. Such an approach has been applied in this study, based on terrestrial palynomorphs of two well-dated deep-marine sediment cores of Paleocene to middle Eocene age: IODP Hole U1356A (Wilkes Land margin, East Antarctica) and ODP Hole 1172D (East Tasman Plateau, southwest Pacific Ocean) (Fig.1.5).

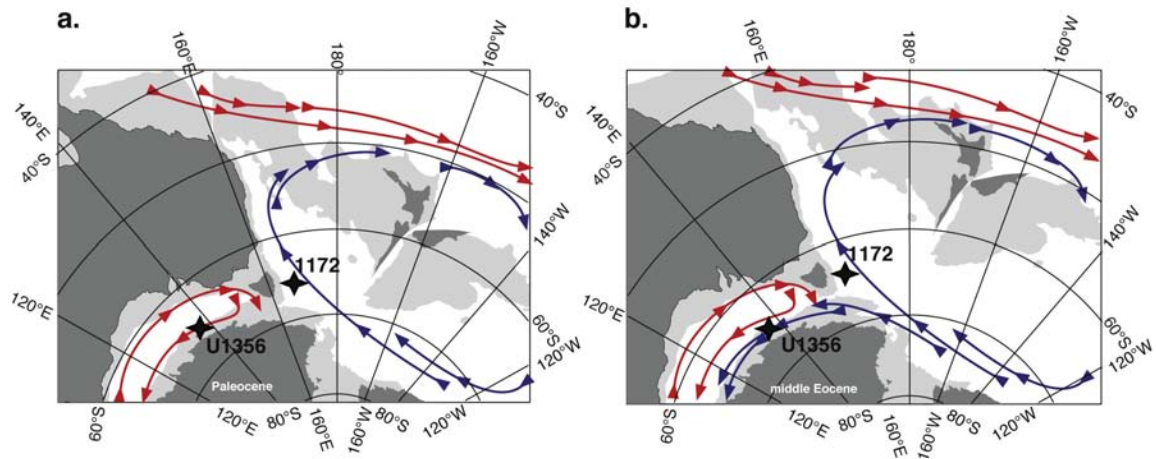


Figure 1.5. Paleogeographic reconstructions of the East Antarctic/Australian sector of the Southern Ocean for the early Paleocene (left) and the middle Eocene (right). Warm and cold surface-water currents are marked by red and blue arrows, respectively. Positions of IODP Site U1356 and ODP Site 1172 are indicated by stars. Dark grey areas indicate present-day land, light grey areas are submerged continental blocks above 300 m (after Bijl, 2011).

IODP Site U1356 ($63^{\circ}19'S$, $168^{\circ}49'E$; Fig. 1.5) is located at the transition between the continental rise and the abyssal plain close to the Wilkes Land margin (Expedition 318 Scientists, 2011). The paleolatitudes of the Wilkes Land margin and Site U1356 are nearly identical to the present-day positions. For this study only the early Eocene to middle Eocene sequence was analysed from this hole. Lithologically, the early Eocene succession consists of bioturbated claystones with intercalated fine sandstone beds. The middle Eocene succession is characterized by interbedded sandstones, diamictites, silty claystones, and siltstones (Expedition 318 Scientists, 2011). The studied succession comprises mid-shelf sediments of the early Eocene (53.9–51.9 Ma), separated by a ~ 3 myr-long hiatus, with an interval from the latest early Eocene to middle Eocene (49.3 – 46 Ma; Tauxe et al., 2012). The age control of the Eocene strata at Site U1356 is based on the integration of magnetostratigraphic and dinoflagellate cyst-based biostratigraphic data of Tauxe et al. (2012).

Cores from the ODP Site 1172 were extracted from a water depth of ~ 2620 m on the western side of the East Tasman Plateau (ETP; $43^{\circ}57.6' S$, $149^{\circ}55.7' E$; Fig. 1.5) (Shipboard Scientific Party, 2001a). During the early Paleogene, the ETP was located at $\sim 65^{\circ}S$, much closer to Antarctica than today (e.g., Cande and Stock, 2004). The present study focuses on the middle Paleocene to the early Eocene sequence from this hole. Lithologically, the middle Paleocene to early Eocene succession of ODP Site 1172 consists mainly of grey to greyish brown clay- and siltstones with low abundances of calcareous and siliceous microfossils (Shipboard Scientific Party, 2001b; Röhl et al., 2004). Environmentally, the succession is interpreted to reflect very shallow to restricted marine conditions, with marked runoff from the nearby shores (Röhl et al., 2004). The age model of the studied sequence is based on the magneto- and chemostratigraphically calibrated dinoflagellate cyst zonation of Bijl et al. (2013b).

Surface marine currents from the Australo-Antarctic region were strongly influenced by the deepening and widening of the Tasmanian Gateway (Stickley et al., 2004b; Bijl et al.,

2013a). During the Paleocene and early Eocene, the Pacific sector of the ETP was under the persistent influence of the relatively cool Tasman Current; in contrast, the Wilkes Land margin at the Australo-Antarctic Gulf was bathed by the low-latitude-derived warm Proto-Leeuwin Current (Huber et al., 2004; see Fig. 1.5). Onset at ~49–50 Ma, a westbound Antarctic Counter Current flowed from the Pacific sector of the Tasmania region to the Australo-Antarctic Gulf linked to deepening of the Tasmanian Gateway (Bijl et al., 2013a; see Fig. 1.5). An accelerated deepening and widening of the Tasmanian Gateway took place close to the middle-late Eocene boundary (~35.5 Ma) that led to the inflow of relatively warm Australo-Antarctic Gulf waters through the Tasmanian Gateway into the southwest Pacific region during the early Oligocene (Stickley et al., 2004b). The paleoceanographic reorganizations outlined above had important influences on the terrestrial climate conditions of the Australo-Antarctic region during the early Paleogene (Bijl et al. 2013a). This is mainly based on the comparison of MBT/CBT and sporomorph-based temperatures (same data presented in this study for Site U1356; see Chapter 2), with dinoflagellate biogeography and sea surface temperatures from the same region (see Bijl et al. 2013a).

1.5 Proxy for reconstructing vegetation: Pollen and spores

In this study, a total of 225 palynological samples were analysed for pollen and spores content, 145 taken from the Eocene interval of Site U1356 and 80 from the middle Paleocene to early Eocene interval of Site 1172. Palynological slides from Site U1356 were prepared in the present study following the protocols at the Institute of Geosciences of Goethe University Frankfurt and the Laboratory of Palaeobotany and Palynology of Utrecht University (see Fig. 1.6 for the laboratory processing applied). Samples from Site 1172 were supplied by the Laboratory of Palaeobotany and Palynology of Utrecht University.

Samples were analysed using a light microscope at 200x magnification. Up to 12 slides were necessary for counting 100 to 300 sporomorphs due to the low abundances of sporomorphs in many of the studied samples. Details of the morphological characteristics were observed at 1000x magnification. The taxonomical classification of sporomorphs were carried out following mainly Couper (1960), Harris (1965), Stover and Partridge (1973), Truswell (1983), Raine et al. (2008), and Truswell and Macphail (2009). The taxonomical affinities were established after Macphail et al. (1994), Raine (1998) and Truswell and Macphail (2009).



Figure 1.6 Steps of the palynological laboratory processing used for samples of Site U1356 at Utrecht University and Goethe University Frankfurt in this study. HCL was used only to dissolve the silica gel during the palynological processing due to the low content of carbonate in all processed samples.

Considering that terrestrial palynomorphs analysed in the present study were deposited in marine environments (see Section 1.4), it becomes indispensable to identify the source region of the studied sporomorphs, in order to obtain better insights into the vegetation and terrestrial climate conditions. In this study, the recovered sporomorphs from Site U1356 and Site 1172 are thought to reflect the vegetation of the Wilkes Land margin and Tasmania, respectively. Generally, terrestrial palynological studies from marine settings rely on the idea that the recorded sporomorphs reflect the vegetation of adjacent

landmasses (e.g., Traverse, 1994a; van der Kaars, 2001). However, in the present study different lines of evidence are presented to further support the provenance of the sediments from the Wilkes Land margin (Site U1356; see Chapters 2 and 3 for an in depth discussion) and Tasmania (Site 1172; See Chapter 4 for an in depth discussion).

Considering that water transportation is responsible for the majority of sporomorph particles deposited in marine settings (e.g., Muller, 1959; Farley, 1987; Traverse, 1994a), the recorded sporomorphs at Site U1356 and Site 1172 were probably transported from the Wilkes Land margin and Tasmania mainly via streams and marine currents as clastic particles. The hydrodynamic sorting during transport of the pollen and spores into the marine setting may result in assemblages dominated by easily transported, more buoyant, sporomorphs (e.g., Holmes, 1994; Traverse, 2008). Hence, the selective nature of marine pollen transport may decrease the diversity of sporomorph types in marine cores compared with terrestrial sites (Moss et al., 2005). The potential bias effects of the hydrodynamic sorting, have been taken into account when interpreting the sporomorph results of IODP Site U1356 and ODP Site 1172 and are further discussed in Chapters 3 and 4.

To further elucidate other potential biases, it appears well possible that pollination strategies may also affect the relative abundances of the sporomorph assemblages deposited in marine settings. This is mainly due to the fact that pollen derived from insect-pollinated species are not likely to be transported over larger distances before they settle and they reach normally lower abundances in the pollen spectrum when compared to wind-pollinated taxa (Jackson, 1994). The studied sporomorph assemblages at Site U1356 and Site 1172 are characterized by low abundances of taxa with living relatives distributed today mainly in tropical settings (e.g., *Arecaceae* [palms]), *Nypa*, *Bombacoideae*). These plants are mainly insect-pollinated (Bush and Rivera, 1998; Barfod et al., 2011) and they appear underrepresented on the sporomorph assemblages of the studied sequences of Site U1356 and Site 1172. Hence, despite of the low abundances reached by these taxa in the present study, their presences have significant ecological and climatological implications and are further discussed in the subsequent chapters.

1.6 Quantitative methods for inferences of diversity and composition of the vegetation

For assessing the vegetation diversity and compositional changes, different techniques were used in the present study:

- (i) Rarefaction: this interpolation technique is derived from the analysis of the relative frequencies of specimens within species, which makes possible the estimation of the number of sporomorph species at a constant sample size (Raup, 1975).
- (ii) Diversity and Evenness indices: Shannon index ($H = - \sum p_n \log_{10} p_n$, with $p_n =$ proportion of individuals that belong to species n) and Evenness ($J = H/H_{max}$)

were calculated as a measure of species diversity. $H=0$ (minimum value) when the sample unit contains a single specie and increases with the number of species. For a given number of species, H reaches its maximum when the individuals are equally distributed among the species (Legendre and Legendre, 1998). When $J = 1$, all species have the same number of individuals. A low value indicates that most of the assemblage is dominated by only few species (Hayek and Buzas, 2010).

- (iii) Species accumulation curves: This method allows meaningful standardization and comparison of the richness patterns from different datasets. The sample-based taxon resampling curves represent the means of richness of repeated re-sampling of a certain number of pooled samples (Gotelli and Colwell, 2001).
- (iv) Detrended Correspondence Analysis (DCA) and Multidimensional Scaling: Both ordination techniques have been mainly applied in palynological studies to assess the overall variation in floral composition through time (e.g., Harrington, 2001; Jaramillo, 2002; Cardenas et al., 2011; Wing and Currano, 2013). DCA is an adaption of correspondence analysis that suppresses the curvature of straight gradients and rescales the axes to remove distortion (Peet et al., 1988). Multidimensional Scaling helps to evaluate similarities and dissimilarities of samples based on any distance matrix (e.g., dissimilarity indices). This technique plots dissimilar objects far apart from each other and similar objects close to one another and does not maximize the variability associated with individual axes of the ordination (Legendre and Legendre, 1998). Multidimensional Scaling was also applied to evaluate the response of sporomorph taxa to a temperature gradient (see Chapter 2 and Supplement of this chapter).
- (v) A parametric statistic t-test, Mann-Whitney test and ANOSIM for the Multidimensional Scaling results were carried out to assess the differences in the floral composition and diversity between the different sporomorph assemblages.

All analyses were performed using the software R for statistical computing (R Development Core Team, 2011) and the package Vegan (Oksanen et al., 2011).

1.7 Paleoclimatic estimations based on pollen and spores

Quantitative paleoclimatic evaluations of sporomorph assemblages have been recently used as a valuable tool in pre-Quaternary climate reconstructions both from terrestrial (e.g., Greenwood et al., 2005; Poole et al., 2005) and marine (Eldrett et al., 2009) sedimentary records. The two approaches most widely applied to pre-Quaternary sporomorph assemblages are the bioclimatic analysis method (Greenwood et al., 2005; see Fig. 1.7) and the coexistence approach (Mosbrugger and Utescher, 1997; see Fig. 1.7). Both methods

rely on the notion that a given fossil taxon has similar ecological requirements as its nearest living relative (NLR). The climatic estimates are based on presence/absence data and are hence independent of the percentages of individual sporomorph taxa. This makes these methods well suited for the climatic evaluation of sporomorph assemblages from marine sediments, in which the hydrodynamic properties of the different grains may result in variations in the percentages of individual taxa with respect to the original assemblages on the continent (see Section 1.5). Although both approaches can work with a single taxon, the interval width typically increases with the number of taxa with NLR used (Mosbrugger and Utescher, 1997; Pross et al., 2000).

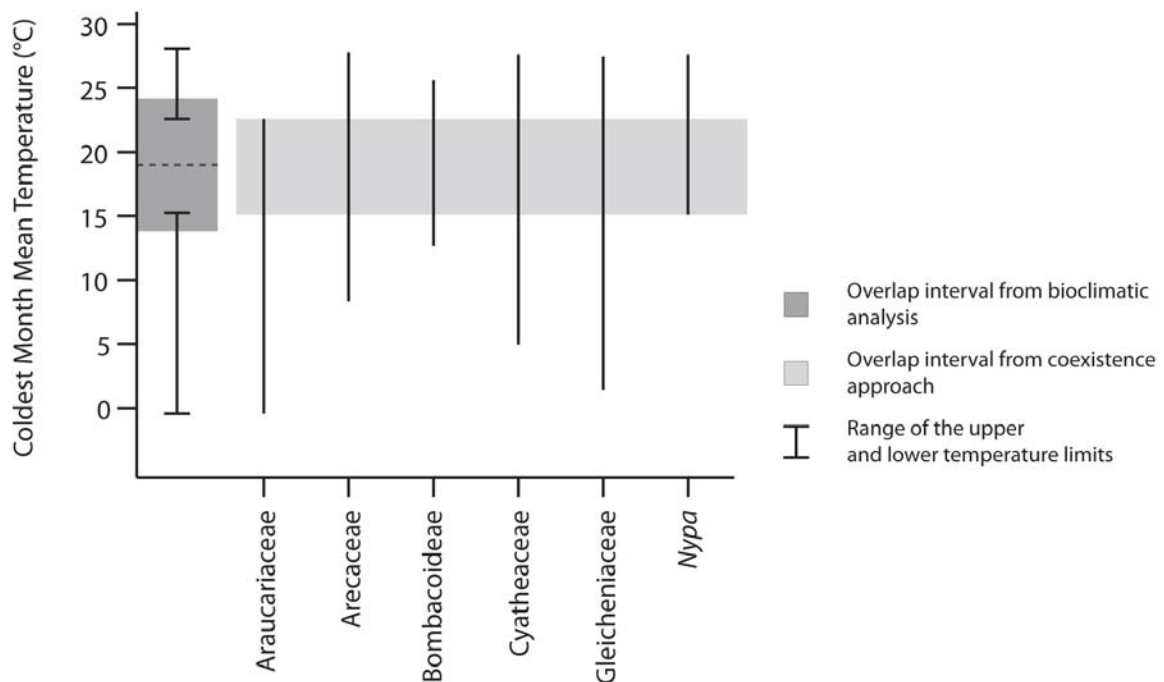


Figure 1.7 Temperature profiles for the Coldest Month Mean Temperature of nearest living relatives (NLRs) of informative taxa used in this study. Shaded areas are derived from the thermal overlap following the bioclimatic analysis (Greenwood et al., 2005) and the coexistence approach (Mosbrugger and Utescher, 1997). The zone of overlap from the bioclimatic analysis was calculated using the 10th percentile of the range from the upper limits of the temperature profiles and 90th percentile of the temperature range from the lower limits of the temperature profiles. The zone of overlap from the coexistence approach reflects the temperature range where all taxa involved in the analysis can coexist. Dashed line shows the mid-point value of the interval obtained from the bioclimatic analysis.

Based on the established botanical affinities, climatic profiles of mean annual temperature (MAT), coldest month mean temperature (CMMT), mean winter temperatures (MWT), warmest month mean temperature (WMMT), mean summer temperatures (MST) and mean annual precipitation (MAP) were generated for each taxon with known NLR. Each profile contains the maximum and minimum values for a range of climate variables with respect to each NLR. The climate profiles used here were mainly from two sources: (i) dataset mainly based on geographical distribution data from the Australian National Herbarium online database (Australian National Herbarium, 2011) and the mathematical climate surface

software ANUCLIM 5.156 (Houlder et al., 1999); provided by David Greenwood (ii) PALAEOFLORA database that contains climatic information for a plant taxon referring to its global distribution (Utescher and Mosbrugger, 2013); provided by Torsten Utescher. After the climate profiles were generated, the bioclimatic analysis and the coexistence approach were applied to the sporomorph data following Greenwood et al. (2005) and Utescher and Mosbrugger (2013), respectively (see Fig. 1.7 for clarification of both methods). Moreover, the same sporomorph-based paleoclimatic approach was applied to previously published sporomorph records from Southeast Australia (Bass Basin, Gippsland Basin, South East Highlands) and New Zealand to further constraint our results from Site 1172.

1.8 Comparison with organic proxies

The absence of biogenic carbonate in high-latitude Paleogene sediments leads to the use of organic approaches for temperature estimations (Bijl et al., 2009). The most recently developed proxies are TEX₈₆ (Schouten et al., 2002) and MBT/CBT (Weijers et al., 2007d). Both proxies are based on Glycerol-dialkyl-glycerol-tetraethers (GDGT) lipids that are synthesized by many phylogenetic groups within the Archea domain and occur ubiquitously in a wide range of environments, such as the marine and lacustrine water columns, lacustrine sediments, surface and deeply buried marine sediments, soil, peat and modern hot springs (see Schouten et al., 2013; and references therein).

The MBT/CBT (methylation index of branched tetraethers/cyclisation ratio of branched tetraethers) proxy for air temperature is a relatively novel organic geochemical tool increasingly employed in terrestrial paleoclimatic studies (e.g., Weijers et al., 2007c; Eberle et al., 2010). This proxy was developed based on the significant correlation between mean annual air temperature and soil pH with branched GDGT distributions in >130 natural soils (Weijers et al., 2007d). This proxy is derived from branched GDGTs produced by a yet unknown group of anaerobic soil bacteria that adapt their core membrane lipid composition to both pH and temperature (Weijers et al., 2007d).

While the CBT is primarily related to the pH of the soil, the MBT is mainly correlated with the annual mean air temperature and, to a lesser extent, negatively correlated with the pH of the soil (Weijers et al., 2007a). If both parameters are combined, it appears that the variation in the MBT is largely explained by both MAT and pH as follows (Weijers et al., 2007d):

$$\text{MBT} = 0.122 + 0.187 \times \text{CBT} + 0.02 \times \text{MAT} \quad (r^2 \text{ 0.77}) \quad (\text{Eq. 1.1})$$

Since these lipids are produced in soil, they are likely to reflect soil temperature rather than air temperature; additionally, like other proxies, results derived from the MBT/CBT proxy may be biased towards summer temperatures (see Schouten et al., 2013 and references therein for further discussion). In this study, a comparison of the sporomorph data with

temperatures derived from MBT/CBT (data provided by Peter Bijl from Utrecht University) is portrayed in Chapter 2.

With regard to TEX₈₆, this technique is based on the relative distribution of isoprenoid GDGTs derived from marine Thaumarchaeota (Schouten et al., 2002; 2013). This proxy relies on the idea that temperature is one of the main factors influencing the relative number of cyclopentane moieties, combined with the observation that the distribution of cyclopentane moieties in marine sediments varied between different latitudes (Schouten et al., 2002; 2013).

Considering that temperature is an important control on GDGT distribution in the marine environment, Schouten et al. (2002) presented a significant correlation between the number of cyclopentane rings of GDGTs and the annual mean sea surface temperatures based on the following index:

$$\text{TEX}_{86} = \frac{(GDGT-2)+(GDGT-3)+(Chenarchaeol\ regio\ isomer)}{(GDGT-1) + (GDGT-2)+(GDGT-3)+(Chenarchaeol\ regio\ isomer)} \quad (\text{Eq.1.2})$$

However, the established correlation by Schouten et al. (2002) is based on a relatively small set (n=44) of surface sediment data. An extended dataset (n=287) with core top data from mainly polar oceans improved the correlation and supported that TEX₈₆ has a strong linear relationship with sea surface temperatures (SSTs) between 5°C and 30°C and might not be directly applicable for the polar oceans (Kim et al., 2008). Moreover, Kim et al. (2010) extended the global core top data set including samples from polar oceans and confirmed the general insensitiveness of TEX₈₆ to temperatures on those latitudes. They also statistically evaluated other GDGT indices other than the ones introduced by Schouten et al. (2002) and founded two new calibrations (i.e., Tex₈₆^L and Tex₈₆^H) with a stronger relationship to SSTs.

The application of TEX₈₆ to higher latitudes is still on debate (see further discussion on Hollis et al., 2012; Bijl et al., 2013a; Pancost et al., 2013, Schouten et al., 2013). In this study, comparisons with SST estimations derived from Tex₈₆^L and Tex₈₆^H of Site 1172 (Bijl et al., 2009; 2013b; Hollis et al., 2014) are provided in Chapter 4.

1.9 Framework of this thesis

Summaries of Chapters 2 – 4 are presented as follows:

Chapter 2, Based on the obtained Eocene sporomorph data for Site U1356, the first continental climate reconstruction of Antarctica for the peak of the early Eocene greenhouse world is provided in this chapter. Our palynological data indicate that the early Eocene vegetation along the Wilkes Land margin was highly diverse and contained thermophilous elements that today are restricted to tropical and subtropical settings (e.g., palms and Bombacoideae). In combination with MBT/CBT paleotemperature results, they

provide strong evidence for near-tropical warmth at least in the coastal lowlands along the Wilkes Land margin. At the same time, vegetation elements that today prefer cool temperate settings were consistently present, suggesting a vegetation zonation by altitude and/or coastline distance. In contrast, the middle Eocene pollen and spores record indicates a dominance of cool temperate, low-diversity forests dominated by *Nothofagus* (southern beech) and conifers. Thermophilous elements are consistently absent and lower temperatures are also suggested by the MBT/CBT data for this time interval. This cooling is further corroborated by sporomorph-derived paleoclimatic information that is mainly based on bioclimatic analyses using the nearest living relative concept. Mean annual temperature (MAT), mean winter (MWT) and summer (MST) temperatures and mean annual precipitation (MAP) are provided in this chapter for the lowland (paratropical) and highland (temperate) biomes. Although the climate estimates presented in this chapter are not representative of the Antarctic continent as a whole, they bear implications for the current debates on the general ability of climate models to reproduce extreme greenhouse conditions and the response of polar ecosystems to increase CO₂ forcing.

Chapter 3, A qualitative and quantitative characterization of Eocene forests along the Wilkes Land margin based on the sporomorph assemblages of Site U1356 is provided in this chapter. The qualitative approach investigates the vegetation structure of forests along the Wilkes Land margin based on the ecological requirements and habitats of the known living relatives of the fossil taxa. The quantitative approach describes the composition and diversity of these ancient forests based on Detrended Correspondence Analysis, rarefaction, species accumulation curves, and diversity indices. A comparison of species richness of the Eocene vegetation from the Wilkes Land margin with modern selected tropical and temperate sites through species accumulations curves further elucidates the characterization of Eocene forests on Antarctica. The results of the combined qualitative and quantitative approach indicate that early Eocene forests along the Wilkes Land margin were characterized by a diverse canopy composed of plants that today occur in tropical settings; their richness pattern was similar to present-day forests from New Caledonia. In contrast, middle Eocene forests were characterized by a canopy dominated by *Nothofagus* and exhibited low richness patterns similar to modern *Nothofagus* forests from New Zealand. Moreover, stratigraphic distribution and characterization of selected taxa through taxonomical remarks and microphotographs are presented in this chapter and in Appendix 1.

Chapter 4, This chapter explores the climate and vegetation dynamics during the early Paleogene on Tasmania based on the middle Paleocene to early Eocene record of Site 1172. Based on the obtained sporomorph data, this study suggests that three vegetation types were thriving on Tasmania under different climate conditions from the middle Paleocene to the early Eocene: (i) warm-temperate forests dominated by gymnosperms that were the dominant vegetation during the middle and late Paleocene; (ii) cool-temperate forests dominated by *Nothofagus* and Araucariaceae that transiently prevailed across the middle/late Paleocene transition interval; and (iii) paratropical forests rich in ferns that were established in the wake of the Paleocene–Eocene Thermal Maximum (PETM). The

presence of cool-temperate forests and the absence of frost sensitive taxa (i.e., palms and Cycadales) during the middle/late Paleocene transition (~59.5 to ~59.0 Ma) indicate notably cooler conditions and harsher winters on Tasmania during this time interval. The integration of our data with the available terrestrial information from the Southwest Pacific region, together with newly generated paleoclimatic estimates, suggests that the replacement of temperate by paratropical forests was indeed regional and strongly linked to the PETM event. Moreover, the comparison of our terrestrial (i.e., floristic and climatic) data from Site 1172 and TEX₈₆-based sea-surface temperatures reveals a strong close coupling between marine and terrestrial evolution during the early Paleogene and a summer bias on the TEX₈₆-derived temperatures.

Chapter 2. Persistent near-tropical warmth on the Antarctic continent during the early Eocene epoch

Jörg Pross^{1,2}, Lineth Contreras¹, Peter K. Bijl³, David R. Greenwood⁴, Steven M. Bohaty⁵, Stefan Schouten⁶, James A. Bendle⁷, Ursula Röhl⁸, Lisa Tauxe⁹, J. Ian Raine¹⁰, Claire E. Huck¹¹, Tina van de Flierdt¹¹, Stewart S.R. Jamieson¹², Catherine E. Stickley¹³, Bas van de Schootbrugge¹, Carlota Escutia¹⁴, Henk Brinkhuis³ and IODP Expedition 318 Scientists.

¹Paleoenvironmental Dynamics Group, Institute of Geosciences, Goethe University Frankfurt, Altenhöferallee 1, 60438 Frankfurt, Germany. ²Biodiversity and Climate Research Centre, Senckenberganlage 25, 60325 Frankfurt, Germany. ³Biomarine Sciences, Institute of Environmental Biology, Laboratory of Palaeobotany and Palynology, Utrecht University, Budapestlaan 4, 3584 CD Utrecht, The Netherlands. ⁴Biology Department, Brandon University, 270 18th Street, Brandon, Manitoba, R7A 6A9, Canada. ⁵National Oceanography Centre Southampton, University of Southampton, European Way, Southampton SO14 3ZH, UK. ⁶Department of Marine Organic Biogeochemistry, NIOZ Royal Netherlands Institute of Sea Research, Post Office 59, 1790 AB Den Burg, Texel, The Netherlands. ⁷Glasgow Molecular Organic Geochemistry Laboratory, School of Geographical and Earth Sciences, University of Glasgow, Glasgow G12 8QQ, UK. ⁸MARUM – Center for Marine Environmental Sciences, University of Bremen, Leobener Straße, 28359 Bremen, Germany. ⁹Scripps Institution of Oceanography, University of California, San Diego, La Jolla, California 92093, USA. ¹⁰Department of Palaeontology, GNS Science, PO Box 30368, Lower Hutt 6009, New Zealand. ¹¹Imperial College London, Department of Earth Science and Engineering, South Kensington Campus, Exhibition Road, London, SW7 2AZ, UK. ¹²Department of Geography, Durham University, Science Laboratories, South Road, Durham, DH1 3LE, UK. ¹³Department of Geology, University of Tromsø, 9037 Tromsø, Norway. ¹⁴Instituto Andaluz de Ciencias de la Tierra, Av. de las Palmeras, 4 18100 Armilla (Granada), Spain.

Published in Nature 488, 73-77

Abstract

The warmest global climates of the past 65 Million years (Myr) occurred during the early Eocene epoch (about 55-48 million years ago), when the Equator-to-pole temperature gradients were much smaller than today (Greenwood and Wing, 1995; Bijl et al., 2009) and atmospheric carbon dioxide levels were in excess of one thousand parts per million by volume (Yapp, 2004; Beerling and Royer, 2011). Recently, the early Eocene has received considerable interest because it may provide insight into the response of the Earth's climate and biosphere to high atmospheric CO₂ levels that are expected for the near future (Meinshausen et al., 2011) as a consequence of unabated anthropogenic carbon emissions (Zachos et al., 2008; Beerling and Royer, 2011). Climatic conditions of the early Eocene “greenhouse world” are poorly constrained in critical regions, particularly Antarctica. Here

we present a well-dated record of early Eocene climate on Antarctica from an ocean sediment core recovered off the Wilkes Land coast of East Antarctica. The information from biotic climate proxies (pollen and spores) and independent organic geochemical climate proxies (indices based on branched tetraether lipids) yields quantitative, seasonal temperature reconstructions for the early Eocene greenhouse world on Antarctica. We show that the climate in lowland settings along the Wilkes Land coast (at a palaeolatitude of about 70° south) supported the growth of highly diverse, near-tropical forests characterized by mesothermal to megathermal floral elements including palms and Bombacoideae. Notably, winters were extremely mild (warmer than 10°C) and essentially frost-free despite polar darkness, which provides a critical new constraint for the validation of climate models and for understanding the response of high-latitude terrestrial ecosystems to increased carbon dioxide forcing.

2.1 Introduction

The climate and ecosystem evolution on Antarctica before the onset of continental-scale glaciation at the Eocene/Oligocene transition (~33.9 Myr ago) is still poorly resolved owing to the obliteration or coverage of potential archives by the Antarctic ice sheet. Available data are primarily based on records from the Antarctic Peninsula, which are only partially representative of climate and ecosystem conditions on the Antarctic mainland (Anderson et al., 2011). Terrestrial proxy data generally indicate cool temperate conditions supporting a vegetation dominated by podocarpaceous conifers during the Palaeocene (~65-56 Myr ago) and southern beech (*Nothofagus*) during the middle Eocene (~49-37 Myr ago), followed by the final demise of angiosperm-dominated woodlands as a result of Cenozoic cooling and the development of the Antarctic cryosphere around Eocene-Oligocene boundary times (Francis, 1996; Poole et al., 2005; Truswell and Macphail, 2009). This virtually makes the terrestrial realm of the high southern latitudes a climatic *terra incognita* for the peak warmth of the Cenozoic greenhouse world.

We apply terrestrial palynology and palaeothermometry based on the methylation index of branched tetraethers (MBT) and the cyclization ratio of branched tetraethers (CBT) to a new sedimentary record from the Wilkes Land margin, East Antarctica, recovered by the Integrated Ocean Drilling Program (IODP Expedition 318 Site U1356; Expedition 318 Scientists, 2011; Fig. 2.1). These datasets provide the framework for the first terrestrial climate reconstructions for the early Eocene of Antarctica. The record presented here comprises a succession of mid-shelfal sediments with excellent chronostratigraphic control (Supplementary Fig. S2.1), representing early Eocene (53.6-51.9 Myr ago) greenhouse conditions and, separated by a ~2 Myr hiatus, an interval of cooling presumed within the latest early Eocene to middle Eocene (49.3-46 Myr ago; here informally referred to as “mid-Eocene”). Palynological and geochemical evidence independently supports the contention that the Wilkes Land sector of Antarctica is indeed the source region for the Eocene terrestrial palynomorphs and biomarkers present in the sediment core from Site U1356 (see Supplementary Information).

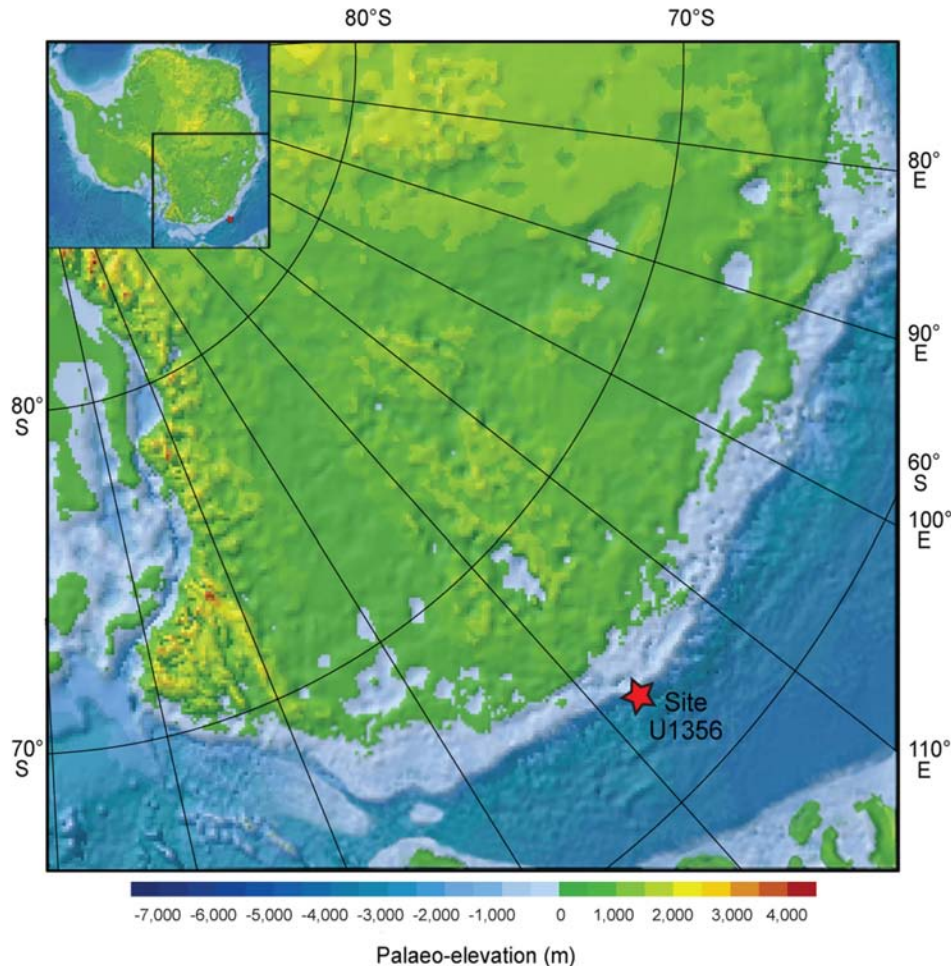


Figure 2.1 Site location and continental setting of Antarctica at early Eocene times. Pre-glacial topographical reconstruction for Antarctica during Eocene–Oligocene times. Reconstructed elevations are used here to define minimum elevations for the early Eocene (Supplementary Information). The reconstruction indicates the likely presence of extensive lowlands along the Wilkes Land margin and higher-altitude settings in the hinterland, both of which represent the main catchment area for the terrestrial climate proxies (sporomorphs and biomarkers) studied at Site U1356. Palaeotopography after Wilson et al. (2012); early Eocene coordinates obtained from the Ocean Drilling Stratigraphic Network after Hay et al. (1999).

2.2 Results and Discussion

Non-metric multidimensional scaling techniques show that the Eocene sporomorph assemblages at Site U1356 represent two main biomes (Fig. 2.2 and Supplementary Information). A highly diverse paratropical rainforest biome prevailed during the early Eocene, probably occupying the coastal lowlands of the Wilkes Land margin. This biome includes numerous mesothermal to megathermal taxa characteristic of modern subtropical to tropical settings in Australia, New Guinea and New Caledonia (Kershaw, 1988). In addition to ferns and tree ferns (*Lygodium*, Cyatheaceae), it is characterized by the presence of palms (Arecaceae), Bombacoideae (Malvaceae), *Strasburgeria* (Strasburgeriaceae), *Beauprea* (Proteaceae), *Anacolosa* (Olacaceae) and *Spathiphyllum* (Araceae) (Fig. 2.2). Although these additional taxa occur only in low abundance, their presence is highly significant. Because they are pollinated by insects, their pollen dispersal in extant rainforests is generally restricted to less than 100m (Bush and Rivera, 1998). Hence, even

low percentages of their pollen in the Site U1356 record indicate that these plants formed a substantial part of the Wilkes Land margin vegetation.

The palm and Bombacoideae pollen not only represent the southernmost documented occurrences for both taxa during the Eocene, but, importantly, imply that winter temperatures remained substantially above freezing. Extant palms occur naturally only in regions with a coldest-month mean temperature (CMMT) of $\geq 5^{\circ}\text{C}$ (Greenwood and Wing, 1995). Because their cold-season temperature requirements increase further when palms grow under a high partial pressure of atmospheric CO_2 , the CMMT implied by palms during the early Eocene greenhouse world was at least 8°C (Royer et al., 2002). Even warmer conditions are suggested by the record of Bombacoideae, which today occur where $\text{CMMT} > 10^{\circ}\text{C}$. Because even the most winter-hardy extant palms are severely damaged by short-term freezing, with a series of consecutive years of unfavourable climate eventually being lethal (Larcher and Winter, 1981), winters must have been essentially frost-free.

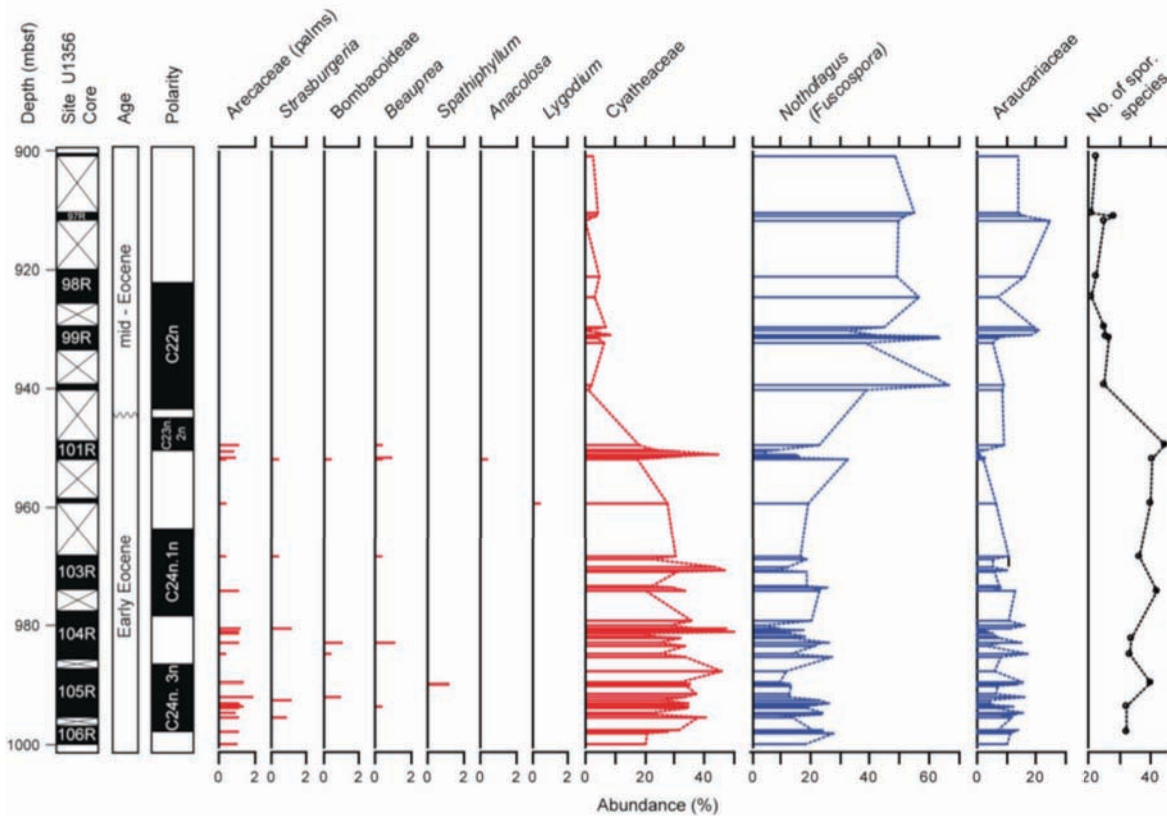


Figure 2.2 Data from Site U1356 for the early to mid-Eocene. (a) Core recovery, m.b.s.f, metres below sea floor; (b) Geological age; (c) Relative abundances of selected sporomorphs representative of the paratropical and temperate rainforest biomes, and (d) relative abundances of Proteaceae pollen. Data based on samples with counts ≥ 90 specimens; (e) Number of sporomorph species rarefied at 280 grains. The number of sporomorph species from the early Eocene is significantly higher than that from the mid-Eocene (Mann-Whitney test, $P < 0.000005$).

Sporomorphs representing a lower-diversity temperate rainforest biome, with taxa characteristic of extant forests in montane settings of Australia, New Caledonia, New Guinea and New Zealand (Kershaw, 1988), typically account for, 30% of sporomorphs during the early Eocene. Characteristic taxa include *Nothofagus (fusca* type), Araucariaceae, Proteaceae and *Podocarpus*; mesothermal to megathermal, frostsensitive taxa are consistently absent. Judging from its floral composition, this temperate rainforest

biome occupied cooler environments of Wilkes Land located farther inland and/or at higher elevations, and therefore provides insight into the climate conditions deeper within the Antarctic continent. The coeval existence of a temperate rainforest biome in the hinterland and a paratropical rainforest in the lowlands of the Wilkes Land margin indicates a pronounced continental interior to-coastal temperature gradient during the early Eocene.

A markedly different vegetation pattern is documented for the mid-Eocene time interval, with a strong expansion of the *Nothofagus* dominated temperate rainforest biome and the near-extirpation of the paratropical rainforest biome; notably, the remainder of the latter biome is devoid of megathermal elements (Fig. 2.2). Hence, our data suggest that the temperate rainforest biome became dominant over the entire catchment area of Site U1356, also extending into the coastal regions, and that relict mesothermal components of the paratropical rainforest biome persisted only in localized pockets along the Wilkes Land margin. These shifts in dominance and floral composition indicate a strong cooling, which in light of the cold-season sensitivity of meso- and megathermal taxa was particularly pronounced in winter temperatures, and a strong weakening of the temperature gradient between coastal and montane regions of the Wilkes Land margin.

To quantify further the sporomorph-derived palaeoclimatic information, we carried out bioclimatic analyses using the nearest living relative concept (Greenwood et al., 2005) to reconstruct the mean annual temperature (MAT), the mean winter and summer temperatures (MWT and MST) (Fig. 2.3), and the mean annual precipitation (Supplementary Fig. S2.5). These results were critically assessed through a comparison with reconstructions using a different methodology that also relies on the nearest living relative concept (the coexistence approach of Mosbrugger and Utescher, 1997; see Supplementary Information). Because the two recognized biomes represent distinct environments with different climatic conditions, our approach allows a spatiotemporally differentiated view of the climate evolution of Wilkes Land from early Eocene peak warmth through the onset of mid-Eocene cooling. Our temperature estimates for the paratropical rainforest biome show that climate along the Wilkes Land margin was generally warm until at least 51.9 Myr ago. Most samples indicating temperatures of 16 ± 5 °C for MAT, 11 ± 5 °C for MWT and 21 ± 5 °C for MST, although a small number also yields colder and warmer values (Fig. 2.3). A markedly cooler climate emerges for the temperate rainforest biome, in particular for MAT and MWT, for which most samples yield values of 9 ± 3 °C and 5 ± 2 °C, respectively. For MST, the data show a strong scatter between 14 ± 1 °C and 18 ± 3 °C, and the values overlap partly with those for the paratropical rainforest biome. For both biomes, the mean annual precipitation was persistently more than 100 cm yr^{-1} (Supplementary Information).

For the mid-Eocene interval, our reconstructions based on the relicts of the paratropical rainforest biome suggest a pronounced cooling, although this trend is partly within the error limits of the data. The estimated MAT is 14 ± 3 °C, which represents a decline of ~ 2 °C from the early Eocene. Our data also indicate a decline in MWT and MST, although these trends are again within the error limits. Temperatures reconstructed for the temperate

rainforest biome are comparable to those from the early Eocene, which is consistent with there being no major changes in the composition of this biome between both intervals.

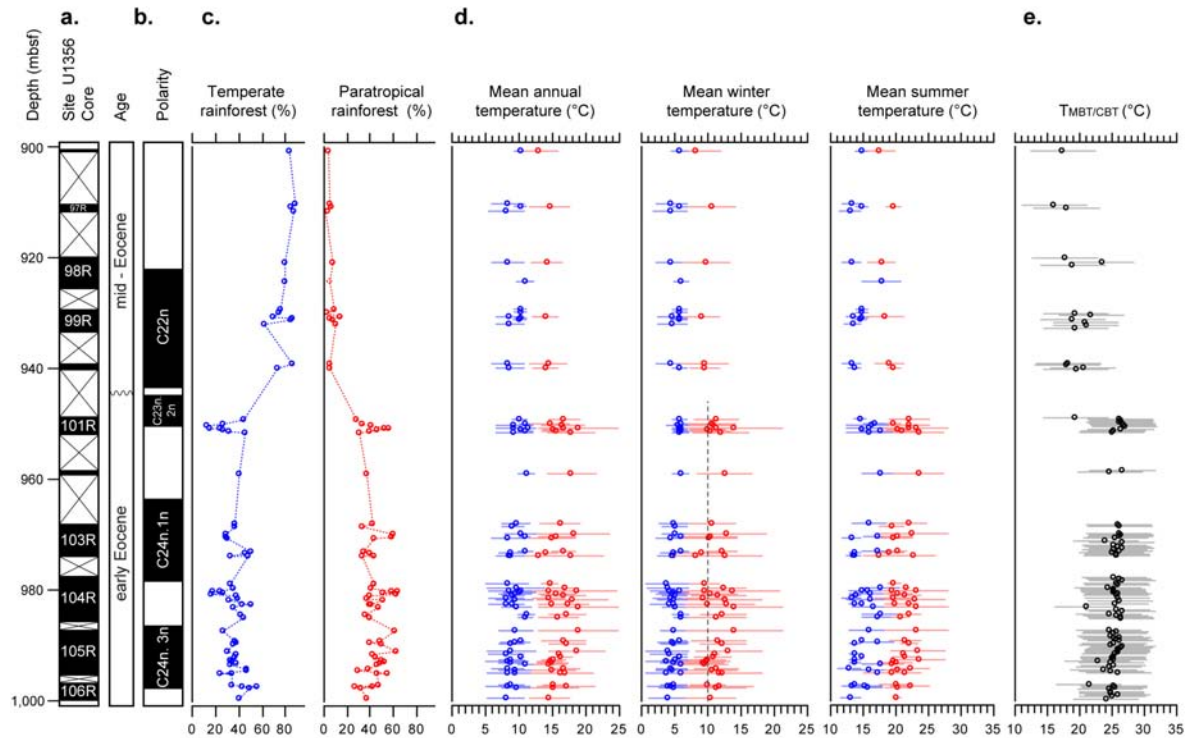


Figure 2.3 Climate reconstruction for the Wilkes Land sector of Antarctica during the early and mid-Eocene derived from Site U1356. (a) Core recovery; (b) Geological age (c) Relative abundances of sporomorphs representing the temperate and paratropical rainforest biomes; (d) Estimates of Mean Annual Temperature, Mean Winter Temperature and Mean Summer Temperature for the temperate (blue) and paratropical (red) rainforest biomes based on the methodology of Greenwood et al. (2005). Error bars represent the minimum and maximum estimate returned using that method. The vertical dashed marks the minimum requirements of Bombacoideae for the mean temperature of the coldest month; (e) Temperatures derived from the MBT/CBT index with horizontal error bars indicating the calibration standard error (± 5 °C). This error refers to absolute temperature estimates across all environmental settings of the modern calibration; thus, the error of the within-record variation is much smaller. Relative sporomorph abundances and sporomorph-based climate estimates based on samples with counts ≥ 90 specimens.

Independent support for a warm terrestrial climate during the early Eocene and marked cooling during the mid-Eocene comes from our MBT/CBT palaeothermometry data (Fig. 2.3). Soil temperatures of ~ 24 – 27 °C are estimated for the early Eocene, and, ~ 17 – 20 °C for the mid-Eocene. These temperatures fall close to the MSTs derived for the paratropical rainforest biome. This suggests that the branched tetraethers in Site U1356 sediments originated from coastal lowland soils of the Wilkes Land sector of Antarctica and could imply a bias of the MBT/CBT proxy towards summer temperatures, although such a bias has not been observed in modern mid-latitude climates (Supplementary Information).

Our data, which provide continental temperature reconstructions for the high southern latitudes during the early Eocene greenhouse world, show that paratropical conditions persisted in the lowlands of the Wilkes Land margin of Antarctica from at least 53.9 to 51.9 Myr ago. Notably, our estimates yield a constraint on Antarctic winter temperatures during peak greenhouse conditions. The CMMT and MWT estimates of ≥ 10 °C and 11 ± 5 °C,

respectively, compare favourably with deep-water temperatures of ~ 11 °C in the marine realm at this time (Lear, 2000; Zachos et al., 2008). Because early Eocene deep waters were sourced from downwelling surface waters in the high southern latitudes off Antarctica (Thomas et al., 2003), winter temperatures in these regions cannot have dropped much below 11 °C. Although our MWT estimates are not representative of the Antarctic continent as a whole, they bear implications for the current debates on the general ability of climate models to reproduce extreme greenhouse conditions and the response of polar ecosystems to increased CO₂ forcing.

When run with conservative estimates of atmospheric CO₂ levels for the early Eocene, fully coupled climate models yield high-latitude terrestrial winter temperatures considerably below freezing (Shellito et al., 2003), and they produce warm (that is, above-freezing) winters in the terrestrial high latitudes only when radiative forcing is strongly enhanced (Huber and Caballero, 2011). Hence, our winter temperatures for Wilkes Land provide a critical reference point for understanding the climate dynamics of the early Eocene greenhouse world. They are in remarkably close agreement with simulated MWTs for the Wilkes Land region when radiative forcings equivalent to 2,240 ppmv. and 4,480 ppmv. CO₂ are applied (Huber and Caballero, 2011), suggesting that enhancing radiative forcing in models may help resolve the persistent data–model mismatch. However, factors other than extremely high atmospheric greenhouse gas forcing may have contributed to the winter warmth along the Wilkes Land sector of Antarctica. They include winter cloud radiative forcing over high-latitude land masses (Abbot et al., 2009), possibly connected to high ocean-to-land moisture transport (Abbot and Tziperman, 2008). Our precipitation estimates (Supplementary Fig. S2.5) and the presence of rainforest biomes consistently suggest high moisture availability throughout the year, thus lending support for this mechanism being in operation in the Wilkes Land sector of Antarctica. A high moisture flux from the ocean was facilitated by the presence of extremely warm surface waters in the Australo-Antarctic gulf, resulting from the subtropically derived, clockwise-flowing proto-Leeuwin current (Huber et al., 2004). Warm surface waters off Wilkes Land are documented by mass occurrences of the subtropical dinoflagellate cyst *Apectodinium* (Bijl et al., 2013a).

Our data also provide new insights into the physiological ecology of high-latitude forests, which are subject to seasonally extreme changes in light levels. The, 50 days of polar darkness on the Wilkes Land margin poses severe constraints on the plants' carbon gain by photosynthesis and carbon loss by respiration. Because carbon loss by respiration typically increases with temperature (Tjoelker et al., 2001), it has been argued that polar winters must have been cool rather than warm (Read and Francis, 1992). Our MBT/CBT temperature data, which under the most conservative (that is, 'coldest') assumption represent MST, are typically between 24 and 27 °C for the early Eocene (Fig. 2.3). They are similar to, although possibly slightly warmer than, the terrestrial MST predicted by climate models using high radiative forcing (20–25 °C; Huber and Caballero, 2011). Over a wide range of CO₂ forcing, the models yield a temperature seasonality of the order of 10 °C, thus suggesting a MWT of 10–15 °C. This evidence, which is strictly independent of

our vegetation-based climate reconstructions, contradicts the scenario of cold winters on Wilkes Land, therefore suggesting that respiration losses under a highly seasonal polar light regime were compensated for by a factor other than temperature. We suggest that the high atmospheric CO₂ levels of the early Eocene greenhouse climate were a decisive factor in the physiological ecology of high-latitude forests, most probably through causing a reduction in carbon respiration during the polar winter (Beerling and Osborne, 2002) and an increase in photosynthetic carbon gain during the growing season (DeLucia et al., 1999).

Our new data from the peak early Eocene greenhouse world indicate that a highly diverse forest vegetation containing evergreen elements can successfully colonize high-latitude, warm winter environments when atmospheric CO₂ levels are high. Depending on the thresholds in atmospheric CO₂ required by such plants, the duration of polar winters and the temperatures at which such forcing factors become significant, these results have important implications for the composition of high-latitude terrestrial ecosystems in a future anthropogenic greenhouse world with high atmospheric CO₂ levels and drastic polar amplification of warming.

2.3 Methods summary

Palynology. Between 10 and 15 g of sediment were processed per sample. The dried sediment was weighed and spiked with *Lycopodium* spores to facilitate the calculation of absolute palynomorph abundances. Chemical processing comprised treatment with 30 % HCl and 38 % HF for carbonate and silica removal, respectively. Ultrasonication was used to disintegrate palynodebris. Residues were sieved over a 10- μ m mesh and mounted on microscope slides, which were analyzed at 200x and 1000x magnification. A detailed, step-by-step processing protocol is given in Supplementary Information.

Sporomorph-based climate reconstructions. Bioclimatic analyses were carried out following Greenwood and Christophel (2005), but with data sources including Southern Hemisphere taxa, allowing the development of climatic profiles for each taxon as described in Supplementary Information. The results of the bioclimatic analyses were critically assessed through the application of the coexistence approach (Mosbrugger and Utescher, 1997) to the data set using the same underlying database. Supplementary Table S2.1 lists all taxa that were evaluated through the bioclimatic analyses and the coexistence approach, their botanical affinity and the nearest living relatives used in the analyses.

Organic geochemistry. For MBT/CBT analyses, freeze-dried, powdered samples were extracted with an accelerated solvent extractor using a 9:1 (v/v) dichloromethane (DCM):methanol solvent mixture. The obtained extracts were separated over an activated Al₂O₃ column, using 9:1 (v/v) hexane:DCM, 1:1 (v/v) hexane: DCM, 1:1 (v/v) ethylacetate:DCM and 1:1 (v/v) DCM:methanol, into apolar, ketone, ethylacetate and polar fractions, respectively. The polar fractions containing the branched tetraether lipids were analysed by HPLC/APCI-MS (high-performance liquid chromatography/atmospheric

pressure chemical ionization mass spectrometry) using an Agilent 1100 LC/MSD SL. MBT/CBT indices were calculated and converted into temperature estimates as described in Supplementary Information.

Acknowledgements

This research used samples and data provided by the Integrated Ocean Drilling Program (IODP). The IODP is sponsored by the US National Science Foundation and participating countries under the management of Joint Oceanographic Institutions, Inc. Financial support for this research was provided by the German Research Foundation to J.P. (grant PR 651/10) and U.R. (grant RO 1113/6), the Biodiversity and Climate Research Center (BIK-F) of the Hessian Initiative for Scientific and Economic Excellence (LOEWE) to J.P., the Netherlands Organisation for Scientific Research to H.B. and S.S. (VICI grant), the Natural Sciences and Engineering Research Council of Canada to D.R.G. (grant DG 311934), the Natural Environment Research Council to S.M.B. (grant Ne/J019801/1), J.A.B. (grant Ne/I00646X/1) and T.v.d.F. (grant Ne/I006257/1), the National Science Foundation to L.T. (grant OCE 1058858) and the New Zealand Ministry of Science and Innovation to J.I.R.. We thank J. Francis, S. Gollner and M. Huber for discussions, and B. Coles, E. Hopmans, K. Kreissig, A. Mets, J. Ossebaar, B. Schminke and N. Welters for technical support

2.4 Supplementary Information for Chapter 2

2.4.1 Site description, lithology and depositional setting

Integrated Ocean Drilling Program (IODP) Site U1356 (coordinates: 63°18.6138' S, 135°59.9376' E) is located ~300 km off Wilkes Land, Antarctica, at the transition between the continental rise and the abyssal plain. Water depth is 3992 meters (Expedition 318 Scientists, 2011).

The lowermost 110 meters of sediments recovered at IODP Site U1356 (895.5 to 1000.08 meters below sea floor [mbsf], lithostratigraphic Units X and XI) are dated as Early to Middle Eocene in age based on the integration of dinoflagellate cyst (dinocyst) biostratigraphy and magnetostratigraphy (Expedition 318 Scientists, 2011); see also Section 2.4.2 – Age model for the Eocene of IODP Site U1356). Unit X (Cores -96R to -100R; 895.5 to 948.8 mbsf) consists of interbedded stratified and massive sandstones, diamictites, silty claystones, and siltstones exhibiting graded bedding and parallel lamination. Intraformational clasts occur abundantly in the fining-upward sandstones. In the lowermost intervals of Unit X, distinctive reddish brown silty claystones are repetitively interbedded at the decimeter- to meter-scale with greenish gray and brown, laminated sandy mudstones (Expedition 318 Scientists, 2011). Unit XI (Cores -101R to -106R; 948.8 to 1000.08 mbsf) consists predominantly of dark green, bioturbated claystone that is faintly stratified (millimetre- to meter-scale) as defined by colour variations (light to dark bands), and subordinate laminated siltstone and sandstone interbeds. Based on information from

dinocyst assemblages, sediments of Units X and XI were deposited in mid-shelfal settings (Expedition 318 Scientists, 2011).

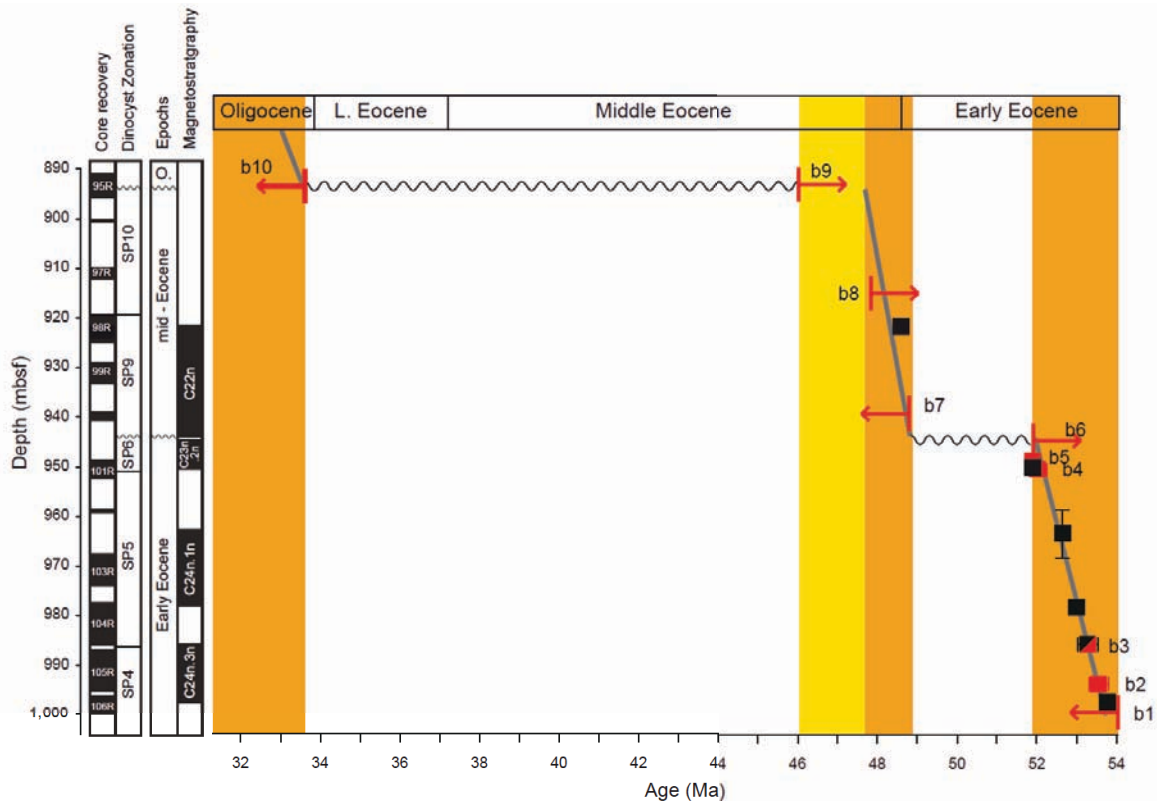
2.4.2 Age model for the Eocene of IODP Site U1356

An age-depth plot for the Eocene interval of IODP Site U1356 is presented in Supplementary Figure S2.1 and discussed in the following.

The coeval presence of the dinocyst species *Impagidinium cassiculum* and *Samlandia delicata* in the lowermost samples from IODP Site U1356 correlates to dinocyst zones NZE2b of Crouch and Brinkhuis (2005) and SPDZ4 as described in Bijl (2011). At the Tawanui section in New Zealand, NZE2b correlates to nannoplankton zone NP10, indicating an early Eocene age (correlated to magnetochron C24) (Gradstein et al., 2004). Core -105R Section 6W contains the First Occurrence (FO) of *Schematophora obscura*, thus being correlative to the upper part of the NZE2b zone of Crouch (2001) and Crouch and Brinkhuis (2005). This makes the oldest magnetic reversal in Core U1356A-106R (at 997.80 mbsf) the C24r–C24n.3n reversal. The FO of *Dracodinium waipawaense* is tentatively correlated to nannoplankton zone NP11 in New Zealand (Crouch, 2001). At Site U1356, we find the FO of *D. varielongitutum*, which is the Northern Hemisphere ecophenotype of *D. waipawaense* (Bijl et al., 2011), correlated to a magnetic reversal between Cores U1356A-105R and -104R (~986 mbsf) that we here assign to the C24n.3n–C24n.2r boundary. The overlying cores (U1356-104R and -103R) bear few biostratigraphic datums that would allow for a high-resolution correlation to other sites; all dinocyst species present correlate to Subchron C24n (Bijl et al., 2011). The top of Core U1356-104R and Core -103R have a normal polarity, which we assign to Subchron C24n.1n based on the presence of *D. varielongitutum* (which has a Last Occurrence [LO] at 51.5 Ma in Northern mid-latitudes (Williams et al., 2004). Core U1356-102R has a reversed polarity and still contains *D. varielongitutum*, allowing a correlation to Subchron C23r. The FOs of *Wetzeliiella samlandica* and *Charlesdowniea columna* within Core U1356-101R (at ~951.04 and 948.9 mbsf, respectively) correlate to the onset of C23n. In turn, the reversal found in shipboard magnetostratigraphic analyses (but not replicated by shore-based discrete sampling) within Core U1356-101R (~950 mbsf) is tentatively correlated to the C23r–C23n.2n reversal.

Dinocyst assemblages and palynofacies in Core U1356-100R and above are distinctly different from those observed further downhole. Relative abundances of endemic Antarctic species such as *Vozzhennikovia apertura*, *V. stickleyae*, *Spinidinium schellenbergii* and *Deflandrea antarctica* increase dramatically, and the palynofacies assemblages contain significantly higher amounts of terrestrial debris. Between Cores U1356-101R and -100R, the LOs of *Wetzeliiella samlandica*, *Homotryblium tasmaniense* and *Palaeocystodinium golzowense* are identified. These species are typical for the early Eocene (Bijl et al., 2011). *Arachnodinium antarcticum* has its FO within Core -100R. At ODP Sites 1172 and 1171, *Arachnodinium antarcticum* has a FO within the ranges of *Charlesdowniea coleothrypta* and *C. edwardsii*. These two species are also found in the Ashley Mudstone, New Zealand,

where they are restricted to nannoplankton zone NP13 (Hollis et al., 2009). This nannoplankton zone correlates to Magnetochron C22. At Site U1356, we find both these *Charlesdowniea* species from Core -99R section 2W to Core -98R Section 1W, but based on the presence of *Arachnodinium antarcticum* we assign the normal polarity in Cores -100R, -99R and -98R up to -98R section 2W to C22n. The absence of *Enneadocysta multicornuta* and *Enneadocysta dictyostila* in Cores U1356-100R through -96R allows this entire interval to be attributed to Subchron C21r or older (~46 Ma) (Williams et al., 2004).



Supplementary Figure S2.1. Age-depth plot for the Eocene interval of IODP Site U1356. Plotted are dinocyst events (red) and shipboard magnetic reversals (black). Orange shading indicates which time intervals are recovered, interval shaded in yellow is uncertain. Grey line represents best fit through the biostratigraphic control points. Biostratigraphic labels are as follows: b1 = first occurrence (FO) *Impagidinium cassiculum*; b2 = FO *Schematophora obscura*; b3 = FO *Dracodinium varilongitudum/waipawaense*; b4 = FO *Wetzeliella samlandica*; b5 = FO *Charlesdowniea columna*; b6 = last occurrence (LO) *Palaeocystodinium golzowense*; b7 = FO *Arachnodinium antarcticum*; b8 = LO *Damassadinium crassimuratum*; b9 = LO *in situ Membranophoridium perforatum*; b10 = FO *Malvinia escutiana*. The error bar connected to the magnetostratigraphic datum at 963.83 mbsf indicates the uncertainty of its stratigraphic position (± 4.83 m) resulting from core loss during drilling operations. Ages based on the GTS 2004 time scale (Gradstein et al., 2004), with refinements by Westerhold et al. (2008).

Within Section U1356-95R-3, we recognize the FOs of the Eocene species *Enneadocysta multicornuta*, *E. dictyostila*, *Deflandrea* sp. A *sensu* Brinkhuis et al. (2003), *Schematophora speciosa*, *Reticulosphaera actinocoronata*, *Turbiosphaera sagena* and *Stoveracysta kakanuiensis*. All these species have magnetostratigraphically calibrated FOs in the middle to late Eocene (Subchrons C21n, C20r, C16n.1r, C16n.1r, C15r, C15r, and C13r, respectively). Concomitantly, this sample level also contains the FO of *Malvinia escutiana*; The FO of this species has been calibrated to the Oligocene isotope event 1 (Oi-1) in the Southwest Atlantic Ocean (Houben et al., 2011). The LO is not defined at the type locality (DSDP Site 511), but the species ranges at least to 31.5 Ma (Houben et al., 2011). The coeval FOs of all abovementioned species suggest a hiatus between Sections U1356-

95R-3 and -95R-4 that covers at least the time interval correlated to the FO of *Enneadocysta multicornuta* and the Oi-1 isotope event. According to the GTS2004 time scale (Gradstein et al., 2004), the duration of this hiatus spans the time interval from at least 46 Ma to 33.6 Ma. The overlying strata contain numerous dinocyst taxa that have FOs during the time period covered by the hiatus.

2.4.3 Methods

2.4.3.1. Palynology

Processing and counting

A total of 145 palynological samples, taken from the Eocene interval of Site U1356 at a resolution of 20-30 cm, were processed using identical protocols at the Institute of Geosciences of Goethe University Frankfurt and the Laboratory of Palaeobotany and Palynology of Utrecht University.

Samples were crushed to chips with diameters of several millimeters and oven-dried (60°C) for several days. Subsequently, they were weighed and transferred into plastic bottles with screw-on caps. A tablet containing a known amount of *Lycopodium* spores (Lund University Batch Number 483216; 18,583 ±4.1 % spores per tablet) was added to each sample to facilitate the calculation of absolute (i.e., specimens per gram of dry sediment) palynomorph abundances. Samples were wetted with 10 % Agepon wetting detergent, and subsequently 10 % HCl was added when no carbonate was present; an excess of 30 % HCl was added to calcareous samples. The sample solutions were allowed to settle overnight and then decanted; subsequently, water was added, and the samples were centrifuged (2000 rpm, 5 minutes) and decanted again. Silicates were dissolved by adding an excess of 38 % HF and shaking the sample bottles on a shaker table for 2 hours. Subsequently, water was added and the samples were allowed to settle overnight. After decanting, an excess of 30 % HCl was added to remove silica gels. After centrifuging (2000 rpm, 5 minutes) and decanting again, the sample bottles were filled to halfway with 38 % HF and shaken on a shaker table for 2 hours, then filled up with distilled water and allowed to settle overnight. After decanting, silica gels were removed again by adding an excess of 30 % HCl, centrifuging (2000 rpm, 5 minutes), decanting, thoroughly rinsing with distilled water, and centrifuging and decanting again. The organic residue was sieved through a 250 µm nylon mesh to remove large particles, and the filtrate was subsequently sieved over a 10 µm mesh; an ultrasonic bath was used in the sieving process to disintegrate palynodebris. To separate heavier particles (pyrite and heavy minerals) from the organic residue, the entire residue was placed in a ceramic bowl that was kept floating in an ultrasonic bath for 5 minutes. The residue in the ceramic bowl was subsequently decanted, and the organic material, which remains in suspension during this process, was transferred into a glass vial. This residue was centrifuged (2000 rpm, 5 minutes) and decanted before diluted glycerol was added. The residue was then transferred to microscope slides, and slide preparations

were made using glycerine jelly as a mounting medium and nail polish for sealing. For each sample, between 2 and 12 slides (average: 5 slides) were prepared and evaluated.

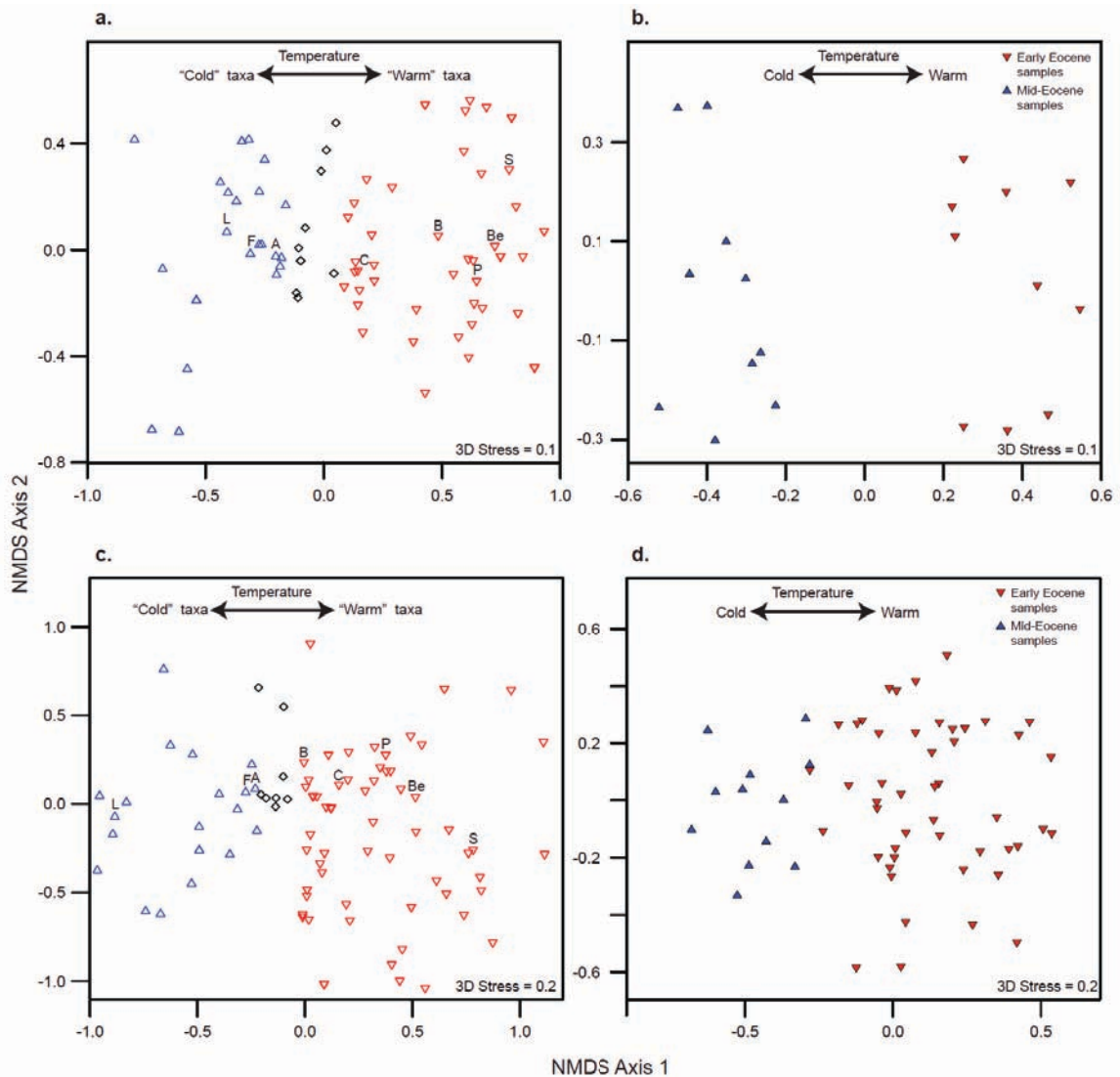
Whenever possible, 300 sporomorphs (excluding bisaccate pollen grains and reworked sporomorphs) were analysed per sample; this required the analysis of up to 12 slides per sample. Only samples with counting sums ≥ 90 sporomorphs (excluding bisaccate pollen grains and reworked sporomorphs) were used for further evaluation.

For the calculation of sporomorph percentages, bisaccate pollen grains and reworked sporomorphs were excluded from the counting sums; bisaccate pollen is generally overrepresented in marine sporomorph assemblages due to its particularly high buoyancy and resistance to degradation (Rossignol-Strick and Paterne, 1999; Traverse, 2008). The botanical affinities of the sporomorphs and the nearest living relatives (NLR) of their parent plants were determined using mainly Macphail et al. (1994), APSA Members (2007), Raine et al. (2008) and Truswell and Macphail (2009). The NLR are presented in Supplementary Table S2.1.

Statistical evaluation of sporomorph assemblages

Statistical and species richness analyses were performed using the software R for statistical computing (R Development Core Team, 2011) and the package VEGAN (Oksanen et al., 2011). To evaluate similarities and dissimilarities of samples and assess the response of sporomorph taxa to gradients resulting from environmental forcing factors, non-metric Multidimensional Scaling (NMDS) was performed using the function *metaMDS*. Due to the variation in sample sizes, the NMDS was applied separately to counts of ~ 100 and ~ 300 specimens. The dataset based on sample sizes of ~ 100 specimens also includes the counts of the first 100 specimens from all samples that ultimately yielded counting sums of 300 specimens. Relative sporomorph abundances from the two datasets were used as input to run the *metaMDS* function. The Bray-Curtis dissimilarity index was used as the distance parameter, and a three-dimensional ordination was selected because of the lower stress value obtained; however, for visual simplification the NMDS results are represented in two-dimensional view in Supplementary Figure S2.2. The function performed square root transformation and Wisconsin double standardization to give equal weight to all species and a better ordination. Additionally, *metaMDS* function returned the best solution after several random starts.

Based on the NMDS results, two separate clusters were obtained for the samples from the early and mid-Eocene (Supplementary Figure S2.2). The magnitude of the difference (early vs. mid-Eocene samples) was tested by analysis of similarities (ANOSIM) using the same parameters as in the NMDS analysis (i.e., square root transformation, Wisconsin double standardization, Bray-Curtis dissimilarity index). Statistical values derived from ANOSIM (R statistic = 0.91, $P < 0.01$ at counts of ~ 300 individuals; R statistic = 0.56, $P < 0.01$ at counts of ~ 100 individuals) demonstrate that the overall difference between the early and mid-Eocene samples are statistically significant.

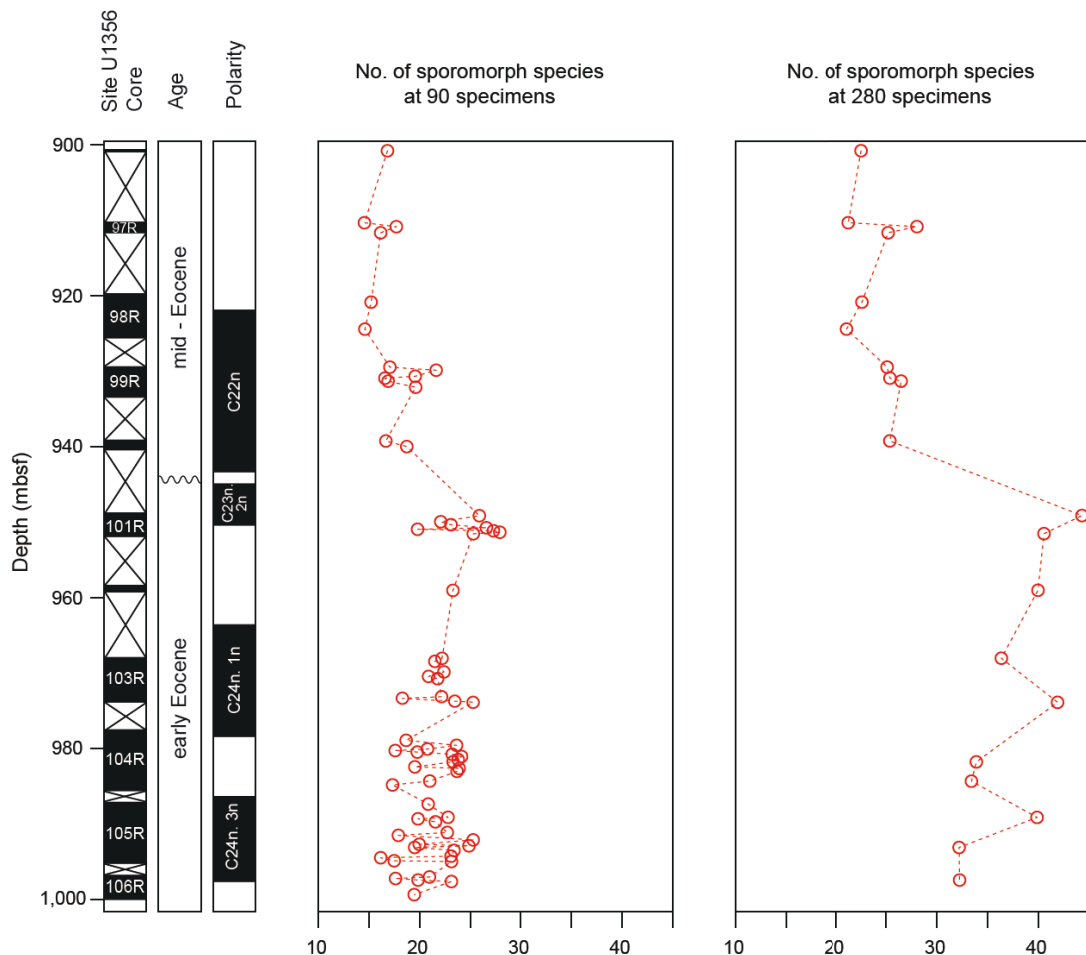


Supplementary Figure S2.2. Two-dimensional view of non-metric multidimensional scaling (NMDS) results for sporomorph data from the Eocene of IODP Site U1356. (a) Sporomorph species scores for samples with ~300 specimens. Red triangles: “warm” taxa, blue triangles: “cold” taxa, diamonds: uncertain or intermediate temperature preferences; (b) Sample scores for early and mid-Eocene samples with ~300 specimens; (c) Sporomorph species scores for samples with ~100 specimens. Red triangles: “warm” taxa, blue triangles: “cold” taxa, diamonds: uncertain or intermediate temperature preferences; (d) Sample scores for early and mid-Eocene samples with ~100 specimens. Selected key taxa are marked with letters directly above respective symbols. A = Araucariaceae; B = Bombacoideae; Be = *Beauprea*; F = *Nothofagus (fusca type)*; L = *Nothofagus (subgenus Lophozonia)*; S = *Strasburgeria*; P = Arecaceae (palms).

Based on sporomorph taxa for which the climatic requirements of their nearest living relatives (NLRs) are particularly well constrained, values along Axis 1 for the species scores in Supplementary Figure S2.2 represent primarily a temperature gradient. Sporomorphs can be attributed to two main biomes based on their distribution along Axis 1. The “warm” taxa, with nearest living relatives today occurring in the subtropical to tropical lowlands of New Guinea and New Caledonia (Paijmans, 1976; Morat, 1993), indicate a megathermal, paratropical rainforest biome. The “cold” taxa, with nearest living relatives today occurring in New Zealand and montane settings of New Guinea and New Caledonia (e.g., Kershaw, 1988), indicate a temperate rainforest biome. Taxa that are located in the central area along Axis 1 (i.e., between the “warm” and “cold” taxa) occurred

in both main biomes and/or may have responded primarily to environmental variables other than temperature.

Species richness (i.e., number of sporomorph species) was calculated using rarefaction. This interpolation technique is derived from an analysis of the relative frequencies of specimens within species and makes it possible to compare the estimated species richness at a constant sample size (Raup, 1975). Rarefaction was performed at 280 and 90 individuals (Supplementary Figure S2.3). The results suggest that the sporomorph species richness at Site U1356 was higher for the early Eocene (mean = 21.9 species/sample, with standard deviation ± 2.7 species/sample, $n = 52$, rarefied at 90 individuals; 37.5 ± 4.4 species/sample, $n = 10$, rarefied at 280 individuals) than for the mid-Eocene (17.3 ± 2.03 species/sample, $n = 14$, rarefied at 90 individuals; 24.3 ± 2.3 species/sample, $n = 10$, rarefied at 280 individuals). The significance of these differences was assessed through a Mann-Whitney test. The obtained P values indicate that the species richness of the early Eocene is significantly higher than that of the mid-Eocene ($P < 0.000001$ at 90 individuals; $P < 0.000005$ at 280 individuals).



Supplementary Figure S2.3. Number of sporomorph species from the Eocene of IODP Site U1356. Values are derived from the rarefaction analysis at 90 (left column) and 280 specimens (right column).

Quantitative climate reconstructions based on sporomorph assemblages

The method of bioclimatic analysis is essentially the same as described by Greenwood and others (Greenwood et al., 2005), but with data sources focused on Southern Hemisphere (mainly Australian) taxa enabling climatic profiles to be developed for each sporomorph taxon. The first step in the bioclimatic analysis is to identify as many sporomorph taxa with NLRs as possible from the fossil floras. Climatic profiles are then produced for each NLR with respect to various climate parameters such as mean annual temperature (MAT), mean winter temperature (MWT), coldest month mean temperature (CMMT), mean summer temperature (MST), and mean annual precipitation (MAP). For this, we obtained geographical distribution data from the Australian National Herbarium online database (Australian National Herbarium, 2011) and determined the climate profile for each NLR taxon using the mathematical climate surface software ANUCLIM 5.1 (Houlder et al., 1999). Each profile contains the maximum and minimum values for a range of climate and related environmental variables with respect to an individual NLR taxon. To determine the climate envelope that accommodated a majority of taxa from a given fossil assemblage with respect to a given climate parameter, the zone of overlap was calculated using the 10th percentile (as lower limit) and 90th percentile (as upper limit) of the total range for all NLRs represented in that assemblage. The estimate in bioclimatic analysis is presented as the midpoint between the lower and upper limits, with the error spanning from the lower to the upper limit. The sporomorph taxa that were utilised in this study and their NLRs can be found in Supplementary Table S2.1. Only samples with at least 5 NLRs with climate profiles were used in our analysis.

To test the fidelity of results derived from this reconstruction, we carried out quantitative reconstructions for the same climate parameters based on the Coexistence Approach (CA) of Mosbrugger and Utescher (1997). This approach is also based on the NLR concept, i.e., the assumption that the climatic requirements of the fossil taxa are similar to those of their NLRs. The aim of the CA is to identify for a given fossil flora the range for a specific climate parameter in which a maximum number of NLRs of this flora can coexist. Coexistence ranges are calculated separately for each climate parameter; together they are considered the best description of the palaeoclimatic situation under which the fossil flora had lived. The climatic requirements of the NLRs are from the same sources as those used for the bioclimatic analyses *sensu* Greenwood et al. (2005) (see above). This enables us to compare the output of both methodologies based on an internally consistent database. The width of a coexistence interval for a given climate parameter determines the resolution of the CA with respect to this parameter. Although the CA can in principle work with a single taxon, the interval width typically increases with the number of taxa with NLR used (Mosbrugger and Utescher, 1997; Pross et al., 2000). In this study, we only use climate values derived from the CA if the evaluation of a sample is based on ≥ 5 NLRs.

Fossil taxon	Biome	Botanical affinity			
		Taxon	Source	NLR used for climate analysis	Data-base
<i>Anacolosidites acutullus</i>		Olacaceae?/Santalaceae	Raine et al., 2008		
Anacolosidites luteoides		Olacaceae (<i>Anacolosa</i>)	Raine et al., 2008	<i>Anacolosa</i>	1
Araucariacites spp.	T	Araucariaceae	Raine et al., 2008	Araucariaceae	1, 2
Arecipites spp.	P	Arecaceae	Nichols et al., 1973	Arecaceae	1
Baculatisporites spp./Osmundacidites spp.	T	Osmundaceae	Raine et al., 2008	Osmundaceae	1
<i>Beaupreaidites</i> spp.		Proteaceae (<i>Beauprea</i>)	Raine et al., 2008		
<i>Bluffopollis scabratus</i>		Strasburgeriaceae (<i>Strasburgeria</i>)	Jarzen and Pocknall, 1993		
Bombacacidites sp. A	P	Bombacoideae		Bombacoideae (all Australian species)	1
Bombacacidites? "protocostatus"	P	Bombacoideae?		Bombacoideae (all Australian species)	1
<i>Brevitricolpites</i> sp. (<i>Brownlowia</i> type)		<i>Brownlowia</i> ?	Comparison with Perveen et al., 2010		
Crassorettriletes vanraadshooveni	P	<i>Lygodium</i>	Germeraad et al., 1968	<i>Lygodium</i>	1
Cyathidites spp.	P	Probably Cyatheaceae	Mohr, 2001	Cyatheaceae	1
<i>Dilwynites granulatus</i>		Araucariaceae (<i>Wollemia</i>)	Macphail et al., 1995		
<i>Foveotrilites lacunosus</i>		<i>Huperzia</i>	Raine et al., 2008		
Gleicheniidites spp.	T	Gleicheniaceae	Raine et al., 2008	<i>Dicranopteris</i> , <i>Diplopterygium</i> , <i>Gleichenia</i> , <i>Sticherus</i>	1
<i>Intratrirporopollenites notabilis</i> ?		Sterculioideae?, Bombacoideae?, Tilioideae?	Raine et al., 2008		
Kuylisporites waterbolkii	P	Cyatheaceae (<i>Cyathea</i> , <i>Cnemidaria</i>)	Raine et al., 2008	Cyatheaceae (<i>Cyathea</i> , <i>Cnemidaria</i>)	1, 2
<i>Malvacipollis</i> spp.		Euphorbiaceae (<i>Austrobuxus</i> , <i>Dissiliaria</i> , <i>Petalostigma</i>); Eumalvoideae?	Raine et al., 2008		
Margocolporites cf. cribellatus	P	Caesalpiniaceae? (similar to <i>Margocolporites vanwijhei</i>)	Muller, 1981	<i>Caesalpinia</i> (all Australian species)	1
Myricipites harrisii	P/T	Casuarinaceae, possibly also Myricaceae	Raine et al., 2008	Casuarinaceae (all Australian species)	1
Myrtacidites spp.		Myrtaceae	Raine et al., 2008		
Myrtacidites tenuis	P	Myrtaceae, <i>Eucalyptus</i> ?	Harris, 1965	<i>Eucalyptus</i>	1
Nothofagidites asperus complex	T	Nothofagaceae (<i>Nothofagus</i> subg. <i>Lophozonia</i>)	Truswell and Macphail, 2009	<i>N. cunninghamii</i> , <i>N. moorei</i>	1
Nothofagidites cf. N. emarcidus complex	T	Nothofagaceae (<i>Nothofagus</i>)	Truswell and Macphail, 2009	all subgenera (including <i>Brassospora</i>)	1, 2
Nothofagidites flemingii complex	T	Nothofagaceae (<i>Nothofagus</i> subg. <i>Nothofagus</i>)	Raine et al., 2008	Nothofagaceae (<i>Nothofagus</i> subg. <i>Fuscospora</i>)	1, 2
Nothofagidites lachlaniae complex	T	Nothofagaceae (<i>Nothofagus</i> subg. <i>Fuscospora</i>)	Raine et al., 2008	Nothofagaceae (<i>Nothofagus</i> subg. <i>Fuscospora</i>)	1, 2
Nothofagidites sp. undifferentiated	T	Nothofagaceae (<i>Nothofagus</i>)		all subgenera (including <i>Brassospora</i>)	1, 2
Phyllocladidites mawsonii	T	<i>Lagarostrobos</i>	Raine et al., 2008	<i>Lagarostrobos</i>	1, 2

Supplementary Table S2.1. Botanical and climatological background data for fossil sporomorph taxa from the Eocene of Site U1356. Known botanical affinities, assigned nearest living relatives and sources of the developed climate profiles are indicated. Fossil sporomorph taxa used in the climatic evaluation through the bioclimatic analysis and the CA are printed in boldface. P = Paratropical rainforest biome, T = Temperate rainforest biome. Databases used for climate profiles: 1 – distribution geocode (latitude, longitude, altitude) records from Australian National Herbarium specimen information register online (<http://www.anbg.gov.au/cgi-bin/anhsir>), and bioclimatic envelopes from BIOCLIM (ANUCLIM 6.1; Houlder et al., 1999); 2 – point occurrence and climate data from South America, New Caledonia, New Zealand and New Guinea, including Mitchell (1991), Norstog and Nicholls (1997), Read et al. (2005), Duarte et al. (2012) and Mundo et al. (2012).

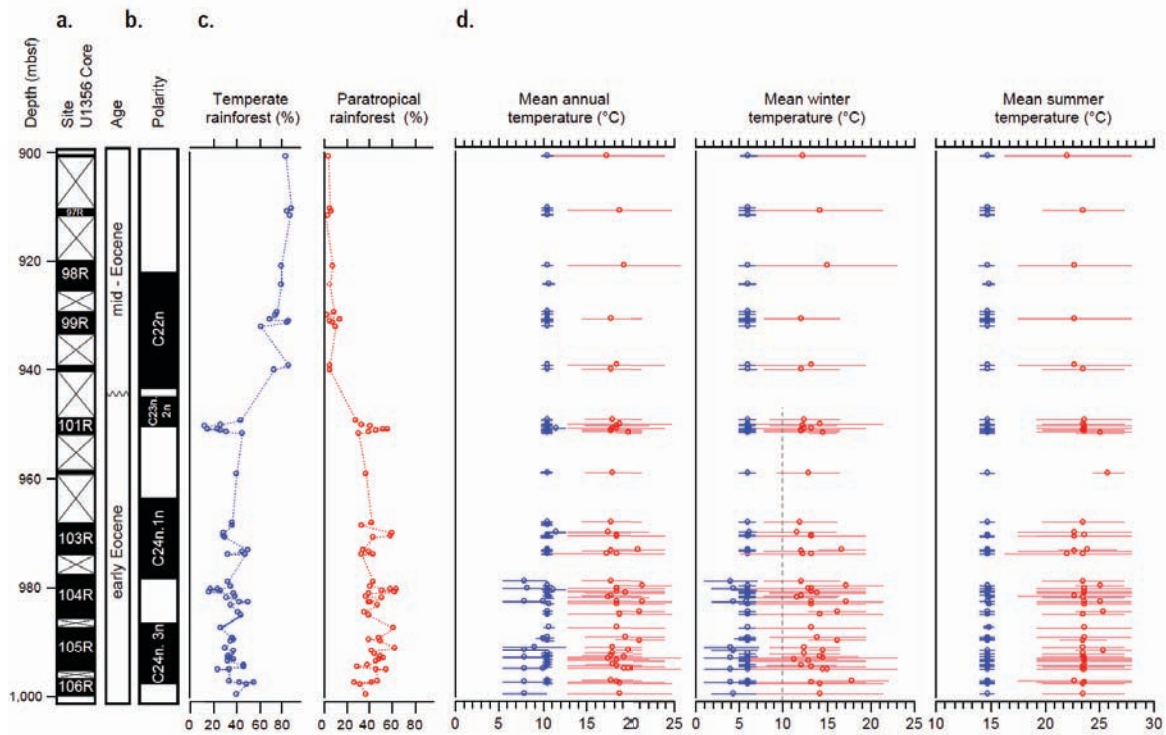
Fossil taxon	Biome	Botanical affinity			
		Taxon	Source	NLR used for climate analysis	Data-base
<i>Podocarpidites</i> spp.	T	Podocarpaceae mainly <i>Podocarpus</i>	Raine et al., 2008	<i>Podocarpus</i>	1, 2
<i>Polycolpoporopollenites</i> sp.		Polygalaceae?			
<i>Polypodiaceosporites</i> sp.		Polypodiaceae?			
<i>Proteacidites</i> cf. <i>amolosexinus</i>		Proteaceae (<i>Knightia excelsa</i> type)	Raine et al., 2008		
<i>Proteacidites annularis</i>	P	Proteaceae (<i>Xylomelum occidentale</i> or <i>Lambertia</i>)	Raine et al., 2008	<i>Xylomelum</i> (all Australian species)	1
<i>Proteacidites adenanthoides</i> cf.	P	Proteaceae (<i>Adenanthos</i>)	Raine et al., 2008	<i>Adenanthos</i>	1
<i>Proteacidites pseudomoides</i> cf.	P	Proteaceae (<i>Carnarvon</i> type, cf. <i>Lomatia</i>)	Raine et al., 2009	<i>Carnarvon</i>	1
<i>Proteacidites</i> cf. <i>spiniferus</i>		Proteaceae (cf. <i>Embothrium</i>)	Raine et al., 2008		
<i>Proteacidites parvus</i>	T	Proteaceae (<i>Belladena montana</i> type)	Raine et al., 2008	<i>Belladena montana</i>	1
<i>Proteacidites reticulosabratus</i>	P	Proteaceae (<i>Gevuina/Hicksbeachia</i> type)	Raine et al., 2008	<i>Gevuina</i> , <i>Hicksbeachia</i>	1, 2
<i>Proteacidites symphyonemoides</i>	T	Proteaceae (<i>Symphyonema</i> , <i>Petrophile</i>)	Raine et al., 2008	<i>Symphyonema</i> , <i>Petrophile</i>	1
<i>Psilamonocolpites</i> spp. (Including <i>Cycadopites</i> spp.)	P	Arecaceae/Gymnospermopsida for <i>Cycadopites</i> spp.	Raine et al., 2008	Cycadales: <i>Bowenia</i> , <i>Lepidozamia</i> , <i>Macrozamia</i>	1, 2
<i>Spathiphyllum</i> sp.		Araceae (<i>Spathiphyllum</i>)	Hesse and Zetter, 2007		
<i>Stereisporites</i> sp.		Sphagnaceae	Truswell & Macphail, 2009		
<i>Stereisporites</i> (<i>Tripunctisporis</i>) sp.		Sphagnaceae?			
<i>Triporoletes</i> cf. <i>reticulatus</i>		cf. <i>Riccia beyrichiana</i>	Raine et al., 2008		
<i>Tubulifloridites</i> sp.		Asteraceae subf. Tubuliflorae	Raine et al., 2008		

Supplementary Table S2.1 (continued).

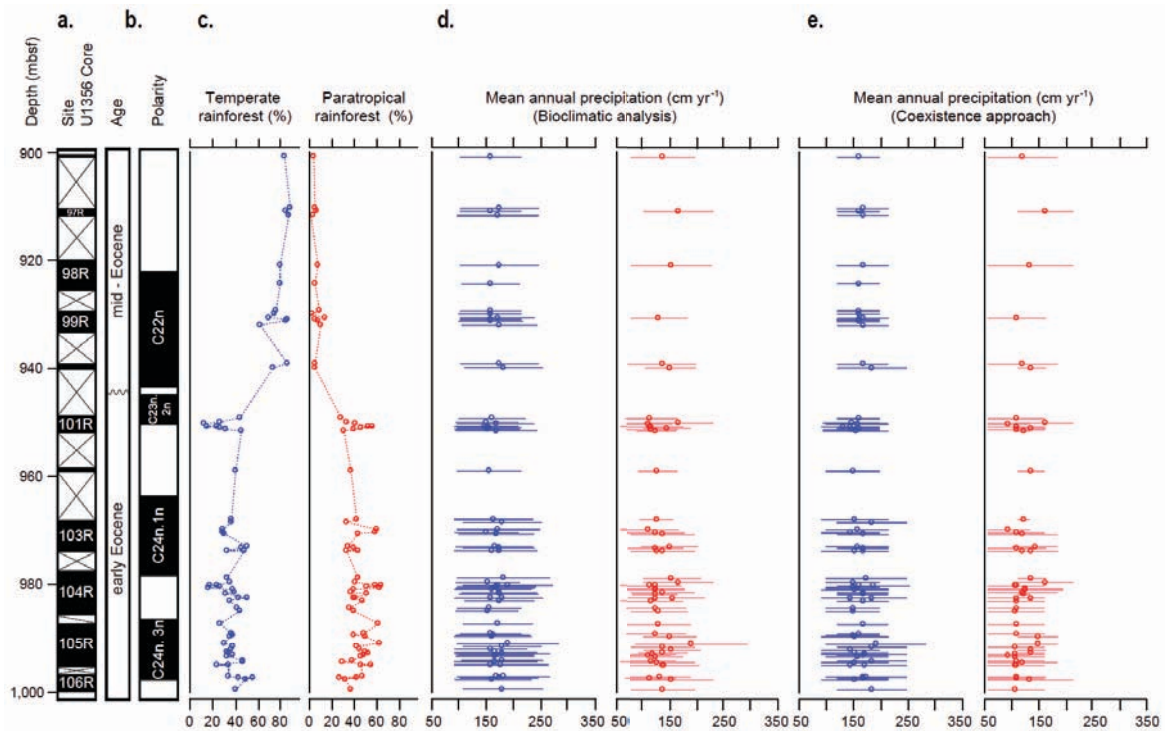
Summarizing the above, the differences between the methodologies of the bioclimatic analysis *sensu* Greenwood et al. (2005) and the CA *sensu* Mosbrugger and Utescher (1997) are as follows: In CA, a lower bound with respect to a given climate parameter is defined by the minimum value of a single taxon-NLR; likewise, the upper bound is defined by the maximum value of another taxon-NLR. These values provide the coexistence interval where all taxa overlap; “outliers” (i.e., taxa whose climate profiles sit outside of the zone of overlap of the majority of taxa) are arbitrarily excluded. In bioclimatic analysis, however, in order to exclude outliers the zone of overlap is calculated using the 10th percentile (lower limit) and 90th percentile (upper limit) of the total range for all taxa recorded for a single sample. The estimate derived for an assemblage in bioclimatic analysis is presented as the midpoint of the two extremes, with the error plotted as the lower and upper bounds. Hence, the “error bar” in bioclimatic analysis corresponds to the coexistence interval derived through the CA.

The comparison of the climate estimates through the bioclimatic analyses and the CA is based on the evaluation of the same taxa (see Supplementary Table S2.1 for a list of taxa). The application of the two methodologies yields consistent results for all climate parameters evaluated (Figure 2.3 in main text, Supplementary Figures S2.4 and S2.5). This indicates that our quantitative reconstructions are robust, thus providing a reliable basis for further interpretations. For all temperature parameters reconstructed, the CA intervals show a clear separation of the temperature intervals of the temperate rainforest and the

paratropical rainforest biomes, with the intervals of both biomes only overlapping in very few samples. Estimated MAP is very similar in both reconstruction methods, with a tendency towards higher values for the temperate rainforest biome than for the paratropical rainforest biome (Supplementary Figure S2.5).



Supplementary Figure S2.4. Temperature reconstructions for the Wilkes Land sector of Antarctica during the early and mid-Eocene derived from Site U1356. Reconstructions are based on the Coexistence Approach of Mosbrugger and Utescher (1997). (a) Core recovery; (b) Age model; (c) Relative abundances of sporomorphs representing the temperate and paratropical rainforest biomes; (d) Coexistence intervals for mean annual temperature, mean winter temperature and mean summer temperature for the temperate (blue) and paratropical (red) rainforest biomes. Blue respectively red bars delineate widths of coexistence intervals, with same-colour dots marking the centers of these intervals. Data based on samples with counts ≥ 90 specimens.



Supplementary Figure S2.5. Precipitation reconstructions for the Wilkes Land sector of Antarctica during the early and mid-Eocene derived from Site U1356. (a) Core recovery; (b) Age model; (c) Relative abundances of sporomorphs representing the temperate and paratropical rainforest biomes; (d) Mean annual precipitation as reconstructed through bioclimatic analyses following Greenwood et al. (2005). Horizontal error bars represent the minimum and maximum precipitation values as returned from the method; (e) Coexistence intervals for mean annual precipitation as reconstructed through the Coexistence Approach of Mosbrugger and Utescher (1997). Blue respectively red bars delineate widths of coexistence intervals, with same-colour dots marking the centers of these intervals.

2.4.3.2 Organic geochemistry

Organic compounds were extracted from 100 powdered and freeze-dried sediment samples with dichloromethane (DCM)/methanol (MeOH) (9:1, v/v) by using the accelerated solvent extraction technique (Dionex). Excess solvent was removed using rotary evaporation under vacuum. The total extracts were separated in apolar, ketone, ethyl acetate (EtOAc), and polar fractions over an activated Al₂O₃ column using hexane:dichloromethane (DCM) (9:1, v/v), hexane:DCM (1:1, v/v), EtOAc:DCM (1:1 v/v), and DCM:MeOH (1:1, v/v), respectively.

Glycerol dialkyl glycerol tetraether (GDGT) analyses

The polar fractions were dissolved in a (99:1; v/v) hexane/propanol solvent and filtered using a 0.45 µm, 4-mm-diameter polytetrafluoroethylene (PTFE) filter. Subsequently, they were analyzed using high-performance liquid chromatography/atmospheric pressure positive ion chemical ionization mass spectrometry (HPLC/APCI-MS); HPLC/APCI-MS analyses were carried out following Schouten et al. (2007) using an Agilent 1100 series LC/MSD SL separation and a Prevail Cyano column (2.1 x 150 mm, 3 mm; Alltech) maintained at 30°C. The GDGTs were eluted using a changing mixture of hexane and

propanol as follows: 99% hexane : 1% propanol for 5 minutes, then a linear gradient to 1.8% propanol in 45 minutes. Flow rate was 0.2 ml per minute. Single ion monitoring was set to scan the 10 [M+H]⁺ ions of the branched GDGTs and crenarchaeol with a dwell time of 237 ms for each ion.

MBT/CBT mean annual air temperature proxy

The MBT/CBT proxy for mean annual air temperature is derived from branched GDGT membrane lipids produced by a yet unknown group of anaerobic soil bacteria (Weijers et al., 2007d), although a branched GDGT was recently found in soil Acidobacteria (Sinninghe Damsté et al., 2011). A suite of different branched GDGTs are recognized in different soils and named as follows: GDGTs I, II and III contain none, one or two extra methyl branches and can contain either one (Ib; IIb; IIIb) or two (Ic; IIc, IIIc) cyclopentyl moieties. Studies show that there is strong relation between ambient pH of the soil and the amount of cyclopentyl moieties incorporated in the branched GDGTs (Weijers et al., 2007a; Peterse et al., 2009). This is expressed in the cyclisation ratio of branched tetraethers (CBT) (Weijers et al., 2007a):

$$CBT = -\log \left(\frac{([Ib] + [IIb])}{([I] + [II])} \right) \quad (\text{Eq. 2.1})$$

with the following correlation equation:

$$CBT = 3.33 - 0.38 * \text{pH} \quad (R^2 = 0.70) \quad (\text{Eq. 2.2})$$

The amount of methyl groups incorporated in the branched GDGTs (MBT) strongly correlates with mean annual air temperature and pH (Weijers et al., 2007a):

$$MBT = \frac{[I + Ib + Ic]}{[I + Ib + Ic] + [II + IIb + IIc] + [III + IIIb + IIIc]} \quad (\text{Eq. 2.3})$$

with the following equation:

$$MBT = 0.867 - 0.096 * \text{pH} + 0.021 * \text{MAT} \quad (R^2 = 0.82) \quad (\text{Eq. 2.4})$$

Correlation of MBT with MAT and CBT yields the following equation (Weijers et al., 2007a):

$$MBT = 0.122 + 0.187 * \text{CBT} + 0.020 * \text{MAT} \quad (R^2 = 0.77) \quad (\text{Eq. 2.5})$$

This calibration equation has a relatively large error (5 °C), and thus absolute values have to be interpreted with care. However, this calibration error is a systematic error that applies *between* different environmental settings; *within* settings, this error is reduced as much of the environmental variables causing the scatter in the calibration (e.g., vegetation type, hydrology and/or seasonality) are locally less variable. Thus, the point-to-point error within

a given record is less than the calibration error, but larger than the analytical error (ca. 0.5 °C). This means that temperature trends in the MBT/CBT record of Site U1356, such as the mid-Eocene cooling, are likely significant despite being smaller than the calibration error. Unfortunately, it is not possible to give an exact estimate of the error, and therefore we conservatively give the calibration error as the error in the MBT/CBT record (Fig. 2.3 in main text). For a detailed discussion on this topic we refer to the Supplementary Information of the paper by Tierney et al. (2010).

In marine sedimentary records, notably those from shelfal settings, branched GDGTs were also recognized; they were interpreted to originate from continental soils, with soil erosion and runoff further transporting the molecules into the marine realm (Hopmans et al., 2004; Kim et al., 2006; Walsh et al., 2008). Later studies recognized the *in situ* production of branched GDGTs in sediments of some marine settings, though their concentrations remained relatively low compared to archaeal isoprenoid GDGTs (Peterse et al., 2009). However, BIT values, a proxy for the relative amount of soil-derived branched GDGTs *versus* aquatic archaeal GDGTs (Hopmans et al., 2004), were consistently >0.16 and up to 0.57 in our record, suggesting considerable input of soil-derived GDGTs. Furthermore, we observed substantial amounts of terrestrial debris in the palynological slides, suggesting that the input of soil organic matter was relatively large on the Wilkes Land margin when compared to the amount of marine organic matter. Hence, we argue that, should any marine production of branched GDGTs have occurred, it is heavily diluted by the branched GDGTs that originated from Antarctic soils.

The processes involved in the transport from terrestrial soils to the Antarctic shelf imply that the MBT/CBT temperature signal yields an integration over a larger area and a larger time interval. However, as it has been described for Late Quaternary deglaciations (Weijers et al., 2007b) and the Palaeocene-Eocene Thermal Maximum in the Arctic Ocean (Weijers et al., 2007c), MBT/CBT records show in general no large temporal offsets (<1 kyr) when compared to other climate records.

In mid-latitude soils, branched GDGT production over a seasonal cycle does not show any seasonal pattern, but a seasonal bias could not be excluded (Weijers et al., 2011). Indeed, in the high latitudes, soil bacterial activity should theoretically increase strongly during the summer months. Thus, the MBT/CBT proxy potentially could be biased towards summer. The comparison of our MBT/CBT data with our seasonal pollen-based climate reconstructions from the Wilkes Land margin provides evidence for a warm-season bias in the MBT/CBT proxy when applied to high-latitude settings. They are in line with results from the Eocene of the Canadian Arctic, where a comparison of oxygen isotopes from biogenic phosphate with MBT/CBT data yielded a good correspondence of warmest month temperatures with the MBT/CBT proxy (Eberle et al., 2010).

2.4.4. Source area of terrestrial palynomorphs, biomarkers and GDGTs

The interpretation of the terrestrial palynomorph and biomarker record from Site U1356 depends critically on the origin of the material studied. Evidence from palynology and isotope geochemistry independently suggests that the vast majority of this material is derived from the Wilkes Land margin of Antarctica and its hinterland (rather than from other, lower-latitude landmasses or being reworked), thus providing direct insights into the vegetation and climate dynamics on the Antarctic mainland.

2.4.4.1 Palynological evidence

Terrestrial palynomorph records in marine sediments reflect the vegetation of adjacent landmasses. Factors influencing the transport and deposition of sporomorphs in marine sediments include the hydrodynamic properties of the sporomorphs, their resistance to degradation, and the transportation mechanisms, the latter mainly being aquatic (i.e., via runoff and surface-water currents) and/or eolian (Traverse, 2008). Although eolian transport is the prevalent transportation mechanism for pollen from arid environments with negligible fluvial activity (Traverse, 1994b), aquatic transport through rivers and surface-water currents is responsible for the majority of sporomorphs deposited in marine settings (Muller, 1959; Farley, 1987). The distance of Site U1356 to the Wilkes Land coastline during the Eocene was on the order of 300 km. A mid-shelfal location is suggested by the composition of dinocyst assemblages at Site U1356, which contain only low abundances of typically oceanic taxa such as *Cerebrocysta* spp. and *Impagidinium* spp. (Expedition 318 Scientists, 2011). In contrast, the direct distance to the South Australian Margin during that time amounted to ~1200 km; however, due to the clockwise nature of the Proto-Leeuwin Current that bathed the coasts of southern Australia, West Tasmania and the Wilkes Land sector of Antarctica during the early and middle Eocene (Sloan and Rea, 1996; Huber et al., 2004), any transport of material from southern Australia by surface-water currents would have had to occur over a considerably larger distance. Similarly, any source area on Tasmania would have required a transport over ~1200 km. In light of these transport trajectories, a major input from Australia and/or Tasmania to the assemblages at Site U1356 is highly unlikely. This is particularly true for pollen from insect-pollinated taxa such as Arecaceae (palms) and Bombacoideae. Such taxa are extremely underrepresented in the pollen rain owing to their low pollen production, which reduces their susceptibility to long-distance transport; this holds particularly true for megathermal forest environments (Kershaw and Hyland, 1975).

Additional palynological evidence against any long-distance transport from adjacent lower-latitude environments (notably Australia) comes from the composition of sporomorph assemblages. If the sporomorph assemblages from the Eocene of Site U1356 were the result of long-distance transport from southern Australia and/or Tasmania, their composition should mimic those of coeval sporomorph records from these regions. In southern Australia, micro- and megaflores of early and middle Eocene age are known from various locations (Stover and Evans, 1973; Stover and Partridge, 1973; MacPhail, 1999;

see compilations by Kemp, 1978; Martin, 1978; Macphail et al. 1994 and Greenwood et al. 2003). Because sporomorph percentage data are only available for selected taxa from the abovementioned studies, any evaluation of the similarities respectively differences between microfloras from southern Australia and Site U1356 has to be based on a taxon-by-taxon comparison rather than on numerical similarity indices. Although early Eocene sporomorph assemblages from southern Australia exhibit strong similarities to the early Eocene record from Site U1356, important differences exist. For instance, *Cupanieidites* spp., *Ilexpollenites* spp., and *Santalumidites* spp. are characteristic elements of early Eocene sporomorph assemblages of southern Australia (Macphail et al., 1994; Greenwood et al., 2003), but do not occur in the U1356 record. Middle Eocene sporomorph assemblages from southern Australia (notably the Gippsland Basin; Macphail et al., 1994) exhibit a strong dominance of *Nothofagidites* spp. (*brassii* group) types (50-60 %), whereas the mid-Eocene record of Site U1356 is dominated by *Nothofagidites* spp. (*fusca* group) types (38-68 %). Similarly, *Myricipites harrisii* reaches percentages of up to 30 % in southern Australia (Macphail et al., 1994), but only attains ~4 % at Site U1356. On the other hand, *Gambierina edwardsii* is consistently present in the Early and mid-Eocene assemblages of Site U1356, whereas in southern Australia this taxon become extinct in the earliest Eocene (Partridge, 1999). This mismatch not only highlights the difference between Eocene sporomorph assemblages of southern Australia and Site U1356, but also suggests that the parent plants of this taxon were able to survive on Antarctica into mid-Eocene times (Truswell and Macphail, 2009).

A Tasmanian source for the early Eocene sporomorph assemblages at Site U1356 can also be excluded. Early Eocene records from Tasmania exhibit a relatively low diversity, with a dominance of *Podocarpidites* spp., *Myricipites harrisii*, and *Nothofagidites* spp. (*brassii* group) (Macphail et al., 1994; Pole and Macphail, 1996). In contrast, the early Eocene record at Site U1356 represents a highly diverse angiosperm forest. Notably, percentages of *Nothofagidites* spp. (*brassii* group) are much lower (<5 %) than on Tasmania (~35 %), and *Nypa* pollen as encountered on Tasmania (Pole and Macphail, 1996) is not present.

The palynological assemblages from the early and mid-Eocene of Site U1356 contain numerous reworked pollen and spores of Palaeozoic (mainly Permian) and Mesozoic (Triassic, Jurassic and Cretaceous) age (Expedition 318 Scientists, 2011). Based on their relatively dark exine colours, which range from pale yellow to orange and brown, they can be reliably distinguished from contemporaneous Eocene material. The presence of these reworked elements is characteristic for circum-Antarctic marine sediments, including those off Wilkes Land (Truswell, 1983). Their abundances show a clear decrease with increasing distance from the Antarctic continent, which implies that they originate from Antarctica rather than from other landmasses (Truswell, 1983). Thus, their consistent presence in the Eocene record of Site U1356 further corroborates an Antarctic origin for the sporomorph assemblages.

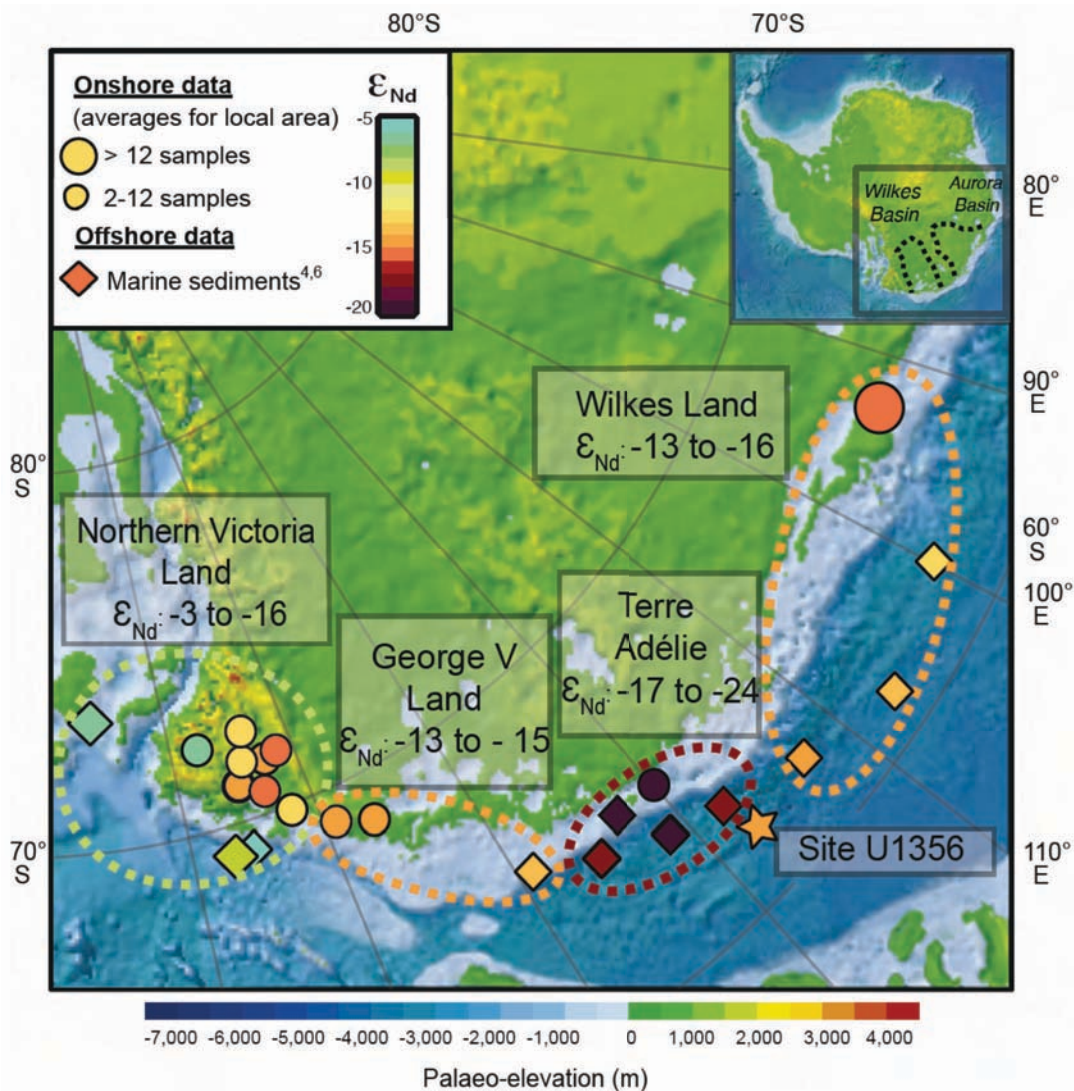
Laboratory contamination as a potential source of the sporomorphs from thermophilous taxa can be ruled out because (i) the palynological samples processing was carried out in

two palynological laboratories (Institute of Geosciences, Frankfurt University, and Laboratory of Palaeobotany and Palynology, Utrecht University), and the samples processed in both laboratories have consistently yielded thermophilous taxa in the Lower Eocene of Site U1356; (ii) the palynological laboratory in Frankfurt has been newly set up in 2008, and since then no material containing such taxa has been processed at this facility; (iii) the thermophilous sporomorphs encountered exhibit the same state of preservation and, based on their exine coloration (which is a sensitive indicator for the taphonomic/diagenetic history of sporomorphs; compare, e.g., Pross et al., 2007), have undergone the same taphonomic/diagenetic history as the other members of the sporomorph assemblages from the Lower Eocene of Site U1356.

2.4.4.2 Constraints on Eocene sediment source based on Nd isotope geochemistry

To further constrain the provenance of Eocene sediments from Site U1356, we analysed bulk sediment samples for their neodymium isotopic composition. ^{143}Nd is produced by the decay of radioactive ^{147}Sm , which results in variations in the $^{143}\text{Nd}/^{144}\text{Nd}$ in natural rocks dependent on their age and lithology. Since Sm/Nd ratios tend to behave conservatively during weathering and erosion, Nd isotopic compositions of detrital marine sediments are valuable indicators of the continental source area (e.g., Goldstein and Hemming, 2003).

Seven samples from the Eocene of Site U1356, representing major core lithologies between 910.77 and 997.57 mbsf, were subjected to flux fusion digestion on board of the research vessel JOIDES Resolution (Expedition 318 Scientists, 2011). Solutions were shipped back to Imperial College London, pre-concentrated with an iron co-precipitation step, and passed through a two-step column chemistry to separate Nd from the sample matrix. The rare earth elements (REEs) were separated from the sample matrix using 1M HNO_3 and 4M HCl on Tru Spec resin. Subsequently, Nd was separated from the other REEs using a modified procedure after Pin and Zalduegui (1997) with 0.2M HCl on Ln Spec resin. Neodymium isotope analyses were performed on the Imperial College London Nu Plasma multiple collector inductively coupled plasma mass spectrometer in static mode. A $^{146}\text{Nd}/^{144}\text{Nd}$ ratio of 0.7219 was applied to correct for instrumental mass bias using the exponential law. Tests with doped standards showed that interferences from ^{144}Sm can be adequately corrected, if the ^{144}Sm contribution is less than 0.1% of the ^{144}Nd signal. Interferences for all our samples were significantly below this level. Repeat analysis of the JNd_i isotopic standard during three measurement sessions yielded a precision of 0.3 to 0.4 epsilon units on $^{143}\text{Nd}/^{144}\text{Nd}$ (2s standard deviation; n = 7 to 16). All sample results were corrected relative to the accepted JNd_i $^{143}\text{Nd}/^{144}\text{Nd}$ ratio of 0.512115 (Tanaka et al., 2000). Parallel processing of two BCR-2 rock standards, which went through the same initial preparation steps as all samples on board the JOIDES Resolution, yielded values within error of the results reported by Weis et al. (2006). Procedural blank levels of < 300 pg were at least a factor of 1000 lower than the sample concentrations analysed and hence not significant.



Supplementary Figure S2.6. Neodymium isotopic compositions for Eastern Antarctica. Individual Nd isotopic compositions represent onland outcrops (circles) and marine sediment samples (predominantly core-tops; diamonds) (modified after Pierce et al., 2011). Eocene Antarctic topography is after Wilson et al. (2012), with early Eocene coordinates derived from the Ocean Drilling Stratigraphic Network following Hay et al. (1999). The colour coding reflects the modern Nd isotopic composition of samples, with the exception of Site U1356, where the colour coding reflects the early to mid-Eocene Nd isotopic composition. Sectors highlighted in circled areas are simplified provenance areas as derived from the combined insights from outcrop and sediment data (for further details see Pierce et al., 2011 and text).

Results show a range of ϵ_{Nd} values from -13.9 to -15.0 for Eocene bulk sediments with an average value of -14.4 ± 0.9 (2s standard deviation) (ϵ_{Nd} is defined as the deviation of a measured $^{143}Nd/^{144}Nd$ ratio from the chondritic value in parts per 10,000). Such values are typical for Proterozoic continental crust, which can be found in sparse outcrops along the East Antarctic margin (Fitzsimons, 2000). Where direct outcrops are missing, glaciogenic and terrestrial sediments can be used to infer the geology under the ice (Roy et al., 2007; Goodge and Fanning, 2010; Pierce et al., 2011). Following this approach, four broad geological source areas can be defined in the vicinity of Site U1356 (from east to west): (i) the high-elevation area of Northern Victoria Land ($\epsilon_{Nd} = -3$ to -16), (ii) the George V Land area, dominated by drainage from the Wilkes Basin ($\epsilon_{Nd} = -13$ to -15), (iii) the old cratonic area of Terre Adélie ($\epsilon_{Nd} = -17$ to -24), and (iv) the Proterozoic Wilkes Land margin,

dominated by drainage from the Aurora Basin ($\epsilon_{Nd} = -13$ to -16) (see Supplementary Figure S2.6 for references and further information). In light of these data, Eocene sediments at Site U1356 are tightly matched in their Nd isotopic composition by the George V Land and the Wilkes Land areas

2.4.5. Reconstruction of Antarctic palaeotopography for the early Eocene

Detail on Antarctic palaeotopography during the early Eocene is extremely limited, especially in East Antarctica where the crustal evolution is poorly known. There is geomorphological evidence that enhanced river incision occurred at this time in the Transantarctic Mountains, suggesting the climate experienced a wet phase (Baroni et al., 2005). Although such patterns are not identified in Wilkes Land due to a lack of bedrock exposure, modeling suggests that fluvial incision was dominant across the continent because the large-scale river networks are preserved under the ice at the present day (Jamieson and Sugden, 2008; Jamieson et al., 2010). The inference is that topography in much of Antarctica was probably higher than at present. Consequently, we use a recent reconstruction of palaeotopography for the Eocene-Oligocene boundary (Wilson et al., 2012) to infer a minimum elevation for the Wilkes Land region during the early Eocene. This is the best constrained pre-ice sheet reconstruction currently available for Antarctica because it employs offshore sediment volumes identified using coherent seismic reflectors and adjusted for changes in density to limit the amount of eroded material that is restored to the continent. The reconstructed landscape adjusts the present-day topography to account for evolution via glacial erosion, thermal subsidence, volcanic activity, rifting in the Ross Sea, and isostatic loading associated with the distribution of ice, sediment and water. The result is a palaeotopography that suggests parts of the present Wilkes Land basin may have been above sea level at the Eocene-Oligocene boundary. We interpret this topography as representing minimum elevations for early Eocene Wilkes Land.

2.4.6. Comparison with other Antarctic records of Eocene terrestrial environments

Current knowledge of the long-term terrestrial climate evolution of Antarctica through the Palaeogene is highly incomplete and based on reconstructions from a relatively small number of stratigraphically discontinuous records from around the Antarctic margin. Prior to recovery of the lower Eocene section in Hole U1356A during IODP Expedition 318, no reports of strata of equivalent age were available from the East Antarctic margin – neither from outcrop sections nor Antarctic shelf cores. Thus, there are no palaeobotanical datasets from East Antarctica to which we can directly compare our results from Site U1356. Previous studies, however, allow us to place the early Eocene terrestrial climate information derived from Site U1356 in the broader context of the long-term climate evolution of Antarctica through the Eocene.

In the Ross Sea, fossil evidence of middle–late Eocene coastal vegetation is preserved in displaced glacial erratic boulders deposited in moraines of the McMurdo Sound area at a palaeolatitude of $\sim 78^\circ\text{S}$ (Harwood and Levy, 2000). Fossil wood, leaves and sporomorphs

described from these erratics indicate the presence of cool-temperate rainforests in the coastal region and valleys along the Transantarctic Mountains during the middle–late Eocene that were dominated by shrubs and trees of Araucariaceae, Podocarpaceae and Nothofagaceae (Askin, 2000; Francis, 2000; Pole et al., 2000). A sporomorph assemblage with similar components is also documented in the latest Eocene interval of the nearby CIROS-1 drillhole (Mildenhall, 1989). On the other side of East Antarctica, in the Prydz Bay region, strata of middle–late Eocene age recovered at ODP Sites 742 and 1166 contain sporomorph assemblages that are also interpreted to indicate the presence of cool-temperate rain forests or rainforest scrub vegetation (Truswell, 1991; Macphail and Truswell, 2004). Gravity cores collected to the west of Prydz Bay on the Mac. Robertson Shelf containing material of late Palaeocene and middle–late Eocene age have also been recovered (Quilty et al., 1999), but the sporomorph assemblages from these cores have not been documented in detail. In summary, published palaeo-vegetation records from the East Antarctic margin do not span the entire Eocene interval. Currently available records from the Ross Sea and Prydz Bay are confined to the middle–late Eocene and are comparable with the 'mid-Eocene' sporomorph assemblages documented in Cores U1356A-100R to -96R. Notably, the early Eocene pollen assemblages of Cores U1356A-106R to -101R, which document the presence of near-tropical rainforests, stand out as being unique amongst all existing records from the East Antarctic margin.

A wealth of information on Eocene palaeo-vegetation is also available from the Antarctic Peninsula, but, as with records from East Antarctica, there are no well-dated sections that document the evolution of terrestrial environments from the peak of early Eocene warmth through the onset of middle–late Eocene cooling. Eocene fossil wood, leaf, and sporomorph assemblages have been described from both King George Island and Seymour Island (see summary in Francis et al., 2008). Outcrop exposures of the La Meseta Formation on Seymour Island, located on the eastern Weddell Sea side of the Antarctic Peninsula, have yielded extensive evidence for cool-temperate forests that became less diverse as climatic conditions cooled from the middle to late Eocene. Sporomorph assemblages from cores retrieved off Seymour Island and near the South Orkney Islands provide similar indications for cool-temperate forests in the middle–late Eocene (Mohr, 1990; 2001; Warny and Askin, 2011).

The age of the lowermost La Meseta Formation has been a subject of debate. Dinocyst biostratigraphy indicates a latest early Eocene-to-middle Eocene age (Wrenn and Hart, 1988; Coccozza and Clarke, 1992), whereas strontium isotope dating suggests an early Eocene age (Dutton et al., 2002; Ivany et al., 2008). Precise age determination using the strontium isotope method, however, is not possible in the lowermost stratigraphic units (TELMs 2–5) of the La Meseta Formation due to a large degree of scatter in strontium isotope values (compare Fig. 8 in Dutton et al., 2002) and the low-amplitude variability of the early-to-middle Eocene marine strontium isotope curve (McArthur and Howarth, 2004). Additionally, recent calibrations of dinocyst biostratigraphic events in Eocene drillcores recovered during ODP Leg 189 (Tasman Gateway) (Brinkhuis et al., 2003; Stickley et al., 2004a; Williams et al., 2004; Bijl, 2011; Bijl et al., 2011) provide a considerably more

refined age control than that available for earlier studies. The presence of the dinocyst taxa *Enneadocysta diktyostila* (presented in Cocozza and Clarke, 1992 as *Areosphaeridium* cf. *diktyoplokum*, but thereafter emended to *E. diktyostila*), *Arachnodinium antarcticum* and *Thalassiphora pelagica sensu stricto* throughout the section (Wrenn and Hart, 1988; Cocozza and Clarke, 1992) indicates an age of <46 Ma (Stickley et al., 2004a; Williams et al., 2004; Bijl, 2011; Bijl et al., 2011), suggesting that the La Meseta Formation is entirely middle-to-late Eocene in age. Thus, we conclude that there are no age-equivalent records of early Eocene vegetation from Seymour Island that we can compare with the Site U1356 record.

Numerous Eocene sections containing fossil wood and leaves have also been reported from King George Island, which is part of the South Shetland Islands in the northern region of the Antarctic Peninsula. These sections are poorly dated, constrained only to the late Palaeocene to late Eocene (see summary in Francis et al., 2008). The majority of the floral evidence from these deposits indicates cool-temperate forests dominated by *Nothofagus* species. One exception to this characterization is a diverse leaf and sporomorph assemblage from the Fossil Hill Formation on King George Island, which contains taxa affiliated with both subantarctic and tropical regimes (Cao, 1992; Li, 1992). The age of this section is broadly constrained to the late Palaeocene–middle Eocene, so it is unclear if and to what extent this assemblage is correlative to part of the early–middle Eocene record from Site U1356.

Truswell (1997) presented sporomorph assemblages from four samples taken from RV *Sonne* gravity core S36-22/SL off western Tasmania. Based on their sporomorph content, the samples are assigned to the upper part of the *Proteacidites asperopolus* zone of Stover and Partridge (1973), which is correlative to magnetochron C21 and therefore falls into the middle Eocene. The sporomorph assemblages from gravity core S36-22/SL are similar to those from the mid-Eocene of Site U1356 in that they lack tropical elements such as palms and Bombacoideae, but also contain considerable amounts of *Araucariacites* spp., *Nothofagidites* spp., *Cyathidites* spp., *Myricipites harrisii*, *Podocarpidites* spp., *Proteacidites* spp., and *Phyllocladidites mawsonii*. However, the diversity of the assemblages from core S36-22/SL is higher than in assemblages from the mid-Eocene of Site U1356 due to occurrences of taxa such as *Cupanieidites orthotheichus*, *Ilexpollenites* sp., *Liliacidites* spp., and *Myrtaceidites parvus* that are not recorded at Site U1356. Because of this diversity difference and the less pronounced dominances of temperate rainforest elements such as *Araucariacidites* spp. and *Nothofagidites* spp., the sporomorph assemblages from core S36-22/SL indicate slightly warmer conditions than those from the mid-Eocene of Site U1356, but markedly cooler conditions than those from the early Eocene of Site U1356.

Perhaps the most appropriate comparison for the early Eocene sporomorph record from Site U1356 is with plant-fossil assemblages from western Tasmania. Diverse early Eocene floral assemblages (mostly consisting of cuticles) are described from tidal estuary and freshwater deposits at Strahan-Regatta Point – a site approximately positioned at ~66°S at

that time (Pole, 2007). They provide evidence of mesothermal rainforests with MATs between 12 and 20 °C, but also contain *Nypa* mangrove palms and a species of Rhizophoraceae with affinities to extant mangroves (Pole, 2007). Recently, Carpenter et al. (2012) published megafloral and palynological evidence for terrestrial MATs of ~24 °C from the Lowana Road outcrop section on Tasmania (palaeolatitude: ~65 °S). The maximum age of the Lowana Road fossils is ~53 Myr; its minimum age is less well constrained, but estimated at ~52 Myr based on a combination of presence/absence data from dinocysts and pollen. These findings make the Lowana Road fossils partially age-equivalent to the early Eocene assemblages from the Wilkes Land margin of Antarctica. Hence, these data from relatively high southern latitudes – although not representing climate conditions on Antarctica – provide confirmation that the surprisingly warm climatic estimates derived for the peak of the EECO for the Wilkes Land margin of Antarctica are realistic.

2.4.7. Remarks on Sporomorph Taxa

Key sporomorph taxa from the Eocene of Site U1356 are discussed below, with selected forms presented in Supplementary Figure S2.7.

Anacolosidites luteoides Cookson and Pike 1954

Remarks: This distinctive species is here recorded in the lower Eocene of Site U1356, which constitutes the first record of this taxon for Antarctica. The taxon has been previously described from the Palaeogene of New Zealand (Raine et al., 2008) and the lower and middle Eocene of Australia (Stover and Partridge, 1973).

Botanical affinity: *Anacolosa* (Olacaceae) (Raine et al., 2008).

Modern distribution: Tropics and southern Africa (Macphail et al., 1994).

Genus *Araucariacites* Cookson ex Couper 1953

Remarks: This genus occurs commonly in the early and mid-Eocene interval of Site U1356.

Botanical affinity: *Araucaria* and *Agathis* (Araucariaceae) (Raine et al., 2008).

Modern distribution: Southern hemisphere (Hill, 1994).

Genus *Arecipites* Wodehouse 1933 emend. Nichols et al. 1973

Remarks: The genus *Arecipites* includes monosulcate pollen grains with a sulcus tapered at the ends and an exine with a tectate structure. These forms may exhibit columellae in optical section. The exine can be psilate, scabrate, pitted or scrobiculate, but forms with true reticulate sculpture are not included within the genus (Nichols et al., 1973).

Cycadopites includes monosulcate pollen grains with a sulcus extending along the full length of the grain. *Arecipites* differs from *Cycadopites* in that members of the former have a sulcus that is open at the ends (Nichols et al., 1973; Jansonius et al., 1998), and they lack any structure within the exine (e.g., Nichols et al., 1973). *Arecipites* spp. at Site U1356 include pollen grains mainly attributable to *A. pseudotranquillus* and *A. punctatus*

following Nichols et al. (1973). Pollen grains with characteristic morphological features of the genus *Arecipites* occur consistently, albeit in low numbers in the lower Eocene of Site U1356, representing the first record of this taxon for Antarctica.

Botanical affinity: Palms (Arecaceae) (Nichols et al., 1973).

Modern distribution: Tropical to warm temperate regions (Macphail et al., 1994).

Bluffopollis scabratus (Couper 1954) Pocknall and Mildenhall 1984

Remarks: The occurrence of this distinctive species in the lower Eocene of Site U1356 represents the first record of this taxon for Antarctica. Previously identified occurrences include the Palaeocene? to Miocene of southern Australia (Jarzen and Pocknall, 1984), and the Palaeogene and Neogene of New Zealand (Raine et al., 2008).

Botanical affinity: *Strasburgeria* (Jarzen and Pocknall, 1984).

Modern distribution: New Caledonia (Macphail et al., 1994).

Genus ***Bombacacidites*** Couper 1960 emend. Krutzsch 1970

Remarks: The genus *Bombacacidites* has been proposed for fossil pollen grains with the typical morphological characteristics of the extant family Bombacaceae. *Bombacacidites* has a distinct columellate layer and lacks a post-vestibulum (endexine interlamellarly split) as it is characteristic of the genus *Intratropipollenites* (Jansonius and Hills, 1976).

***Bombacacidites* sp. A**

Diagnosis: *Bombacacidites* type, mid-sized (~40 µm), amb subcircular, brevitricolporate, costae 2-4 µm wide, exine 1-2 µm thick, semitectate, reticulate, luminae 1-2 µm wide.

Remarks: Some specimens of *Bombacacidites* sp. A are similar to *Intratropipollenites notabilis* of Stover and Evans (Stover and Evans, 1973). Although a detailed description of the apertures is not available, the illustration of *I. notabilis* by Stover and Evans (1973) (Plate 3, Fig. 4) suggests the presence of a vestibulum (or fastigium, if the grain is brevitricolporate). Specimens of *Bombacacidites* sp. A occur in the lower Eocene of Site U1356, which constitutes the first Cenozoic record of *Bombacacidites* on Antarctica.

Botanical affinity: Malvaceae, subfamily Bombacoideae *sensu* Bayer and Kubitzki (2003).

Bombacacidites sp. A is similar to pollen from extant taxa such as *Bombax globosum*, *Cavanillesia arborea* and *Ochroma pyramidale* (Roubik and Moreno, 1991; Bush and Rivera, 1998; Members, 2007). *Bombax* and *Cavanillesia* are well nested within the subfamily Bombacoideae, while *Ochroma* has unresolved phylogenetic relations, but is consistently basal to both the Malvoideae and Bombacoideae subfamilies (Duarte et al., 2011).

Modern distribution: Neotropics, with some species occurring in the Old World tropics (Bayer and Kubitzki, 2003).

Genus ***Cyathidites*** Couper 1953

Remarks: Specimens grouped within the fossil genus *Cyathidites* comprise laevigate and simple trilete spores. In the present study, they were subdivided into three informal groups based on size: *Cyathidites* spp. <25 µm; *Cyathididites* spp. 25 to 50 µm (mainly *C. minor*); *Cyathididites* spp. >50 µm (mainly *C. australis*).

Botanical affinity: Probably Cyatheaceae (Mohr, 2001), but also possibly other fern families such as Pteridaceae.

Modern Distribution: The family Cyatheaceae is geographically widespread, but occurs mainly in tropical and warm temperate regions (Macphail et al., 1994).

Crassoretiriletes vanraadshooveni Germeraad et al. 1968

Botanical affinity: *Lygodium* (Germeraad et al., 1968).

Modern distribution: Tropical to warm temperate regions, including Indo-Malaysia and Australia (Macphail et al., 1994).

Dilwynites granulatus Harris 1965

Remarks: This specie occurs commonly in the lower and mid-Eocene of Site U1356. It is distinguished from *Araucariacites australis* by its relatively coarse, granulate ornamentation (Truswell and Macphail, 2009).

Botanical affinity: *Wollemia* (Araucariaceae) (Dettmann and Jarzen, 2000).

Modern distribution: Restricted to southeastern Australia (Jones et al., 1995).

Gambierina edwardsii (Cookson and Pike 1954) Harris 1972

Remarks: Specimens of *G. edwardsii* occur in the lower and mid-Eocene of Site U1356. *Gambierina edwardsii* and *G. rudata* became extinct in southeastern Australia during the earliest Eocene, while their stratigraphic ranges in New Zealand are Palaeogene to Early Eocene and Late Cretaceous to Palaeocene, respectively (Wanntorp et al., 2011).

Botanical affinity: Unknown.

Genus ***Malvacipollis*** Harris 1965

Remarks: Specimens here attributed to *Malvacipollis* spp. correspond mainly to *Malvacipollis diversus* and *Malvacipollis subtilis sensu* Stover and Partridge (1973).

Botanical affinity: Euphorbiaceae (genera *Austrobuxus* and *Dissiliaria*; Martin, 1974) and possibly Eumalvoideae (Raine et al., 2008).

Modern distribution: *Austrobuxus* and *Disillaria*: Southwest Pacific region (Martin, 1974); Eumalvoideae: Subtropics to temperate regions (Baum et al., 2004).

Myricipites harrisii (Couper 1953) Dutta and Sah 1970

Botanical affinity: Casuarinaceae, possibly also Myricaceae (Raine et al., 2008). Modern distribution: Casuarinaceae: Indo-Malaysia and Australia (Macphail et al., 1994); Myricaceae: mainly tropics, but also Northwest Europe (Punt et al., 2002).

Genus ***Nothofagidites*** Potonié 1960

Remarks: Specimens belonging to the fossil genus *Nothofagidites* have been assigned to four main complexes following Macphail et al. (1994) and Truswell and Macphail (2009). These are: *Nothofagidites asperus* complex, *Nothofagidites lachlaniae* complex, *Nothofagidites flemingii* complex, and *Nothofagidites* spp. cf. *N. emarcidus* complex.

Botanical affinity: *Nothofagidites asperus* complex: *Nothofagus*, subgenus *Lophozonia*; *Nothofagidites lachlaniae* complex: *Nothofagus*, subgenus *Fuscospora*; *Nothofagidites*

flemingii complex: *Nothofagus*, subgenus *Nothofagus*. *Nothofagidites emarcidus* is related to the extant subgenus *Brassospora*, although Truswell and Macphail (2009) suggest that some specimens assigned to *Nothofagidites* spp. cf. *N. emarcidus* may represent immature pollen grains of other taxa. The *Nothofagidites lachlaniae* complex and the *Nothofagidites flemingii* complex are often referred to as *fusca* type.

Modern distribution: *Lophozonia*: Eastern Australia, New Zealand and South America; *Fuscospora*: Tasmania, New Zealand and South America (Macphail et al., 1994).

Genus ***Proteacidites*** Cookson 1950

Remarks: *Proteacidites* represents one of the most common and diverse angiosperm pollen genera in the Cretaceous and Cenozoic of the Southern Hemisphere (Sauquet and Cantrill, 2007). For the Eocene of Site U1356, 28 morphotypes belonging to the genus *Proteacidites* were identified.

Botanical affinity: Proteaceae. Some *Proteacidites* morphotypes from Site U1356 can be linked to extant genera (compare Supplementary Table S2.1).

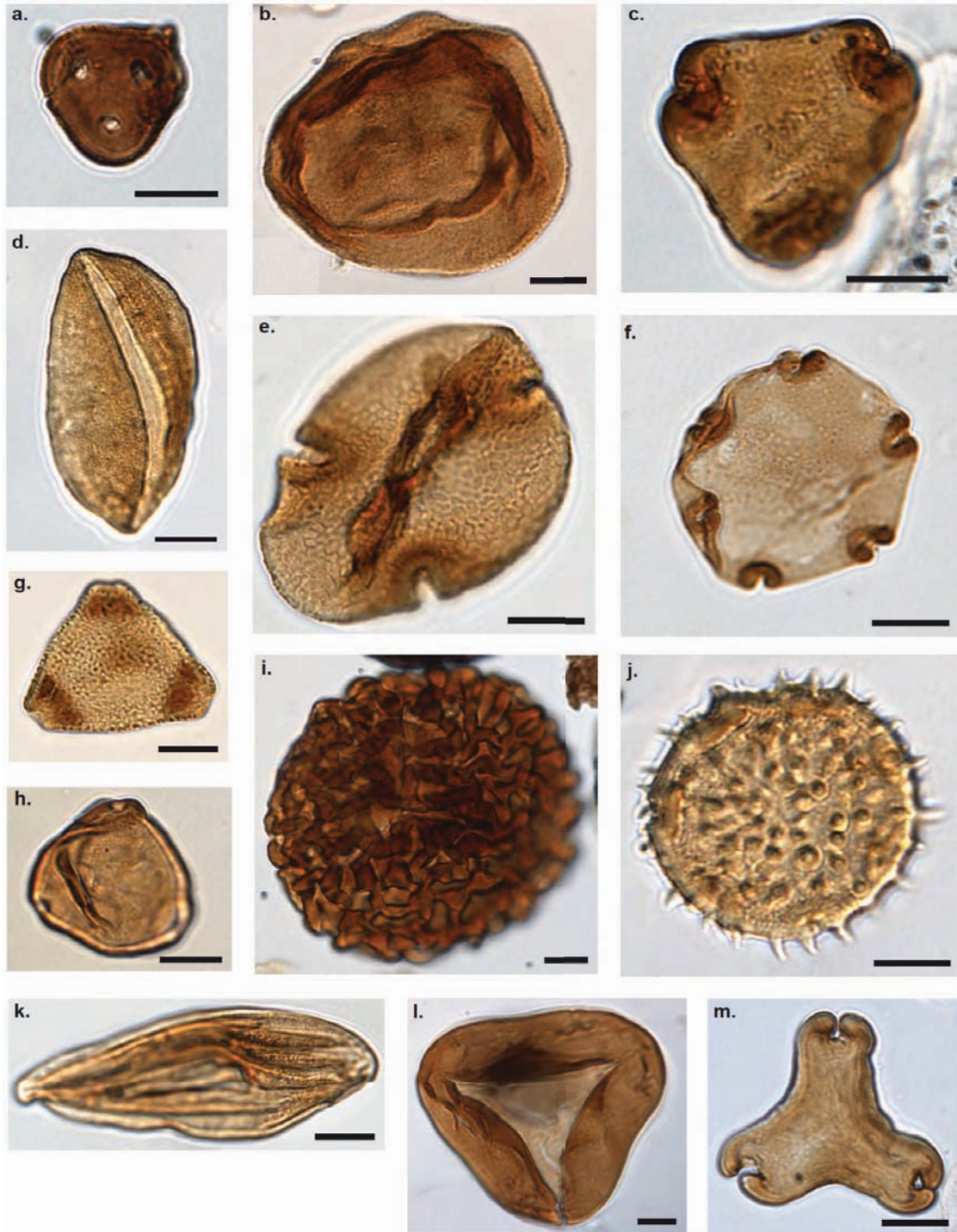
Modern distribution: Tropical to temperate regions of the southern hemisphere (Sauquet and Cantrill, 2007).

Spathiphyllum type *sensu* Muller (1981)

Remarks: The exposed endexine between the ribs, the presence of a columellate infratectum and narrow ribs allow to differentiate members of the genus *Spathiphyllum* from the genus *Ephedripites* (see Hesse and Zetter, 2007, for details).

Botanical affinity: *Spathiphyllum* (Araceae).

Modern distribution: Tropics (Govaerts and Frodin, 2002).



Supplementary Figure S2.7. Photomicrographs of key sporomorph taxa from the Eocene of IODP Site U1356. (a) *Anacolisidites luteoides* (*Anacolosa*); (b) *Araucariacites australis* (*Araucariaceae*); (c) *Bluffopollis scabratus* (*Strasburgeria*); (d) *Arecipites punctatus* (*Arecaceae*, palms); (e) *Bombacacidites* sp. A (*Bombacoideae*); (f) *Nothofagidites flemingii* (*Nothofagus*, *fusca* type); (g) *Proteacidites reticulosabratus* (*Proteaceae*); (h) *Myricipites harrisii* (*Casuarinaceae/Myricaceae*); (i) *Crassoretitriletes vanraadshooveni* (*Lygodium*); (j) *Malvacipollis* cf. *diversus* (*Euphorbiaceae*, *Eumalvoideae*); (k) *Spathiphyllum* sp. (*Spathiphyllum*); (l) *Cyathidites australis* (*Cyatheaceae*); (m) *Gambierina edwardsii*. Scale bars: 10 μ m.

Chapter 3. Early to Middle Eocene vegetation dynamics at the Wilkes Land Margin (Antarctica)

Lineth Contreras^{1,2}, Jörg Pross^{1,2}, Peter K. Bijl³, Andreas Koutsodendris¹, J. Ian Raine⁴, Bas van de Schootbrugge¹, Henk Brinkhuis^{3,5}

¹Paleoenvironmental Dynamics Group, Institute of Geosciences, Goethe University Frankfurt, Altenhöferallee 1, 60438 Frankfurt, Germany. ²Biodiversity and Climate Research Centre, Senckenberganlage 25, 60325 Frankfurt, Germany. ³Department of Earth Sciences, Faculty of Geosciences, Utrecht University. Laboratory of Palaeobotany and Palynology, Budapestlaan 4, 3584 CD Utrecht, The Netherlands. ⁴Department of Palaeontology, GNS Science, PO Box 30368, Lower Hutt 6009, New Zealand. ⁵NIOZ Royal Netherlands Institute for Sea Research, P.O. Box 59, 1790 AB Den Burg, Texel, The Netherlands.

*Published in Review of Palaeobotany and Palynology 197, 119-142**

Abstract

The early Eocene epoch was characterized by extreme global warmth, which in terrestrial settings was characterized by an expansion of near-tropical vegetation belts into the high latitudes. During the middle to late Eocene, global cooling caused the retreat of tropical vegetation to lower latitudes. In high-latitude settings, near-tropical vegetation was replaced by temperate floras. This floral change has recently been traced as far south as Antarctica, where along the Wilkes Land margin paratropical forests thrived during the early Eocene and temperate *Nothofagus* forests developed during the middle Eocene. Here we provide both qualitative and quantitative palynological data for this floral turnover based on a sporomorph record recovered at Integrated Ocean Drilling Program (IODP) Site U1356 off the Wilkes Land margin. Following the nearest living relative concept and based on a comparison with modern vegetation types, we examine the structure and diversity patterns of the Eocene vegetation along the Wilkes Land margin. Our results indicate that the early Eocene forests along the Wilkes Land margin were characterized by a diverse canopy composed of plants that today occur in tropical settings; their richness pattern was similar to that of present-day forests from New Caledonia. The middle Eocene forests were characterized by a canopy dominated by *Nothofagus* and exhibited richness patterns similar to modern *Nothofagus* forests from New Zealand.

* Appendix 1 Taxonomy Site U1356 belongs to this chapter and is also published in Review of Palaeobotany and Palynology 197, 119-142

3.1 Introduction

Characterized by very low equator-to-pole temperature gradients and global warmth extending into polar regions, the Eocene represents the most recent epoch of extreme greenhouse conditions (e.g., Zachos et al., 2001; 2008; Bijl et al., 2009; Huber and Caballero, 2011). Eocene warmth peaked during the Early Eocene Climatic Optimum (EECO; 51 – 53 Ma), followed by high-latitude cooling through the middle and late Eocene (e.g., Miller et al., 1987; Zachos et al., 2001; 2008). The final step of this global cooling occurred around Eocene-Oligocene times when continental ice sheets rapidly expanded across Antarctica and global icehouse conditions started to develop (e.g., Zachos et al., 1994; 2001; 2008; Barrett, 1996).

The extreme greenhouse warmth during the EECO facilitated the expansion of tropical to subtropical vegetation belts into polar latitudes. For the Arctic, macrofloral remains document the existence of forests during the early Eocene similar to the present-day swamp-cypress and broadleaf floodplain vegetation in southeastern North America (e.g., Eberle and Greenwood, 2011, and references therein). In the southern high latitudes, early Eocene paleobotanical records from South Australia, Tasmania and New Zealand reflect the presence of broadleaf paratropical vegetation, notably including records of the mangrove palm *Nypa* (Kemp, 1978; Macphail et al., 1994; Greenwood et al., 2003; Raine et al., 2009; Carpenter et al., 2012). Coeval floras from central Patagonia and central Chile were highly diverse, including taxa with a mainly tropical distribution such as Lauraceae and *Annona* (e.g., Gayó et al., 2005; Wilf et al., 2005). In contrast, middle Eocene vegetation was characterized by the expansion of temperate *Nothofagus*-conifer forests in New Zealand, Australia, Chile, and Argentina (e.g., Kemp, 1978; Macphail et al., 1994; Hinojosa and Villagran, 1997; Greenwood et al., 2003; Barreda and Palazzesi, 2007).

On the Antarctic continent, paratropical rainforests thrived along the Wilkes Land margin during the early Eocene; during the middle Eocene, they were replaced by temperate *Nothofagus*-dominated rainforests (Pross et al., 2012). The presence of *Nothofagus*-dominated forests is also documented for the middle and late Eocene on the Antarctic Peninsula (Francis et al., 2008; Warny and Askin, 2011) and East Antarctica (Askin, 2000; Francis, 2000; Pole et al., 2000; Macphail and Truswell, 2004; Truswell and Macphail, 2009); towards the Oligocene, increasingly cooler conditions resulted in a herb-moss tundra vegetation that was fully developed by Miocene times (Askin and Raine, 2000; Lewis et al., 2008; Truswell and Macphail, 2009; Anderson et al., 2011).

Qualitative and quantitative analyses of fossil sporomorph assemblages have been widely applied to decipher vegetation dynamics during the Paleogene (e.g., Harrington, 2001; Wing and Harrington, 2001; Crouch and Visscher, 2003; Wing et al., 2003; Jaramillo et al., 2010). The qualitative approach is used to decipher the structure of past vegetation communities considering the physiognomies of present-day ecosystems (Specht et al., 1992). It is based on the notion that the physical characteristics of vegetation developing under similar climates in widely separated geographical regions are highly similar

irrespective of the number of common taxa (e.g., Wolfe, 1978; Woodward, 1987; Prentice et al., 1992; Woodward et al., 2004).

The quantitative approach assesses the diversity and composition patterns of vegetation records (e.g., Jaramillo, 2002; Harrington, 2004; Jardine and Harrington, 2008). This approach allows interpretation of ancient vegetation dynamics by means of modern ecological criteria. The application of species accumulation curves has, for instance, revealed that early Eocene Arctic ecosystems comprised forests with a richness similar to that found in Holocene forests from southeastern North America (Harrington et al., 2012). Although combined qualitative and quantitative analyses have become available for high-latitude Eocene sporomorph datasets from the Northern Hemisphere (e.g., Harrington, 2001; Wing and Harrington, 2001; Harrington and Jaramillo, 2007), this approach has not yet been applied to Paleogene pollen records from the Southern Hemisphere.

In light of the above, we here characterize the early to middle Eocene vegetation along the Wilkes Land margin of Antarctica based on sporomorph assemblages recovered from IODP Site U1356. Besides documenting the stratigraphic distribution of the sporomorph taxa in the Site U1356 record, we describe selected taxa through photomicrographs and taxonomical remarks. Moreover, we investigate the vegetation structure along the Wilkes Land margin based on the ecological requirements and habitats of the known living relatives of Eocene taxa. In addition, we use quantitative methods (rarefaction, diversity indices and Detrended Correspondence Analysis) to describe the diversity and composition of these ancient forests. Finally, we compare the species richness patterns of the Eocene vegetation from the Wilkes Land margin to those characterizing the vegetation at selected tropical and temperate sites in New Caledonia and New Zealand during the late Holocene.

3.2 Study site

The early to middle Eocene sporomorph-bearing strata studied here were recovered at IODP Site U1356, which is located off the Wilkes Land coast (63°19'S, 168°49'E) of Antarctica at the transition between the continental rise and the abyssal plain (Expedition 318 Scientists, 2011). This site has evolved into a key location for deciphering the paleoclimatic evolution of the high southern latitudes during the Paleocene (Pross et al., 2012; Bijl et al., 2013a; Houben et al., 2013; Passchier et al., 2013). The paleolatitudes of Wilkes Land and Site U1356 are nearly identical to the present-day positions, which implies that the Wilkes Land margin was subject to polar darkness for about 50 days per year. The distance of Site U1356 to the paleo-shoreline during the Eocene was on the order of 300 km (Pross et al., 2012).

The age control of the Eocene strata at Site U1356 is based on the integration of magnetostratigraphic and dinoflagellate cyst-based biostratigraphic data. The Eocene sedimentary sequence recovered dates back to early Eocene times (53.9 – 51.9 Myr); it is separated from latest early Eocene to middle Eocene (49.3 – 46 Myr; here informally referred to as “mid-Eocene”) strata by a ~3 Myr-long hiatus (Pross et al., 2012; Tauxe et al., 2012). Lithologically, the early Eocene succession consists of bioturbated claystones with intercalated fine sandstone beds. The mid-Eocene succession is characterized by

interbedded sandstones, diamictites, silty claystones, and siltstones (Expedition 318 Scientists, 2011).

3.2.1 Constraints on sporomorph source area

Several lines of paleoceanographical, palynological and isotope geochemical evidence suggest that the Eocene sporomorphs recovered at Site U1356 are primarily derived from the Wilkes Land margin rather than from other, lower-latitude landmasses (compare also Pross et al., 2012, and Supplementary Information accompanying that paper for an in-depth discussion). The transport and deposition of sporomorphs in the marine realm depends on the hydrodynamic characteristics of the sporomorphs, their resistance to degradation, and the transportation mechanisms, which can be aquatic (i.e., through runoff and surface-water currents) and/or eolian (Traverse, 2008). Whereas sporomorphs from arid settings are mainly transported via atmospheric processes (Traverse, 1994b), aquatic transport through fluvial activity and surface-water currents is responsible for the majority of sporomorphs deposited in marine settings (Muller, 1959; Farley, 1987). Whereas the distance of Site U1356 to the Wilkes Land coast during the Eocene was only ~300 km, the direct distance to the coast of South Australia amounted to ~1200 km; however, due to the clockwise-flowing Proto-Leeuwin Current that bathed the coasts of South Australia, western Tasmania and Wilkes Land during the early and middle Eocene (Sloan and Rea, 1996; Huber et al., 2004; Bijl et al., 2011), the surface-water transport of sporomorphs from southern Australia would have required an even larger distance.

Similarly, any source area of sporomorphs on western Tasmania would have required a surface-water transport over ~1200 km (Pross et al., 2012). Hence, an input from Australia and/or Tasmania to the sporomorph assemblages at Site U1356 is highly unlikely. This holds particularly true for insect-pollinated canopy species of rain forests; the fact that they are strongly underrepresented in the pollen spectra of tropical forests (Bush and Rivera, 1998) further reduces their susceptibility to long-distance transport. In line with these considerations, remarkable differences exist between the Eocene sporomorph records of Site U1356 and coeval records from Southern Australia (see compilations by Kemp, 1978; Martin, 1978; Macphail et al., 1994; Greenwood et al., 2003) and western Tasmania (Pole and Macphail, 1996; Truswell, 1997; Carpenter et al., 2012). Because percentage data are only available for few sporomorph taxa in the studies cited above, similarities and differences between sporomorph assemblages from southern Australia and Site U1356 have to be evaluated through a taxon-by-taxon comparison rather than via numerical similarity indices (compare also Supplementary Information of Pross et al., 2012). Although early Eocene sporomorph spectra from southern Australia are strongly similar to those from the Eocene of Site U1356, important differences exist. For example, *Cupanieidites* spp., *Ilexpollenites* spp., and *Santalumidites* spp. do not occur in early Eocene strata from Site U1356, but are typical of coeval sporomorph spectra from southern Australia (Macphail et al., 1994; Greenwood et al., 2003). Whereas the mid-Eocene sporomorph spectra from Site U1356 are dominated by *Nothofagidites* spp. (*fusca* group) types, their middle Eocene counterparts from southern Australia (e.g., Macphail et al., 1994) show a dominance of *Nothofagidites* spp. (*brassii* group) types. *Myricipites harrisii* only reaches ~4 % at Site U1356, but attains up to 30 % in southern Australia (Macphail et al., 1994).

Tasmania can also be excluded as a source region for the early Eocene sporomorphs from Site U1356. Early Eocene sporomorph spectra from Tasmania are of relatively low

diversity and are dominated by *Podocarpidites* spp., *Myricipites harrisii*, and *Nothofagidites* spp. (*brassii* group) (Macphail et al., 1994; Pole and Macphail, 1996). In contrast, the early Eocene sporomorphs from Site U1356 are highly diverse. In particular, *Nypa* pollen as occurring on Tasmania (Pole and Macphail, 1996) is not present, and percentages of *Nothofagidites* spp. (*brassii* group) are markedly lower (<5 %) than on Tasmania (~35 %).

Independent support for an Antarctic provenance comes from the Neodymium isotopic composition of the Eocene sediments at Site U1356. Neodymium isotope ratios are valuable indicators of the continental source areas of detrital marine sediments (e.g., Goldstein and Hemming, 2003). Neodymium data from Eastern Antarctica exhibit a tight match between the Eocene sediments at Site U1356 and those from the George V Land and Wilkes Land areas, thus suggesting that the main sediment input to Site U1356 during the Eocene was from the Wilkes Land margin (see Supplementary Information of Pross et al., 2012, for details).

In a more general sense, near-tropical conditions must have prevailed along the Wilkes Land margin during the early Eocene in order to facilitate the growth of many of the plants that are reflected by the Site U1356 sporomorph record and are being portrayed in this paper. Evidence for such climate conditions comes from three biotic and organic geochemical proxy records that are completely independent from the sporomorph assemblages as well as from recent climate modeling (Huber and Caballero, 2011), the biogeography of palms (Trénel et al., 2007) and other megathermal plants (Bartish et al., 2011), and dated molecular palm phylogenies (Baker and Couvreur, 2013). The proxy records comprise organic geochemical terrestrial (MBT/CBT; Pross et al., 2012) and marine (TEX₈₆) paleothermometry (Bijl et al., 2013a), and mass occurrences of the tropical dinoflagellate cyst genus *Apectodinium* (Bijl et al., 2013a). They consistently indicate that the climatic boundary conditions along the Wilkes Land margin during the early Eocene were favourable for the development of a paratropical vegetation as evidenced by the Site U1356 sporomorph record and as discussed in the following.

3.3 Methods

In total, 145 samples from the Lower and mid-Eocene of Site U1356 were analyzed for their sporomorph assemblages. The samples are from clay- and siltstones. They were processed following standard palynological techniques including drying, weighting, treatment with HCl (10%) and HF (38%), and sieving through a 10µm nylon mesh. Separation of heavier particles was carried out in an ultrasonic bath, and slide preparations were made using glycerine jelly as a mounting medium. Whenever possible, 300 sporomorphs were determined per sample using a Zeiss Axioskop light microscope at 200x magnification; morphological details of sporomorphs were investigated using a magnification of 1000x. Reworked sporomorphs (e.g., Appendix 1, Plate VIII), which are mainly from the Permian, Triassic and Cretaceous, were excluded from the counting sums; they could be readily identified based on their relatively dark colors and their stratigraphic ranges as described by Dettmann (1963), Helby et al. (1987) and Raine et al. (2008). The determination and taxonomical classification of sporomorphs were carried out following Couper (1960), Harris (1965), Truswell (1983), Raine et al. (2008), and Truswell and

Macphail (2009); botanical affinities were established after Macphail et al. (1994), Raine (1998), APSA Members (2007) and Truswell and Macphail (2009).

To quantitatively analyse the Eocene sporomorph assemblages of Site U1356, six different techniques were employed:

(i) Detrended Correspondence Analysis (DCA), a multivariate statistical technique, was applied to evaluate the overall variation in floral composition. This method is based on the principles of the correspondence analysis that summarizes variation in the composition of the assemblages in a small number of dimensions. DCA was developed to suppress the curvature of straight gradients and because distances in the ordination space do not have a consistent meaning in terms of compositional change (Hill and Gauch, 1980). Due to the different sample sizes, relative sporomorph abundance data were used as an input to perform the DCA, and only samples with counts ≥ 100 individuals were used for the calculations.

(ii) Sander's rarefaction, an interpolation technique, was used to estimate the number of sporomorph species at a constant sample size. This method is derived from an analysis of the relative frequencies of specimens within species (Raup, 1975).

(iii) Species accumulation curves allowing a valid richness comparison between different datasets. The sample-based taxon resampling curves are generated based on random permutations (without replacement) that find the species richness for certain number of pooled samples (Gotelli and Colwell, 2001). The extrapolated exact (mean) richness is based on the estimator Chao ($S_P = S_0 + a1^2/(2*a2)$), where S_P is the extrapolated richness in a pool, S_0 is the observed number of species in the collection, and $a1$ and $a2$ are the number of species occurring only in one or only in two sites in the collection (Oksanen et al., 2011).

(iv) The Shannon index ($H = -\sum p_n \log_{10} p_n$, with p_n = proportion of individuals that belong to species n) was calculated as a measure of species diversity. When H is 0 (minimum value), the sampling unit contains one single species; H increases with the number of species and reaches its maximum when the individuals are equally distributed among the species; it is lower when there is a strong dominance by one or few species (Legendre and Legendre, 1998). Only samples with counts ≥ 100 individuals were used for the calculations.

(v) Evenness ($J = H/H_{max}$) was calculated as a measure of the abundance distribution of a population. When $J = 1$, all species have the same number of individuals. A low value indicates that most of the assemblage is dominated by only few species (Hayek and Buzas, 2010).

(vi) A parametric statistic t-test was carried out to assess the differences in the floral composition and diversity between the early and mid-Eocene sporomorph assemblages.

All analyses were performed using the software R for statistical computing (R Development Core Team, 2011) and the package Vegan (Oksanen et al., 2011). All sporomorph data and numerical results (along with the respective R code) for Site U1356, are permanently archived and accessible at PANGAEA database (www.pangaea.de; doi:10.1594/PANGAEA.810464; see also supplementary file `supplemdataU1356.xlsx`).

To compare the richness of the Eocene sporomorph assemblages from Site U1356 to that of modern vegetation types, species accumulation curves were generated for two Holocene sporomorph records from sites with similar climate conditions with regard to mean annual temperature, (MAT), mean winter and summer temperatures (MWT and MST), and mean annual precipitation (MAP) as those previously reconstructed for the early and mid-Eocene of the Wilkes Land margin by Pross et al. (2012; compare Table 3.1). Moreover, the similarity of the climatic conditions between the modern sites and the paleoclimatic conditions for the early and middle Eocene records yield insights into the physiognomy of ancient forests. In this respect, we follow the concept that the physical characteristics of a vegetation growing under similar climatic conditions are highly similar irrespective of their floral composition (e.g., Wolfe, 1978; Woodward, 1987; Prentice et al., 1992; Woodward et al., 2004).

The most direct approach to compare the Eocene sporomorph assemblages from Site U1356 to recent counterparts would be to utilize (sub-)tropical pollen records of Holocene age from directly comparable marine depositional settings. However, no such records exist from regions with climate conditions closely similar to those reconstructed for the early and mid-Eocene of the Wilkes Land margin. As a basis for a comparison with Holocene assemblages representing comparable climate conditions, we therefore selected terrestrial sporomorph records. With regard to a comparison of species richness patterns, this approach is justified based on the fact that the selective process of the sporomorph transport into marine depositional settings decreases rather than increases the diversity of sporomorph types when compared to adjacent terrestrial sites (Moss et al., 2005). This implies that the sporomorph richness at Site U1356 can only be lower, but not higher than at archives from the adjacent terrestrial catchment area.

For a comparison with the early Eocene sporomorph assemblages from Site U1356, we used previously published late Holocene (~6.0 kyr BP) sporomorph data from the Plum Swamp locality (Core 2 of Stevenson et al. 2001), which is located in a lowland setting at 10 m above sea level (a.s.l.) on the southwest coast of New Caledonia (22°16' S, 166°37' E; Fig. 3.1). The sporomorph assemblages from the Plum Swamp core are characterized by, in the order of decreasing abundances, Casuarinaceae, *Pandanus* (Pandanaceae), *Macaranga* (Euphorbiaceae), Poaceae, Myrtaceae, and *Araucaria* (Stevenson et al., 2001). Based on the sporomorph assemblages, the Plum Swamp area was surrounded by littoral forests and lowland rainforest until ~3.0 kyr BP (Stevenson et al., 2001). The present-day distribution of montane and lowland settings in New Caledonia is comparable with the Eocene paleotopography as reconstructed for the Wilkes Land margin of Antarctica by Wilson et al. (2012). To achieve maximum comparability between the sporomorph records

from the Lower Eocene of Site U1356 and Plum Swamp, taxa that are strongly overrepresented in the pollen rain and predominantly mirror the local vegetation at the Plum Swamp locality (i.e., Cyperaceae pollen and fern spores) were excluded from that dataset following Stevenson et al. (2001).

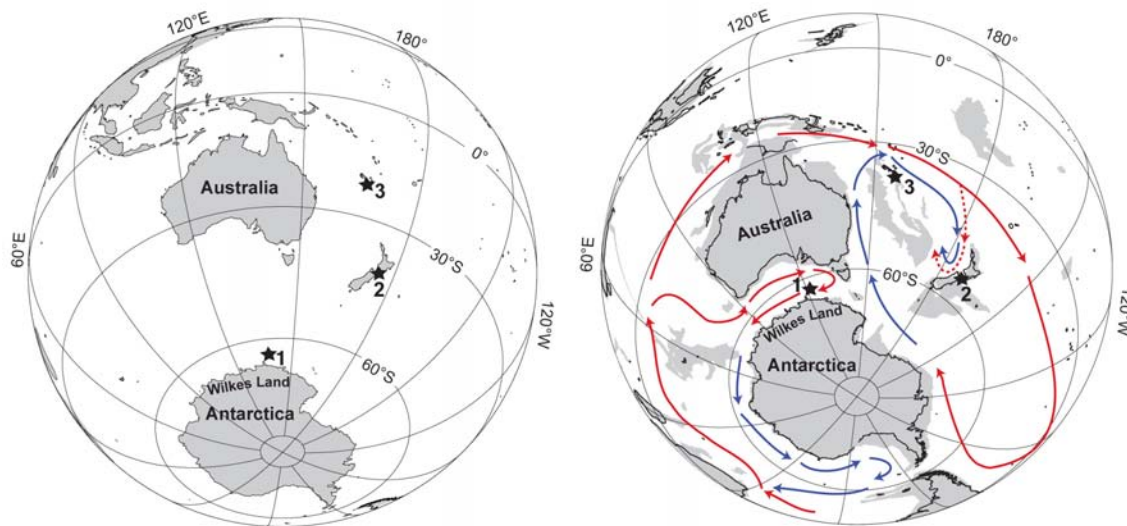


Figure 3.1 Maps of Oceania and Antarctica showing the present-day (right) and early-middle Eocene (left) continental configuration with locations of localities discussed in the text. 1. IODP Site U1356; 2. Plum Swamp, New Caledonia; 3. Wallaceville Swamp, New Zealand. Maps derived from the Ocean Drilling Stratigraphic Network (ODSN, <http://www.odsn.de/odsn/services/paleomap/paleomap.html>) after Hay et al. (1999). Eocene ocean currents after Huber et al. (2004).

As a basis for the comparison with the mid-Eocene sporomorph assemblages from Site U1356, a late Holocene sporomorph record from the Wallaceville Swamp in New Zealand ($41^{\circ}9'$, $175^{\circ}4'$, compare Fig. 3.1) was employed; the Wallaceville Swamp, measuring roughly $5 \times 1.6 \text{ km}^2$, is located in a basinal setting at an altitude of 140 m a.s.l., with surrounding hills rising over 240 m a.s.l. (Mildenhall and Moore, 1983). The sporomorph record evaluated here is based on the late Holocene ($\sim 5.0 \text{ kyr BP}$) palynological dataset from the cores R27/f7529 and R27/f7530 of Harris and Mildenhall (1984). In both cores, the sporomorph assemblages are characterized in order of decreasing abundance by *Nothofagus* (*fusca* group), *Gleichenia circinata* (Gleicheniaceae), Podocarpaceae, *Dacrydium cupressinum* (Podocarpaceae), *Leptospermum* (Myrtaceae), and *Cyathea* (Cyatheaceae) (Harris and Mildenhall, 1984). The present-day vegetation of the Wallaceville swamp is characterized by remnants of the *Nothofagus* forest that dominated the area since $\sim 5.0 \text{ kyr BP}$ (Harris and Mildenhall, 1984). A particularly high comparability between the mid-Eocene sporomorph record from Site U1356 and that from the late Holocene of the Wallaceville Swamp is warranted by the fact that both records are dominated by *Nothofagus* pollen grains.

3.4 Results

3.4.1. Composition and diversity of sporomorph assemblages at Site U1356

A total of 161 sporomorph types were identified in the Eocene of Site U1356; the stratigraphic distribution and relative abundances of all taxa that were encountered in at least two individuals are presented in Fig. 3.2. The three major botanical groups represented by the sporomorphs (i.e., angiosperms, gymnosperms and pteridophytes) appear in varying relative abundances (Fig. 3.3). In the order of decreasing abundances, the assemblages are dominated by *Nothofagidites* spp., *Cyathidites* spp. and *Araucariacites* spp., which are commonly recorded in both the early and mid-Eocene intervals. The early Eocene is generally characterised by a higher number of sporomorph taxa than the mid-Eocene. The occurrences of several sporomorph taxa that consistently reach only low abundances ($\leq 5\%$ of total non-reworked sporomorphs) are confined to specific core intervals. In particular, 45 taxa (including *Arecipites* spp., *Bluffopollis scabratus* and *Margocolporites cribellatus*) only occur in the Lower Eocene, whereas one taxon (i.e., *Dilwynites tuberculatus*) only occurs in the mid-Eocene strata (Fig. 3.2).

The DCA results of the entire sporomorph record yield significantly different values of the Axis 1 sample scores for the early and mid-Eocene intervals (Fig. 3.3). The two groups marked by different sporomorph assemblages are portrayed in the following sections.

3.4.1.1. Early Eocene (53.9 – 51.9 Ma)

Generally, the sporomorph assemblages are dominated by pteridophyte spores, which on average account for ~40% of all non-reworked sporomorphs and are represented mainly by spores of the genus *Cyathidites* spp. (botanical affinity: probably Cyatheaceae). Angiosperm pollen grains reach on average ~25% of all sporomorphs, even if *Nothofagus*, which is known to produce extremely high amounts of pollen and therefore tends to be strongly overrepresented in the pollen rain (e.g., Dodson, 1976), is excluded (Fig. 3.3). Abundantly occurring angiosperm elements are, in the order of decreasing abundances, *Nothofagidites* spp. (mainly *fusca* type; *Nothofagus*), *Proteacidites* spp. (Proteaceae), *Malvacipollis* spp. (Euphorbiaceae/Malvaceae), and *Myricipites harrisii* (probably Casuarinaceae). Gymnosperms are abundant (~20%) and mainly represented by *Araucariacites* spp. and *Dilwynites granulatus* (both Araucariaceae) (Fig. 3.2). Rare, but characteristic tropical angiosperm elements include, in the order of decreasing abundances, *Arecipites* spp. (Arecaceae), *Bluffopollis scabratus* (*Strasburgeria*), *Bombacacidites* sp. A (Bombacoideae), *Anacolosidites luteoides* (*Anacolosia*), and *Spathiphyllum* type (*Spathiphyllum*). Other angiosperm pollen types with unknown botanical affinities are registered in low abundances ($\leq 5\%$, see Fig. 3.2) or represented only by one specimen.

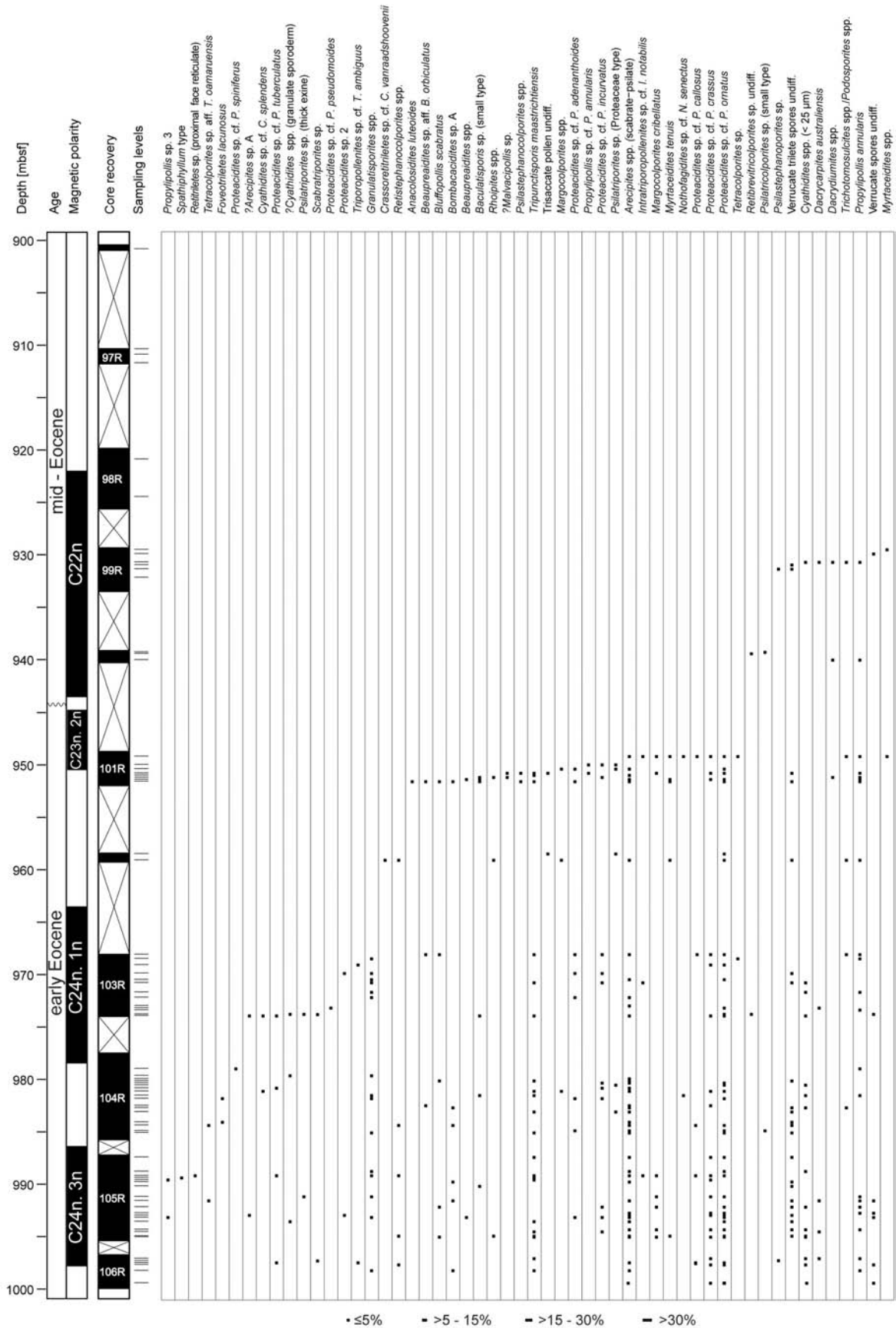


Figure 3.2 Semiquantitative range chart of sporomorphs identified in the Eocene of IODP Site U1356 for samples with counts higher than 100 individuals. The range chart contains all sporomorph taxa that were encountered in at least two specimens. Age model after Pross et al. (2012) and Tauxe et al. (2012).

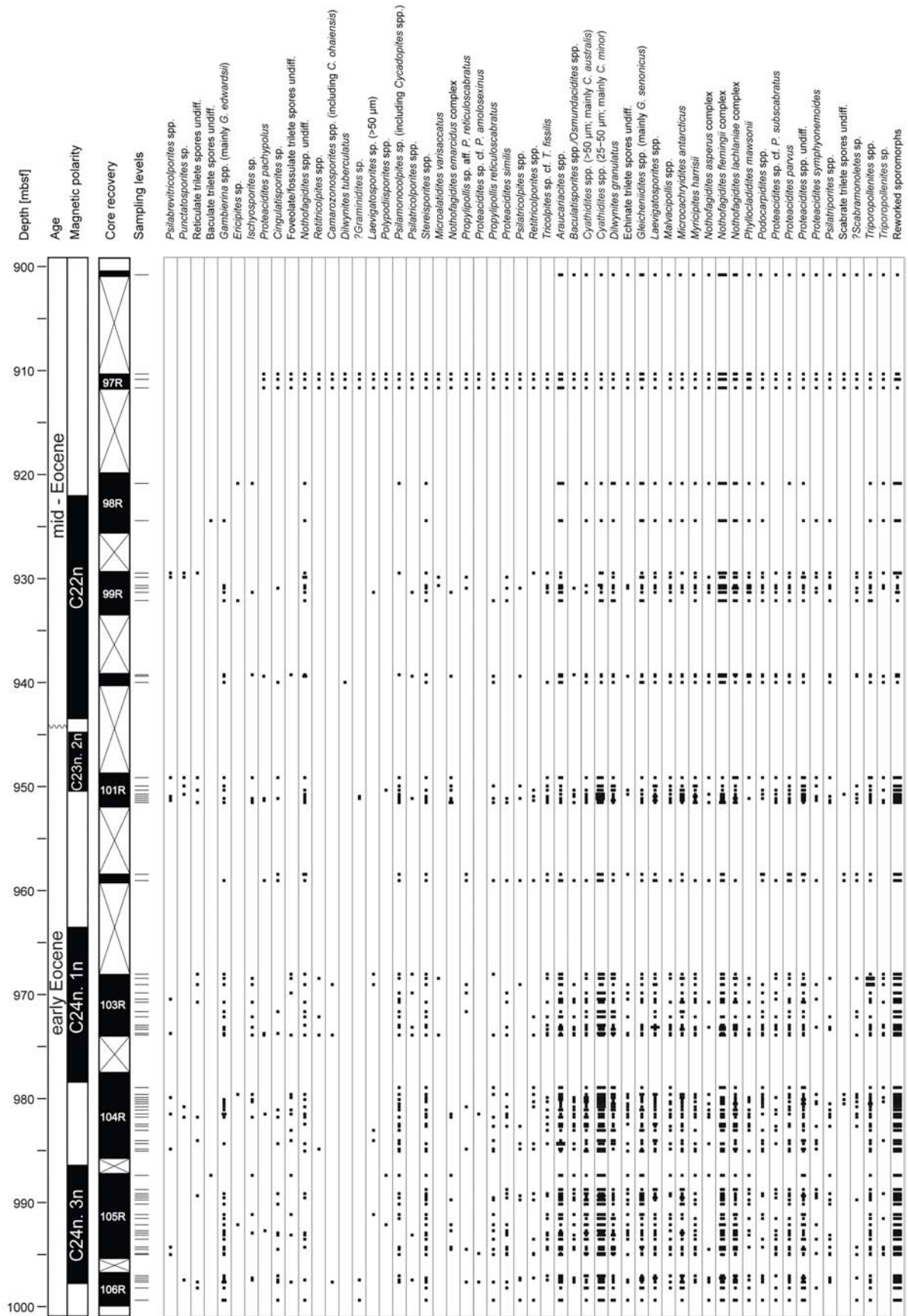


Fig. 3.2. (Continued)

Quantitatively, the early Eocene sporomorph record is characterized both by a high number of sporomorph species and a high diversity. Based on rarefied values, the number of sporomorph species is 25.1 ± 2.37 (mean \pm SD) species/sample at 100 individuals (Fig. 3.3). Shannon diversity index results are between 2.31 and 3.06, with an average of 2.66 ± 0.19 (Fig. 3.3). Evenness (J) values are between 0.69 and 0.84, with a mean of 0.77 ± 0.03 (Fig. 3.3).

3.4.1.2. Mid-Eocene (49.3 – 46 Ma)

Generally, the mid-Eocene sporomorph record is marked by high abundances of *Nothofagidites* spp. (mainly *fusca* type; *Nothofagus*) accounting for ~50% of total non-reworked sporomorphs. Abundantly occurring angiosperm pollen taxa are, in the order of decreasing abundances, *Proteacidites* spp. (Proteaceae), *Malvacipollis* spp. (Euphorbiaceae/Malvaceae) and *Myricipites harrisii* (probably Casuarinaceae); these taxa reach similar abundances as during the early Eocene. Gymnosperms are represented mainly by *Araucariacites* spp. and *Dilwynites granulatus* (both Araucariaceae), both of which reach slightly higher abundances (~30%) than during the early Eocene. Pteridophytes are represented by, in the order of decreasing abundances, *Cyathidites* spp. (probably Cyatheaceae), *Gleicheniidites* spp. (Gleicheniaceae) and *Osmundacidites* spp./*Baculatisporites* spp. (Osmundaceae); they are markedly less abundant (~10%) than during the early Eocene (Fig. 3.2).

Quantitatively, the mid-Eocene sporomorph assemblages are characterized by a lower number of sporomorph species and a lower diversity than those from the early Eocene. Based on rarefied values, the number of sporomorph species is 19.73 ± 2.38 species/sample at 100 individuals (Fig. 3.3). The Shannon diversity index yields values between 2.08 and 2.64, with an average of 2.31 ± 0.16 (Fig. 3.3). Evenness (J) values are between 0.62 and 0.79, with a mean of 0.69 ± 0.05 (Fig. 3.3).

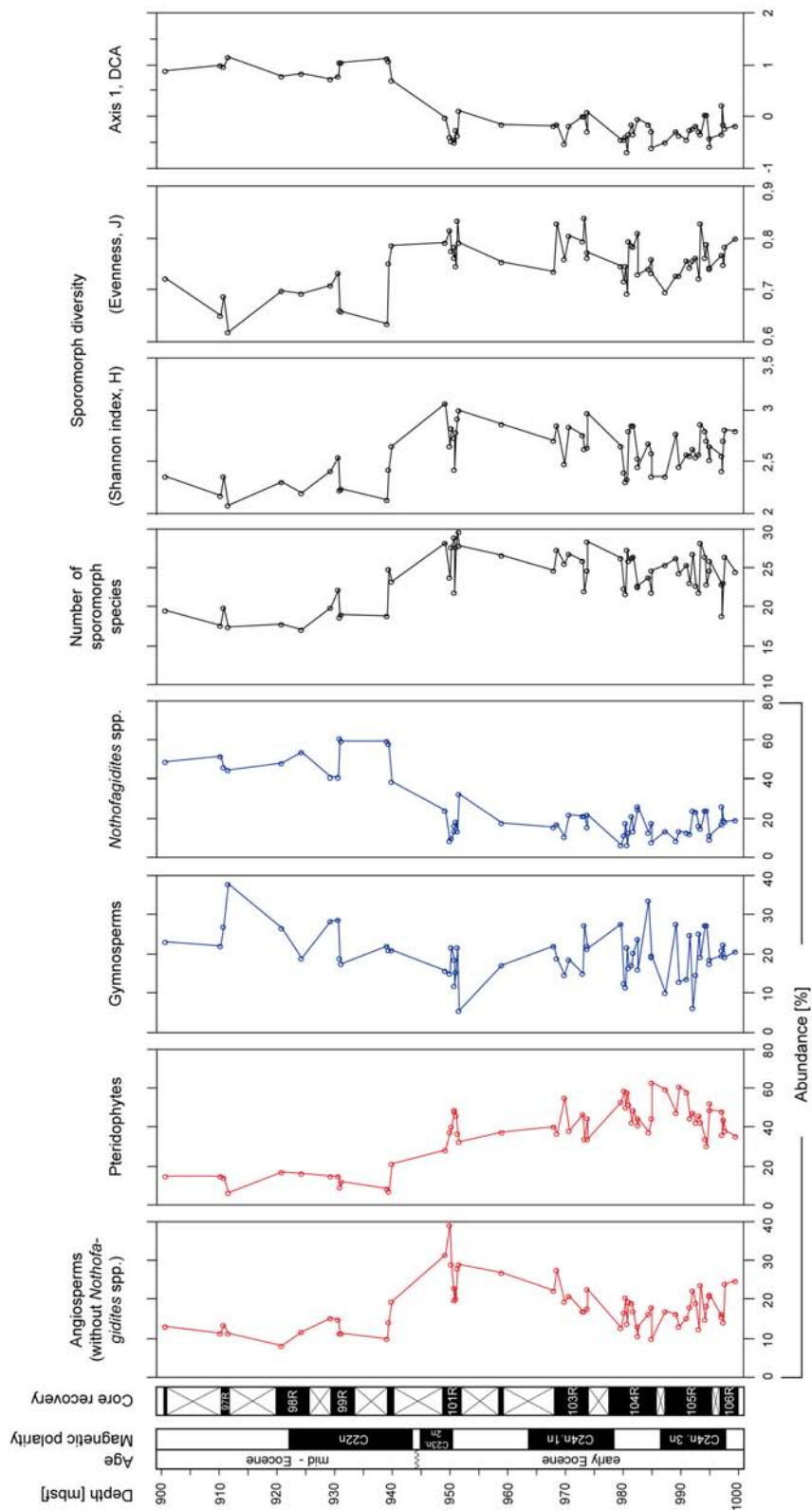


Figure 3.3 Diversity and Detrended Correspondence Analysis (DCA) results for IODP Site U1356. Relative abundances of *Nothofagidites* spp., pteridophytes, gymnosperms, angiosperms (excluding *Nothofagidites* spp.) are given for all samples with counts ≥ 100 sporomorphs. Numbers of sporomorph species are based on Sander's rarefaction analysis with samples rarefied at 100 individuals. The Shannon and evenness diversity indices were calculated for all samples with counts ≥ 100 individuals. The results of the DCA are derived from the Axis 1 sample scores, showing two distinctive compositional groups for the early and mid-Eocene samples.

3.5 Discussion

3.5.1. Qualitative characterization of vegetation structure

3.5.1.1. Early Eocene (53.9 – 51.9 Ma)

The sporomorph record from Site U1356 provides evidence for paratropical rainforests thriving along the Wilkes Land margin during the early Eocene. This evidence is mainly based on the documentation of plant taxa that today are restricted to tropical and subtropical settings, notably *Arecaceae* (palms), *Bombacoideae*, *Strasburgeria*, *Beauprea*, *Spathiphyllum*, *Anacolosa*, and *Lygodium*. The coeval presence of plants that today are restricted to temperate climate regimes such as *Nothofagus* (subgenera *Fuscospora* and *Nothofagus*) suggests that the vegetation along the Wilkes Land margin was subject to a climatic gradient that resulted from differences in elevation and/or the proximity to the coastline. Whereas paratropical rainforests dominated the lowlands and coastal regions, temperate forests probably prevailed in higher-elevation settings in the hinterland (Pross et al., 2012).

Based on the botanical affinities of the sporomorphs from Site U1356, the early Eocene forests in the lowlands of the Wilkes Land margin consisted of overstorey and understorey vegetation. Considering the known botanical affinities of the encountered sporomorphs, the overstorey comprised taxa such as *Bombacoideae*, *Strasburgeria*, *Arecaceae*, and *Proteaceae*. Extant *Bombacoideae* are trees with a pantropical distribution (Bayer and Kubitzki, 2003); they commonly occur both in dry regions and rainforests (e.g., Fedorov, 1966; Pennington et al., 2009). Extant representatives of the genus *Strasburgeria* are trees (Dickison, 2007) that form a part of the canopy of dense, evergreen forests on New Caledonia (Jaffré, 1995). Modern *Arecaceae* are well represented within the canopy and understorey of tropical forests (e.g., Pajmans, 1976; Morley, 2000). *Proteaceae* such as *Carnarvonia* (pollen taxon: *Proteacidites pseudomoides*) and *Gevuina/Hicksbeachia* (*Propylipollis reticuloscabratus*) are trees that form part of rainforests in Australia and New Caledonia (Specht et al., 1992). Apart from typical tropical taxa, the overstorey of the lowland vegetation may also have comprised *Araucariaceae* and *Podocarpus*. Extant *Araucariaceae* are tall trees in tropical to temperate forests restricted to the South American and Southwest Asia-Western Pacific region (Kershaw and Wagstaff, 2001). *Podocarpaceae* trees occur in tropical to temperate forests across a wide elevation range from high- (>2000 m a.s.l.) to lowland areas (Kershaw, 1988; Punyasena et al., 2011).

The understorey vegetation was probably dominated by shade ferns such as *Cyatheaceae*, *Osmundaceae* and *Huperzia*, an epiphyte that today thrives from the tropics to the Arctic and Subantarctic zones (Chinnock, 1998). Another element of the understorey was the evergreen herb *Spathiphyllum*, which is today restricted to wet settings in tropical forests (Govaerts and Frodin, 2002). Extant *Cyatheaceae*, which at least partially thrive well under low-light conditions (Volkova et al., 2009), are part of the shrub layer of tropical to temperate forests in lowland and mountainous areas (e.g., Jaffré, 1995; Veblen et al.,

1996); based on this distribution pattern, Cyatheaceae may have been part of the understorey of both the lowland and the hinterland vegetation along the Wilkes Land margin. Whereas present-day osmundaceous ferns occur from intermittent shade to high-light-level settings, osmundaceous ferns have been attributed to the understorey in the Late Cretaceous vegetation of the Otway Basin, southeastern Australia (Specht et al., 1992).

In addition, findings of pollen from Proteaceae shrubs such as *Adenanthos* (pollen taxon: *Proteacidites adenanthoides*), *Xylomelum* (*Propylipollis annularis*), *Beauprea* (*Beaupreaidites* spp.), and *Symphyonema* (*Proteacidites symphyonemoides*) together with pollen probably derived from *Eucalyptus* (*Myrtaceidites tenuis*) and Casuarinaceae (*Myricipites harrisii*) indicate the presence of an open-forest community characterized by sclerophyllous vegetation; such communities are widespread in areas with intermediate water availability (Martin, 1978; Specht and Specht, 1999). Hence, their presence suggests the existence of pockets with relatively dry conditions along the Wilkes Land margin.

Pollen grains attributable to *Anacolosia* (*Anacolosidites luteoides*) and Myrtaceae (*Myrtaceidites* spp.) occur in variable abundances within the early Eocene interval of Site U1356. As is the case with Proteaceae, the nearest living relatives of these taxa represent both shrubs and trees (George, 1984; Hill, 1994; Wilson, 2011). Hence, their role within the early Eocene vegetation along the Wilkes Land margin is difficult to constrain; they may have been part of the overstorey and/or understorey part of the forests.

A number of climate parameters for the Plum Swamp area (New Caledonia) are comparable with paleoclimatic estimates derived from the early Eocene record of Site U1356 (Pross et al., 2012; compare Table 3.1). Whereas MAP and MST as registered at Plum Swamp compare favorably with the respective values for the early Eocene of the Wilkes Land margin, MWT at Plum Swamp is markedly higher (Table 3.1). This apparent shortcoming in the comparability of MWT values results from the lack of a perfect modern analogue for early Eocene high-latitude climates because of the low meridional temperature gradients during that time (e.g., Huber and Caballero, 2011). However, abundant precipitation, high MST and frost-free conditions during winter are the most important factors in determining the composition and latitudinal distribution of vegetation growing in tropical to near-tropical climates (Hutchins, 1947; Morley, 2000). Considering that the early Eocene forests along the Wilkes Land margin thrived under the climate conditions required for the establishment of extant tropical rainforests, the structure of the vegetation may also be considered as similar to that of such forests. Based on this notion, the early Eocene vegetation along the Wilkes Land margin was probably characterized by multi-storeyed forests with a highly diverse tree component and a floristically varied understorey (Jaffré, 1995; Morley, 2000). However, in any such comparison the low incident solar radiation at higher latitudes is exposed to needs to be taken into account. For instance, the amount of light received by understory vegetation in a dense forest at higher latitudes would be very low; under these conditions only shade plants and cryptogams can survive (Specht et al., 1992).

Climate parameter	Early Eocene (Site U1356)	Plum Swamp (New Caledonia)*	mid-Eocene (Site U1356)	Wallaceville Swamp (New Zealand)*
MAT	16 ± 3°C	23.1°C	9.4 ± 1.5°C	10.5°C
MWT	11 ± 4°C	20.3°C	4.3 ± 1.5°C	6°C
MST	21 ± 3°C	25.7°C	14.2 ± 1°C	15°C
MAP	132 ± 55 cm/yr	150.3 cm/yr	160 ± 53 cm/yr	164 cm/yr

* Present-day data

Table 3.1. Comparison between paleoclimatic estimates derived from the early and mid-Eocene sporomorph assemblages from IODP Site U1356 (Pross et al., 2012) and present-day climate conditions at the Plum Swamp (New Caledonia; Pesin et al., 1995) and Wallaceville Swamp (New Zealand; NIWA, 2012) localities. MAT: Mean annual temperature; MWT: Mean winter temperature, MST: Mean summer temperature; MAP: Mean annual precipitation. Paleoclimatic estimates for the early and mid-Eocene sporomorph assemblages from IODP Site U1356 are from Pross et al. (2012) and were generated following the bioclimatic analysis approach of Greenwood et al. (2005).

Based on present-day climatological parameters and community physiological processes, Specht et al. (1992) examined the relationships between the structures of present-day forests and those from Late Cretaceous high-latitude (~65°) settings with a MAT between 16.5 and 19°C. They concluded that the Late Cretaceous vegetation comprised tall open forests with a conical-shaped crown that enabled some light to penetrate the understorey. In light of the comparable paleolatitude and temperature regime, these findings have relevance for the early Eocene forests from the Wilkes Land margin; they suggests that these forests were probably also characterized by a relatively tall open canopy with a conical-shaped crown.

3.5.1.2. Mid-Eocene (49.3 – 46 Ma)

Based on the mid-Eocene sporomorph record from Site U1356, the Wilkes Land margin was characterized by *Nothofagus*-dominated forests at that time; Araucariaceae were also present in high abundances. Today, cool temperate forests dominated by *Nothofagus* are confined to New Zealand and to Tasmania (Kershaw, 1988). Extant Araucariaceae predominantly thrive in the lower mid-latitudes (Kershaw and Wagstaff, 2001), but are also found in cool temperate Valdivian rainforests of Chile where Araucariaceae stands occur in mountainous areas from 37°20' to 40°20' S (Veblen, 1982).

Based on the established botanical affinities of the sporomorphs identified at Site U1356, the overstorey vegetation along the Wilkes Land Margin during the mid-Eocene was dominated by *Nothofagus*; further overstorey elements were Araucariaceae, *Podocarpus*, *Lagarostrobos* (pollen taxon: *Phyllocladidites mawsonii*), and *Gevuina/Hicksbeachia* (*Propylipollis reticulosabratus*).

The understorey vegetation was composed by Osmundaceae, Cyatheaceae and probably Proteaceae; notably, Cyatheaceae were less common than during the early Eocene. Records of *Xylomelum* (*Propylipollis annularis*), *Symphyonema* (*Proteacidites symphyonemoides*), and Casuarinaceae (*Myricipites harrisii*) suggest the presence of a sclerophyllous community. Gleicheniaceae represent a further common element throughout the mid-Eocene record. Today, members of this family occur in habitats affected by intermittent waterlogging (Specht et al., 1992) and often thrive at the margins of rainforests (Chinnock and Bell, 1998). The co-occurrence of *Nothofagus*, *Podocarpus*, Araucariaceae, and Proteaceae, which together formed the forest canopy, with sclerophyllous Proteaceae and with Gleicheniaceae that potentially indicate waterlogged soils might indicate the development of an ecological gradient in some patches along the Wilkes Land margin. A similar palynological association from the Upper Cretaceous of the Otway Basin, southeastern Australia, has been postulated to represent the vegetation response to a gradient from well-drained, nutrient-rich soils to seasonally waterlogged, nutrient-poor soils (Specht et al., 1992).

The climate parameters available for the Wallaceville Swamp (New Zealand) are consistent with the paleoclimatic estimates from the mid-Eocene record of Site U1356 (Pross et al., 2012; compare Table 3.1). Following the same concept as for the early Eocene, the structure of the mid-Eocene forests from the Wilkes Land margin may thus have been similar to that of the modern forests around Wallaceville Swamp. Specifically, considering the structure of the present-day *Nothofagus* forests in New Zealand (McGlone et al., 1996), the mid-Eocene forests along Wilkes Land margin were probably characterized by a single canopy layer dominated by *Nothofagus* and open understories.

3.5.2. Quantitative characterization of vegetation

As described above, the early and mid-Eocene sporomorph records from Site U1356 represent two markedly different floral assemblages. Quantitatively, these differences are reflected by the results of DCA and rarefaction analysis as well as the diversity indices (Fig. 3.3 and Table 3.2) and species accumulation curves (Fig. 3.4).

With regard to the output of the DCA, the Axis 1 sample scores reflect two distinct sporomorph assemblages from the early and mid-Eocene (Fig. 3.3 and Table 3.2). The diversity and richness patterns derived from the diversity indices (H and J), rarefaction analysis (Fig. 3.3) and species accumulation curves (Fig. 3.4) show that the early Eocene forests contained a significantly higher number of taxa than those from the mid-Eocene (Table 3.2). In addition, the early Eocene assemblages on average do not only comprise a significantly higher number of species per sample, but are also characterized by a more equitable abundance distribution of its taxa when compared to the mid-Eocene assemblages (Fig. 3.3 and Table 3.2).

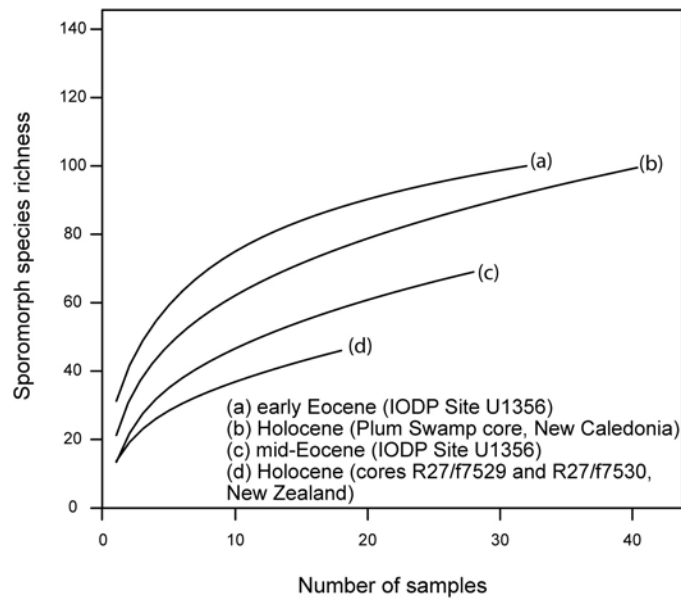


Figure 3.4 Species accumulation curves derived from the Eocene sporomorph data of IODP Site U1356 and from the Holocene sporomorph data from the Plum Swamp (New Caledonia; Stevenson et al., 2001) and cores R27/f7529 and R27/f7530 from the Wallaceville Swamp (New Zealand; Harris and Mildenhall, 1984). Data from IODP Site U1356 are presented separately for the early and mid-Eocene intervals.

Both the early Eocene vegetation at the Wilkes Land margin and extant forests from New Caledonia are located close to the ecotone between tropical and temperate forests and can be classified as paratropical rainforests *sensu* Morley (2000). The term was originally introduced by Wolfe (1979) for forests that exhibit similar physical characteristics of extant evergreen rain forests that are delimited by the 20 – 25°C MAT isotherms, and occupy the coastal lowlands between 17° and 26° N. Additionally, compared to evergreen rainforests in the equatorial zone, paratropical forests are floristically less diverse, with fewer megathermal elements and more frost-tolerant species (Morley, 2000). Hence, the coeval existence of frost-tolerant taxa (e.g., Araucariaceae, *Nothofagus*, Podocarpaceae) and megathermal elements (e.g., Bombacoideae, Arecaceae) as observed for the vegetation along the early Eocene Wilkes Land margin and as highlighted by Morley (2000) prompt us to here use the term “paratropical” in a broader sense following Morley (2000).

Although the floral composition of the vegetation from New Caledonia and the Wilkes Land margin during the early Eocene is different because many clades such as *Gambierina edwardsii*, *Intratropollenites notabilis* and *Proteacidites incurvatus* were extirpated in the southern latitudes during the Cenozoic, and the geological history of New Caledonia has strongly influenced the floral evolution (Lowry, 1996), the observed richness patterns exhibit similar trends. This is evidenced through the comparison of the species accumulation curves (Fig. 3.4) from the early Eocene record from the Wilkes Land margin and late Holocene (~6.0 kyr BP) palynological data from New Caledonia (Plum Swamp core; Stevenson et al., 2001).

Analysis	Early Eocene		mid-Eocene		r<(t-test)
	Mean	(SD)	Mean	(SD)	
Rarefaction (100 individuals)	25.1	2.37	19.73	2.38	<0.001
Shannon index (H)	2.66	0.19	2.31	0.16	<0.001
Evenness (J)	0.77	0.03	0.69	0.05	<0.001
DCA (Axis 1, sample scores)	-0.26	0.2	0.93	0.16	<0.001

Table 3.2. Summary of quantitative results and significance of the parametric t-test for the comparison between the early and mid-Eocene sporomorph assemblages from IODP Site U1356.

Both the mid-Eocene record from the Wilkes Land margin and the late Holocene record from the Wallaceville Swamp in New Zealand (Harris and Mildenhall, 1984) are dominated by *Nothofagus* and exhibit similar richness patterns (Fig. 3.4). Richness values of the assemblages from the mid-Eocene interval at Site U1356 are slightly higher than those of the Holocene assemblages (Fig. 3.4). This is likely due to the fact that the higher time condensation characterizing regimes with low sedimentation rates and the larger source area for sporomorph assemblages deposited in an offshore setting (as it both is the case for the record from Site U1356) probably increases the sporomorph species richness.

At tropical latitudes, forests grow under small annual temperature variations (Morley, 2000). Modern ecological studies have shown that diversity benefits from high temperatures in combination with high water availability; hence, species richness tends to be higher at tropical latitudes (e.g., Francis and Currie, 2003; Kreft and Jetz, 2007; Jansson and Davies, 2008). A similar picture emerges when the species richness and climate data from Plum Swamp (New Caledonia) and Wallaceville Swamp (New Zealand) are compared. Plum Swamp is characterized by a markedly higher species richness than Wallaceville Swamp (see Fig. 3.4 for comparison); it also exhibits higher mean winter and summer temperatures (MWT = 20.3°C, MST = 25.7°C) than Wallaceville Swamp (MWT = 6°C, MST = 15°C; compare Table 3.1), although the mean annual precipitation is similarly high at both sites (150–164 cm/yr).

For the Eocene of the Wilkes Land margin, the available climate reconstructions suggest markedly higher temperatures during the early Eocene (MWT = ~11°C, MST = ~21°C) than during the mid-Eocene (MWT = ~4°C, MST = ~14°C), whereas the mean annual precipitation was similar during both intervals (~130–160 cm/yr; Table 3.1). Considering the similarities between the early and mid-Eocene diversity records from the Wilkes Land margin with the diversity records from New Caledonia and New Zealand, respectively, it appears that under similar precipitation conditions diversity patterns were primarily

controlled by the prevailing temperature regime. These findings may be particularly noteworthy in light of the long annual period of darkness along the high-latitude Wilkes Land margin, which amounted to ~50 days per year (Pross et al., 2012). They suggest that photoperiod was not obstacle to the development of high plant diversities at high southern latitudes during the Eocene greenhouse world, which is in agreement with recent findings from the Arctic (Harrington et al., 2012).

3.6 Conclusions

The early and mid-Eocene sporomorph assemblages from Site U1356 represent two different vegetation types along the Wilkes Land margin. The early Eocene vegetation was probably multi-storeyed, with a tall, relatively open canopy and diverse overstorey containing taxa such as Bombacoideae, *Strasburgeria*, palms and Proteaceae; the understorey vegetation was probably dominated by ferns. In contrast, the mid-Eocene vegetation was predominantly characterized by cool temperate forests with a single canopy layer dominated by *Nothofagus* and open understories dominated by ferns. Both during the early and the mid-Eocene, the forests contained sclerophyllous vegetation elements; this suggests the presence of patches with reduced water availability along the Wilkes Land margin. Quantitatively, the sporomorph assemblages from the early and mid-Eocene are characterized by significant differences with regard to composition and diversity. The early Eocene assemblages exhibit a high diversity, with sporomorph species richness patterns comparable to those of present-day forests from New Caledonia; in contrast, the mid-Eocene assemblages are markedly less diverse and exhibit a sporomorph species richness similar to that observed in present-day cool temperate forests from New Zealand.

Acknowledgments

J. Stevenson provided palynological data from the Plum Swamp core, New Caledonia. B. O'Hara is thanked for advice on the numerical analyses. Discussions with A. Kershaw and P. Moss are gratefully acknowledged. L. Lyachenko, B. Schminke and N. Welters are thanked for technical support. We thank two anonymous referees for their constructive reviews. This work was funded through the German Research Foundation (DFG; grant PR 651-10) and the Biodiversity and Climate Centre Frankfurt (BiK-F).

Chapter 4. Terrestrial climate dynamics in the Tasmanian sector of the Southwest Pacific Ocean during the Paleocene-Eocene deduced from a marine pollen record (ODP Site 1172, East Tasman Plateau)

Lineth Contreras^{1,2}, Jörg Pross^{2,3}, Peter K. Bijl⁴, Robert B. O'Hara², J. Ian Raine⁵, Apy Sluijs⁴, Henk Brinkhuis^{4,6}

¹Paleoenvironmental Dynamics Group, Institute of Geosciences, Goethe University Frankfurt, Altenhöferallee 1, 60438 Frankfurt, Germany. ²Biodiversity and Climate Research Centre, Senckenberganlage 25, 60325 Frankfurt, Germany. ³Paleoenvironmental Dynamics Group, Institute of Geosciences, Heidelberg University, Im Neuenheimer Feld 234, 69120 Heidelberg, Germany. ⁴Department of Earth Sciences, Faculty of Geosciences, Utrecht University. Laboratory of Palaeobotany and Palynology, Budapestlaan 4, 3584 CD Utrecht, The Netherlands. ⁵Department of Palaeontology, GNS Science, P.O. Box 30368, Lower Hutt 5040, New Zealand. ⁶NIOZ Royal Netherlands Institute for Sea Research, P.O. Box 59, 1790 AB Den Burg, Texel, The Netherlands.

Published in Climate of the Past 10, 1401 – 1420[†]

Abstract

Reconstructing the early Paleogene climate dynamics of terrestrial settings in the high southern latitudes is important to assess the role of high-latitude physical and biogeochemical processes in the global climate system. However, whereas a number of high-quality Paleogene climate records has become available for the marine realm of the high southern latitudes over the recent past, the long-term evolution of coeval terrestrial climates and ecosystems is yet poorly known. We here explore the climate and vegetation dynamics on Tasmania from the middle Paleocene to the early Eocene (60.7 – 54.2 Ma) based on a sporomorph record from Ocean Drilling Program (ODP) Site 1172 on the East Tasman Plateau. Our results show that three distinctly different vegetation types thrived on Tasmania under a high-precipitation regime during the middle Paleocene to early Eocene, with each type representing different temperature conditions: (i) warm-temperate forests dominated by gymnosperms that were dominant during the middle and late Paleocene (excluding the middle/late Paleocene transition); (ii) cool-temperate forests dominated by southern beech (*Nothofagus*) and araucarians that transiently prevailed across the middle/late Paleocene transition interval (~59.5 to ~59.0 Ma); and (iii) paratropical forests rich in ferns that were established during and in the wake of the Paleocene–Eocene Thermal Maximum (PETM). The transient establishment of cool-temperate forests lacking any frost-sensitive elements (i.e., palms and cycads) across the middle/late Paleocene transition interval indicates markedly cooler conditions, with the occurrence of frosts in winter, on Tasmania during that time. The integration of our sporomorph data with previously published TEX₈₆-based sea-surface temperatures from ODP Site 1172 documents that the vegetation dynamics on Tasmania were closely linked with the temperature evolution in the Tasman sector of the Southwest Pacific region. Moreover, the

[†] Text of the published version was adapted to British English

comparison of our season-specific climate estimates for the sporomorph assemblages from ODP Site 1172 with the $\text{TEX}_{86}^{\text{L}}$ - and $\text{TEX}_{86}^{\text{H}}$ -based temperature data suggests a warm bias of both calibrations for the early Paleogene of the high southern latitudes.

4.1 Introduction

The Southern Ocean is an important region for early Cenozoic (65–34 Ma) climates, being the dominant region for deep-water formation during that time (Thomas et al., 2003; Sijp et al., 2011; Hollis et al., 2012). South Pacific sea-surface and global intermediate water temperatures increased from the late Paleocene to the early Eocene, with maximum warmth during the Early Eocene Climatic Optimum (EECO; 53–51 Ma), followed by a cooling trend during the middle and late Eocene (Zachos et al., 2001; 2008; Bijl et al., 2009; Hollis et al., 2012). This cooling trend ultimately culminated in the establishment of a continental-scale ice shield on Antarctica during the earliest Oligocene (e.g., Zachos et al., 1994; 2008; Barrett, 1996), which represented a decisive step in the Earth's transition from a “greenhouse” into an “icehouse” world.

Organic geochemical surface-water temperature proxy records from the high-latitude Southwest Pacific Ocean (notably TEX_{86} ; Bijl et al., 2009) closely mirror trends in the benthic foraminiferal oxygen isotope data from the late Paleocene to the early Oligocene (Zachos et al., 2001; 2008), which lends further support to the suggestions that the southern ocean was the main region for deep-water formation (Thomas et al., 2003). Irrespective of the calibration used, Southwest Pacific TEX_{86} -derived sea-surface temperatures (SSTs) were relatively cool during the early and middle Paleocene. During the late Paleocene and early Eocene, SSTs gradually rose to tropical values ($>26^{\circ}\text{C}$), with maxima being reached during the Paleocene-Eocene Thermal Maximum (PETM; Sluijs et al., 2011) and the EECO (Bijl et al., 2009; Hollis et al., 2009; 2012). Towards the end of the early Eocene (49–50 Ma), a pronounced SST cooling of $\sim 4^{\circ}\text{C}$ occurred on the Australo-Antarctic margin; this cooling has been attributed to the onset of westbound surface-water throughflow across the Tasmanian Gateway (Bijl et al., 2013a). A similar cooling trend is registered for surface waters off New Zealand (Hollis et al., 2009; 2012) and in the Tasman sector of the Southwest Pacific Ocean (Bijl et al., 2009; Hollis et al., 2012). Strikingly low SSTs are recorded for the high-latitude Southwest Pacific Ocean during the interval spanning the middle/late Paleocene transition (59.5–59.0 Ma); TEX_{86} -derived SST decreased by $\sim 3^{\circ}\text{C}$ during that time (Bijl et al., 2009; Hollis et al., 2012; 2014). Along with this SST drop, lowered sea level and marked bathyal erosion suggest that a transient growth of an Antarctic ice sheet may have occurred (Hollis et al., 2014).

While an increasing amount of data has become available on the marine climate evolution in the southern high latitudes during the early Paleogene, the coeval terrestrial climate dynamics of that region are yet poorly documented (e.g., Passchier et al., 2013). For the Paleocene, paleobotanical records reflect the thriving of temperate, gymnosperm-rich forests dominated by podocarps in Southeast Australia (e.g., Macphail et al., 1994; Greenwood et al., 2003; Greenwood and Christophel, 2005), on Seymour Island

(Antarctica; Askin, 1990), and in New Zealand (Mildenhall, 1980; Raine et al., 2009). In contrast, highly diverse angiosperm forests containing taxa that today are restricted to tropical environments characterize the early Eocene vegetation in the higher-latitude Southwest Pacific region. This vegetation is widely known from Southeast Australia (Macphail et al., 1994; Greenwood et al., 2003; Greenwood and Christophel, 2005), Tasmania (Truswell, 1997; Carpenter et al., 2012) and New Zealand (Raine et al., 2009; Handley et al., 2011); notably, it also thrived on the Wilkes Land margin of the Antarctic continent, i.e., at paleo-latitudes of $\sim 70^\circ$ South (Pross et al., 2012; Contreras et al., 2013).

The pronounced vegetation turnover from temperate forests during the Paleocene to near-tropical forests during the early Eocene suggests a marked, climatically driven change in terrestrial environments in the high southern latitudes. However, the transitional process between these two vegetation types and the underlying change in terrestrial climate conditions of the Southwest Pacific region have remained poorly understood. The gaps in the documentation of terrestrial climate dynamics during the early Paleogene appear particularly pronounced considering the coeval datasets for the marine realm from the same region (Bijl et al., 2009; 2013a; Hollis et al., 2009; 2012; 2014). This is due to the fact that prior paleobotanical studies are mainly based on stratigraphically discontinuous outcrops that provided only limited insights into the Paleocene and early Eocene vegetation of the region (Greenwood et al., 2003). In addition, available studies on sporomorphs from the early Paleogene of the Southwest Pacific region have predominantly focussed on the taxonomical characterization of the assemblages and the generation of biostratigraphic schemes (e.g., Stover and Evans, 1973; Stover and Partridge, 1973; Truswell, 1997; MacPhail, 1999). In any case, estimates of terrestrial temperatures in the high southern latitudes and a comparison with the currently available SST estimates from the marine realm can strongly enhance the understanding of the climate evolution in the high southern latitudes during the early Paleogene.

In light of the above, we here explore the vegetation response to high-southern-latitude climate forcing from the Paleocene to the “hothouse” conditions of the early Eocene based on a new, chronostratigraphically well-calibrated (Bijl et al., 2013b) sporomorph record from Ocean Drilling Program (ODP) Site 1172 off eastern Tasmania. We quantitatively evaluate the compositional variations of the sporomorph assemblages and carry out quantitative sporomorph-based paleoclimatic reconstructions. For a further assessment of the terrestrial climatic conditions in the Southwest Pacific region, we apply the same paleoclimate reconstruction approach to previously published sporomorph records from Southeast Australia (Bass Basin, Gippsland Basin, Southeast Highlands) and New Zealand. Finally, we compare our terrestrial paleoclimate estimates with previously published TEX_{86} - (i.e., $\text{TEX}_{86}^{\text{L}}$ and $\text{TEX}_{86}^{\text{H}}$ calibrations; Kim et al., 2010) based SST reconstructions from the same site (Bijl et al., 2009; 2013b; Hollis et al., 2014) in order to contribute to a better understanding of the early Paleogene climate dynamics in the high southern latitudes.

4.1.2 Regional setting and paleoceanography

During the early Paleogene, Tasmania and the ETP were located at $\sim 65^{\circ}\text{S}$, much closer to Antarctica than today (Exon et al., 2004b). Paleoceanographic patterns as determined by winds and gateway configuration were likely vital for regional climates on land (Sijp et al., 2011). The study site was located close to the Tasmanian promontory, which hampered deep ocean exchange between the Southwest Pacific and the Australo-Antarctic Gulf for most of the early Paleogene (Shipboard Scientific Party, 2001b; Stickley et al., 2004; Fig. 4.1). During the Paleocene and early Eocene, the Tasman region was under the persistent influence of the Antarctic-derived Tasman Current; in contrast, the Australo-Antarctic Gulf (west of Tasmania) was bathed by the low-latitude-derived Proto-Leeuwin Current (Huber et al., 2004; Sijp et al., 2011; see Fig. 4.1). This paleoceanographic configuration determined marine biogeographical patterns in the region (Huber et al., 2004; Bijl et al., 2011; 2013a). The onset of the deepening of the Tasmanian Gateway at $\sim 49\text{--}50$ Ma initiated a westbound Antarctic Counter Current flowing along the Antarctic margin from the Pacific into the Australo-Antarctic Gulf (Bijl et al., 2013a). Continued rifting through the Eocene and accelerated deepening of the Tasmanian Gateway (~ 35.5 Ma) led to the inflow of Australo-Antarctic Gulf waters through the Tasmanian Gateway into the southern Pacific during the early Oligocene (Stickley et al., 2004; Sijp et al., 2011). These paleoceanographic reorganizations had important effects on terrestrial climates in the Australo-Antarctic region (Bijl et al., 2013a).

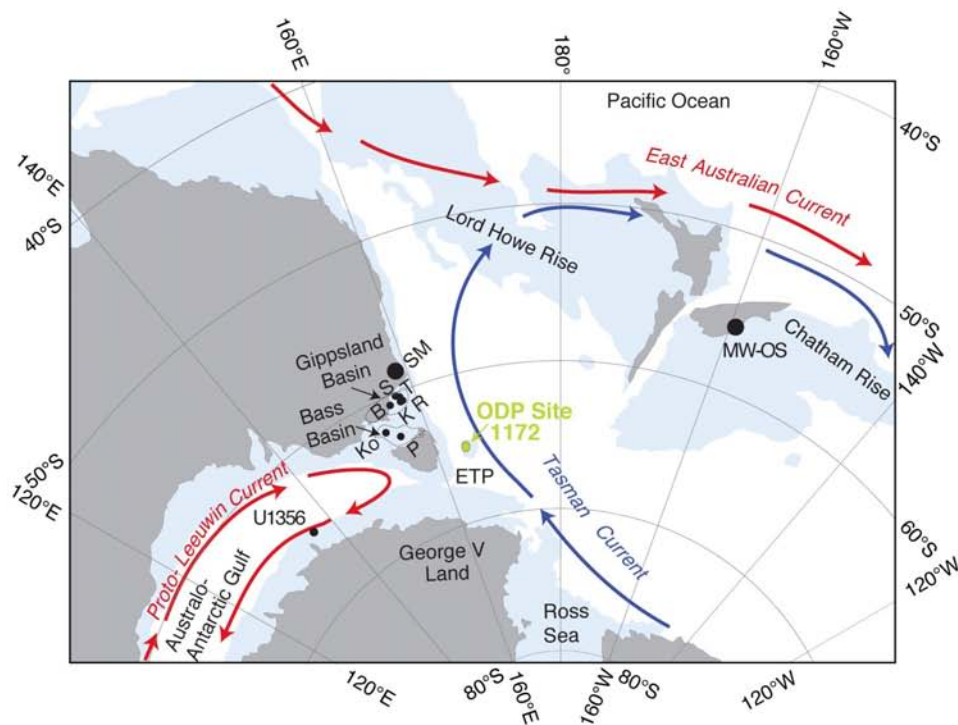


Figure 4.1 Map of the Southwest Pacific Ocean showing the early Eocene (~ 53 Ma) continental configuration, illustrating modern continents (gray), areas shallower than 300 m (blue) and locations of ODP Site 1172 and localities listed in Table 4.1. SM = Southern Monaro Sections (Southeast Highlands), B = Burong-1, K = Kingfish-8, Ko = Konkon-1, MW-OS = Middle Waipara and Otaio River sections, P = Poonboon-1, R = Roundhead-1, S = Sweetlips-1, T = Turrum-4, ETP = East Tasman Plateau. Modified after Cande and Stock (2004) and Sluijs et al. (2011).

4.2 Material and methods

The middle Paleocene to early Eocene strata studied here were recovered at ODP Site 1172, which is located ~100 km east of Tasmania on the western side of the East Tasman Plateau (ETP; 43°57.6' S, 149°55.7' E; Fig. 4.1) (Shipboard Scientific Party, 2001a).

4.2.1 Age model, lithology and depositional environment

We here follow the corrected sample depths for ODP Hole 1172D as published in Sluijs et al. (2011) based on detailed correlation of the X-ray fractionation core scanning to the γ -ray downhole log. The age model of the studied sequence is based on the magnetostratigraphy, chemostratigraphy and dinoflagellate cyst (dinocyst) biostratigraphy as presented in Bijl et al. (2013b). For the interval studied (60.7–54.2 Ma), the age model is based on three magnetic reversals confidently correlated to the Geomagnetic Polarity Time Scale (GPTS) of Vandenberghe et al. (2012), the PETM (~56 Ma), which exhibits a negative carbon isotope excursion of ~3‰ between 611.89 and 611.86 rmbfsf (revised meters below sea floor) (Sluijs et al., 2011), and several dinocyst first and last occurrence data that have been calibrated regionally following Crouch et al. (2014). The magnetostratigraphic age model for the Paleocene section (Röhl et al., 2004) was adjusted by Bijl et al. (2010) on the basis of the recognition of the PETM in Core 1172D-15R (611.8 rmbfsf; Sluijs et al., 2011). The missing interval between Cores 16R and 17R (~620 rmbfsf) represents a ~1.3-Ma-long hiatus that spans the time interval correlative to between infra-Subchrons C26n and C25n (57.7–59 Ma; Bijl et al., 2010; 2013b).

The upper 60 cm of section in Core 17R (i.e., below the hiatus) are heavily disturbed and have many sediment characteristics more consistent with Core 16R than with the underlying sediment (Röhl et al., 2004). We therefore follow Röhl et al. (2004) in their suggestion that this interval represents caved material of late Paleocene age. The Middle Paleocene to lower Eocene succession of ODP Site 1172 consists mainly of gray to grayish brown clay- and siltstones with low abundances of calcareous and siliceous microfossils (Shipboard Scientific Party, 2001a; Röhl et al., 2004). Environmentally, the succession is interpreted to reflect very shallow to restricted marine conditions, with marked runoff from the nearby shores (Röhl et al., 2004).

Any study on sporomorphs from marine sediments critically relies on the identification of the source region in order to provide meaningful paleoclimatic information. An in-depth discussion of this issue is provided in Section 4.4.1 (“Constraints on sporomorph source region”).

4.2.2 Sample processing and data analysis

Eighty-nine samples from the Paleocene and Eocene of ODP Site 1172, originally processed at the Laboratory of Palaeobotany and Palynology, Utrecht University (Bijl et

al., 2011), were here reanalysed for terrestrial palynomorphs. Sample processing followed standard palynological techniques, including treatment with HCl (10%) and HF (38%) and sieving through a 15 µm nylon mesh (e.g., Pross, 2001). The microscope slides were prepared using glycerine jelly as a mounting medium. The residues and slide preparations are stored in the collection of the Laboratory of Palaeobotany and Palynology at Utrecht University. Whenever possible, 300 sporomorphs (excluding reworked specimens) were analysed per sample and determined to the species level; this required the analysis of up to six slides per sample. The analyses were performed using a light microscope at 200x magnification; morphological details were studied with a magnification of 1000x. Sporomorph identifications are mainly based on Couper (1960), Harris (1965), Stover and Partridge (1973), Truswell (1983), Raine et al. (2008), and Truswell and Macphail (2009). The botanical affinities are given following Macphail et al. (1994), Raine (1998), and Truswell and Macphail (2009). All sporomorph data (including photomicrographs of key taxa) are provided in the Supplementary Information.

Rarefaction was applied to evaluate sporomorph diversity; this allows to estimate the number of sporomorph species at a constant sample size (Raup, 1975). Detrended Correspondence Analysis (DCA) is an ordination technique that was used to analyse floral composition change through time.

To constrain the source region of the sporomorphs from ODP Site 1172, we compared the floristic composition of our record with coeval sporomorph records from Southeast Australia (Bass Basin – data from Blevin 2003; Gippsland Basin – Department of Primary Industries, 1999; Southeast Highland sections – Taylor et al., 1990) and New Zealand (Middle Waipara and Otaio River sections – Pancost et al., 2013) using DCA (see Fig. 4.1 for locations and Table 4.1 for further details and references). From all records derived from drillholes, only data from core or sidewall core samples were evaluated to avoid potential contamination by caving. To exclude a bias as it could have been introduced into our comparison through different taxonomic criteria, we have standardized all datasets using broader groups of taxa (e.g., *Gleicheniidites* spp./*Clavifera* spp., *Phyllocladidites* spp., *Nothofagidites* spp. [*fusca* group]) when necessary. Due to the differences in sample sizes, sporomorph percentages were used as input for the DCA, and only samples with counts ≥ 100 individuals were evaluated.

Section	Region	Age	Pollen Biozone	Authors
Southern Monaro sections	highlands of southeastern Australia	60 – 58 Ma	Lygiestepollenites balmei	Taylor et al., 1990
Burong-1	onshore Gippsland Basin	late Paleocene	Upper L. balmei	* Partridge and Macphail, 1997
Kingfish-8	offshore Gippsland Basin	early Eocene	Lower Malvacipollis diversus	* Partridge, 1992
Konkon-1	Bass Basin	middle to late Paleocene, early Eocene	L. balmei and Lower M. diversus	+ Partridge, 2003
Otaio and Middle Waipara sections	New Zealand	58 – 56 Ma		Pancost et al. 2013
Poonboon-1	Bass Basin	late Paleocene, early Eocene	Upper L. balmei, Lower M. diversus	+ Partridge, 2003
Roundhead-1	offshore Gippsland Basin	middle to late Paleocene, early Eocene	L. balmei, Lower M. diversus	* Partridge, 1989
Sweetlips-1	offshore Gippsland Basin	middle to late Paleocene	L. balmei	* Partridge, 1989
Turrum-4	offshore Gippsland Basin	middle to late Paleocene	L. balmei	* Partridge, 1993
Turrum-4	offshore Gippsland Basin	middle to late Paleocene	L. balmei	* Partridge, 1993

Table 4.1 Sporomorph datasets evaluated in this study from the Southeast Australia (Bass Basin, Gippsland Basin, Southeast Highlands) and New Zealand (Middle Waipara and Otaio River sections). Asterisks indicate data derived from palynological reports in Department of Primary Industries (1999); Plus signs denote data derived from the Appendix C of Blevin (2003). Biozones and ages are based on Stover and Evans (1973), Stover and Partridge (1973) and Partridge (2006).

4.2.3 Sporomorph-based climate reconstructions

Quantitative sporomorph-based climate estimates were carried out following the bioclimatic analysis approach of Greenwood et al. (2005). For each taxon with a known nearest living relative (NRL; Table 4.2), climatic profiles were generated with regard to mean annual temperature (MAT), coldest month mean temperature (CMMT), warmest month mean temperature (WMMT), and mean annual precipitation (MAP). The climate profiles are derived from (i) the dataset of Pross et al. (2012), which is mainly based on distribution data from the Australian National Herbarium online database (Australian National Herbarium, 2011) and the mathematical climate surface software ANUCLIM 5.156 (Houlder et al., 1999), and (ii) the PALAEOFLORA database, which contains climatic information for a plant taxon based on its global distribution (Utescher and Mosbrugger, 2013). Following Greenwood et al. (2005), the climatic values for each assemblage were calculated based on the zone of overlap of the majority of taxa from that

Fossil taxon	Botanical affinity	Source	NLR used for climate analysis	database
Araucariacites spp.	Araucariaceae	Raine et al., 2008	Araucariaceae	1, 2
Arecipites spp.	Arecaceae	Nichols et al., 1973	Arecaceae	1
Baculatisporites spp.	Osmundaceae	Raine et al., 2008	Osmundaceae	1
<i>Banksiaeidites arcuatus</i>	Proteaceae (<i>Banksia</i> , <i>Dryandra</i> , <i>Musgravea</i>)	Raine et al., 2008		
<i>Beaupreaidites cf. diversiformis</i>	Proteaceae (<i>Beauprea</i>)	Raine et al., 2008		
<i>Caryophyllidites sp.</i>	Caryophyllaceae	Raine et al., 2008		
<i>Ceratosporites spp.</i>	<i>Lycopodiaceae</i> , <i>Selaginellaceae</i>	Raine et al., 2008		
Crassorettriletes cf. vanraadshooveni	<i>Lygodium</i>	Germeraad et al., 1968	<i>Lygodium</i>	1
Cyathidites spp.	Probably Cyatheaceae	Mohr, 2001	Cyatheaceae	1
Cycadopites spp.	Cycadales	Raine et al., 2008	Cycadales: <i>Bowenia</i> , <i>Lepidozamia</i> , <i>Macrozamia</i> <i>Dacrycarpus</i>	1
Dacrycarpites australiensis	Podocarpaceae (<i>Dacrycarpus dacrydioides</i>)	Raine et al., 2008		1
Dacrydiumites florinii	Podocarpaceae (<i>Dacrydium</i>)	Raine et al., 2008	<i>Dacrydium</i>	1
Dacrydiumites spp.	Podocarpaceae (<i>Dacrydium</i>)	Raine et al., 2008	<i>Dacrydium</i>	1
<i>Dilwynites granulatus</i>	Araucariaceae (<i>Wollemia/Agathis</i>)	Macphail et al., 2013		
<i>Dilwynites tuberculatus</i>	Araucariaceae (<i>Wollemia/Agathis</i>)	Macphail et al., 2013		
<i>Ephedripites sp.</i>	<i>Ephedra</i>			
Gleicheniidites senonicus	Gleicheniaceae	Raine et al., 2008	<i>Dicranopteris</i> , <i>Diplopterygium</i> , <i>Gleichenia</i> , <i>Sticherus</i>	1

Table 4.2 List of fossil sporomorph taxa from the Middle Paleocene to Lower Eocene of ODP Site 1172 with known botanical affinities and literature source, the nearest living relative (NLR) used in the climate reconstruction, and database where climate profiles of the NLRs are derived from. Database (1) = PALAEOFLORA (Utescher and Mosbrugger, 2013), Database (2) = Pross et al. (2012). Taxa used in the climatic evaluation are printed in boldface.

Fossil taxon	Botanical affinity	Source	NLR used for climate analysis	database
Gleicheniidites spp.	Gleicheniaceae	Raine et al., 2008	<i>Dicranopteris</i> , <i>Diplopterygium</i> , <i>Gleichenia</i> , <i>Sticherus</i>	1
<i>Intratropopollenites</i> <i>cf. notabilis</i>	Sterculioideae?, Bombacoideae?, Tilioideae?	Raine et al., 2008		
Malvacipollis diversus	Euphorbiaceae (<i>Austrobuxus</i> , <i>Dissiliaria</i> , <i>Petalostigma</i>); Eumalvoideae?	Raine et al., 2008	Euphorbiaceae	1
Microalatidites spp.	Podocarpaceae (cf. <i>Phyllocladus</i>)	Raine et al., 2008	<i>Phyllocladus</i>	1
Microcachrydites antarcticus	Podocarpaceae (<i>Microstrobos</i> , <i>Microcachrys tetragona</i>)	Raine et al., 2008		
Myricipites harrisii	Casuarinaceae, possibly also Myricaceae	Raine et al., 2008	Casuarinaceae (all Australian species)	1
Myrtaceidites spp.	Myrtaceae	Raine et al., 2008	Myrtaceae	1
Nothofagidites asperus complex	Nothofagaceae (<i>Nothofagus</i> subg. <i>Lophozonia</i>)	Truswell and Macphail, 2009	<i>N. cunninghamii</i> , <i>N.</i> <i>moorei</i>	1
Nothofagidites brachyspinulosus complex	Nothofagaceae (<i>Nothofagus</i> subg. <i>Fuscospora</i>)	Truswell and Macphail, 2009	Nothofagaceae (<i>Nothofagus</i> subg. <i>Fuscospora</i>)	2
Nothofagidites emarcidus complex (including <i>N. endurus</i>)	Nothofagaceae (<i>Nothofagus</i>)	Truswell and Macphail, 2009	all subgenera (including <i>Brassospora</i>)	2
Nothofagidites flemingii complex	Nothofagaceae (<i>Nothofagus</i> subg. <i>Nothofagus</i>)	Raine et al., 2008	Nothofagaceae (<i>Nothofagus</i> subg. <i>Fuscospora</i>)	2
Nothofagidites lachlaniae complex	Nothofagaceae (<i>Nothofagus</i> subg. <i>Fuscospora</i>)	Raine et al., 2008	Nothofagaceae (<i>Nothofagus</i> subg. <i>Fuscospora</i>)	2
Nothofagidites sp.1	Nothofagaceae (<i>Nothofagus</i>)		all subgenera (including <i>Brassospora</i>)	2
Nothofagidites spp. undifferentiated	Nothofagaceae (<i>Nothofagus</i>)		all subgenera (including <i>Brassospora</i>)	2
Osmundacidites spp.	Osmundaceae	Raine et al., 2008	Osmundaceae	1
<i>Parvisaccites</i> <i>catastus</i>	Podocarpaceae (<i>Halocarpus</i>)	Raine et al., 2008		

Table 4.2 (continued)

Fossil taxon	Botanical affinity	Source	NLR used for climate analysis	database
<i>Phyllocladidites mawsonii</i>	<i>Lagarostrobos</i>	Raine et al., 2008	<i>Lagarostrobos</i>	2
<i>Podocarpidites ellipticus</i>	Podocarpaceae (<i>Podocarpus</i>)	Raine et al., 2008	<i>Podocarpus</i>	1
<i>Podocarpidites exiguus</i>	Podocarpaceae	Raine et al., 2008		
<i>Proteacidites adenanthoides</i>	Proteaceae (<i>Adenanthos</i>)	Raine et al., 2008	<i>Adenanthos</i>	2
<i>Proteacidites annularis</i>	Proteaceae (<i>Xylomelum occidentale</i> or <i>Lambertia</i>)	Raine et al., 2008	<i>Xylomelum</i> (all Australian species)	2
<i>Proteacidites</i> cf. <i>amolosexinus</i>	Proteaceae (<i>Knightsia excelsa</i> type)	Raine et al., 2008		
<i>Proteacidites</i> cf. <i>adenanthoides</i>	Proteaceae (<i>Adenanthos</i>)	Raine et al., 2008	<i>Adenanthos</i>	2
<i>Proteacidites parvus</i>	Proteaceae (<i>Bellenden montana</i> type)	Raine et al., 2008	<i>Bellenden montana</i>	2
<i>Proteacidites reticuloscabratus</i>	Proteaceae (<i>Gevuina/Hicksbeachia</i> type)	Raine et al., 2008	<i>Gevuina</i> , <i>Hicksbeachia</i>	2
<i>Proteacidites symphyonemoides</i> / <i>P. pseudomoides</i>	Proteaceae (<i>Symphyonema</i> , <i>Carnarvonia</i>)	Raine et al., 2008	<i>Symphyonema</i> , <i>Petrophile</i>	2
<i>Pseudowinterapollis</i> sp.	Winteraceae	Raine et al., 2008		
<i>Retitriletes</i> cf. <i>rosewoodensis</i>	Lycopodiaceae (<i>Lycopodium</i>)	Raine et al., 2008		
<i>Retitriletes facetus</i>	Lycopodiaceae (<i>Lycopodium</i>)	Raine et al., 2008		
<i>Rubinella</i> cf. <i>major</i>	<i>Leptolepis</i> ?	Raine et al., 2008		
<i>Spinizonocolpites prominatus</i>	<i>Nypa</i> (Arecaceae)	Muller 1968	<i>Nypa</i>	1
<i>Stereisporites</i> sp.	Sphagnaceae	Truswell and Macphail, 2009		
<i>Triporoletes</i> cf. <i>reticulatus</i>	cf. <i>Riccia beyrichiana</i>	Raine et al., 2008		
<i>Troporopollenites ambiguus</i>	Proteaceae (<i>Telopea truncata</i> , <i>Oreocallis pinnata</i>)	Raine et al., 2008		
<i>Tripunctisporites maastrichtiensis</i>	Sphagnaceae?			

Table 4.2 (continued)

assemblage with respect to a given climate parameter. This overlap interval was calculated using the 10th percentile (as lower limit) and 90th percentile (as upper limit) of the total range of the NLRs recorded in that assemblage. The climate estimate is given as the midpoint between the lower and upper limits, with the error spanning from the lower to the upper limit. Only samples with counts ≥ 100 individuals were used in the climate reconstructions.

Paleoclimate estimates based on the NLR concept may be influenced by a number of factors that need to be considered prior to the application of NLR-based reconstruction methods (e.g., Mosbrugger and Utescher, 1997; Mosbrugger, 1999; Pross et al., 2000; Utescher et al., 2000). These factors include (i) the potential misidentification of the fossil taxa and/or NLRs; (ii) the potentially incomplete coverage of the climatic tolerances of the NLRs; (iii) potentially unidentified differences between the climatic tolerances of fossil taxa and their NLRs; and (iv) a weakening of the connection between fossil taxa and NLRs the further one goes back in time. Generally, these issues become increasingly important with the age of the floras analyzed and may diminish the significance of the results (e.g., Poole et al., 2005). They can, however, be identified and corrected via the application of multi-proxy approaches. In particular, the NLR concept has been successfully applied to both macrofloral and sporomorph assemblages from the early Paleogene of the higher southern latitudes (Greenwood et al., 2003; Carpenter et al., 2012; Pross et al., 2012; Contreras et al., 2013); the validity of the NLR-based results has been demonstrated through the comparison with data from other, independent proxies.

4.2.4 Statistical examination of the connection between floristic composition and temperature

To examine the correlation between the floristic composition of our sporomorph record from ODP Site 1172 (as represented by DCA Axis 1 sample scores; Figs. 4.2, 4.4) and $\text{TEX}_{86}^{\text{L}}$ - and $\text{TEX}_{86}^{\text{H}}$ -derived SST values from the same site (Bijl et al., 2013b; Hollis et al., 2014), we applied a state space model. State space models or dynamic linear models allow data distributed along time to be interpreted as the combination of several components, such as trends, or seasonal or regressive components (Petris et al., 2009; see West and Harrison, 1997, for further details on the advantages and development of the method). In essence, we modelled the dynamics of the 'true' (but unknown) SST and DCA Axis 1 sample scores in time, and modelled the observed values as deviations from these true values.

The model was fitted with a Bayesian approach. The likelihood is defined by Equations (4.1) and (4.2), with both SST and DCA for each time point where either one or both was measured. We compared 60 SST data points with our 40 values of the DCA Axis 1 scores. Because only six of the SST data points and DCA Axis 1 sample scores are from the exact same depths, we treated the missing data with multiple imputation; in essence, we estimated them as extra parameters to be estimated (e.g., Gelman et al., 2003). The cross-covariance between two points was calculated following Equation (4.3) and the final

correlation using Equation (4.4).

$$SST_i \sim N(x_{SST}(t(i)), t_{SST}^2) \quad (\text{Eq. 4.1})$$

$$DCA_i \sim N(x_{DCA}(d(i)), t_{DCA}^2) \quad (\text{Eq. 4.2})$$

$$\Delta d \begin{pmatrix} \sigma_{11}^2 & \rho\sigma_{11}\sigma_{22} \\ \rho\sigma_{11} & \sigma_{22} \end{pmatrix} + \begin{pmatrix} \sigma_{SST}^2 & 0 \\ 0 & \sigma_{DCA}^2 \end{pmatrix} \quad (\text{Eq. 4.3})$$

$$\text{corr}(SST, DCA) = \frac{\Delta t \rho \sigma_{DCA} \sigma_{SST}}{\sqrt{(\Delta t + \tau_{DCA}^2)(\Delta t \sigma_{SST}^2 + \tau_{SST}^2)}} \quad (\text{Eq. 4.4})$$

The model was fitted using OpenBUGS run through the BRugs package (Thomas et al., 2006) of the R software for statistical computing (R Development Core Team, 2011) fitted in a Bayesian framework using the BRugs package. The R script and further explanation of the analysis is given in the Supplementary Information.

4.3 Results

4.3.1 Sporomorph results from ODP Site 1172

Of the 89 palynological samples processed from the Middle Paleocene to Lower Eocene of ODP Site 1172, 40 samples yielded sporomorph counts ≥ 100 individuals and were further used in our analyses. The preservation of sporomorphs is generally good. A total of 197 sporomorph types were identified. A range chart with the relative abundances of key taxa is presented in Fig. 4.2; a full account of the identified taxa and their abundance data along with photomicrographs of key taxa is provided in the Supplementary Information. Based on rarefied values, the entire study interval is characterized by rich sporomorph assemblages (mean \pm s.d. = 29.2 ± 3.4 taxa/sample at 100 individuals, $n = 40$). Remarkably low sporomorph species numbers are recorded for the samples corresponding to the PETM (22.8 and 24.5 species/sample at 100 individuals; Fig. 4.2).

The DCA results of our sporomorph record yield distinctly different values for the Axis 1 and Axis 2 sample scores (Fig. 4.3a). They allow to define three sample groups, with each sample group being characteristic for specific time intervals of our record (Fig. 4.3a). These intervals are: (i) the middle (60.7 – 59.5 Ma) and late Paleocene (59.0 – 55.6 Ma); (ii) the middle/late Paleocene transition (~ 59.5 to ~ 59.0 Ma); and (iii) the early Eocene including the PETM (55.6 – 54.2 Ma). All three sample groups comprise characteristic sporomorph assemblages that are portrayed in the following.

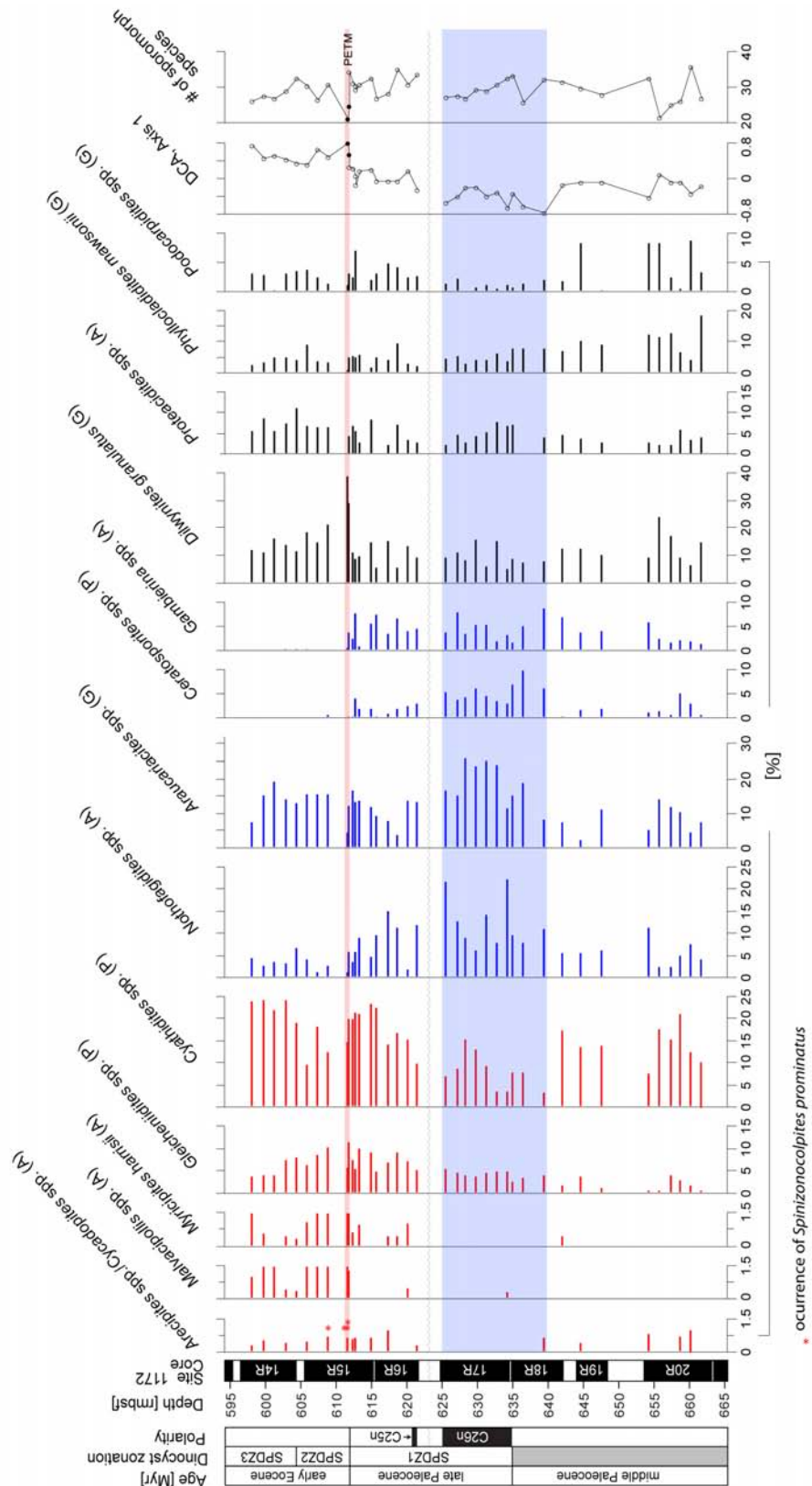


Figure 4.2 Relative abundances of selected sporomorph taxa ([A] angiosperms, [G] gymnosperms, [P] pteridophytes) representative of the middle Paleocene to early Eocene assemblages from ODP Site 1172. DCA Axis 1 scores represent the fluctuations in floristic composition between samples. Relative abundances and DCA results are based on samples with counts ≥ 100 individuals only. Numbers of sporomorph species are rarefied at 100 individuals. The intervals corresponding to the middle/late Paleocene transition and PETM are marked by horizontal blue and red bars, respectively. Age model and dinocyst zonation after Bijl et al. (2013b).

4.3.1.1 Middle Paleocene (60.7 – 59.5 Ma) and late Paleocene (59.0 – 55.6 Ma) intervals

The sporomorph assemblages from the middle and late Paleocene intervals (excluding the middle/late Paleocene transition, see below) are represented by 20 samples. They are dominated by gymnosperm pollen, which on average accounts for 45% of all sporomorphs. The gymnosperm pollen is represented mainly, in the order of decreasing abundances, by *Podocarpidites* spp. (botanical affinity: Podocarpaceae; podocarps), *Dilwynites granulatus* (*Wollemia* [Wollemi pine]/*Agathis* [Kauri]; Macphail et al., 2013), *Phyllocladidites mawsonii* (*Lagarostrobos franklinii*; Huon pine), and *Araucariacites* spp. (*Araucariaceae*; *Agathis* [Kauri] and *Araucaria*) (Fig. 4.2). Other abundant sporomorphs are, in the order of decreasing abundances, *Cyathidites* spp. (probably Cyatheaceae), *Nothofagidites* spp. (*Nothofagus*; southern beech), *Gambierina* spp., *Gleicheniidites* spp. (*Gleicheniaceae*), and *Ceratosporites* spp. (*Lycopodiaceae*, *Selaginellaceae*).

Although the sporomorph assemblages from the middle to late Paleocene have very similar floristic compositions, differences exist with regard to the percentages of some taxa (Fig. 4.2). For instance, the early part of the middle Paleocene exhibits relatively high (~30%) percentage of podocarpaceous pollen (mainly *Podocarpidites* spp. [*Podocarpaceae*; podocarps] and *Phyllocladidites mawsonii* [*Lagarostrobos franklinii*; Huon pine]). In contrast, the latest Paleocene is characterized by lower abundances of these taxa (~14%), but exhibits higher percentages of *Cyathidites* spp. (~18%) and the constant presence of *Myricipites harrisii* (probably *Casuarinaceae*; sheoak). Remarkably, both the middle and late Paleocene are characterized by the presence of *Arecipites* spp. (*Arecaceae*; palms) and *Cycadopites* spp. (*Cycadales*).

4.3.1.2 Middle/late Paleocene transition interval (59.5 – 59.0 Ma)

The sporomorph assemblages of the middle/late Paleocene transition interval are represented by ten samples. They exhibit higher percentages of *Araucariacites* spp. (*Araucariaceae*; ~19%), *Nothofagidites* spp. (*Nothofagus*; ~13%), and *Ceratosporites* spp. (*Lycopodiaceae*, *Selaginellaceae*; ~6%) than the assemblages from the under- and overlying Paleocene strata described in Section 4.3.1.1 above (Fig. 4.2). Other abundant taxa are, in the order of decreasing abundances, *Cyathidites* spp. (*Cyatheaceae*), *Dilwynites granulatus* (*Wollemia/Agathis*) and *Gleicheniidites* spp. (*Gleicheniaceae*). The percentages of podocarpaceous types (*Podocarpidites* spp. [*Podocarpaceae*] and *Phyllocladidites mawsonii* [*Lagarostrobos franklinii*]) are lower (~10%) than in assemblages from the under- and overlying middle and late Paleocene. Notably, the assemblages from the middle/late Paleocene transition interval are devoid of *Arecipites* spp. (*Arecaceae*; palms) and *Cycadopites* spp. (*Cycadales*) pollen.

4.3.1.3 PETM and early Eocene interval (55.6 – 54.2 Ma)

Assemblages from the PETM are documented in two samples with counts ≥ 100 individuals. They are characterized by high percentages (up to 39%) of *Dilwynites granulatus* (*Wollemia/Agathis*). Other abundant taxa are, in the order of decreasing abundances, *Cyathidites* spp. (Cyatheaceae), *Araucariacites* spp. (Araucariaceae), and *Gleicheniidites* spp. (Gleicheniaceae). The assemblages of the PETM interval are further characterized by the presence of *Malvacipollis* spp. (Euphorbiaceae, probably Eumalvoideae) and *Myricipites harrisii* (probably Casuarinaceae). Findings of *Spinizonocolpites prominatus* (*Nypa* palm) are restricted to the PETM and the earliest Eocene (Fig. 4.2).

Sporomorph assemblages of the early Eocene interval are documented in 8 samples. They show in general very high percentages (mean: 20%) of *Cyathidites* spp. (probably Cyatheaceae; Fig. 4.2). Other abundant taxa are, in the order of decreasing abundances, *Dilwynites granulatus* (*Wollemia/Agathis*), *Araucariacites* spp. (Araucariaceae), *Podocarpidites* spp. (Podocarpaceae), and *Phyllocladidites mawsonii* (*Lagarostrobos franklinii*). The early Eocene interval is also characterized by relatively high percentages of *Proteacidites* spp. (~7%) and the constant presence of *Malvacipollis* spp. (Euphorbiaceae, probably Eumalvoideae), *Myricipites harrisii* (probably Casuarinaceae), *Arecipites* spp. (Arecaceae; palms), and *Cycadopites* spp. (Cycadales).

4.3.2 Sporomorph-based paleoclimate estimates

The paleoclimate estimates derived from the sporomorph assemblages from ODP Site 1172 are presented in Fig. 4.4. Weighted averages with their respective propagated errors are given in Table 4.3. For the middle Paleocene (60.7–59.5 Ma), all reconstructed temperature parameters yield relatively cool values (MAT = 9 – 16°C; CMMT = 5 – 9°C; WMMT = 15 – 22°C). A pronounced further cooling is documented in all temperature parameters for the middle/late Paleocene transition interval (59.5–59.0 Ma). The reconstructed values represent the lowest temperatures of the entire record; values are 8 – 14°C for MAT, 4 – 7°C for CMMT and 15 – 20°C for WMMT (see Fig. 4). Markedly higher temperatures prevailed during the late Paleocene (59.0–55.6 Ma) and early Eocene (55.6–54.2 Ma), with estimates for that interval being on the order of 11 – 22°C for MAT, 6 – 18°C for CMMT and 17 – 26°C for WMMT. The highest temperatures of the entire study interval are recorded for the Paleocene/Eocene transition interval (including the PETM); MAT, CMMT and WMMT reached values of ~22°C, ~18°C and ~26°C, respectively, during that time (Fig. 4.4). The sporomorph-based MAP estimates yield high (138 – 208 cm/yr; see Fig. 4.4 and Table 4.3), near-constant values throughout the sequence studied.

Age	Location	SST (°C)	MAT (°C)	CMMT (°C)	WMMT (°C)	MAP (cm/year)
early Eocene	ODP Site 1172	23.4 ± 1.7 (L) 27.8 ± 2.5 (H)	12.5 ± 3.8	6.9 ± 3.8	19.3 ± 3.7	180 ± 86
	Bass Basin		20.2 ± 4.8	12.3 ± 3.4	24.8 ± 2.4	198 ± 114
	Gippsland Basin		17.2 ± 6.4	9.1 ± 6	21.3 ± 3	201 ± 119
	Otaio section		18.9 ± 3.4	11.8 ± 1.1	24.1 ± 0.4	125 ± 24
late Paleocene	ODP Site 1172	22 ± 1.2 (L) 25.5 ± 1.1 (H)	12.7 ± 5.2	7.4 ± 3.3	20.9 ± 2.9	172 ± 98
	Bass Basin		15.8 ± 5.8	9.3 ± 4	21.5 ± 2.9	195 ± 112
	Gippsland Basin		15.8 ± 5.9	8.6 ± 4.1	20.4 ± 3.6	200 ± 108
	Southern Morano sections		15.3 ± 6.4	8.5 ± 3.8	20.7 ± 4.1	194 ± 105
	Middle Waipara section	14 ± 1.6 (L) 19.3 ± 1.7 (H)	15.2 ± 2.8	6.9 ± 2.4	15.1 ± 2.9	179 ± 98
middle/late Paleocene transition	ODP Site 1172	16.5 ± 1.5 (L) 21.2 ± 1.1 (H)	10.6 ± 3.9	5.9 ± 2.8	15 ± 2.4	177 ± 86
middle Paleocene	ODP Site 1172	18.1 ± 1.9 (L) 23.5 ± 1 (H)	11.2 ± 4.6	6.4 ± 3.5	15.2 ± 3.1	181 ± 89
	Bass Basin		14.8 ± 8.7	7.5 ± 5.1	19.9 ± 4.5	205 ± 121
	Gippsland Basin		14.1 ± 5.8	7.5 ± 4.4	19.3 ± 3.6	198 ± 99

Table 4.3. Sporomorph-based climate estimates for Paleocene to early Eocene records from Southeast Australia (Bass Basin, Gippsland Basin, Southeast Highlands), New Zealand (Middle Waipara and Otaio River sections) and ODP Site 1172. SST values given for each stratigraphic interval represent average values of the data of Bijl et al. (2013b) and Hollis et al. (2014), with (H) and (L) denoting TEX_{86}^H (calibration error $\pm 2.5^\circ\text{C}$) respectively TEX_{86}^L (calibration error $\pm 4.0^\circ\text{C}$). Sporomorph-derived climate estimates are based on the methodology of Greenwood et al. (2005) and are presented with the weighted averages and their respective propagated errors (See Supplementary Information for further details). MAT = Mean Annual Temperature, CMMT = Coldest Month Mean Temperature, WMMT= Warmest Month Mean Temperature, MAP = Mean Annual Precipitation.

4.4 Interpretation

4.4.1 Constraints on sporomorph source region

Several lines of evidence suggest that eastern Tasmania was the main source of the sporomorphs encountered in the Middle Paleocene to Lower Eocene of ODP Site 1172. The distance of this site to the paleo-shoreline of eastern Tasmania during the Paleocene–early Eocene was on the order of ~ 100 km, whereas the minimum distance to George V Land (Antarctica) amounted to ~ 500 km (Fig. 4.1). A Tasmanian source is further suggested based on the distribution pattern of reworked Permian and Triassic sporomorphs. The assemblages from ODP Site 1172 are characterized by the constant presence of elements reworked from Permian and Triassic strata (e.g., *Cannanoropollis* spp.,

Protohaploxypinus spp., *Alisporites* spp.; see Supplementary Information, Plate II); the percentages of reworked sporomorphs reach up to 16% of the total assemblages. A similar input of reworked Permian and Triassic material is known for sporomorph assemblages from Paleocene–Eocene strata along the Australo-Antarctic Gulf (Otway Basin; Harris, 1965) and from the Eocene of the Wilkes Land margin (Contreras et al., 2013). In the Tasmania region, reworked Permian and Triassic sporomorphs are recorded in the Paleocene–Eocene of the Bass Basin (Partridge et al., 2003) as well as in Eocene strata off western Tasmania and on the South Tasman Rise (Truswell, 1997). This pattern is consistent with the fact that sporomorph-bearing sediments of Permian and Triassic age occur in several regions of Tasmania (e.g., Playford, 1965; Truswell, 1978; Calver et al., 1984). In contrast, reworked sporomorphs on the continental shelf off George V Land (Antarctica; Fig. 4.1) comprise only taxa with Cretaceous and Cenozoic ages (Truswell, 1983). A similar picture emerges for the Cenozoic of the Gippsland Basin where Permian and Triassic sporomorphs occur only sporadically and in low numbers (see reports in Department of Primary Industries, 1999).

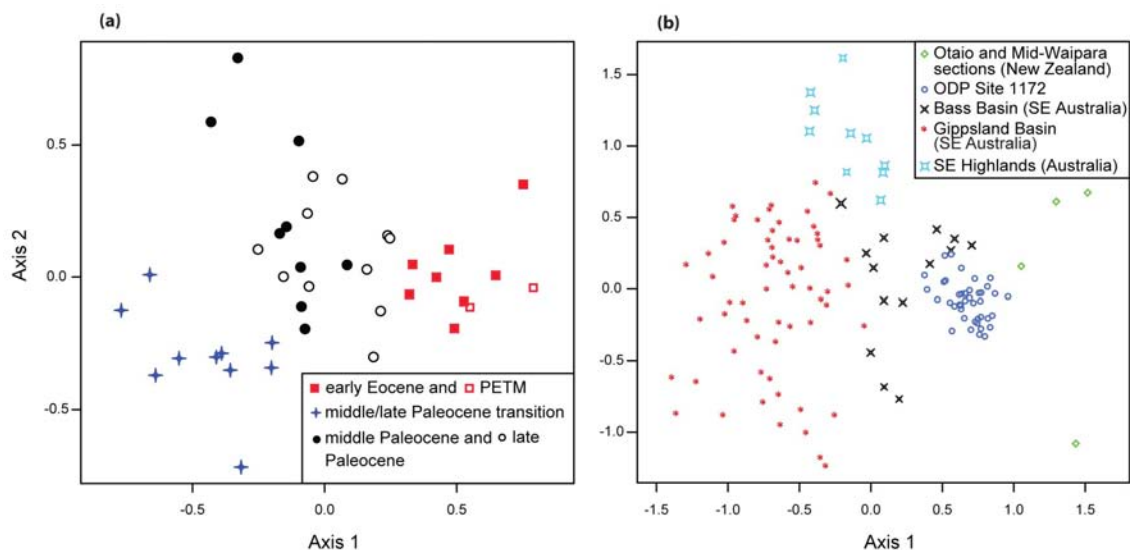


Figure 4.3 Comparison of the floristic composition based on the DCA sample scores for (a) middle Paleocene to early Eocene sporomorph assemblages from ODP Site 1172; (b) Paleocene/early Eocene sporomorph assemblages from Southeast Australia (Bass Basin, Gippsland Basin, Southeast Highlands), New Zealand (Middle Waipara and Otaio River sections) and ODP Site 1172. Results are based on samples with counts ≥ 100 individuals.

A further constraint on the source of the sporomorphs at ODP Site 1172 comes from the DCA-based comparison of the floristic composition of the Site 1172 record with other coeval Paleocene–Eocene sporomorph records from Southeast Australia (Bass and Gippsland Basins, Southeast Highlands) and New Zealand (Middle Waipara and Otaio River sections) (Fig. 4.3b; see Fig. 4.1 and Table 4.1 for site locations and details on records). It suggests marked differences in floristic compositions between most records, a result that can be further corroborated for the Bass and Gippsland Basins based on carbon-isotope data from both basins. The Paleocene–Eocene successions of these basins exhibit distinctly different bulk carbon isotope values, which is interpreted to reflect the signal from different plant communities contributing to the organic carbon input into the basins

during that time (Boreham et al., 2003). However, despite the floristic differences between the records analysed, there is a remarkable similarity in DCA scores between the records from ODP Site 1172 and the Bass Basin (Fig. 4.3b), which is located mainly on the shelf off northern Tasmania, but also extends into Northeast Tasmania (Moore et al., 1984). This similarity further corroborates the scenario of a Tasmanian source for the ODP Site 1172 sporomorph assemblages.

4.4.2 Floristic and climatic evolution

Based on our qualitative and quantitative results from the sporomorph record from ODP Site 1172, three main vegetation types prevailed on Tasmania from the middle Paleocene to early Eocene. These vegetation types (i) exhibit different floristic compositions based on the DCA results (Figs. 4.2 and 4.3a), (ii) show similar diversities based on the rarefaction results (Fig. 4.2), and (iii) represent specific climatic conditions based on our sporomorph-derived paleoclimatic reconstructions (Fig. 4.4). The floristic characteristics and climatic requirements of all three vegetation groups are discussed in the following sections.

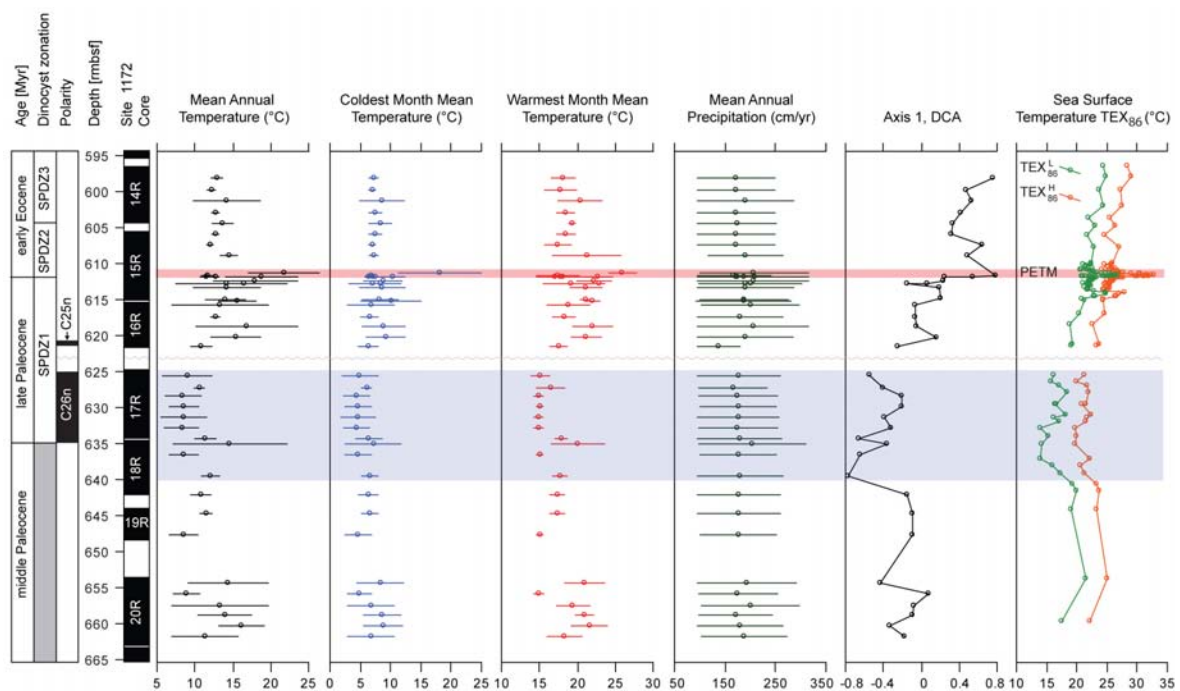


Figure 4.4 Comparison of the sporomorph-derived climate estimates, SST values based on $\text{TEX}_{86}^{\text{L}}$ and $\text{TEX}_{86}^{\text{H}}$, and DCA Axis 1 sample scores from the Middle Paleocene to Lower Eocene of ODP Site 1172. Sporomorph-derived climate estimates are based on the methodology of Greenwood et al. (2005). Error bars represent the minimum and maximum estimates determined using that method. SST data are from and Hollis et al. (2014). Sporomorph-derived climate estimates and DCA results are based on samples with counts ≥ 100 individuals only. The intervals corresponding to the middle/late Paleocene transition and the PETM are marked by horizontal blue and red bars, respectively. Age model and dinocyst zonation after Bijl et al. (2013b).

4.4.2.1 Middle Paleocene (60.7 – 59.5 Ma) and late Paleocene (59.0 – 55.6 Ma) intervals

During both time intervals, the flora of Tasmania was characterized by gymnosperm-rich forests dominated by podocarps; Araucariaceae, ferns, Proteaceae and *Nothofagus* were further important components of the vegetation. Arecaceae (palms) and Cycadales were present during both time intervals. Although the middle Paleocene and late Paleocene forests exhibited a strongly similar composition, important differences existed. Podocarps reached a markedly stronger dominance during the middle Paleocene than during the late Paleocene, whereas the late Paleocene was characterized by higher abundances of ferns (mainly Cyatheaceae) and the presence of Casuarinaceae (Fig. 4.2).

With regard to modern analogues, these forests bear resemblance to the extant warm-temperate, Podocarpaceae-dominated forests of Southeast Australia and New Zealand (e.g., Kershaw, 1988). Based on the structure of extant temperate forests from the southern latitudes (Kershaw, 1988; Enright and Hill, 1995; Veblen et al., 1996; Reid et al., 1999), the overstorey of Tasmanian forests during the middle and late Paleocene was dominated by Podocarpaceae and, to a somewhat lesser extent, Araucariaceae and *Nothofagus*. The understorey, in turn, was likely dominated by ferns, with Cyatheaceae being particularly abundant during the late Paleocene. Considering the habitats of their extant representatives, Arecaceae (palms), Cycadales, Proteaceae, and Casuarinaceae formed parts of both the over- and understorey (compare Johnson and Wilson, 1993; Hill, 1994; Morley, 2000; Jones, 2002).

Climatically, the presence of tree ferns (i.e., Cyatheaceae), Arecaceae and Cycadales implies mild climates with no or merely rare frost events. Owing to physiological constraints (including manoxylic wood, large, unprotected buds, soft, water-rich tissues, and a near-absence of frost-“hardening” mechanisms), all these plants are unable to cope with sustained freezing (Sakai and Larcher, 1987; Wing and Greenwood, 1993); today, they only occur in settings with CMMT $\geq 5.5^{\circ}\text{C}$ (Greenwood and Wing, 1995; Utescher and Mosbrugger, 2013).

4.4.2.2 Middle/late Paleocene transition interval (59.5 – ~59.0 Ma)

Across the middle/late Paleocene boundary, the warm-temperate forests characterizing the vegetation on Tasmania during most of the middle and late Paleocene as described above were transiently replaced by cool-temperate forests dominated by *Nothofagus* (mainly *N. fusca* type) and Araucariaceae. Ferns, podocarps and Proteaceae were further prominent components of this vegetation. Palms (Arecaceae) and Cycadales, as they occurred both during the preceding part of the middle (60.7–59.5 Ma) and the subsequent part of the late Paleocene (59.0–55.6 Ma; see above), were absent (Fig. 4.2). In light of the age control and the temporal resolution of our record, these cool-temperate forests prevailed on Tasmania for ~0.5 Ma (based on the duration of elevated *Nothofagus* percentages) respectively ~0.3 Ma (based on the absence of tropical to subtropical indicators such as palms and

Cycadales). The 1.3-Myr-long hiatus precludes us from firmly determining the complete duration of the cold interval in the mid-Paleocene (Fig. 4.2), however from marine records from New Zealand we deduce a duration of 0.5 Ma (Waipara section and ODP Site 1121; Hollis et al., 2014).

Today, vegetation dominated by *Nothofagus* (*N. fusca* type) is typical of cool-temperate forests from southern Australia and New Zealand (Kershaw, 1988). Considering the structure of such forests (e.g., McGlone et al., 1996; Reid et al., 1999), the vegetation thriving during the middle/late Paleocene transition interval was characterized by a canopy dominated by *Nothofagus* and open understories dominated by ferns (mainly Cyatheaceae and the parent plants of *Ceratosporites* spp. [Lycopodiaceae, Selaginellaceae]). Araucariaceae were also present. Because extant members of Araucariaceae are tall trees generally confined to the lower mid-latitudes (Kershaw and Wagstaff, 2001), their presence appears at first sight incompatible with an occurrence of cool-temperate forests. However, members of the genus *Araucaria* also thrive in cold temperate forests in mountainous areas of Chile (Veblen, 1982) and can withstand frost events as cold as -15°C (Prentice et al., 1992), which supports our observation that Araucariaceae were a component of the cool-temperate forests of Tasmania across the middle/late Paleocene transition.

Based on the overall floristic evidence, Tasmania witnessed a transient period of cooler conditions lasting from ~ 59.5 to ~ 59.0 Ma. In light of the frost sensitivity of Areaceae, Cycadales and Cyatheaceae (compare Section 4.4.2.1), the decline or total absence of these taxa across the middle/late Paleocene transition (Fig. 4.2) suggests harsher winters (with particularly frequent and/or cold frost events) during that time. Such lower temperatures are corroborated by the comparison with coeval $\text{TEX}_{86}^{\text{L}}$ - and $\text{TEX}_{86}^{\text{H}}$ -based SST data from ODP Site 1172 (Bijl et al., 2009; 2013b; Hollis et al., 2014). For the interval from ~ 59.4 to ~ 59.0 Ma, they show the lowest values of the entire Paleocene–Eocene SST record (Fig. 4.4, Table 4.3).

4.4.2.3 PETM and Early Eocene interval (55.6 – 54.2 Ma)

During the early Eocene, the composition of the forests on Tasmania was distinctly different from that of the temperate forests thriving during the Paleocene (Figs. 4.2, 4.3a); the underlying floristic turnover coincides with the onset of the PETM (see DCA Axis 1 sample scores in Fig. 4.2). Based on our sporomorph data, the early Eocene vegetation was dominated by ferns and different angiosperms (mainly Proteaceae, Casuarinaceae and Euphorbiaceae/Eumalvoideae). Remarkably, taxa that were common during the Paleocene (e.g., *Ceratosporites* spp. [Lycopodiaceae, Selaginellaceae] and *Gambierina* spp. [extinct clade]) declined dramatically in abundance or disappeared completely during that time (Fig. 4.2). Because extant Selaginellaceae and Lycopodiaceae are cosmopolitan families (Jermy, 1990; Øllgaard, 1990), it is difficult to connect the disappearance of these taxa on Tasmania during the earliest Eocene with specific ecological and climatic conditions.

The coexistence of frost-tolerant (e.g., Araucariaceae, Podocarpaceae) and thermophilous taxa (e.g., Casuarinaceae, Arecaceae [palms]) suggests the presence of paratropical forests *sensu* Morley (2000). In particular, the occurrence of *Nypa* from the PETM onward into the early Eocene suggests the presence of tropical mangrove vegetation along the coast of Tasmania. A similar vegetation, also containing thermophilous taxa such as *Nypa* and *Gymnostoma* (Casuarinaceae), is documented in early Eocene macrofloras from western Tasmania (Pole, 2007; Carpenter et al., 2012). Hence, forests on Tasmania during the early Eocene consisted temporarily of at least two vegetation associations: (i) A mangrove association characterized by *Nypa*, which is only recognized during the PETM and the earliest Eocene, and (ii) a paratropical association characterized by the coexistence of frost-tolerant taxa (i.e., Araucariaceae, Podocarpaceae and *Nothofagus*) and thermophilous elements such as palms and Casuarinaceae.

Considering the ecology of the nearest living relatives of the plants represented by the encountered sporomorphs, the overstorey vegetation during the early Eocene comprised taxa such as Araucariaceae, Podocarpaceae and *Nothofagus*, whereas the understorey was probably dominated by ferns (mainly Cyatheaceae). Members of the Proteaceae, Casuarinaceae, Cycadales, Arecaceae (palms), and Euphorbiaceae/Eumalvoideae may have been both components of the over- and the understorey (Johnson and Wilson, 1993; Hill, 1994; Morley, 2000; Jones, 2002).

The number of sporomorph species registered at ODP Site 1172 remained relatively constant from the middle Paleocene to the early Eocene (Fig. 4.2). This observation is in contrast to Southeast Australia, where sporomorph assemblages from non-marine and marginal marine settings (Partridge, 1976) exhibit a considerably higher diversity during the early Eocene than during the Paleocene (Macphail et al., 1994; see Section 4.4.3.2. below). The reasons behind this discrepancy may be sought in the particularly high sea level during the early Eocene as it is recorded regionally based on sedimentological and paleontological data from ODP Site 1172 (Exon et al., 2004a) and globally (Miller et al., 2005; Cramer et al., 2011). Owing to the selective nature of marine sporomorph transport as a function of transport distance (e.g., Moss et al., 2005), the higher sea level during the early Eocene than during the Paleocene potentially caused a diversity decrease of the sporomorph assemblages at ODP Site 1172 (see also below).

Our data suggest that the floristic change connected to the PETM is similar to that registered for the early Eocene. However, unravelling the exact anatomy of vegetation change across the PETM at ODP Site 1172 is difficult due to the low sporomorph yields in the respective sediments at that site. In addition, the interpretation of the available data is hampered by the sea-level rise during the PETM (Sluijs et al., 2011); the transgression-induced change in depositional setting towards more distal conditions may have caused a bias in the composition and diversity patterns of sporomorph assemblages, with the resulting assemblages being skewed towards a dominance of easily transported sporomorphs (compare Traverse, 1994; 2008). In light of this bias, the high abundances (up to 39%; Fig. 4.2) of *Dilwynites granulatus* (*Wollemia/Agathis*) and the remarkably low

diversities (Fig. 4.2) in the PETM samples from ODP Site 1172 likely represent a change in depositional setting rather than a true paleoecological signal. This interpretation is supported by the higher abundances of the same species (~35%) in early Paleogene sediments deposited in distal environments of the Bass Basin when compared to the markedly lower abundances (~10%) in coeval sediments from nearshore settings in the same basin (see reports in Partridge et al., 2003). Nevertheless, our data show that the environmental perturbations connected to the PETM had a profound impact on the vegetation on Tasmania. They lead to the extirpation of various ferns (e.g., *Perinomonoletes* spp., *Ceratosporites* spp. [Lycopodiaceae, Selaginellaceae]) and angiosperms (e.g., *Gambierina rudata*, *Nothofagidites* sp. 1 [*Nothofagus*]), and the appearance of new angiosperms mainly within the Proteaceae family (e.g., *Proteacidites grandis*).

4.4.3 Integration with other terrestrial vegetation records and temperature estimates from the southern high latitudes

Our results from ODP Site 1172 yield a ~6.5-Ma-long vegetation record for the Tasman sector of the SW Pacific region spanning from the middle Paleocene to the early Eocene. To obtain insights into the potential regional differentiation of terrestrial ecosystems and climates in the high southern latitudes during that time, we have integrated our data from ODP Site 1172 with the available information on terrestrial ecosystems and temperatures from other parts of the SW Pacific domain. Our integration is augmented by newly generated temperature estimates for previously published sporomorph records from Southeast Australia and New Zealand (see Tables 4.1 and 4.3 for further information on records evaluated and results). Because other continuous, stratigraphically well-calibrated vegetation records across the middle/late Paleocene transition interval are not yet available for the SW Pacific region, we focus our comparison on the middle Paleocene, late Paleocene and early Eocene.

4.4.3.1 Middle and late Paleocene

Paleobotanical records for the middle and late Paleocene are well known from Southeast Australia (e.g., Bass Basin – Macphail et al., 1994; Blevin, 2003; Gippsland Basin – Stover and Partridge, 1973; Macphail et al., 1994; Department of Primary Industries, 1999). In summary, the middle and late Paleocene vegetation in this region consisted predominantly of warm temperate forests characterized by podocarps, Araucariaceae and ferns; angiosperms were represented mainly by Proteaceae (e.g., Taylor et al., 1990; Macphail et al., 1994; Greenwood et al., 2003; Greenwood and Christophel, 2005). Similar warm temperate forests dominated by podocarps and Araucariaceae, and with a strong contribution of Proteaceae, thrived on New Zealand (Mildenhall, 1980; Raine et al., 2009). Based on our results, Podocarpaceae together with Araucariaceae, Cyatheaceae and Proteaceae were also the prevailing group of plants during the middle and late Paleocene on Tasmania (Fig. 4.2; compare also Section 4.4.2.1). However, important floristic differences existed between Southeast Australia, New Zealand and Tasmania (Fig. 4.3b);

they are mainly based on the restriction of certain sporomorph taxa to specific regions (e.g., *Liliacidites* spp., *Cibotioidites tuberculiformis* – New Zealand; *Ilexpollenites* spp. – Southeast Australia [Bass and Gippsland Basins, Southeast Highlands]; *Tripunctisporis maastrichtiensis* – New Zealand, Bass Basin and Tasmania). Despite the differences in floristic composition, the remarkable dominance of Podocarpaceae and Araucariaceae in Southeast Australia, Tasmania and New Zealand suggests that warm-temperate forests dominated by gymnosperms were the prevalent vegetation type in the Southwest Pacific region during the middle and late Paleocene. Moreover, thermophilous taxa such as palms, Olacaceae (*Anacolosa*) and Cupanieae first appeared and/or increased significantly in abundance and diversity during the latest Paleocene in Southeast Australia (Kemp, 1978; Macphail et al., 1994). On New Zealand, typical tropical taxa (e.g., Cupanieae, *Austrobuxus* [Euphorbiaceae], *Nypa*) also begin to appear during the latest Paleocene prior to the PETM (Crouch and Brinkhuis, 2005; Raine et al., 2009). Hence, the arrival of thermophilous elements indicates the onset of warmer conditions in the Southwest Pacific region during the latest Paleocene. A scenario of warm conditions is further corroborated by MAT estimates reaching $\sim 18^{\circ}\text{C}$ as derived from latest Paleocene macrofloras in Southeast Australia (Greenwood et al., 2003).

Considering our sporomorph-based climate estimates for Southeast Australia and Tasmania (Table 4.3), temperatures were higher during the late Paleocene than during the middle Paleocene. Hence, the overall climatic and vegetation signal suggests that terrestrial settings across the Southwest Pacific region consistently experienced a pronounced warming during the late Paleocene.

4.4.3.2 PETM and Early Eocene

The effects of the PETM on terrestrial ecosystems in the high southern latitudes are yet poorly constrained. Available records from Southeast Australia (Bass and Gippsland Basins) covering the PETM and the earliest Eocene suggest the widespread presence of *Nypa* during that time (Partridge, 1976). Climatically, this indicates a MAT $>21.7^{\circ}\text{C}$ (Utescher and Mosbrugger, 2013). For the South Island of New Zealand, sporomorph data from nearshore marine sediments document the development of *Nypa* mangrove swamps and the appearance of pollen from the thermophilous subfamily Cupanieae connected to the PETM interval (Handley et al., 2011); moreover, the PETM is characterized by a percentage increase of fern spores as well as of Euphorbiaceae/Eumalvoideae and Myrtaceae pollen at the expense of gymnosperm pollen percentages (Handley et al., 2011). Similarly, sporomorph data for the North Island of New Zealand as available from the Tawanui section show the presence of *Nypa* pollen connected to the PETM (Crouch and Visscher, 2003). However, besides a marked increase of *Dilwynites granulatus* (*Wollemia/Agathis*) pollen, no other significant changes in floristic composition occur (Crouch and Visscher, 2003). Considering that the PETM sediments of the Tawanui section are part of a transgressive systems tract (Crouch and Brinkhuis, 2005; Sluijs et al., 2008), the high abundances of *Dilwynites granulatus* (*Wollemia/Agathis*) may represent a taphonomic rather than a paleoecological signal as suggested for the sporomorph record of

the PETM from ODP Site 1172 (see Section 4.4.2.3).

With regard to the early Eocene, the majority of vegetation records in the Southwest Pacific region come from Southeast Australia; they suggest that by early Eocene times the warm temperate, conifer-dominated forests of the late Paleocene had been replaced by more diverse, meso- to megathermal angiosperm forests (Macphail et al., 1994; Greenwood et al., 2003; Greenwood and Christophel, 2005). Although sporomorph percentages are extremely variable within the available records from Southeast Australia, Araucariaceae, Casuarinaceae, Euphorbiaceae/Eumalvoideae, Proteaceae, and ferns are generally the dominant taxa; typical tropical elements such as *Nypa*, *Anacolosa* and Cupanieae are also recorded (Kemp, 1978; Macphail et al., 1994). This trend in vegetation development during the early Eocene is also documented for Tasmania.

On New Zealand, early Eocene sporomorph assemblages exhibit a mixed Paleocene-Eocene character, with a continued high abundance of conifer pollen (Crouch and Visscher, 2003; Raine et al., 2009). However, thermophilous taxa such as Cupanieae, Casuarinaceae and Euphorbiaceae (*Austrobuxus*) are constantly present in these records (Pocknall, 1990; Raine et al., 2009), and Casuarinaceae pollen abruptly started to dominate the sporomorph assemblages from ~54.5 Ma onwards (Raine et al., 2009). On the Wilkes Land margin (Antarctica), paratropical vegetation has been recorded during the early Eocene (53.9–51.9 Ma) with the notable presence of thermophilous taxa such as Arecaceae (palms) and Bombacoideae (Pross et al., 2012; Contreras et al., 2013),

With regard to temperature conditions, early Eocene macrofloras from Southeast Australia suggest a MAT of ~19°C from ~56 to ~53 Ma (Greenwood et al., 2003), which is very similar to our MAT estimates for coeval sporomorph records (~55.8–54.3 Ma; lower Malvacipollis diversus zone of Partridge, 2006; Table 4.1) from the Bass and Gippsland Basins (~18°C; Table 4.3). On the Wilkes Land margin, climatic estimates for the early Eocene (53.9–51.9 Ma) suggest a MAT of ~16°C for the lowland regions (Pross et al., 2012). Although occasionally MAT values as high as ~23°C are recorded during the earliest Eocene at ODP Site 1172, the MATs for this time interval are on the order of 12 – 14°C (Fig. 4.4). This is markedly lower than those from Southeast Australia, and even lower than those from the Wilkes Land margin. Considering that our sporomorph-derived climate data from ODP Site 1172 mainly reflect climate conditions along the coast of eastern Tasmania (compare discussion on sporomorph source region in Section 4.4.1), these relatively low values may suggest that the eastern part of Tasmania was influenced by the relatively cool Tasman Current (Fig. 4.1). However, this argument is not supported by the TEX₈₆-derived SSTs from ODP Site 1172 for the early Eocene, which are much higher (mean: 23°C - TEX₈₆^L, 28°C - TEX₈₆^H; Bijl et al., 2013b). Terrestrial, macroflorally derived temperatures on the order of 24°C from western Tasmania (Carpenter et al., 2012) suggest that this region was significantly warmer than the eastern part of Tasmania. Alternatively, another potential explanation for this discrepancy is that the sea-level rise during the early Eocene biased the composition of the sporomorph assemblages at ODP

Site 1172 (compare Section 4.4.2.3) towards a dominance of easily transported and/or particularly abundant sporomorphs indicative of cool conditions at the expense of rarer sporomorphs indicative of warmer conditions. This scenario is supported by the fact that many thermophilous plants from the Lower Eocene of the Southwest Pacific region (e.g., *Arecaceae* [palms], *Cupanieae*, *Ilex*, *Nypa*) are mainly insect-pollinated (Bush and Rivera, 1998; Barfod et al., 2011). Hence, these taxa reach only low abundances in pollen spectra when compared to wind-pollinated taxa, and they are not likely to be transported over larger distances before they settle (Jackson, 1994).

Despite of the potential bias on the early Eocene sporomorph assemblages at Site 1172, the supraregional replacement of temperate forests by paratropical forests during the early Eocene on Southeast Australia, New Zealand and Tasmania and the widespread occurrence of *Nypa* palms during the PETM in the same regions consistently indicate a pronounced reorganization of the vegetation during the early Eocene in the high southern latitudes connected to the PETM.

4.4.5 Integration with other precipitation records from the southern high latitudes

Based on our paleoclimatic results from the sporomorph record of ODP Site 1172, MAP on Tasmania was relatively constant (~180 cm/yr) from the middle Paleocene to the early Eocene (Fig. 4.4; Table 4.3). These values are comparable to the present-day precipitation received by rainforests in western Tasmania at ~42 °S (185 cm/yr, Corinna; Bureau of Metereology, 2012), along the west coast of the South Island of New Zealand (212 cm/yr; Westport; NIWA, 2012), northern Australia (180 cm/year, Darwin Botanic Gardens; Bureau of Metereology, 2012) and on the east coast of New Caledonia (197 cm/year, Puoébo; Pesin et al., 1995). The high-precipitation regime on Tasmania during the early Paleogene as deduced from the sporomorphs is further corroborated by the dominance of the dinocyst genus *Senegalinium* at ODP Site 1172 during this time interval (Sluijs et al., 2011); this genus is characterized by many freshwater-tolerant species (Sluijs et al., 2005; Brinkhuis et al., 2006). Hence, the observed *Senegalinium* dominance, which is best explained by substantial freshwater input, is well compatible with high precipitation on Tasmania and a resulting strong freshwater influx on the Tasmanian continental shelf during the early Paleogene.

Because of the general lack of precipitation data from other sites at high southern latitudes we can mainly compare our estimates from Tasmania with values deduced from other coeval paleobotanical records. Based on our results from sporomorph assemblages from Southeast Australia (Table 4.3), this region experienced similarly high precipitation (MAP: ~200 cm/yr) during the early Paleogene; this is consistent with MAP mean estimates (186–240 cm/yr) as derived from macrofloral records from the Upper Paleocene to Lower Eocene of the same region (Greenwood et al., 2003). On the Wilkes Land margin (Antarctica), high precipitation values (MAP mean: ~132 cm/yr) are also suggested for the early Eocene (Pross et al., 2012). These high precipitation values (>100 cm/yr) have been

corroborated recently by alkaline major element geochemistry for Eocene sediments from Antarctica (Passchier et al., 2013).

Based on the overall precipitation data, Tasmania and the Australia-Antarctic region experienced high rainfall conditions during the early Paleogene, comparable with present-day rainforests from southern latitudes. This lends support to modeling studies that include high atmospheric humidity as an important warming mechanism for the higher latitudes (e.g., Abbot et al., 2009).

4.4.6 Comparison with marine temperature evolution

Based on our sporomorph data (as evidenced in the Axis 1 sample scores of the DCA results, which represent the variation in floristic composition along the studied interval; Fig. 4.4) and the $\text{TEX}_{86}^{\text{L}}$ and $\text{TEX}_{86}^{\text{H}}$ data of Bijl et al. (2009; 2013b) and Hollis et al. (2014), there is a strong correlation between the vegetation composition on eastern Tasmania and SST at ODP Site 1172 (Fig. 4.4). This connection is clearly borne out by our results from the state space model, where there is a very strong correlation of 0.997 when DCA Axis 1 sample scores are compared with $\text{TEX}_{86}^{\text{L}}$ (95% highest posterior density: 0.633–0.999 based on Equation [4.4]; compare Section 4.2.4) and 0.978 when DCA Axis 1 sample scores are compared with $\text{TEX}_{86}^{\text{H}}$ (95% highest posterior density: 0.879–0.997 based on Equation [4.4]; compare Section 4.2.4). Hence, the strong correlation between the temperature variability derived from TEX_{86} and the floristic composition recorded at ODP Site 1172 demonstrates the impact of temperature on the vegetation dynamics in the Southwest Pacific region during the early Paleogene.

A close coupling between the temperature evolution in the marine and the terrestrial realms is also evident through the comparison of our sporomorph-based temperature estimates (notably WMMTs) with the TEX_{86} -derived SSTs (Fig. 4.4 and Table 4.3); it is only during the early Eocene that the pronounced warming trend recorded by $\text{TEX}_{86}^{\text{L}}$ and $\text{TEX}_{86}^{\text{H}}$ is not clearly reflected in the sporomorph-based temperature estimates, likely due to the sea-level increase during the early Eocene (compare Sections 4.4.2.3 and 4.4.3.2).

The terrestrial, sporomorph-derived MATs are markedly cooler than the SSTs derived from $\text{TEX}_{86}^{\text{L}}$ and $\text{TEX}_{86}^{\text{H}}$ (Fig. 4.4), which based on the traditional perception of the TEX_{86} proxy are supposed to represent surface-water MAT (e.g., Schouten et al., 2002). At the same time, the TEX_{86} -derived SSTs are closely related to the sporomorph-derived WMMTs (Fig. 4.4, Table 4.3). These observations suggest that TEX_{86} -based temperatures may be biased towards warm conditions when applied to early Paleogene records from the high southern latitudes. Such a warm (summer) bias has also been suggested for other early Paleogene records from the high southern latitudes based on different multiproxy approaches (Bijl et al., 2009; 2013a; Sluijs et al., 2011; Hollis et al., 2012; Pancost et al., 2013).

4.5 Conclusions

The middle Paleocene to early Eocene vegetation on Tasmania as reconstructed from the sporomorph record of ODP Site 1172 was characterized by three different forest types that thrived in high-precipitation regimes under different temperature conditions. These forest types were: (i) warm-temperate rainforests dominated by Podocarpaceae during the middle and late Paleocene; (ii) cool-temperate rainforests dominated by *Nothofagus* and Araucariaceae that transiently prevailed across the middle/late Paleocene transition interval (iii) paratropical rainforests dominated by Cyatheaceae during the early Eocene with the remarkable presence of the mangrove palm *Nypa* during the PETM and the earliest Eocene. The comparison with other, previously published floral records from the Southwest Pacific region (including Southeast Australia and New Zealand) supports the validity of our data for Tasmania. It shows that temperate forests were replaced by paratropical forests during the early Eocene throughout the Southwest Pacific region. This reorganisation in vegetation composition included an increase in fern (mainly Cyatheaceae) and angiosperm abundances (e.g., Proteaceae, Euphorbiaceae/Eumalvoideae, Casuarinaceae) at the expense of gymnosperms (mainly podocarps).

The integration of terrestrial (i.e., floristic) and previously published marine (i.e., TEX₈₆-based SST) climate information from ODP Site 1172 shows that the surface-water cooling of ~3°C across the middle/late Paleocene transition interval (~59.5 to ~59.0 Ma) was paralleled by a transient demise of frost-sensitive plants (i.e., palms and cycads) and the establishment of cool-temperate forests dominated by *Nothofagus* and Araucariaceae on Tasmania. This suggests that cooler conditions (and notably harsher winters with strong and/or frequent frosts) prevailed on Tasmania during that time.

In light of the statistically robust connection between the floristic composition of the sporomorph record from ODP Site 1172 and the previously published TEX₈₆-based SST record from the same site, the vegetation dynamics on Tasmania during the middle Paleocene to early Eocene were mainly driven by temperature; precipitation remained high (with a MAP mean of ~180 cm/yr) throughout that time. Based on the comparison of our sporomorph-derived temperatures with the TEX₈₆-based SSTs, we conclude that TEX₈₆^L- and TEX₈₆^H-derived temperatures for the high southern latitudes of the early Paleogene are likely biased towards summer conditions.

Acknowledgments

This research used samples and data provided by the Ocean Drilling Program (ODP). ODP was sponsored by the U.S. National Science Foundation and participating countries under management of Joint Oceanographic Institutions (JOI) Inc. Discussions with C. Hollis and A. Partridge are gratefully acknowledged. G. Harrington and L. Dupont are thanked for their constructive reviews. N. Welters is thanked for technical support and processing of samples. Support through the German Research Foundation (DFG; grant PR 651-10) and the Biodiversity and Climate Centre Frankfurt (BiK-F) is gratefully acknowledged. P.K.

Bijl thanks the LPP Foundation and the Netherlands Organisation for Scientific Research (NWO) for funding VENI grant # 863.13.002. The European Research Council under the European Community's Seventh Framework Program provided funding for this work by ERC Starting Grant #259627 to A. Sluijs.

4.6 Supplementary Information for Chapter 4

Supplementary table with all sporomorph data for this study is provided in `supplemdata1172.xlsx` and accessed through [doi:10.5194/cpd-10-291-2014](https://doi.org/10.5194/cpd-10-291-2014).

4.6.1 State space models

State space models assume there is an underlying “true” system, and what we observe is corrupted by observational noise. In particular, we assume that the “true” DCA axis score and Sea Surface Temperature (SST) evolve according to a bivariate Wiener process (e.g., Varughese and Pienaar, 2013), i.e. if $\mathbf{x}(t) = \{x_{DCA}(t), x_{SST}(t)\}$ is a vector of the DCA axis score and SST,

$$\mathbf{x}(t + Dt) \sim \text{MVN}(\mathbf{x}(t), Dt \mathbf{S}) \quad (\text{Eq. 4.5})$$

where \mathbf{S} is a covariance matrix:

$$\mathbf{\Sigma} = \begin{Bmatrix} \sigma_{DCA}^2 & \sigma_{DCA}\sigma_{SST}\rho \\ \sigma_{DCA}\sigma_{SST}\rho & \sigma_{SST}^2 \end{Bmatrix} \quad (\text{Eq. 4.6})$$

Thus, the “true” DCA axis score and SST both diffuse over time, and if they are correlated, the off-diagonal term in \mathbf{S} will be non-zero and can be read as a correlation between the true values.

We assume that the observed values of the DCA axis score and SST are corrupted by random noise, which we assume is independent and normally distributed:

$$SST_i \sim N(x_{SST}(t(i)), \tau_{SST}^2) \quad (\text{Eq. 4.7})$$

$$DCA_i \sim N(x_{DCA}(d(i)), \tau_{DCA}^2) \quad (\text{Eq. 4.8})$$

The correlation between observations decays with time, but we can estimate the correlation between SST and DCA based on:

$$\text{corr}(SST, DCA) = \frac{\Delta t \rho \sigma_{DCA} \sigma_{SST}}{\sqrt{(\Delta t + \tau_{DCA}^2)(\Delta t \sigma_{SST}^2 + \tau_{SST}^2)}} \quad (\text{Eq. 4.9})$$

We compared 60 SST datapoints with our 40 values of the DCA Axis 1 scores. Because only six of the SST datapoints and DCA Axis 1 sample scores are from the exact same depths, we estimated the values of DCA Axis 1 sample scores and SST through multiple imputation (e.g., Nakagawa and Freckleton, 2008); the missing data are treated as extra variables that are estimated in the same model. We took a Bayesian approach to the model fitting, which requires setting prior distributions on the parameters and missing data. The initial “true” values, $x_{DCA}(t)$ and $x_{SST}(t)$, were given independent normal priors with mean zero and standard deviation of 100. s_{DCA} , s_{SST} , t_{DCA} and s_{SST} were all given uniform priors between 0 and 100, and the prior for the correlation, r , was a uniform distribution between -1 and 1.

Two chains were run and after a burn-in of 10^6 iterations, a further 10^5 iterations were run, thinned to every 10^{th} iteration to give a total of 20,000 draws from the posterior. The R script for the analysis is given below.

R code script for the state space model

(written by Robert B. O’Hara)

```
# Read in data, and merge into one data frame
DCA=read.xls("To bob.xlsx", sheet=2)
SST=read.xls("To bob.xlsx", sheet=3)
names(SST)=c("Depth", "SST")

Data=merge(DCA,SST, by="Depth", all=T)
Data=Data[order(Data$Depth),]

# write.csv(Data, file="DCA_SST.csv")

# Write data for BUGS
DataToBUGS=list(NObs=nrow(Data), DCA=Data$DCA1, SST=Data$SST, Time=Data$Depth)
bugsData(DataToBUGS, "DCA_SSTbugs.txt")

# DataToBUGS=source("DCA_SSTbugs.txt")$value

# Plot the data
svg("Data.svg", width=8, height=6)
par(mfrow=c(2,1), mar=c(2,4,3,1), oma=c(2,0,0,0))
plot(DataToBUGS$Time, DataToBUGS$DCA, type="l", xlab="", ylab="DCA")
points(DataToBUGS$Time, DataToBUGS$DCA, pch=19, col=1+!is.na(DataToBUGS$SST),
       cex=0.5)
points(DataToBUGS$Time[!is.na(DataToBUGS$SST)],
       DataToBUGS$DCA[!is.na(DataToBUGS$SST)], pch=19, col=2, cex=0.5)
mtext("First DCA Coordinate", 3, line=0.5, adj=0.1)

plot(DataToBUGS$Time, DataToBUGS$SST, type="l", xlab="", ylab="Temperature")
points(DataToBUGS$Time, DataToBUGS$SST, pch=19, col=1+!is.na(DataToBUGS$DCA),
       cex=0.5)
points(DataToBUGS$Time[!is.na(DataToBUGS$DCA)],
       DataToBUGS$SST[!is.na(DataToBUGS$DCA)], pch=19, col=2, cex=0.5)
```

```

mtext("Sea Surface Temperature", 3, line=0.5, adj=0.1)
mtext("Depth", 1, line=2.53)
dev.off()

# Plot data with both SST and DCA
svg("Joint.svg", width=6, height=6)
par(mfrow=c(1,1), mar=c(4.1,4.1,1,1), oma=c(0,0,0,0))
plot(DataToBUGS$SST, DataToBUGS$DCA, xlab="Sea Surface Temperature", ylab="DCA
score")
dev.off()

# Look at the correlation between values where we have both
cor(DataToBUGS$SST, DataToBUGS$DCA, use="c")

# The BUGS model: 2D diffusion + observation error
TheModel=function() {
  for(t in 1:NObs) {
    SST[t] ~ dnorm(X[t,1], tauSST)
    DCA[t] ~ dnorm(X[t,2], tauDCA)
  }
  for(p in 1:2) {
    X[1,p] ~ dnorm(0,0.0001)
  }
  for(t in 2:NObs) {
    for(p in 1:2) {
      for(pp in 1:2) {
        TauT[t,p,pp] <- Tau[p,pp]/max(sqrt(Time[t] - Time[t-1]),0.00001)
      }
    }
    X[t,1:2] ~ dmnorm(X[t-1,1:2], TauT[t,,])
  }
  for(p in 1:2) {
    SD.tau[p] ~ dunif(0,100)
    Sigma[p,p] <- SD.tau[p]*SD.tau[p]
    Sigma[p,3-p] <- rho*SD.tau[p]*SD.tau[3-p]
  }
  rho ~ dunif(-1,1)
  Tau[1:2,1:2] <- inverse(Sigma[,])

  Var[1,1] <- Sigma[1,1] + 1/tauSST
  Var[2,2] <- Sigma[2,2] + 1/tauDCA
  for(p in 1:2) {
    StdDev[p] <- sqrt(Var[p,p])
    Var[p,3-p] <- Sigma[p,3-p]
    for(pp in 1:2) {
      Corr[p,pp] <- Var[p,pp]/sqrt(Var[p,p]*Var[pp,pp])
    }
  }
  sdSST ~ dunif(0,100); tauSST <- pow(sdSST,-2)
  sdDCA ~ dunif(0,100); tauDCA <- pow(sdDCA,-2)
}
writeModel(TheModel, "BUGSmodel.bug")

# Function to simulate initial values for the MCMC
SimInits=function(dat) {

```

```

#dat=DataToBUGS
Use=!is.na(dat$SST) & !is.na(dat$DCA)
DCA.lm=lm(dat$DCA[Use]~dat$SST[Use])
DCA.newdata=data.frame(SST=dat$SST[is.na(dat$DCA)])
DCApred=rnorm(sum(is.na(dat$DCA)),                                predict(DCA.lm,
newdata=DCA.newdata),sd(resid(DCA.lm))/sqrt(2))
DCAinit=ifelse(!is.na(dat$DCA), dat$DCA, DCApred)

SST.lm=lm(dat$SST[Use]~dat$DCA[Use])
SST.newdata=data.frame(DCAT=dat$DCA[is.na(dat$DCA)])
SSTpred=rnorm(sum(is.na(dat$SST)),                                predict(SST.lm,
newdata=SST.newdata),sd(resid(SST.lm))/sqrt(2))
SSTinit=ifelse(!is.na(dat$SST), dat$SST, SSTpred)

list(
  DCA=ifelse(!is.na(dat$DCA), NA, DCApred),
  SST=ifelse(!is.na(dat$SST), NA, SSTpred),
  X=cbind(
    rnorm(length(dat$DCA), DCAinit, sd(DCAinit)/sqrt(2)),
    rnorm(length(dat$SST), SSTinit, sd(SSTinit)/sqrt(2)) ),
    sdDCA=sd(dat$DCA, na.rm=T)/4, sdSST=sd(dat$SST, na.rm=T)/4,
    SD.tau=rgamma(2,10,100), rho=rbeta(1,48,2)
  )
)
# SimInits(DataToBUGS)

# Run BUGS
NChains=2 # 2 chains (mixes well, but takes time to converge)
bugsInits(replicate(NChains, SimInits(DataToBUGS), simplify=F), NChains,
  paste("DCA_SSTinits", 1:NChains, ".txt", sep=""))

modelCheck("BUGSmodel.bug")
modelData("DCA_SSTbugs.txt")
modelCompile(NChains)
modelInits(paste("DCA_SSTinits", 1:NChains, ".txt", sep=""))

# Burn in for 10^6 iterations
# Could do in 1 line, but sometimes BUGS traps, and this lets it continue
modelUpdate(1e4, thin=10) # 10k
modelUpdate(1e4, thin=10) # 20k
modelUpdate(1e4, thin=10) # 30k
modelUpdate(1e4, thin=10) # 40k
modelUpdate(1e4, thin=10) # 50k
modelUpdate(1e4, thin=10) # 60k
modelUpdate(1e4, thin=10) # 70k
modelUpdate(1e4, thin=10) # 80k
modelUpdate(1e4, thin=10) # 90k
modelUpdate(1e4, thin=10) # 100k

modelSaveState("DCA_SST1mInits")
# Record interesting variables
samplesSet("StdDev")
samplesSet("sdDCA")
samplesSet("sdSST")
samplesSet("rho")

```

```

# Run for another 10^5 iterations, thin to every 10
modelUpdate(1e3, thin=10) # 1k
modelUpdate(1e3, thin=10) # 2k
modelUpdate(1e3, thin=10) # 3k
modelUpdate(1e3, thin=10) # 4k
modelUpdate(1e3, thin=10) # 5k
modelUpdate(1e3, thin=10) # 6k
modelUpdate(1e3, thin=10) # 7k
modelUpdate(1e3, thin=10) # 8k
modelUpdate(1e3, thin=10) # 9k
modelUpdate(1e3, thin=10) # 10k

# Check convergence by eye
samplesHistory("rho")

# Save posteriors
samplesStats("*")
samplesCoda("*", "BasicModel")

rho=samplesSample("rho")

library(MCMCglmm) # only for posterior.mode

posterior.mode(rho)
HPDInterval(rho)

```

4.6.2. Weighted averages and propagated errors

Weighted averages were calculated following Equation (4.10) and their corresponding standard deviations (i.e., propagated errors) using Equation (4.11), μ is each climatic estimate, and σ is the error of each climatic estimate. For all climatic estimates with their corresponding errors see supplementary file `supplemdata1172.xlsx`. The R script for these calculations is given below.

$$\bar{\mu} = \frac{1}{\sum_{i=1}^n \frac{1}{\sigma_i^2}} \sum_{i=1}^n \frac{1}{\sigma_i^2} \mu_i \quad (\text{Eq. 4.10})$$

$$std = \sqrt{\frac{1}{n-1} \sum_{i=1}^n (\bar{\mu} - \mu_i)^2 + \frac{1}{n-1} \sum_{i=1}^n \sigma_i^2} \quad (\text{Eq. 4.11})$$

R code script for the weighted averages and propagated errors

(written by Robert B. O'Hara)

```

Table3=read.xls("all data for Table 3.xlsx", sheet=1, as.is=TRUE)
Table3$Group=paste(Table3$Location, Table3$Age, sep="_")

Table3$MAT...C.=as.numeric(Table3$MAT...C.)

```



```
Table3$MAP...cm.year.=as.numeric(Table3$MAP...cm.year.)
Table3$MAP.error=as.numeric(Table3$MAP.error)
Table3$CMMT...C.=as.numeric(Table3$CMMT...C.)
Table3$WMMT...C.=as.numeric(Table3$WMMT...C.)
```

```
an1=lm(MAT...C.~Group+0, weights=MAP...cm.year.^-2, data=Table3)
```

```
GetMeanVar=function(vals, sds) {
  if(length(vals)==0) { res=c(mean=-1, sd=-1) } else {
  if(length(vals)==1) { res=c(mean=vals, sd=sds) } else {
    mean=weighted.mean(vals, sds^-2)
    var=var(vals) + sum(sds^2)/(length(vals)-1)
    res=c(mean=mean, sd=sqrt(var))
  }
}
res
}
```

```
by(Table3, list(Table3$Location, Table3$Age), function(df) {
#df=Table3[Table3$Location=="Otaio Section" & Table3$Age=="early Eocene",]
res=rbind(GetMeanVar(df$MAT...C., df$MAT.error),
  GetMeanVar(df$MAP...cm.year., df$MAP.error),
  GetMeanVar(df$CMMT...C., df$CMMT.error),
  GetMeanVar(df$WMMT...C., df$WMMT.error))
colnames(res)=c("Mean", "STDDev")
rownames(res)=c("MAT", "MAP", "CMMT", "WMMT")
res
})
```

4.6.3. Selected sporomorph taxa

Plate I.

All specimens are from the Paleocene and Eocene of ODP Site 1172. Scale bars equal 10 μm .

1. *Gleicheniidites senonicus* Ross, 1949; Sample 17R-4, 40–42 cm (629.87–629.89 rmbsf), Slide 4, England-Finder coordinates L9.
2. *Evansispora senonica* Raine, 2008; Sample 17R-7, 20–22 cm (634.17–634.19 rmbsf), Slide 1, E35.
3. *Cyathidites australis* Couper, 1953; Sample 15R-5, 134–136 cm (612.85–612.87 rmbsf), Slide 1, C24/3.
- 4.-5. *Ceratosporites* spp. complex; Sample 15R-5, 134–136 cm (612.85–612.87 rmbsf), Slide 2, P38; Sample 15R5, 124–126 cm (612.75–612.77 rmbsf), Slide 1, M26/4.
6. *Podocarpidites exiguus* Harris, 1965; Sample 20R-5, 40–43 cm (660.18–660.21 rmbsf), Slide 1, Q28/3.
7. *Phyllocladites mawsonii* Cookson, 1947 ex Couper, 1953; Sample 20R-5, 40–43 cm (660.18–660.21 rmbsf), Slide 1, M20.
8. *Araucariacites australis* Cookson, 1947; Sample 17R-6, 40–42 cm (631.37–631.39 rmbsf), Slide 1, O22.

9. *Dilwynites granulatus* Harris, 1965; Sample 19R-1, 40–42 cm (644.58–644.6 rmbsf), Slide 2, Q22.
10. *Spinizonocolpites prominatus* (McIntyre) Stover and Evans, 1973; Sample 15R-4, 135–137 cm (611.36–611.38 rmbsf), Slide 1, E28/1.
11. *Cycadopites follicularis* Wilson & Webster, 1946; Sample 15R-3, 40–42 cm (608.9–608.92 mbsf), Slide 2, M33/1.
12. *Arecipites* sp.; Sample 14R-3, 40–42 cm (599.74–599.76 rmbsf), Slide 4, N20/4.

Plate II.

All specimens are from the Paleocene and Eocene of ODP Site 1172. Scale bars equal 10 μ m.

1. *Banksieaeidites arcuatus* Stover in Stover and Partridge 1973, Sample 15R-7, 40–42 cm (614.91–614.93 rmbsf), Slide 2, G15/4.
2. *Propylipollis latrobensis* (Harris) Martin and Harris, 1974; Sample 15R-6, 50–52 cm (613.51–613.53 rmbsf), Slide 1, X19/1.
3. *Proteacidites teuixinus* Stover in Stover and Partridge, 1973; Sample 15R-5, 114–115 cm (612.65–612.66 rmbsf), Slide 1, E16/2.
4. *Proteacidites adenanthoides* Cookson, 1950; Sample 15R-5, 5–7 cm (611.56–611.58 rmbsf), Slide 1, U32.
5. *Myricipites harrisii* (Couper) Dutta and Sah, 1970; Sample 15R-5, 44–45 cm (611.95–611.96 rmbsf), Slide 1, Q20.
6. *Gambierina edwardsii* (Cookson and Pike) Harris, 1972; Sample 20R-5, 40–43 cm (660.18–660.21 rmbsf), Slide 2, V22/1.
7. *Malvacipollis subtilis* Stover in Stover and Partridge, 1973; Sample 15R-5, 19–21 cm (611.7–611.72 rmbsf), Slide 1, X29.
8. *Nothofagidites* cf. *endurus* (Cookson) Harris, 1965; Sample 20R-1, 40–42 cm (654.18–654.20 rmbsf), Slide 2, N24.
9. *Nothofagidites brachyspinulosus* (Cookson) Harris, 1965; Sample 15R-3, 40–42 cm (608.9–608.92 rmbsf), Slide 2, Y49.
10. *Alisporites* sp.; Sample 18R-6, 40–42 cm (641.97–641.99 rmbsf), Slide 1, R26/4 [reworked].
11. *Cannanoropollis* sp.; Sample 20R-4, 40–42 cm (658.67–658.69 rmbsf), Slide 2, Q29/2 [reworked].
12. *Protohaploxylinus* sp.; Sample 20R-5, 40–43 cm (660.18–660.21 rmbsf), Slide 1, C28/3 [reworked].



Plate I.

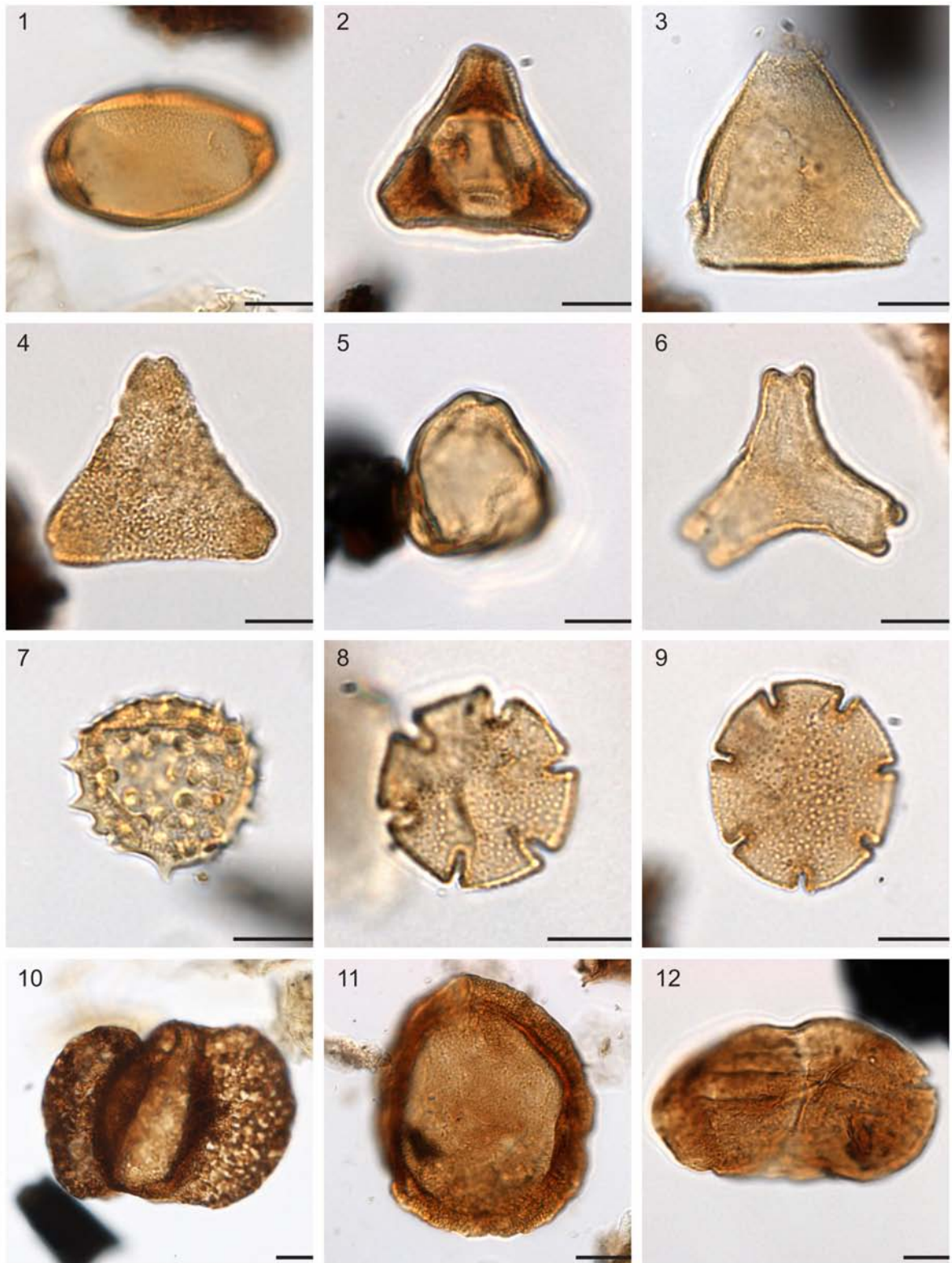


Plate II.

Chapter 5. Conclusions and Outlook

5.1 Conclusions

This study yields new quantitative, mean annual and seasonal temperatures derived from sporomorph records of well-dated marine sediments deposited on east Antarctica and Tasmania during the early Paleogene. Particularly, the present study presents the first terrestrial climate reconstruction of the early Eocene on Antarctica and provides the first continental evidence of the recently traced cooling event that took place during the middle/late Paleocene transition.

Particularly, on east Antarctica, the sporomorph-based climatic estimations of Site U1356 from this study combined with MBT/CB derived temperatures from the same hole suggest that the climate in lowland settings along the Wilkes Land coast (at a paleolatitude of $\sim 70^\circ$ south) was near-tropical during the early Eocene (53.9 – 51.9 Ma). Based on the sporomorph results presented in this study, we concluded that the extremely high temperatures during this time interval allowed the growing of highly diverse, near-tropical forests characterized by thermophilous elements such as palms and Bombacoideae. Moreover, the sporomorph-based climatic estimations reflect that winters were extremely mild (warmer than 10°C) and essentially frost-free despite the polar darkness during the early Eocene along the Wilkes Land margin. Considering the 50 days of polar darkness for a latitude of 70°S , this study provides evidence that the photoperiod was not an obstacle to the development of high plant diversities at higher latitudes and that the high atmospheric concentration of CO_2 during the early Eocene was probably an important factor in the physiological adaptation of high-latitude forests.

With regard to the mid-Eocene record (49.3 – 46 Ma), the sporomorph assemblages from the present study reflect that temperate forests dominated by *Nothofagus* were the prevailing vegetation along the Wilkes Land margin during this time interval. The dominance of temperate forests together with the absence of thermophilous elements reflects cooler conditions during the mid-Eocene when compared to the early Eocene record. This conclusion is further supported by the lower temperatures derived from the MBT/CBT proxy and the sporomorph-based climatic reconstructions presented in this study.

The combined quantitative and qualitative analyses of the vegetation used in this study reflect that two types of markedly different vegetation were thriving along the Wilkes Land margin during the early and mid-Eocene times. Quantitatively, these differences are reflected on the results of DCA and rarefaction analyses as well as on the diversity indices and species accumulation curves portrayed in the present study. Qualitatively, the results from this study reflect that the early Eocene vegetation was probably multi-storeyed, with a tall, relatively open canopy and diverse overstorey. In contrast, the mid-Eocene vegetation was predominantly characterized by cool temperate forests with a single canopy layer dominated by *Nothofagus*. Moreover, the comparison of the diversity results from the

present study with modern (i.e., Holocene) records through species accumulation curves suggests that the early Eocene forests along the Wilkes Land margin were characterized by richness patterns similar to present-day forests from New Caledonia. In contrast, mid-Eocene forests along the Wilkes Land margin were characterized by similar richness to modern *Nothofagus* forests from New Zealand.

The results provided in this study from Site 1172 suggest that three different vegetation types were thriving on Tasmania, under different temperature conditions from the middle Paleocene to the early Eocene. During the middle to late Paleocene, warm-temperate forests dominated by gymnosperms were the prevailing vegetation on Tasmania. These warm-temperate forests were transiently replaced by cool-temperate forests dominated by *Nothofagus* and Araucariaceae during the middle/late Paleocene transition (~59.5 to ~59.0 Ma). The consistent absence of frost sensitive elements (i.e., palms and cycads) across the middle/late Paleocene transition interval, together with the transient establishment of cool-temperate forests, indicate markedly cooler conditions, with harsher winters on Tasmania during that time. Moreover, based on the present study results, it is possible to infer that paratropical forests were established on Tasmania during the early Eocene and that this vegetation replacement was strongly related to the PETM event. The integration with available information of terrestrial vegetation and climatic conditions from other regions along the southwest Pacific region further supports the validity of the sporomorph data derived from Site 1172. This integration was augmented by newly generated climate estimates in the present study of previously published sporomorph records from Southeast Australia and New Zealand.

Based on the paleoclimate results from ODP Site 1172, we suggest that MAP on Tasmania was nearly constant (~180 cm/yr) from the middle Paleocene to the early Eocene. On East Antarctica, the MAP estimates from Site U1356 reflect an average of ~132 cm/yr during the early Eocene and a mean of 160 cm/yr for the mid-Eocene record. Hence, based on the estimated precipitation data from both sites, it is possible to establish that the Australo-Antarctic region experienced high rainfall conditions (>100 cm/yr) during the early Paleogene comparable with MAP values of present-day rainforests from southern latitudes. These precipitation values support modeling studies that include high atmospheric humidity as an important mechanism for warming the higher latitudes during the early Paleogene.

The integration of the sporomorph results of Site 1172 from this study with previously published TEX₈₆-based SSTs from the same hole documents that the vegetation dynamics on Tasmania were closely linked with the temperature evolution of the marine realm from the same region. Moreover, the comparison of our sporomorph-based climatic estimates from Site 1172 with the TEX₈₆^L- and TEX₈₆^H-based temperature data suggests a warm-season bias of both calibrations for the early Paleogene when applied to high southern latitudes.

5.2 Outlook

A major obstacle in understanding the ecosystem and climatic conditions from Antarctica during the Cenozoic is the general lack of well-dated terrestrial records from this region (Lewis et al., 2008). The present study provides new climatic and vegetation data from the Wilkes Land margin (east Antarctica) for the Eocene based on chronostratigraphically well-calibrated (Bijl et al., 2013b) sporomorph records. However, the results from the present study do not represent the terrestrial conditions of Antarctica as a whole during the early to middle Eocene. Hence, the documentation of floral assemblages from strata with well-constrained ages from other regions in Antarctica appears indispensable to elucidate the terrestrial ecosystems on polar regions during the greenhouse conditions of the early Paleogene. Any such effort focusing on the early Eocene should take into account the presence of the low-latitude-derived warm Proto-Leeuwin Current as an important mechanism for warming the terrestrial settings along the Australo-Antarctic Gulf (Bijl et al., 2013a). Hence, it appears possible that the extremely warm conditions that characterized the Wilkes Land margin during the early Eocene might be only recorded in localities where the Proto-Leeuwin Current had influence during this time interval.

The “equable climate problem” can be explained as a response to increased radiative forcing in the form of very high ρCO_2 (Huber and Caballero, 2011). However, additional factors such as the relative humidity have also been thought to play an important role on the extremely warm higher latitudes (equable climates) during the early Paleogene (Abbot et al., 2009). Although this study presents new MAP estimates from high southern latitudes during the early Paleogene, a comparison with other proxies (e.g., deuterium/hydrogen [D/H]; alkaline major element geochemistry) seems indispensable to further explore the effects of high atmospheric humidity on higher latitudes during the early Paleogene.

Comparison with other southern latitudes records appears essential to understand the connection between climate and vegetation during the early Paleogene from a regional point of view. In this study a preliminary comparison in Sections 1.2, 2.4.6 and 4.4.3 is presented. However, further studies would first have to focus on a critical assessment of the ages given for the different floras along the high southern latitudes mainly for data derived from South America and Antarctica. Particularly, no radiometric ages are available for paleobotanical records from Argentina and Chile with the exception of the macrofloras studied by Wilf et al. (2005) of the early Eocene. Moreover, early Eocene records have been thought to be founded on the Antarctic peninsula (Ivany et al., 2008). However, dinocyst-based evaluation of the age for these records suggests that the early Eocene is not recorded in this region (compare Section 2.4.6). The scarcity of comparable sites, as outlined above, indicates that few records along high southern latitudes are directly comparable with the obtained data from the present study.

The vegetation effects of the PETM along high southern latitudes are still insufficiently constrained. Most of the studies related to this time interval are focused on marine pollen records from New Zealand (Crouch and Visscher, 2003; Crouch and Brinkhuis, 2005;

Handley et al., 2011). Moreover, the new results presented in this study from Site 1172 reflect that the current marine records of the PETM from the high southern latitudes are probably biased toward easily transported sporomorphs, due to the high sea level during this time interval (Contreras et al., 2014; see Chapter 4). Additionally to this potential bias, the obtained sporomorph data of Site 1172 for the PETM interval are characterized by extremely low counting sums. Considering these evidences, it seems possible that future sporomorph analyses at Site 1172, may have not provided relevant results to constrain the terrestrial conditions during the PETM interval. Hence, it becomes indispensable to compare with potential terrestrial PETM records that were not affected by sea level change during this time interval. In such an effort, a particular emphasis should be placed on high-resolution studies of terrestrial records with well-constrained ages.

The middle/late Paleocene transition cooling event has been recently traced on marine records from the southwest Pacific region (Hollis et al., 2014). The SSTs recorded during this time interval indicates cooler conditions comparable to the cooler conditions at ~34 Ma when first major ice sheets of the Cenozoic appeared on Antarctica (Bijl et al., 2009; 2013b). Moreover, current studies in the southwest Pacific region reveal a short-lived ice sheet growth on Antarctica during this time interval (Hollis et al., 2014). The results provided in the present study are in good agreement with the inferred extremely cool conditions on Antarctica during this time interval. However, they are currently the only terrestrial evidence of this transient cooling event. Hence, in order to obtain more insights into the mechanisms involved in this short-lived cooling, it seems indispensable to apply an integrated perspective that takes into account an assessment of the terrestrial conditions including different localities along high southern latitudes.

Acknowledgements

The completion of this PhD thesis would not have been possible without the help of many people that were supporting me in different ways before and during my stay in Germany. I am very grateful to all of them.

First of all, my thanks go to Juan Carlos Berrío, José Ignacio Martínez, Carlos Jaramillo and Vladimir Torres who were my first supervisors and the people that inspired me to study palynology, paleoclimatology and statistics. They were really supportive during the first part of my career and it was thanks to their motivation that I was able to start a PhD far away from home. Thank you for your inspiration!

On the way to start my PhD in Germany, I mainly would like to say thanks to Bas van de Schootbrugge who interviewed me for the PhD position and who motivated me to start a new life in another country. Thanks, Bas, for making me feel very comfortable on my arrival in Germany and for all your invaluable support during my process here.

I would specially like to say thanks to my main supervisor Jörg Pross and to the opportunity to work on this interesting project. Thank you for all the solutions to the problems that you have provided to me. Also for your reviews, critical comments, and innumerable inputs to my study. All of them have been essential for the development of this thesis.

I would like to say thanks to all the colleagues and professors from the Institute of Paleontology of Frankfurt University. I sincerely thank Silke Voigt for her cooperation in the last state of my thesis. I am very grateful to Cornelia Anhalt, who has always been efficient and kind with every request for the development of this project. I would specially thank my friends Ulrike Wacker and Jessica Zirkel for all the experiences and support during the PhD process. I am very grateful to Claudia Jung, Miriam Koch and Friederike Adomat for their kindness and all the nice experiences that we spent together. Special thanks go to Andreas Koutsodendris for all the academic and personal support, also thanks to your girls: Woula and Maya for making me feel part of the family when I visited your home. Additionally, for the last part of this process, I would like to say thanks to Angela Fraguas and Sietske Batenburg who were really supportive and friendly since they arrived in the department; thanks for giving me such good energy for finishing!

I sincerely thank Peter Bijl from Utrecht University who has been one of the most important persons for making possible this PhD thesis due to his expertise on the early Paleogene from the Southern Ocean and his valuable cooperation with my research. Henk Brinkhuis and Stefan Schouten were also really supportive and inspiring on the first part of this PhD thesis.

I would like specially to say thanks to Ian Raine who was the person that helped me with the identification of some pollen and spores presented in this study and for giving a strong value to the taxonomical work.

I say thanks to Carlos Cuartas, Linda Adam and Bob O'hara for their fast but very useful help with the software R for statistical computing that saved me a lot of time for getting the paleoclimatic estimates and statistical results presented in this thesis.

I sincerely thank Ulrike Wacker for writing the German abstract for this thesis. I also thank Ulrich Kotthoff for his review and last contributions to this abstract.

I would like specially to thank the Language Service of the Goethe Graduate Academy (GRADE) for reviewing the English of some sections (i.e., Abstract, Introduction, Chapter 5 and Acknowledgements) of this thesis.

I am very grateful to all people whom I have met during these last almost four years and who have been really supportive on the scientific part of this study. Some of them I do not know in person, but the discussion during conferences, meetings or through mail, really enhanced the final product of this study. These people include Alan Partridge, Alexander Houben, Appy Sluijs, Bob O'Hara, Carlota Escutia, Chris Hollis, David Greenwood, Heiko Pälike, Janelle Stevenson, Jerry Dickens, Monica Carvallo, Patrick Moss, Peter Kershaw, Sabine Gollner, Steve Bohaty, Steven Higgins, Torsten Utescher and Ursula Röhl.

I specially say thanks to Lara Lyachenko, Bärbel Schminke, Natasha Welters and Niklas Löffler for their technical support.

I would like to thank my dear friends Angelo Plata, Ivonne Rodríguez, Jennifer Betancourt, Linda Adam, Carlos Magallanes, Fernando Mantilla, Carlos Cuartas, Mario Andrés Pachón, Atenea González, Vanessa Gleiß, Isabel Stümpel and my sister Jenni Contreras for not forgetting about me, and for giving me so much support through your calls, meetings or mails.

Finalmente, quiero dar muchas gracias a mi mamá por estar siempre pendiente de mi, y ser la persona que con su amor y sabiduría siempre me hace ver el lado positivo de las situaciones y me da muchas fuerzas para continuar. Und dir Arne, für deine Liebe, Freude und Frieden, die mir geholfen haben diese Arbeit zu beenden.

References

- Abbot, D.S., Huber, M., Bousquet, G., Walker, C.C., 2009. High-CO₂ cloud radiative forcing feedback over both land and ocean in a global climate model. *Geophysical Research Letters* 36, L05702.
- Abbot, D.S., Tziperman, E., 2008. Sea ice, high-latitude convection, and equable climates. *Geophysical Research Letters* 35, L03702.
- Anderson, J.B., Warny, S., Askin, R.A., Wellner, J.S., Bohaty, S.M., Kirshner, A.E., Livsey, D.N., Simms, A.R., Smith, T.R., Ehrmann, W., Lawver, L.A., Barbeau, D., Wise, S.W., Kulhanek, D.K., Weaver, F.M., Majewski, W., 2011. Progressive Cenozoic cooling and the demise of Antarctica's last refugium. *Proceedings of the National Academy of Sciences of the United States of America* 108, 11356-11360.
- Askin, R.A., 1989. Endemism and heterochroneity in the Late Cretaceous (Campanian) to Paleocene palynofloras of Seymour Island, Antarctica: implications for origins, dispersal and palaeoclimates of southern floras. *Geological Society London Special Publications* 47, 107-119.
- Askin, R.A., 1990. Campanian to Paleocene spore and pollen assemblages of Seymour Island, Antarctica. *Review of Palaeobotany and Palynology* 65, 105-113.
- Askin, R.A., 2000. Spores and pollen from the McMurdo Sound erratics. *Antarctic Research Series* 76, 161-181.
- Askin, R.A., Raine, J.I., 2000. Oligocene and Early Miocene terrestrial palynology of the Cape Roberts Drillhole CRP-2/2A, Victoria Land Basin, Antarctica. *Terra Antarctica* 7, 493-501.
- APSA Members, 2007. The Australasian Pollen and Spores Atlas V.1.0. Australian National University, Canberra, <http://apsa.anu.edu.au/about>.
- Australian National Herbarium, 2011. ANHSIR: ANH Specimen Information Register, IBIS database, <http://www.anbg.gov.au/cpbr/program/hc/hc-ANHSIR.html>.
- Baker, W.J., Couvreur, T.L.P., 2013. Global biogeography and diversification of palms sheds light on the evolution of tropical lineages. II. Diversification history and origin of regional assemblages. *Journal of Biogeography* 40, 286-298.
- Barfod, A.S., Hagen, M., Borchsenius, F., 2011. Twenty-five years of progress in understanding pollination mechanisms in palms (Arecaceae). *Annals of Botany* 108, 1503-1516.
- Baroni, C., Noti, V., Ciccacci, S., Righini, G., Salvatore, M.C., 2005. Fluvial origin of the valley system in northern Victoria Land (Antarctica) from quantitative geomorphic analysis. *Geological Society of America Bulletin* 117, 212-228.

- Barreda, V., Palazzesi, L., 2007. Patagonian vegetation turnovers during the Paleogene-Early Neogene: Origin of arid-adapted floras. *The Botanical Review* 73, 31-50.
- Barrett, P.J., 1996. Antarctic paleoenvironment through Cenozoic times - a review. *Terra Antarctica* 3, 103-119.
- Barron, E., 1987. Eocene equator-to-pole surface ocean temperatures: A significant climate problem? *Paleoceanography* 2, 729-739.
- Bartish, I.V., Antonelli, A., Richardson, J.E., Swenson, U., 2011. Vicariance or long-distance dispersal: historical biogeography of the pantropical subfamily Chrysophylloideae (Sapotaceae). *Journal of Biogeography* 38, 177-190.
- Baum, D.A., DeWitt Smith, S., Yen, A., Alverson, W.S., Nyffeler, R., Whitlock, B.A., Oldham, R.L., 2004. Phylogenetic relationships of Malvaceae (Bombacoideae and Malvoideae; Malvaceae sensu lato) as inferred from plastid DNA sequences. *American Journal of Botany* 91, 1863-1871.
- Bayer, C., Kubitzki, K., 2003. Malvaceae. In: Kubitzki, K., Bayer, C. (Eds.), *Flowering plants, dicotyledons: Malvales, Capparales, and Non-betalain Caryophyllales*. Springer, Germany, pp. 225-311.
- Beerling, D.J., Osborne, C.P., 2002. Physiological ecology of Mesozoic polar forests in a high CO₂ environment. *Annals of Botany* 89, 329-339.
- Beerling, D.J., Royer, D.L., 2011. Convergent Cenozoic CO₂ history. *Nature Geoscience* 4, 418-420.
- Bijl, P.K., 2011. *Environmental and Climatological Evolution of the Early Paleogene Southern Ocean*. LPP Contribution Series No. 34, Utrecht University, Utrecht, the Netherlands. 213 pp.
- Bijl, P.K., Bendle, J.A., Bohaty, S.M., Pross, J., Schouten, S., Tauxe, L., Stickley, C.E., McKay, R.M., Röhl, U., Olney, M., Sluijs, A., Escutia, C., Brinkhuis, H., Expedition 318 Scientists, 2013a. Eocene cooling linked to early flow across the Tasmanian Gateway. *Proceedings of the National Academy of Sciences of the United States of America* 110, 9645-9650.
- Bijl, P.K., Houben, A.J., Schouten, S., Bohaty, S.M., Sluijs, A., Reichert, G.J., Sinninghe Damsté, J.S., Brinkhuis, H., 2010. Transient Middle Eocene atmospheric CO₂ and temperature variations. *Science* 330, 819-821.
- Bijl, P.K., Pross, J., Warnaar, J., Stickley, C.E., Huber, M., Guerin, R., Houben, A.J.P., Sluijs, A., Visscher, H., Brinkhuis, H., 2011. Environmental forcings of Paleogene Southern Ocean dinoflagellate biogeography. *Paleoceanography* 26, PA1202.
- Bijl, P.K., Schouten, S., Sluijs, A., Reichert, G.J., Zachos, J.C., Brinkhuis, H., 2009. Early Palaeogene temperature evolution of the southwest Pacific Ocean. *Nature* 461, 776-779.

- Bijl, P.K., Sluijs, A., Brinkhuis, H., 2013b. A magneto- and chemostratigraphically calibrated dinoflagellate cyst zonation of the early Palaeogene South Pacific Ocean. *Earth-Science Reviews* 124, 1-31.
- Blevin, J.C., 2003. Petroleum geology of the Bass Basin – Interpretation Report, An Output of the Western Tasmanian Regional Minerals Program. *Geoscience Australia Record* 2003/19.
- Boreham, C.J., Blevin, J.E., Radlinski, A.P., Trigg, K.R., 2003. Coal as a source of oil and gas: a case study from the Bass Basin, Australia. *APPEA Journal* 43, 117-148.
- Brinkhuis, H., Schouten, S., Collinson, M.E., Sluijs, A., Sinninghe Damsté, J.S., Dickens, G.R., Huber, M., Cronin, T.M., Onodera, J., Takahashi, K., Bujak, J.P., Stein, R., van der Burgh, J., Eldrett, J.S., Harding, I.C., Lotter, A.F., Sangiorgi, F., van Konijnenburg-van Cittert, H., de Leeuw, J.W., Matthiessen, J., Backman, J., Moran, K., the Expedition 302 Scientists, 2006. Episodic fresh surface waters in the Eocene Arctic Ocean. *Nature* 441, 606-609.
- Brinkhuis, H., Sengers, S., Sluijs, A., Warnaar, J., Williams, G.L., 2003. Latest Cretaceous–earliest Oligocene and Quaternary dinoflagellate cysts, ODP Site 1172, East Tasman Plateau. *Proceedings of the Ocean Drilling Program, Scientific Results* 189, 1-48.
- Bureau of Metereology, 2012. Climate Data Online, <http://www.bom.gov.au/climate/data/>.
- Bush, M.B., Rivera, R., 1998. Pollen dispersal and representation in a neotropical rain forest. *Global Ecology and Biogeography* 7, 379-392.
- Caldeira, K., Wickett, M.E., 2003. Anthropogenic carbon and ocean pH. *Nature* 425, 365.
- Calver, C.R., Clarke, M.J., Truswell, E.M., 1984. The stratigraphy of a late Palaeozoic borehole section at Douglas River, Eastern Tasmania: a synthesis of marine macro-invertebrate and palynological data. *Papers and proceedings of the Royal Society of Tasmania* 118, 137-161.
- Cande, S.C., Stock, J.M., 2004. Cenozoic reconstruction of the Australia-New Zealand-South Pacific sector of Antarctica. In: Exon, N.F., Kennett, J.P., Malone, M. (Eds.), *The Cenozoic Southern Ocean: Tectonics, Sedimentation and Climate Change Between Australia and Antarctica*. American Geophysical Union, Washington, pp. 5-18.
- Cao, L., 1992. Late Cretaceous and Eocene palynofloras from Fildes Peninsula, King George Island (South Shetland Islands), Antarctica. In: Yoshida, Y., Funali, M., Kaminuma, S., Funali, M., Kaminuma, S., Funali, M., Kaminuma, S. (Eds.), *Recent Progress in Antarctic Earth Science*. Terra Scientific Publishing Company, Tokyo, pp. 363-369.
- Cardenas, M.L., Gosling, W.D., Sherlock, S.C., Poole, I., Pennington, R.T., Mothes, P., 2011. The response of vegetation on the Andean flank in western Amazonia to Pleistocene climate change. *Science* 331, 1055-1058.

- Carpenter, R.J., Jordan, G.J., Macphail, M.K., Hill, R.S., 2012. Near-tropical Early Eocene terrestrial temperatures at the Australo-Antarctic margin, western Tasmania. *Geology* 40, 267-270.
- Chinnock, R.J., 1998. *Huperzia*, Flora of Australia Online, <http://www.anbg.gov.au/abrs/online-resources/flora/>.
- Chinnock, R.J., Bell, G.H., 1998. Gleicheniaceae, Flora of Australia Online, <http://www.anbg.gov.au/abrs/online-resources/flora/>.
- Cocozza, C.D., Clarke, C.M., 1992. Eocene microplankton from La Meseta Formation, Northern Seymour Island. *Antarctic Science* 4, 355-362.
- Collinson, M.E., 2000. Fruit and seed floras from the Palaeocene/Eocene transition and subsequent Eocene in southern England: Comparison and palaeoenvironmental implications. *GFF* 122, 36-37.
- Contreras, L., Pross, J., Bijl, P.K., Koutsodendris, A., Raine, J.I., van de Schootbrugge, B., Brinkhuis, H., 2013. Early to Middle Eocene vegetation dynamics at the Wilkes Land Margin (Antarctica). *Review of Palaeobotany and Palynology* 197, 119-142.
- Contreras, L., Pross, J., Bijl, P.K., O'Hara, R.B., Raine, J.I., Sluijs, A., Brinkhuis, H., 2014. Southern high-latitude terrestrial climate change during the Paleocene–Eocene derived from a marine pollen record (ODP Site 1172, East Tasman Plateau). *Climate of the Past* 10, 1401-1420.
- Couper, R.A., 1960. New Zealand Mesozoic and Cainozoic plant microfossils. *New Zealand Geological Survey Paleontological Bulletin* 32, 1-88.
- Cramer, B.S., Miller, K.G., Barrett, P.J., Wright, J.D., 2011. Late Cretaceous–Neogene trends in deep ocean temperature and continental ice volume: Reconciling records of benthic foraminiferal geochemistry ($\delta^{18}\text{O}$ and Mg/Ca) with sea level history. *Journal of Geophysical Research* 116, C12023.
- Crouch, E.M., 2001. Environmental Change at the time of the Late Paleocene-Eocene Biotic turnover. LPP Contribution Series No. 14, Utrecht University, Utrecht, the Netherlands. 216 pp.
- Crouch, E.M., Brinkhuis, H., 2005. Environmental change across the Paleocene–Eocene transition from eastern New Zealand: A marine palynological approach. *Marine Micropaleontology* 56, 138-160.
- Crouch, E.M., Visscher, H., 2003. Terrestrial vegetation record across the initial Eocene thermal maximum at the Tawanui marine section, New Zealand. In: Wing, S., Gingerich, P.D., Schmitz, B., Thomas, E. (Eds.), *Causes and Consequences of Globally Warm Climates in the Early Paleogene*. Geological Society of America Special Paper 369, Boulder, Colorado, pp. 351-363.

- Crouch, E.M., Willumsen, P.S., Kulhanek, D., Gibbs, S., 2014. A revised Paleocene (Teurian) dinoflagellate cyst zonation from eastern New Zealand. *Review of Palaeobotany and Palynology* 202, 47-79.
- Crowley, J.L., 2000. Carbon dioxide and Phanerozoic climate. In: Huber, B.T., Kennen, G.M., Wing, S.L. (Eds.), *Warm Climates in Earth History*. Cambridge University Press, Cambridge, pp. 425-445.
- Cui, Y., Kump, L.R., Ridgwell, A.J., Charles, A.J., Junium, C.K., Diefendorf, A.F., Freeman, K.H., Urban, N.M., Harding, I.C., 2011. Slow release of fossil carbon during the Palaeocene–Eocene Thermal Maximum. *Nature Geoscience* 4, 481-485.
- DeLucia, E.H., Hamilton, J.G., Naidu, S.L., Thomas, R.B., Andrews, J.A., Finzi, A., Lavine, M., Matamala, R., Mohan, J.E., Hendrey, G.R., Schlesinger, W.H., 1999. Net primary production of a forest ecosystem with experimental CO₂ enrichment. *Science* 284, 1177-1179.
- Department of Primary Industries, 1999. Gippsland Basin biostratigraphic reports, Version 0.5c, in: Minerals and Petroleum Division, G.V. (Ed.). Victoria, Australia.
- Dettmann, M.E., 1963. Upper Mesozoic microfloras from South-eastern Australia. *Proceedings of the Royal Society of Victoria* 77, 1-148.
- Dettmann, M.E., Jarzen, D.M., 2000. Pollen of extant *Wollemia* (Wollemi Pine) and comparisons with pollen of other extant and fossil Araucariaceae. In: Harley, M.M., Morton, C.M., Blackmore, S. (Eds.), *Pollen and Spores: Morphology and Biology*. Royal Botanic Gardens, Kew, UK, pp. 187-203.
- Dickens, G.R., O'Neil, J.R., Rea, D.K., Owen, R.M., 1995. Dissociation of oceanic methane hydrate as a cause of the carbon isotope excursion at the end of the Paleocene. *Paleoceanography* 10, 965-971.
- Dickison, W., 2007. Strasburgeriaceae. In: Kubitzki, K. (Ed.), *Flowering Plants, Eudicots. Berberidopsidales, Buxales, Crossosomatales, Fabales p.p., Geraniales, Gunnerales, Myrtales p.p., Proteales, Saxifragales, Vitales, Zygophyllales, Clusiaceae Alliance, Passifloraceae Alliance, Dilleniaceae, Huaceae, Picramniaceae, Sabiaceae*. Springer, Germany, pp. 446-448.
- Dodson, J.R., 1976. Modern pollen spectra from Chatham Island, New Zealand. *New Zealand Journal of Botany* 14, 341-347.
- Duarte, L.D.S., Prieto, P.V., Pillar, V.D., 2012. Assessing spatial and environmental drivers of phylogenetic structure in Brazilian *Araucaria* forests. *Ecography* 35, 1-9.
- Duarte, M.C., Esteves, G.L., Salatino, M.L.F., Walsh, K.C., Baum, D.A., 2011. Phylogenetic Analyses of *Eriotheca* and Related Genera (Bombacoideae, Malvaceae). *Systematic Botany* 36, 690-701.

- Dutton, A.L., Lohmann, K.C., Zinsmeister, W.J., 2002. Stable isotope and minor element proxies for Eocene climate of Seymour Island, Antarctica. *Paleoceanography* 17, PA000593.
- Eberle, J., Greenwood, D.R., 2011. Life at the top of the greenhouse Eocene world - A review of the Eocene flora and vertebrate fauna from Canada's High Arctic. *Geological Society of America Bulletin* 124, 3-21.
- Eberle, J.J., Fricke, H.C., Humphrey, J.D., Hackett, L., Newbrey, M.G., Hutchison, J.H., 2010. Seasonal variability in Arctic temperatures during early Eocene time. *Earth and Planetary Science Letters* 296, 481-486.
- Eldrett, J.S., Greenwood, D.R., Harding, I.C., Huber, M., 2009. Increased seasonality through the Eocene to Oligocene transition in northern high latitudes. *Nature* 459, 969-973.
- Enright, N.J., Hill, R.S., 1995. *Ecology of the Southern Conifers*. Melbourne University Press, Carlton. 342 pp.
- Exon, N.F., Brinkhuis, H., Robert, C.M., Kennett, J.P., Hill, P.J., Macphail, M.K., 2004a. Tectono-sedimentary history of uppermost Cretaceous through Oligocene sequences from the Tasmanian region, a temperate Antarctic margin. In: Exon, N.F., Kennett, J.P., Malone, M. (Eds.), *The Cenozoic Southern Ocean: Tectonics, Sedimentation, and Climate Change Between Australia and Antarctica*. American Geophysical Union, Washington, pp. 319-344.
- Exon, N.F., Kennett, J.P., Malone, M.J., 2004b. *The Cenozoic Southern Ocean: Tectonics, Sedimentation and Climate Change Between Australia and Antarctica*. American Geophysical Union, Washington. 367 pp.
- Expedition 318 Scientists, 2011. Site U1356. in Escutia, C., Brinkhuis, H., Klaus, A., and the Expedition 318 Scientists. *Proceedings of the Integrated Ocean Drilling Program 318*, 1-103.
- Farley, M.B., 1987. Palynomorphs from surface water of the Eastern and Central Caribbean Sea. *Micropaleontology* 33, 254-262.
- Fedorov, A.A., 1966. The structure of the tropical rain forest and speciation in the humid tropics. *Journal of Ecology* 54, 1-11.
- Fine, P.V.A., Ree, R.H., 2006. Evidence for a time-integrated species-area effect on the latitudinal gradient in tree diversity. *The American Naturalist* 168, 796-804.
- Fitzsimons, I.C.W., 2000. Grenville-age basement provinces in East Antarctica: Evidence for three separate collisional orogens. *Geology* 28, 879-882.
- Francis, A.P., Currie, D.J., 2003. A globally consistent richness-climate relationship for angiosperms. *The American Naturalist* 161, 523-536.
- Francis, J.E., 1996. Antarctic palaeobotany: clues to climate change. *Terra Antarctica* 3, 135-140.

- Francis, J.E., 2000. Fossil wood from Eocene high latitude forests, McMurdo Sound, Antarctica. *Antarctic Research Series* 76, 253-260.
- Francis, J.E., Marensi, S., Levy, R., Hambrey, M., Thorn, V.C., Mohr, B., Brinkhuis, H., Warnaar, J., Zachos, J., Bohaty, S., DeConto, R., 2008. Chapter 8 From Greenhouse to Icehouse – The Eocene/Oligocene in Antarctica. In: Florindo, F., Siebert, M. (Eds.), *Antarctic Climate Evolution*. Elsevier, The Netherlands, pp. 309-368.
- Francis, J.E., Poole, I., 2002. Cretaceous and early Tertiary climates of Antarctica: evidence from fossil wood. *Palaeogeography, Palaeoclimatology, Palaeoecology* 182, 47-64.
- Frederiksen, N.O., Edwards, L.E., Ager, T.A., Sheehan, T.P., 2002. Palynology of Eocene strata in the Sagavanirktok and Canning formations on the north slope of Alaska. *Palynology* 26, 59-93.
- Gayó, E., Hinojosa, L.F., Villagrán, C., 2005. On the persistence of tropical paleofloras in central Chile during the Early Eocene. *Review of Palaeobotany and Palynology* 137, 41-50.
- Gelman, A., Carlin, J.B., Stern, H.S., Rubin, D.B., 2003. *Bayesian Data Analysis* (2nd edition). Chapman and Hall/CRC, Boca Raton, Florida. 696 pp.
- George, A.S., 1984. *Anacolosa*, Flora of Australia Online, <http://www.anbg.gov.au/abrs/online-resources/flora/>.
- Germeraad, J.H., Hopping, C.A., Muller, J., 1968. Palynology of Tertiary sediments from tropical areas. *Review of Palaeobotany and Palynology* 6, 189-198.
- Goldstein, S.L., Hemming, S.R., 2003. 6.17 - Long-lived isotopic tracers in oceanography, paleoceanography, and ice-sheet dynamics. In: Holland, D., Turekian, K.K. (Eds.), *Treatise on Geochemistry*. Pergamon, Oxford, pp. 453-489.
- Goodge, J.W., Fanning, C.M., 2010. Composition and age of the East Antarctic Shield in eastern Wilkes Land determined by proxy from Oligocene-Pleistocene glaciomarine sediment and Beacon Supergroup sandstones, Antarctica. *Geological Society of America Bulletin* 122, 1135-1159.
- Gotelli, N.J., Colwell, R.K., 2001. Quantifying biodiversity: procedures and pitfalls in the measurement and comparison of species richness. *Ecology Letters* 4, 379-391.
- Govaerts, R., Frodin, D.G., 2002. *World Checklist and Bibliography of Araceae (and Acoraceae)*. Royal Botanic Gardens, Kew, UK. 560 pp.
- Gradstein, F.M., Hogg, J.G., Smith, A.G., 2004. *A Geologic Time Scale 2004*. Cambridge University Press, Cambridge. 589 pp.
- Gradstein, F.M., Ogg, J.G., Schmitz, M.D., Ogg, G.M., 2012. *The Geological Time Scale 2012*. Elsevier, Amsterdam. 1176 pp.

- Greenwood, D.R., Archibald, S.B., Mathewes, R.W., Moss, P.T., 2005. Fossil biotas from the Okanagan Highlands, southern British Columbia and northeastern Washington State: climates and ecosystems across an Eocene landscape. *Canadian Journal of Earth Sciences* 42, 167-185.
- Greenwood, D.R., Christophel, D.C., 2005. The origins and Tertiary history of Australian "tropical" rainforests. In: Bermingham, E., Dick, C.W., Moritz, C. (Eds.), *Tropical Rainforests: Past, Present and Future*. The University of Chicago Press, Chicago, pp. 336-373.
- Greenwood, D.R., Moss, P.T., Rowett, A.I., Vadala, A.J., Keefe, R.L., 2003. Plant communities and climate change in southeastern Australia during the early Paleogene. In: Wing, S., Gingerich, P.D., Schmitz, B., Thomas, E. (Eds.), *Causes and Consequences of Globally Warm Climates in the Early Paleogene*. Geological Society of America Special Paper 369, Boulder, Colorado, pp. 365-380.
- Greenwood, D.R., Wing, S.L., 1995. Eocene continental climates and latitudinal temperature gradients. *Geology* 23, 1044-1048.
- Handley, L., Crouch, E.M., Pancost, R.D., 2011. A New Zealand record of sea level rise and environmental change during the Paleocene–Eocene Thermal Maximum. *Palaeogeography, Palaeoclimatology, Palaeoecology* 305, 185-200.
- Harrington, G.J., 2001. Impact of Paleocene/Eocene greenhouse warming on North American paratropical forests. *Palaios* 16, 266-278.
- Harrington, G.J., 2004. Structure of the North American vegetation gradient during the late Paleocene/early Eocene warm climate. *Evolutionary Ecology Research* 6, 36-48.
- Harrington, G.J., Eberle, J., Le-Page, B.A., Dawson, M., Hutchison, J.H., 2012. Arctic plant diversity in the Early Eocene greenhouse. *Proceedings of the Royal Society of London. Series B, Biological Sciences* 279, 1515-1521.
- Harrington, G.J., Jaramillo, C., 2007. Paratropical floral extinction in the Late Palaeocene–Early Eocene. *Journal of the Geological Society, London* 164, 323-332.
- Harris, W.F., Mildenhall, D.C., 1984. Wellington Quaternary palynology: Aranuiian and Otiran pollen diagrams from Soil Bureau site, Taita and Wallaceville Swamp, Hutt Valley, New Zealand. *New Zealand Geological Survey Report PAL 69*, 1-27.
- Harris, W.K., 1965. Basal Tertiary microfloras from the Princetown area, Victoria, Australia. *Palaeontographica Abteilung B* 115, 75-106.
- Harwood, D.M., Levy, R.H., 2000. The McMurdo Erratics: Introduction and overview. *Antarctic Resolution Series* 76, 1-18.
- Hay, W.W., DeConto, R.M., Wold, C.N., Wilson, K.M., Voigt, S., Schulz, M., Wold-Rossby, A., Dullo, W.C., Ronov, A.B., Balukhovskiy, A.N., Söding, M., 1999. Alternative global Cretaceous paleogeography. In: Barrera, E., Johnson, C. (Eds.), *Evolution of the*

- Cretaceous ocean-climate system. Geological Society of America Special Paper 332, Boulder, Colorado, pp. 1-47.
- Hayek, L.C., Buzas, M.A., 2010. Surveying natural populations. Columbia University Press, New York. 590 pp.
- Helby, R., Morgan, R., Partridge, A.D., 1987. A palynological zonation of the Australian Mesozoic. *Memoirs of the Association of Australasian Palaeontologists* 4, 1-94.
- Hesse, M., Zetter, R., 2007. The fossil pollen record of Araceae. *Plant Systematics and Evolution* 263, 93-115.
- Hill, M.O., Gauch, H.G., 1980. Detrended Correspondence Analysis: An improved ordination technique. *Vegetatio* 43, 47-58.
- Hill, R.S., 1994. The history of selected Australian taxa. In: Hill, R.S. (Ed.), *History of the Australian Vegetation: Cretaceous to Recent*. Cambridge University Press, Cambridge, pp. 390-419.
- Hinojosa, L.F., Villagran, C., 1997. Historia de los bosques del sur de Sudamérica. I: Antecedentes climáticos del Terciario del cono sur de América. *Revista chilena de historia natural* 70, 225-239.
- Hinojosa, L.F., Villagrán, C., 2005. Did South American Mixed Paleofloras evolve under thermal equability or in the absence of an effective Andean barrier during the Cenozoic? *Palaeogeography, Palaeoclimatology, Palaeoecology* 217, 1-23.
- Hollis, C.J., Handley, L., Crouch, E.M., Morgans, H.E.G., Baker, J.A., Creech, J., Collins, K.S., Gibbs, S.J., Huber, M., Schouten, S., Zachos, J.C., Pancost, R.D., 2009. Tropical sea temperatures in the high-latitude South Pacific during the Eocene. *Geology* 37, 99-102.
- Hollis, C.J., Tayler, M.J.S., Andrew, B., Taylor, K.W., Lurcock, P., Bijl, P.K., Kulhanek, D.K., Crouch, E.M., Nelson, C.S., Pancost, R.D., Huber, M., Wilson, G.S., Ventura, G.T., Crampton, J.S., Schiøler, P., Philips, A., 2014. Organic-rich sedimentation in the southwest Pacific Ocean associated with Late Paleocene climatic cooling. *Earth-Science Reviews* 134, 81-97.
- Hollis, C.J., Taylor, K.W.R., Handley, L., Pancost, R.D., Huber, M., Creech, J.B., Hines, B.R., Crouch, E.M., Morgans, H.E.G., Crampton, J.S., Gibbs, S., Pearson, P.N., Zachos, J.C., 2012. Early Paleogene temperature history of the Southwest Pacific Ocean: Reconciling proxies and models. *Earth and Planetary Science Letters* 349, 53-66.
- Holmes, P.L., 1994. The sorting of spores and pollen by water: experimental and field evidences. In: Traverse, A. (Ed.), *Sedimentation of Organic Particles*. Cambridge University Press, Cambridge, UK, pp. 9-46.
- Hopmans, E.C., Weijers, J.W.H., Schefuß, E., Herfort, L., Sinninghe Damsté, J.S., Schouten, S., 2004. A novel proxy for terrestrial organic matter in sediments based on branched and isoprenoid tetraether lipids. *Earth and Planetary Science Letters* 224, 107-116.

- Houben, A.J., Bijl, P.K., Pross, J., Bohaty, S.M., Passchier, S., Stickley, C.E., Röhl, U., Sugisaki, S., Tauxe, L., van de Flierdt, T., Olney, M., Sangiorgi, F., Sluijs, A., Escutia, C., Brinkhuis, H., Dotti, C.E., Klaus, A., Fehr, A., Williams, T., Bendle, J.A., Carr, S.A., Dunbar, R.B., Flores, J.A., Gonzalez, J.J., Hayden, T.G., Iwai, M., Jimenez-Espejo, F.J., Katsuki, K., Kong, G.S., McKay, R.M., Nakai, M., Pekar, S.F., Riesselman, C., Sakai, T., Salzmann, U., Shrivastava, P.K., Tuo, S., Welsh, K., Yamane, M., 2013. Reorganization of Southern Ocean plankton ecosystem at the onset of Antarctic glaciation. *Science* 340, 341-344.
- Houben, A.J.P., Bijl, P.K., Guerin, G.R., Sluijs, A., Brinkhuis, H., 2011. *Malvinia escutiana*, a new biostratigraphically important Oligocene dinoflagellate cyst from the Southern Ocean. *Review of Palaeobotany and Palynology* 165, 175-182.
- Houlder, D., Hutchinson, M., Nix, H., McMahon, J., 1999. ANUCLIM User's Guide. Canberra: Centre for Resource and Environmental Studies, Australian National University.
- Huber, M., Brinkhuis, H., Stickley, C.E., Doos, K., Sluijs, A., Warnaar, J., Schellenberg, S.A., Williams, G.L., 2004. Eocene circulation of the Southern Ocean: Was Antarctica kept warm by subtropical waters. *Paleoceanography* 19, PA4026.
- Huber, M., Caballero, R., 2011. The early Eocene equable climate problem revisited. *Climate of the Past* 7, 603-633.
- Hutchins, L.W., 1947. The bases for temperature zonation in geographical distribution. *Ecological Monographs* 17, 325-335.
- IPCC, 2007. The physical science basis. Working group I contribution to the fourth assessment report of the IPCC. Cambridge University Press, Cambridge, UK.
- Ivany, L.C., Lohmann, K.C., Hasiuk, F., Blake, D.B., Glass, A., Aronson, R.B., Moody, R.M., 2008. Eocene climate record of a high southern latitude continental shelf: Seymour Island, Antarctica. *Geological Society of America Bulletin* 120, 659-678.
- Jackson, S.T., 1994. Pollen and spores in Quaternary lake sediments as sensors of vegetation composition: theoretical models and empirical evidence. In: Traverse, A. (Ed.), *Sedimentation of Organic Particles*. Cambridge University Press, Cambridge, pp. 253-286.
- Jaffré, T., 1995. Distribution and ecology of the conifers of New Caledonia. In: Enright, N.J., Hill, R.S. (Eds.), *Ecology of the Southern Conifers*. Melbourne University Press, Melbourne, pp. 171-196.
- Jamieson, S.S.R., Sugden, D.E., 2008. Landscape evolution of Antarctica. In: Cooper, A.K., Barrett, P.J., Stagg, H., Storey, B., Stump, E., Wise, W. (Eds.), *Antarctica: a keystone in a changing world. Proceedings of the 10th International Symposium on Antarctic Earth Sciences*. The National Academic Press, Washington D.C., pp. 39-54.
- Jamieson, S.S.R., Sugden, D.E., Hulton, N.R.J., 2010. The evolution of the subglacial landscape of Antarctica. *Earth and Planetary Science Letters* 293, 1-27.

- Jansonius, J., Hills, L.V., 1976. Genera file of fossil spores. Special publication, Department of Geology and Geophysics, University of Calgary.
- Jansonius, J., Hills, L.V., Hartkopf-Fröder, C., 1998. Genera file of fossil pollen and spores - Supplement 12. Special publication, Department of Geology and Geophysics, University of Calgary.
- Jansson, R., Davies, T.J., 2008. Global variation in diversification rates of flowering plants: energy vs. climate change. *Ecology Letters* 11, 173-183.
- Jaramillo, C., 2002. Response of tropical vegetation to Paleogene warming. *Paleobiology* 28, 222-243.
- Jaramillo, C., Cárdenas, A., 2013. Global warming and neotropical rainforests: a historical perspective. *Annual Review of Earth and Planetary Sciences* 41, 741-766.
- Jaramillo, C., Ochoa, D., Contreras, L., Pagani, M., Carvajal-Ortiz, H., Pratt, L.M., Krishnan, S., Cardona, A., Romero, M., Quiroz, L., Rodriguez, G., Rueda, M.J., de la Parra, F., Moron, S., Green, W., Bayona, G., Montes, C., Quintero, O., Ramirez, R., Mora, G., Schouten, S., Bermudez, H., Navarrete, R., Parra, F., Alvaran, M., Osorno, J., Crowley, J.L., Valencia, V., Vervoort, J., 2010. Effects of rapid global warming at the Paleocene-Eocene boundary on neotropical vegetation. *Science* 330, 957-961.
- Jardine, P.E., Harrington, G.J., 2008. The Red Hills Mine palynoflora: A diverse swamp assemblage from the late Paleocene of Mississippi. *Palynology* 32, 183-204.
- Jarzen, D.M., Pocknall, D.T., 1984. Tertiary *Bluffopollis scabratus* (Couper) Pocknall & Mildenhall, 1984 and modern *Strasburgeria* pollen: a botanical comparison. *New Zealand Journal of Botany* 31, 185-192.
- Jermy, A.C., 1990. Selaginellaceae. In: Kramer, K.U., Green, P.S. (Eds.), *Pteridophytes and Gymnosperms*. Springer, Berlin, pp. 39-45.
- Johnson, L.A.S., Wilson, K.L., 1993. Casuarinaceae. In: Kubitzki, K., Rohwer, J.G., Bittrich, V. (Eds.), *Flowering Plants. Dicotyledons: Magnoliid, Hamamelid and Acryophyllid Families*. Springer, Berlin, pp. 237-242.
- Jones, D.L., 2002. *Cycads of the World*. Reed New Holland, Sydney. 456 pp.
- Jones, W.G., Hill, K.D., Allen, J.M., 1995. *Wollemia nobilis*, a new living Australian genus and species in the Araucariaceae. *Telopea* 6, 173-176.
- Kemp, E.M., 1978. Tertiary climatic evolution and vegetation history in the southeast Indian Ocean region. *Palaeogeography, Palaeoclimatology, Palaeoecology* 24, 169-208.
- Kershaw, A.P., 1988. Australasia. In: Huntley, B., Webb, T. (Eds.), *Vegetation History*. Kluwer Academic Publisher, Dordrecht, The Netherlands, pp. 237-306.
- Kershaw, A.P., Hyland, B.P.M., 1975. Pollen transfer and periodicity in a rain-forest situation. *Review of Palaeobotany and Palynology* 19, 129-138.

- Kershaw, A.P., Wagstaff, B., 2001. The southern conifer family Araucariaceae: history, status and value for paleoenvironment reconstruction. *Annual Review of Ecology and Systematics* 32, 397-414.
- Kim, J.-H., Schouten, S., Buscail, R., Ludwig, W., Bonnin, J., Sinninghe Damsté, J.S., Bourrin, F., 2006. Origin and distribution of terrestrial organic matter in the NW Mediterranean (Gulf of Lions): Exploring the newly developed BIT index. *Geochemistry Geophysics Geosystems* 7, Q11017.
- Kim, J.-H., Schouten, S., Hopmans, E.C., Donner, B., Sinninghe Damsté, J.S., 2008. Global sediment core-top calibration of the TEX₈₆ paleothermometer in the ocean. *Geochimica et Cosmochimica Acta* 72, 1154-1173.
- Kim, J.-H., van der Meer, J., Schouten, S., Helmke, P., Willmott, V., Sangiorgi, F., Koc, N., Hopmans, E.C., Sinninghe Damsté, J.S., 2010. New indices and calibrations derived from the distribution of crenarchaeal isoprenoid tetraether lipids: Implications for past sea surface temperature reconstructions. *Geochimica et Cosmochimica Acta* 74, 4639-4654.
- Kreft, H., Jetz, W., 2007. Global patterns and determinants of vascular plant diversity. *Proceedings of the National Academy of Sciences of the United States of America* 104, 5925-5930.
- Larcher, W., Winter, A., 1981. Frost susceptibility of palms: Experimental data and their interpretation. *Principes* 25, 143-152.
- Lear, C.H., 2000. Cenozoic deep-sea temperatures and global ice volumes from Mg/Ca in benthic foraminiferal calcite. *Science* 287, 269-272.
- Legendre, P., Legendre, L., 1998. *Numerical Ecology*. Elsevier, The Netherlands. 853 pp.
- Lewis, A.R., Marchant, D.R., Ashworth, A.C., Hedenas, L., Hemming, S.R., Johnson, J.V., Leng, M.J., Machlus, M.L., Newton, A.E., Raine, J.I., Willenbring, J.K., Williams, M., Wolfe, A.P., 2008. Mid-Miocene cooling and the extinction of tundra in continental Antarctica. *Proceedings of the National Academy of Sciences of the United States of America* 105, 10676-10680.
- Li, H., 1992. Early Tertiary palaeoclimate of King George Island, Antarctica—evidence from the Fossil Hill flora. In: Yoshida, Y., Funali, M., Kaminuma, S., Funali, M., Kaminuma, S., Funali, M., Kaminuma, S. (Eds.), *Recent Progress in Antarctic Earth Science*. Terra Scientific Publishing Company, Tokyo, pp. 371-375.
- Liu, Z.H., Pagani, M., Zinniker, D., DeConto, R., Huber, M., Brinkhuis, H., Shah, S.R., Leckie, R.M., Pearson, A., 2009. Global cooling during the Eocene-Oligocene climate transition. *Science* 323, 1187-1190.
- Lowry, P.P., 1996. Diversity, endemism, and extinction in the flora of New Caledonia: a Review. In: Peng, C.-I., Lowry, P.P. (Eds.), *Rare, Threatened, and Endangered Floras of the Pacific Rim*. Institute of Botany, Academia Sinica, Taipei, pp. 181-206.

- Macphail, M.K., 1999. Palynostratigraphy of the Murray Basin, inland southeastern Australia. *Palynology* 23, 197-240.
- Macphail, M.K., Alley, N.F., Truswell, E.M., Sluiter, I.R.K., 1994. Early Tertiary vegetation: evidence from spores and pollen. In: Hill, R.S. (Ed.), *History of the Australian Vegetation: Cretaceous to Recent*. Cambridge University Press, Cambridge, pp. 189-261.
- Macphail, M.K., Carpenter, R.J., Iglesias, A., Wilf, P., 2013. First Evidence for Wollemi Pine-type Pollen (*Dilwynites*: Araucariaceae) in South America PLOS ONE 8, e69281.
- Macphail, M.K., Truswell, E.M., 2004. Palynology of Site 116, Prydz Bay, East Antarctica. *Proceedings of the Ocean Drilling Program, Scientific Results* 188, 1-43.
- Martin, H.A., 1974. The identification of some Tertiary pollen belonging to the family Euphorbiaceae. *Australian Journal of Botany* 22, 271-291.
- Martin, H.A., 1978. Evolution of the Australian flora and vegetation through the Tertiary: evidence from pollen. *Alcheringa* 2, 181-202.
- McArthur, J.M., Howarth, R.J., 2004. Strontium isotope stratigraphy. Gradstein, F.M., Ogg, J.G., Smith, A.G. (Eds.), *A Geological Timescale 2004*. Cambridge University Press, Cambridge, UK, pp. 96-105.
- McGlone, M.S., Mildenhall, D.C., Pole, M.S., 1996. History and paleoecology of New Zealand *Nothofagus* forests. In: Veblen, T.T., Hill, R.S., Read, J. (Eds.), *The Ecology and Biogeography of Nothofagus Forests*. Yale University Press, New Haven, pp. 293-353.
- Meinshausen, M., Smith, S.J., Calvin, K., Daniel, J.S., Kainuma, M.L.T., Lamarque, J.F., Matsumoto, K., Montzka, S.A., Raper, S.C.B., Riahi, K., Thomson, A., Velders, G.J.M., Vuuren, D.P.P., 2011. The RCP greenhouse gas concentrations and their extensions from 1765 to 2300. *Climatic Change* 109, 213-241.
- Melendi, D.L., Scafati, L., Volkheimer, W., 2003. Palynostratigraphy of the Paleogene Huitrera Formation in N-W Patagonia, Argentina. *Neues Jahrbuch für Geologie und Paläontologie Abh.* 228, 205-273.
- Mildenhall, D.C., 1980. New Zealand late Cretaceous and Cenozoic plant biogeography: a contribution. *Palaeogeography, Palaeoclimatology, Palaeoecology* 31, 197-233.
- Mildenhall, D.C., 1989. Terrestrial palynology. In: Barrett, P.J. (Ed.), *Antarctic Cenozoic history from the CIROS-1 drillhole, McMurdo Sound*, DSIR Bulletin. DSRI Bulletin 245, DSRI Publishing, Wellington, pp. 119-127.
- Mildenhall, D.C., Moore, P.R., 1983. A late Holocene pollen sequence at Turakirae Head, and climatic and vegetational changes in the Wellington area in the last 10,000 years. *New Zealand Journal of Science* 26, 447-459.
- Miller, K.G., Fairbanks, R.G., Mountain, G.S., 1987. Tertiary oxygen isotope synthesis, sea level history, and continental margin erosion. *Paleoceanography* 2, 1-19.

- Miller, K.G., Kominz, M.A., Browning, J.V., Wright, J.D., Mountain, G.S., Katz, M.E., Sugarman, P.J., Cramer, B.S., Christie-Blick, N., Pekar, S.F., 2005. The Phanerozoic record of global sea-level change. *Science* 310, 1293-1298.
- Mitchell, N.D., 1991. The derivation of climate surfaces for New Zealand, and their application to the bioclimatic analysis of the distribution of kauri (*Agathis australis*). *Journal of the Royal Society of New Zealand* 21, 13-24.
- Mohr, B., 1990. Eocene and Oligocene sporomorphs and dinoflagellate cyst from Leg 113 drill sites, Weddell sea, Antarctica. *Proceedings of the Ocean Drilling Program, Scientific Results* 113, 595-612.
- Mohr, B., 2001. The development of Antarctic fern floras during the Tertiary, and palaeoclimatic and palaeobiogeographic implications. *Palaeontographica Abteilung B* 259, 167-208.
- Moore, W.R., Baillie, P.W., Forsyth, S.M., Hudspeth, J.W., Richardson, R.G., Turner, N.J., 1984. Boobyalla Sub-Basin: a Cretaceous onshore extension of the southern edge of the Bass Basin. *APPEA Journal* 24, 110-117.
- Morat, P., 1993. Our knowledge of the flora of New Caledonia: endemism and diversity in relation to vegetation types and substrates. *Biodiversity Letters* 1, 72-81.
- Morley, R.J., 2000. *Origin and Evolution of Tropical Rain Forests*. John Wiley & Sons, United Kingdom. 362 pp.
- Mosbrugger, V., Utescher, T., 1997. The coexistence approach - a method for quantitative reconstructions of Tertiary terrestrial palaeoclimate data using plant fossils. *Palaeogeography, Palaeoclimatology, Palaeoecology* 134, 61-86.
- Mosbrugger, V., 1999. The nearest living relative method. In: Jones, T.P., Rowe, N.P. (Eds.), *Fossil Plants and Spores: Modern Techniques*. Geological Society, London, pp. 261-265.
- Moss, P.T., Kershaw, A.P., Grindrod, J., 2005. Pollen transport and deposition in riverine and marine environments within the humid tropics of northeastern Australia. *Review of Palaeobotany and Palynology* 134, 55-69.
- Muller, J., 1959. Palynology of recent Orinoco delta and shelf sediments: Reports of the Orinoco Shelf Expedition. *Micropaleontology* 5, 1-32.
- Muller, J., 1981. Fossil pollen records of extant angiosperms. *Botanical Review* 47, 1-142.
- Mundo, I.A., Juñent, F.A.R., Villalba, R., Kitzberger, T., Barrera, M.D., 2012. *Araucaria araucana* tree-ring chronologies in Argentina: spatial growth variations and climate influences. *Trees* 26, 443-458.
- Nakagawa, S. and Freckleton, R.P., 2008. Missing inaction: the dangers of ignoring missing data. *Trends in Ecology and Evolution* 23, 592-596.

- Nichols, D.J., Ames, H.T., Traverse, A., 1973. On *Arecipites* Wodehouse, *Monocolpopollenites* Thomson & Pflug, and the Species "*Monocolpopollenites* *Tranquillus*". *Taxon* 22, 241-256.
- NIWA, 2012. CliFlo: NIWA's National Climate Database on the Web, <http://cliflo.niwa.co.nz/>.
- Norris, R.D., Turner, S.K., Hull, P.M., Ridgwell, A., 2013. Marine ecosystem responses to Cenozoic global change. *Science* 341, 492-498.
- Norstog, K., Nicholls, T.J., 1997. *Biology of the Cycads*. Cornell University Press, Ithaca, New York. 363 pp.
- Oksanen, J., Blanchet, F.G., Kindt, R., Legendre, P., Minchin, P.R., O'Hara, R.B., Simpson, G.L., Solymos, P., Henry, M., Stevens, H., Wagner, H. 2011a. *vegan: Community Ecology Package*. R package version 2.0-2, <http://CRAN.R-project.org/package=vegan>.
- Øllgaard, B., 1990. Lycopodiaceae. In: Kramer, K.U., Green, P.S. (Eds.), *Pteridophytes and Gymnosperms*. Springer, Berlin, pp. 31-39.
- Paijmans, K., 1976. *New Guinea Vegetation*. CSIRO, Canberra. 213 pp.
- Palazzesi, L., Barreda, V., 2007. Major vegetation trends in the Tertiary of Patagonia (Argentina): A qualitative paleoclimatic approach based on palynological evidence. *Flora - Morphology, Distribution, Functional Ecology of Plants* 202, 328-337.
- Pancost, R.D., Hopmans, E.C., Sinninghe Damsté, J.S., 2001. Archaeal lipids in Mediterranean cold seeps: molecular proxies for anaerobic methane oxidation. *Geochimica et Cosmochimica Acta* 65, 1611-1627.
- Pancost, R.D., Taylor, K.W.R., Inglis, G.N., Kennedy, E.M., Handley, L., Hollis, C.J., Crouch, E.M., Pross, J., Huber, M., Schouten, S., Pearson, P.N., Morgans, H.E.G., Raine, J.I., 2013. Early Paleogene evolution of terrestrial climate in the SW Pacific, Southern New Zealand. *Geochemistry, Geophysics, Geosystems* 14, 5413-5429.
- Partridge, A.D., 1976. The geological expression of eustacy in the early Tertiary of the Gippsland Basin. *APPEA Journal* 1976, 73-79.
- Partridge, A.D., 1999. *Late Cretaceous to Tertiary geological evolution of the Gippsland Basin, Victoria*. Melbourne: Latrobe University.
- Partridge, A.D., 2006. Late Cretaceous - Cenozoic palynology zonations Gippsland Basin, Australian Mesozoic and Cenozoic palynology zonations- update to the 2004 Geologic Time Scale. *Geoscience Australia Record* 2006/23.
- Partridge, A.D., Trigg, K.R., Montgomerie, N.R., Blevin, J.E., 2003. Review and compilation of open file micropaleontology and palynology data from offshore Tasmania: An Output of the Western Tasmanian Regional Minerals Program. *Geoscience Australia Record* 2003/7.

- Passchier, S., Bohaty, S.M., Jiménez-Espejo, F., Pross, J., Röhl, U., van de Flierdt, T., Escutia, C., Brinkhuis, H., 2013. Early Eocene to middle Miocene cooling and aridification of East Antarctica. *Geochemistry Geophysics Geosystems* 14, 1399-1410.
- Pearson, P.N., Palmer, M.R., 2000. Atmospheric carbon dioxide concentrations over the past 60 million years. *Nature* 406, 695-699.
- Pearson, P.N., van Dongen, B.E., Nicholas, C.J., Pancost, R.D., Schouten, S., Singano, J.M., Wade, B.S., 2007. Stable warm tropical climate through the Eocene Epoch. *Geology* 35, 211-214.
- Peet, R.K., Knox, R.G., Case, J.S., Allen, R.B., 1988. Putting things in order: the advantages of Detrended Correspondence Analysis. *The American Naturalist* 131, 924-934.
- Pennington, R.T., Lavin, M., Oliveira-Filho, A., 2009. Woody plant diversity, evolution, and ecology in the tropics: perspectives from seasonally dry tropical forests. *Annual Review of Ecology, Evolution, and Systematics* 40, 437-457.
- Pesin, E., Blaize, S., Lacoste, D., 1995. Atlas climatique de la Nouvelle-Calédonie. Météo-France, Nouméa, New Caledonia. 104 pp.
- Peterse, F., Kim, J.-H., Schouten, S., Kristensen, D.K., Koç, N., Sinninghe Damsté, J.S., 2009. Constraints on the application of the MBT/CBT palaeothermometer at high latitude environments (Svalbard, Norway). *Organic Geochemistry* 40, 692-699.
- Petris, G., Petrone, S., Campagnoli, P., 2009. *Dynamic Linear models with R*. Springer, New York. 252 pp.
- Pierce, E.L., Williams, T., van de Flierdt, T., Hemming, S.R., Goldstein, S.L., Brachfeld, S.A., 2011. Characterizing the sediment provenance of East Antarctica's weak underbelly: The Aurora and Wilkes sub-glacial basins. *Paleoceanography* 26, PA4217.
- Pin, C., Zalduogui, J.S., 1997. Sequential separation of light rare-earth elements, thorium and uranium by miniaturized extraction chromatography: Application to isotopic analyses of silicate rocks. *Analytica Chimica Acta* 339, 79-89.
- Playford, G., 1965. Plant microfossils from Triassic sediments near Poatina, Tasmania. *Journal of the Geological Society of Australia* 12, 173-210.
- Pocknall, D.T., 1990. Palynological evidence for the early to middle Eocene vegetation and climate history of New Zealand. *Review of Palaeobotany and Palynology* 65, 57-69.
- Pole, M., 2007. Early Eocene dispersed cuticles and mangrove to rainforest vegetation at Strahan-Regatta Point, Tasmania. *Palaeontologia Electronica* 10, 1-66.
- Pole, M.S., Hill, B.D., Harwood, D.M., 2000. Eocene plant macrofossils from erratics, McMurdo Sound, Antarctica. *Antarctic Research Series* 76, 243-251.
- Pole, M.S., Macphail, M.K., 1996. Eocene *Nypa* from Regatta Point, Tasmania. *Review of Palaeobotany and Palynology* 92, 55-67.

- Poole, I., Cantrill, D., Utescher, T., 2005. A multi-proxy approach to determine Antarctic terrestrial palaeoclimate during the Late Cretaceous and Early Tertiary. *Palaeogeography, Palaeoclimatology, Palaeoecology* 222, 95-121.
- Poole, I., Hunt, R.J., Cantrill, D.J., 2001. A fossil wood flora from King George Island: ecological implications for an Antarctic Eocene vegetation. *Annals of Botany* 88, 33-54.
- Prentice, I.C., Cramer, W., Harrison, S.P., Leemans, R., Monserud, R.A., Solomon, A.M., 1992. A global biome model based on plant physiology and dominance, soil properties and climate. *Journal of Biogeography* 19, 117-134.
- Pross, J., Klotz, S., Mosbrugger, V., 2000. Reconstructing palaeotemperatures for the Early and Middle Pleistocene using the mutual climatic range method based on plant fossils. *Quaternary Science Reviews* 19, 1785-1799.
- Pross, J., 2001. Paleo-oxygenation in Tertiary epeiric seas: evidence from dinoflagellate cysts. *Palaeogeography, Palaeoclimatology, Palaeoecology* 166, 369-381.
- Pross, J., Contreras, L., Bijl, P.K., Greenwood, D.R., Bohaty, S.M., Schouten, S., Bendle, J.A., Röhl, U., Tauxe, L., Raine, J.I., Huck, C.E., van de Flierdt, T., Jamieson, S.S.R., Stickley, C.E., van de Schootbrugge, B., Escutia, C., Brinkhuis, H., IODP Expedition 318 Scientists, 2012. Persistent near-tropical warmth on the Antarctic continent during the early Eocene epoch. *Nature* 488, 73-77.
- Pross, J., Pletsch, T., Shillington, D.J., Ligouis, B., Schellenberg, F., Kus, J., 2007. Thermal alteration of terrestrial palynomorphs in mid-Cretaceous organic-rich mudstones intruded by an igneous sill (Newfoundland Margin, ODP Hole 1276A). *International Journal of Coal Geology* 70, 227-291.
- Punt, W., Marks, A., Hoen, P.P., 2002. Myricaceae. Review of Palaeobotany and Palynology 123, 99-105.
- Punyasena, S.W., Dalling, J.W., Jaramillo, C., Turner, B.L., 2011. Comment on "The response of vegetation on the Andean flank in western Amazonia to Pleistocene climate change". *Science* 333, 1825.
- Quattroccio, M.E., Volkheimer, W., Borromei, A.M., Martínez, M.A., 2011. Changes of the palynofloras in the Mesozoic and Cenozoic of Patagonia: a review. *Biological Journal of the Linnean Society* 103, 380-396.
- Quilty, P.G., Truswell, E.M., O'Brien, P.E., Taylor, F., 1999. Paleocene-Eocene biostratigraphy and palaeoenvironment of East Antarctica: new data from the Mac. Robertson Shelf and western parts of Prydz Bay. *AGSO Journal of Australian Geology and Geophysics* 17, 133-143.
- R Development Core Team, 2011. R: A language and environment for statistical computing. R Foundation for Statistical Computing, <http://www.R-project.org/>. Vienna, Austria.

- Raine, J.I., 1998. Terrestrial palynomorphs from Cape Roberts Project Drillhole CRP-1, Ross Sea, Antarctica. *Terra Antartica* 5, 539-548.
- Raine, J.I., Askin, R.A., 2001. Terrestrial Palynology of Cape Roberts Project Drillhole CRP-3, Victoria Land Basin, Antarctica. *Terra Antartica* 8, 389-400.
- Raine, J.I., Kennedy, E.M., Crouch, E.M., 2009. New Zealand Paleogene vegetation and climate. *GNS Science Miscellaneous Series* 18, 117-122.
- Raine, J.I., Mildenhall, D.C., Kennedy, E.M., 2008. New Zealand fossil spores and pollen: an illustrated catalogue. *GNS Science Miscellaneous Series* 4, <http://data.gns.cri.nz/sporepollen/index.htm>.
- Raup, D.M., 1975. Taxonomic diversity estimation using rarefaction. *Paleobiology* 1, 333-342.
- Read, J., Francis, J., 1992. Responses of some Southern Hemisphere tree species to a prolonged dark period and their implications for high-latitude Cretaceous and Tertiary floras. *Palaeogeography, Palaeoclimatology, Palaeoecology* 99, 271-290.
- Read, J., Hope, G.S., Hill, R.S., 2005. Phytogeography and climate analysis of *Nothofagus* subgenus *Brassospora* in New Guinea and New Caledonia. *Australian Journal of Botany* 53, 297-312.
- Reid, J.B., Hill, R.S., Brown, M.J., Hovenden, M.J., 1999. *Vegetation of Tasmania*. Monotone Art Printers, Hobart. 455 pp.
- Röhl, U., Brinkhuis, H., Sluijs, A., Fuller, M., 2004. On the search for the Paleocene/Eocene Boundary in the Southern Ocean: Exploring ODP Leg 189 Holes 1171D and 1172D, Tasman Sea. In: Exon, N.F., Kennett, J.P., Malone, M. (Eds.), *The Cenozoic Southern Ocean: Tectonics, Sedimentation, and Climate Change Between Australia and Antarctica*. American Geophysical Union, Washington, pp. 113-125.
- Röhl, U., Westerhold, T., Bralower, T.J., Zachos, J., 2007. On the duration of the Paleocene-Eocene Thermal Maximum. *Geochemistry Geophysics Geosystems* 8, Q12002.
- Rosignol-Strick, M., Paterne, M., 1999. A synthetic pollen record of the eastern Mediterranean sapropels of the last 1 Ma: implications for the time-scale and formation of sapropels. *Marine Geology* 153, 221-237.
- Roubik, D.W., Moreno, E., 1991. Pollen and spores of Barro Colorado Island. *Monographs in Systematic Botany* 36, 1-270.
- Roy, M., van de Flierdt, T., Hemming, S.R., Goldstein, S.L., 2007. $^{40}\text{Ar}/^{39}\text{Ar}$ ages of hornblende grains and bulk Sm/Nd isotopes of circum-Antarctic glacio-marine sediments: Implications for sediment provenance in the southern ocean. *Chemical Geology* 244, 507-519.

- Royer, D.L., Osborne, C.P., Beerling, D.J., 2002. High CO₂ increases the freezing sensitivity of plants: Implications for paleoclimatic reconstructions from fossil floras. *Geology* 30, 963-966.
- Sakai, A., Larcher, W., 1987. *Frost Survival of Plants: Responses and Adaptation to Freezing Stress*. Springer-Verlag, Berlin. 321 pp.
- Sauquet, H., Cantrill, D.J., 2007. Pollen diversity and evolution in Proteoideae (Proteales: Proteaceae). *Systematic Botany* 32, 271-316.
- Schouten, S., Hopmans, E.C., Schefuß, E., Sinninghe Damsté, J.S., 2002. Distributional variations in marine crenarchaeotal membrane lipids: a new tool for reconstructing ancient sea water temperatures? *Earth and Planetary Science Letters* 204, 265-274.
- Schouten, S., Hopmans, E.C., Sinninghe Damsté, J.S., 2013. The organic geochemistry of glycerol dialkyl glycerol tetraether lipids: A review. *Organic Geochemistry* 54, 19-61.
- Schouten, S., Huguet, C., Hopmans, E.C., Kienhuis, M.V.M., Sinninghe Damsté, J.S., 2007. Analytical methodology for TEX₈₆ paleothermometry by high-performance liquid chromatography/atmospheric pressure chemical ionization-mass spectrometry. *Analytical Chemistry* 79, 2940-2944.
- Shellito, C.J., Sloan, L.C., Huber, M., 2003. Climate model sensitivity to atmospheric CO₂ levels in the Early-Middle Paleogene. *Palaeogeography, Palaeoclimatology, Palaeoecology* 193, 113-123.
- Shipboard Scientific Party, 2001a. Leg 189 Summary. *Proceedings of the Ocean Drilling Program, Initial Reports 189*, 1-98.
- Shipboard Scientific Party, 2001b. Site 1172. *Proceedings of the Ocean Drilling Program, Initial Reports 189*, 1-149.
- Sijp, W.P., England, M.H., Huber, M., 2011. Effect of the deepening of the Tasman Gateway on the global ocean. *Paleoceanography* 26, PA4207.
- Sinninghe Damsté, J.S., Rijpstra, W.I.C., Hopmans, E.C., Weijers, J.W.H., Foesel, B.U., Overmann, J., Dedysh, S.N., 2011. 13,16-Dimethyl Octacosanedioic acid (*iso*-Diabolic Acid), a common membrane-spanning lipid of acidobacteria subdivisions 1 and 3. *Applied and Environmental Microbiology* 77, 4147-4154.
- Sloan, L.C., Rea, D.K., 1996. Atmospheric carbon dioxide and early Eocene climate: A general circulation modeling sensitivity study. *Palaeogeography, Palaeoclimatology, Palaeoecology* 119, 275-292.
- Sluijs, A., Bijl, P.K., Schouten, S., Röhl, U., Reichert, G.J., Brinkhuis, H., 2011. Southern ocean warming, sea level and hydrological change during the Paleocene-Eocene thermal maximum. *Climate of the Past* 7, 47-61.
- Sluijs, A., Brinkhuis, H., Crouch, E.M., John, C.M., Handley, L., Munsterman, D., Bohaty, S.M., Zachos, J.C., Reichert, G.-J., Schouten, S., Pancost, R.D., Sinninghe Damsté, J.S.,

- Welters, N.L.D., Lotter, A.F., Dickens, G.R., 2008a. Eustatic variations during the Paleocene-Eocene greenhouse world. *Paleoceanography* 23, PA4216.
- Sluijs, A., Brinkhuis, H., Schouten, S., Bohaty, S.M., John, C.M., Zachos, J.C., Reichart, G.J., Sinninghe Damsté, J.S., Crouch, E.M., Dickens, G.R., 2007. Environmental precursors to rapid light carbon injection at the Palaeocene/Eocene boundary. *Nature* 450, 1218-1221.
- Sluijs, A., Pross, J., Brinkhuis, H., 2005. From greenhouse to icehouse; organic-walled dinoflagellate cysts as paleoenvironmental indicators in the Paleogene. *Earth-Science Reviews* 68, 281-315.
- Sluijs, A., Röhl, U., Schouten, S., Brumsack, H.-J., Sangiorgi, F., Sinninghe Damsté, J.S., Brinkhuis, H., 2008b. Arctic late Paleocene-early Eocene paleoenvironments with special emphasis on the Paleocene-Eocene thermal maximum (Lomonosov Ridge, Integrated Ocean Drilling Program Expedition 302). *Paleoceanography* 23, PA1S11.
- Sluijs, A., Schouten, S., Donders, T.H., Schoon, P.L., Röhl, U., Reichart, G.-J., Sangiorgi, F., Kim, J.-H., Sinninghe Damsté, J.S., Brinkhuis, H., 2009. Warm and wet conditions in the Arctic region during Eocene Thermal Maximum 2. *Nature Geoscience* 2, 777-780.
- Sluijs, A., Schouten, S., Pagani, M., Woltering, M., Brinkhuis, H., Sinninghe Damsté, J.S., Dickens, G.R., Huber, M., Reichart, G.-J., Stein, R., Matthiessen, J., Lourens, L.J., Pedentchouk, N., Backman, J., Moran, K., the Expedition 302 Scientists, 2006. Subtropical Arctic Ocean temperatures during the Palaeocene/Eocene thermal maximum. *Nature* 441, 610-613.
- Specht, R.L., Dettmann, M.E., Jarzen, D.M., 1992. Community associations and structure in the Late Cretaceous vegetation of southeast Australasia and Antarctica. *Palaeogeography, Palaeoclimatology, Palaeoecology* 94, 283-309.
- Specht, R.L., Specht, A., 1999. *Australian Plant Communities: Dynamics of Structure, Growth and Biodiversity*. Oxford University Press, Singapore. 492 pp.
- Stevenson, J., Dodson, J.R., Prosser, I.P., 2001. A late Quaternary record of environmental change and human impact from New Caledonia. *Palaeogeography, Palaeoclimatology, Palaeoecology* 168, 97-123.
- Stickley, C.E., Brinkhuis, H., McGonigal, K.L., Chaproniere, G.C.H., Fuller, M., Kelly, D.C., Nürnberg, D., Pfuhl, H.A., Schellenberg, S.A., Schoenfeld, J., Suzuki, N., Touchard, Y., Wei, W., Williams, G.L., Lara, J., Stant, S.A. 2004a. 10. Late Cretaceous–Quaternary Biomagnetostratigraphy of ODP Sites 1168, 1170, 1171, and 1172, Tasmanian Gateway. *Proceedings of the Ocean Drilling Program, Scientific Results* 189, 1-57.
- Stickley, C.E., Brinkhuis, H., Schellenberg, S.A., Sluijs, A., Röhl, U., Fuller, M., Grauert, M., Huber, M., Warnaar, J., Williams, G.L., 2004b. Timing and nature of the deepening of the Tasmanian Gateway. *Paleoceanography* 19, PA4026.

- Stover, L.E., Evans, R., 1973. Upper Cretaceous-Eocene spore-pollen zonation, offshore Gippsland Basin, Australia. *Special Publications of the Geological Society of Australia* 4, 55-72.
- Stover, L.E., Partridge, A.D., 1973. Tertiary and Late Cretaceous spores and pollen from the Gippsland Basin, southeastern Australia. *Proceedings of the Royal Society of Victoria* 85, 237-286.
- Tanaka, T., Togashi, S., Kamioka, H., Amakawa, H., Kagami, H., Hamamoto, T., Yuhara, M., Orihashi, Y., Yoneda, S., Shimizu, H., Kunimaru, T., Takahashi, K., Yanagi, T., Nakano, T., Fujimaki, H., Shinjo, R., Asahara, Y., Tanimizu, M., Dragusanu, C., 2000. JNdi-1: a neodymium isotopic reference in consistency with LaJolla neodymium. *Chemical Geology* 168, 279-281.
- Tauxe, L., Stickley, C.E., Sugisaki, S., Bijl, P.K., Bohaty, S.M., Brinkhuis, H., Escutia, C., Flores, J.A., Houben, A.J.P., Iwai, M., Jiménez-Espejo, F., McKay, R., Passchier, S., Pross, J., Riesselman, C.R., Röhl, U., Sangiorgi, F., Welsh, K., Klaus, A., Fehr, A., Bendle, J.A., Dunbar, R., González, J., Hayden, T., Katsuki, K., Olney, M., Pekar, S.F., Shrivastava, P.K., van de Flierdt, T., Williams, T., Yamane, M., 2012. Chronostratigraphic framework for the IODP Expedition 318 cores from the Wilkes Land Margin: Constraints for paleoceanographic reconstruction. *Paleoceanography* 27, PA2214.
- Taylor, G., Truswell, E.M., McQueen, K.G., Brown, M.C., 1990. Early Tertiary palaeogeography, landform evolution, and palaeoclimates of the Southern Monaro, N.S.W., Australia. *Palaeogeography, Palaeoclimatology, Palaeoecology* 78, 109-134.
- Thomas, A., O'Hara, R.B., Ligges, U., Sturtz, S., 2006. Making BUGS Open. *R News* 6, 12-17.
- Thomas, D.J., Bralower, T.J., Jones, C.E., 2003. Neodymium isotopic reconstruction of late Paleocene-early Eocene thermohaline circulation. *Earth and Planetary Science Letters* 209, 309-322.
- Tierney, J.E., Mayes, M.T., Meyer, N., Johnson, C., Swarzenski, P.W., Cohen, A.S., Russell, J.M., 2010. Late-twentieth-century warming in Lake Tanganyika unprecedented since AD 500. *Nature Geoscience* 3, 422-425.
- Tjoelker, M.G., Oleksyn, J., Reich, P.B., 2001. Modelling respiration of vegetation: evidence for a general temperature - dependent Q_{10} . *Global Change Biology* 7, 223-230.
- Traverse, A., 1994a. Sedimentation of land-derived palynomorphs in the Trinity-Galveston Bay Area, Texas. In: Traverse, A. (Ed.), *Sedimentation of organic particles*. Cambridge University Press, Cambridge, UK, pp. 69-102.
- Traverse, A., 1994b. Sedimentation of palynomorphs and palynodebris: an introduction. In: Traverse, A. (Ed.), *Sedimentation of Organic Particles*. Cambridge University Press, Cambridge, pp. 1-8.
- Traverse, A., 2008. *Paleopalynology*, 2nd edition. Springer, Dordrecht, The Netherlands. 813 pp.

- Trénel, P., Gustafsson, M.H., Baker, W.J., Asmussen-Lange, C.B., Dransfield, J., Borchsenius, F., 2007. Mid-Tertiary dispersal, not Gondwanan vicariance explains distribution patterns in the wax palm subfamily (Ceroxyloideae: Areaceae). *Molecular Phylogenetics and Evolution* 45, 272-288.
- Tripathi, A.K., Delaney, M.L., Zachos, J.C., Anderson, L.D., Kelly, D.C., Elderfield, H., 2003. Tropical sea-surface temperature reconstruction for the early Paleogene using Mg/Ca ratios of planktonic foraminifera. *Paleoceanography* 18, PA1101.
- Truswell, E.M., 1978. Palynology of the Permo- Carboniferous in Tasmania: an interim report. *Geological Survey Bulletin, Tasmania Department of Mines* 56, 1-39.
- Truswell, E.M., 1983. Recycled Cretaceous and Tertiary pollen and spores in Antarctic marine sediments: a catalogue. *Palaeontographica Abteilung B* 186, 121-174.
- Truswell, E.M., 1991. Data Report: Palynology of sediments from Leg 119 drill sites in Prydz Bay, East Antarctic. *Proceedings of the Ocean Drilling Program, Scientific Results* 189, 941-945.
- Truswell, E.M., 1997. Palynomorph assemblages from marine Eocene sediments on the west Tasmanian continental margin and the South Tasman Rise. *Australian Journal of Earth Sciences* 44, 633-654.
- Truswell, E.M., Drewry, D.J., 1984. Distribution and provenance of recycled palynomorphs in surficial sediments of the Ross Sea, Antarctica. *Marine Geology* 59, 187-214.
- Truswell, E.M., Macphail, M.K., 2009. Polar forests on the edge of extinction: what does the fossil spore and pollen evidence from East Antarctica say? *Australian systematic botany* 22, 57-106.
- Utescher, T., Mosbrugger, V., Ashraf, A.R., 2000. Terrestrial climate evolution in northwest Germany over the last 25 million years. *Palaios* 15, 430-449.
- Utescher, T., Mosbrugger, V., 2013. The Palaeoflora Database, <http://www.geologie.unibonn.de/Palaeoflora>.
- van der Kaars, S., 2001. Pollen distribution in marine sediments from the south-eastern Indonesian waters. *Palaeogeography, Palaeoclimatology, Palaeoecology* 171, 341-361.
- Vandenbergh, N., Hilgen, F.J., Speijer, R.P., 2012. The Paleocene Period. In: Gradstein, F.M., Ogg, J.G., Schmitz, M.D., Ogg, G.M. (Eds.), *The Geologic Time Scale 2012*. Elsevier, Amsterdam, pp. 855-922.
- Vanhove, D., Stassen, P., Speijer, R.P., Steurbaut, E., 2011. Assessing paleotemperature and seasonality during the Early Eocene Climatic Optimum (EECO) in the Belgian Basin by means of fish otolith stable O and C Isotopes. *Geologica Belgica* 14, 143-158.
- Varughese, M.M., Pienaar, E.A.D., 2013. Statistical inference for a multivariate diffusion model of an ecological time series. *Ecosphere* 4, art104.

- Veblen, T.T., 1982. Regeneration patterns in *Araucaria araucana* forests in Chile. *Journal of Biogeography* 9, 11-28.
- Veblen, T.T., Hill, R.S., Read, J., 1996. *The Ecology and Biogeography of Nothofagus Forests*. Yale University Press, New Haven. 403 pp.
- Volkova, L., Bennett, L.T., Tausz, M., 2009. Effects of sudden exposure to high light levels on two tree fern species *Dicksonia antarctica* (Dicksoniaceae) and *Cyathea australis* (Cyatheaceae) acclimated to different light intensities. *Australian Journal of Botany* 57, 562-571.
- Walsh, E.M., Ingalls, A.E., Keil, R.G., 2008. Sources and transport of terrestrial organic matter in Vancouver Island fjords and the Vancouver-Washington Margin: A multiproxy approach using $\delta^{13}\text{C}_{\text{org}}$, lignin phenols, and the ether lipid BIT index. *Limnology and Oceanography* 53, 1054-1063.
- Wanntorp, L., Vajda, V., Raine, J.I., 2011. Past diversity of Proteaceae on subantarctic Campbell Island, a remote outpost of Gondwana. *Cretaceous Research* 32, 357-367.
- Warny, S., Askin, R., 2011. Vegetation and organic-walled phytoplankton at the end of the Antarctic greenhouse world: Latest Eocene cooling events. In: Anderson, J.B., Wellner, J.S. (Eds.), *Tectonic, Climatic, and Cryospheric Evolution of the Antarctic Peninsula*. American Geophysical Union Special Publication, 63, Geopress, American Geophysical Union, Washington D.C., pp. 193-210.
- Weijers, J., Schouten, S., Vandendunker, J., Hopmans, E., Sinninghe Damsté, J.S., 2007a. Environmental controls on bacterial tetraether membrane lipid distribution in soils. *Geochimica et Cosmochimica Acta* 71, 703-713.
- Weijers, J.W.H., Bernhardt, B., Peterse, F., Werne, J.P., Dungait, J.A.J., Schouten, S., Sinninghe Damsté, J.S., 2011. Absence of seasonal patterns in MBT-CBT indices in mid-latitude soils RID H-5627-2011. *Geochimica et Cosmochimica Acta* 75, 3179-3190.
- Weijers, J.W.H., Schefuß, E., Schouten, S., Sinninghe Damsté, J.S., 2007b. Coupled thermal and hydrological evolution of tropical Africa over the Last Deglaciation. *Science* 315, 1701-1704.
- Weijers, J.W.H., Schouten, S., Sluijs, A., Brinkhuis, H., Sinninghe Damsté, J.S., 2007c. Warm arctic continents during the Palaeocene–Eocene thermal maximum. *Earth and Planetary Science Letters* 261, 230-238.
- Weijers, J.W.H., Schouten, S., van den Donker, J.C., Hopmans, E.C., Sinninghe Damsté, J.S., 2007d. Environmental controls on bacterial tetraether membrane lipid distribution in soils. *Geochimica et Cosmochimica Acta* 71, 703-713.
- Weis, D., Kieffer, B., Maerschalk, C., Barling, J., de Jong, J., Williams, G.A., Hanano, D., Pretorius, W., Mattielli, N., Scoates, J.S., Goolaerts, A., Friedman, R.M., Mahoney, J.B., 2006. High-precision isotopic characterization of USGS reference materials by TIMS and MC-ICP-MS. *Geochemistry Geophysics Geosystems* 7, Q08006.

- West, M., Harrison, J., 1997. Bayesian Forecasting and Dynamic Models. Springer, New York. 700 pp.
- Westerhold, T., Röhl, U., Raffi, I., Fornaciari, E., Monechi, S., Reale, V., Bowles, J., Evans, H.F., 2008. Astronomical calibration of the Paleocene time. *Palaeogeography, Palaeoclimatology, Palaeoecology* 257, 377-403.
- Wilf, P., Cuneo, N.R., Johnson, K.R., Hicks, J.F., Wing, S.L., Obradovich, J.D., 2003. High plant diversity in Eocene South America: Evidence from Patagonia. *Science* 300, 122-125.
- Wilf, P., Johnson, K.R., Cuneo, N.R., Smith, M.E., Singer, B.S., Gandolfo, M.A., 2005. Eocene plant diversity at Laguna del Hunco and Rio Pichileufu, Patagonia, Argentina. *The American Naturalist* 165, 634-650.
- Williams, G.L., Brinkhuis, H., Pearce, M.A., Fensome, R.A., Weegink, J.W., 2004. Southern Ocean and global dinoflagellate cyst events compared: Index events for the Late Cretaceous–Neogene. *Proceedings of the Ocean Drilling Program, Scientific Results* 189, 1-98.
- Wilson, D.S., Jamieson, S.S.R., Barrett, P.J., Leitchenkov, G., Gohl, K., Larter, R.D., 2012. Antarctic topography at the Eocene-Oligocene boundary. *Palaeogeography, Palaeoclimatology, Palaeoecology* 335, 24-34.
- Wilson, P.G., 2011. Myrtaceae. In: Kubitzki, K. (Ed.), *Flowering Plants, Eudicots. Sapindales, Cucurbitales, Myrtaceae*. Springer, Germany, pp. 212-271.
- Wing, S., Greenwood, D.R., 1993. Fossils and fossil climate: the case for equable continental interiors in the Eocene. *Philosophical Transactions of the Royal Society of London Series B-Biological Sciences* 341, 243-252.
- Wing, S., Harrington, G.J., 2001. Floral response to rapid warming in the earliest Eocene and implication for concurrent faunal change. *Paleobiology* 27, 539-563.
- Wing, S.L., Currano, E.D., 2013. Plant response to a global greenhouse event 56 million years ago. *American Journal of Botany* 100, 1234-1254.
- Wing, S.L., Harrington, G.J., Bowen, G.J., Koch, P.L., 2003. Floral change during the initial Eocene Thermal Maximum in the Powder River Basin, Wyoming. In: Wing, S., Gingerich, P.D., Schmitz, B., Thomas, E. (Eds.), *Causes and Consequences of Globally Warm Climates in the Early Paleogene*. Geological Society of America Special Paper 369, Boulder, Colorado, pp. 425-440.
- Wolfe, J.A., 1978. A paleobotanical interpretation of Tertiary climates in the northern hemisphere. *American Scientist* 66, 694-703.
- Wolfe, J.A., 1979. Temperature parameters of humid to mesic forests of eastern Asia and relation to forests of other regions of northern hemisphere and Australasia. U.S. Geological Survey Professional Paper 1106, 1-37.

- Woodward, F.I., 1987. *Climate and Plant Distribution*. Cambridge University Press, Cambridge. 174 pp.
- Woodward, F.I., Lomas, M.R., Kelly, C.K., 2004. Global climate and the distribution of plant biomes. *Philosophical Transactions of the Royal Society of London Series B-Biological Sciences* 359, 1465-1476.
- Wrenn, J.H., Hart, G.F., 1988. Paleogene dinoflagellate cyst biostratigraphy of Seymour Island, Antarctica. In: Feldmann, R., Woodburne, M.O. (Eds.), *Geology and Paleontology of Seymour Island, Antarctic Peninsula*. Geological Society of America Memoir 169, Geological Society of America, Boulder, Colorado, pp. 321-447.
- Yapp, C.J., 2004. Fe(CO₃)OH in goethite from a mid-latitude North American Oxisol: estimate of atmospheric CO₂ concentration in the Early Eocene "climatic optimum". *Geochimica et Cosmochimica Acta* 68, 935-947.
- Zachos, J., Stott, L.D., Lohmann, K.C., 1994. Evolution of early Cenozoic marine temperatures. *Paleoceanography* 9, 353-387.
- Zachos, J.C., Dickens, G.R., Zeebe, R.E., 2008. An early Cenozoic perspective on greenhouse warming and carbon-cycle dynamics. *Nature* 451, 279-283.
- Zachos, J.C., Pagani, M., Sloan, L., Thomas, E., Billups, K., 2001. Trends, rhythms, and aberrations in global climate 65 Ma to present. *Science* 292, 686-693.
- Zachos, J.C., Wara, M.W., Bohaty, S., Delaney, M.L., Petrizzo, M.R., Brill, A., Bralower, T.J., Premoli-Silva, I., 2003. A transient rise in tropical sea surface temperature during the Paleocene-Eocene thermal maximum. *Science* 302, 1551-1554.

Zusammenfassung

Das frühe Paläogen war durch ein globales Treibhausklima charakterisiert: die klimatischen Bedingungen waren durch hohe Temperaturen gekennzeichnet, des Weiteren waren die Konzentrationen an Treibhausgasen in der Atmosphäre deutlich höher als heute. Das Klima im späten Paläozän war durch eine stetige Erwärmung gekennzeichnet, die im frühen Eozän mit dem „Early Eocene Climatic Optimum“ (EECO; 53–51 Ma) ihren Höhepunkt erreichte. Der generelle Langzeittrend zu wärmeren Bedingungen, wurde von kurzfristigen Ereignissen überlagert, in denen rasche Temperaturanstiege auftraten. Ein solches Ereignis ist das „Paleocene Eocene Thermal Maximum“ (PETM, ~56 Ma). Das PETM ist nicht nur durch eine rasche Erwärmung, sondern auch durch eine negative Kohlenstoffisotopenexkursion von 3-8‰ gekennzeichnet. Auf die warmen Bedingungen folgte im mittleren bis späten Eozän eine Abkühlung in den hohen Breiten. Die Eozän-Oligozän Grenze markiert den Endpunkt dieser Abkühlungsphase: rasant dehnten sich Innlandeismassen im Gebiet der Antarktis aus, die den Beginn globaler „Eishaus“-Bedingungen anzeigen.

Klimatische Trends und die Entwicklung von Ökosystemen während der „Treibhausbedingungen“ des frühen Paläogen sind für das terrestrische Milieu noch nicht ausreichend bekannt. Existierende paleobotanischen Datensätze bieten einen gewissen Einblick in die Vegetation, die in dieser Region im Paläozän und frühen Eozän vorherrschte. Es ist allerdings nötig, Datensätze zu generieren, die aus vollständigen und gut datierten sedimentären Sequenzen stammen. In der vorliegenden Arbeit wurden Pollenanalysen an Tiefsee-Sedimentbohrkernen aus der australisch-antarktischen Region durchgeführt: (i) IODP Site U1356 (*Wilkes Land margin*, Ostantarktis) und (ii) ODP Site 1172 (Osttasmanisches Plateau, südwestpazifischer Ozean).

Die hier untersuchte Sequenz des Bohrkerns, der an der IODP-Site U1356 gezogen wurde, enthält Ablagerungen des mittleren Schelfs. Diese stammen aus dem frühen bis mittleren Eozän (53.9-46 Ma). Die Paläobreiten der Bohrstelle und des *Wilkes Land margin* sind nahezu identisch mit den heutigen Positionen. Lithologisch besteht die Abfolge des frühen Eozän aus bioturbierten Tonsteinen, in die feinkörnige Sandsteinlagen zwischengeschaltet sind. Mit Hilfe eines Altersmodells, das auf Magnetostratigraphie, sowie auf Biostratigraphie (basierend auf Dinoflagellatenzysten) beruht, konnten die eozänen Sedimente des Bohrkerns der Site U1356 stratigrafisch zugeordnet werden.

Des Weiteren wurden Sedimente des Bohrkerns ODP Site 1172 untersucht. Diese umfassen ein Alter vom mittleren Paläozän bis in das frühe Eozän (60.7-54.2 Ma). Sie stellen marine Flachwasserablagerungen dar. Die Position der Site 1172 befindet sich auf dem Osttasmanischen Plateau. Dieses befand sich im frühem Paläogen bei ~65°S und damit sehr viel näher an der Antarktis als heute. Der Bohrkern besteht vorwiegend aus grauen bis graubraunen Ton- und Siltsteinen. Kalkige und kieselige Mikrofossilien kommen nur in

geringer Häufigkeit vor. Das Altersmodell zur zeitlichen Einordnung der Ablagerungen beruht auf Magneto-Chemostratigraphie und Dinoflagellatenzysten-Zonierung.

Die hier vorgestellte Studie umfasst palynologische Untersuchungen an 225 Proben. Zum einen wurden Pollen- und Sporenvergesellschaftungen von 145 Proben aus dem Eozän bestimmt (*IODP Site U1356*), zum anderen 80 Proben aus dem mittleren Paläozän bis frühen Eozän (*ODP Site 1172*). Die Proben wurden mit einem Lichtmikroskop bei 200-facher Vergrößerung untersucht. Allerdings war die Häufigkeit von Sporomorphen in vielen analysierten Proben sehr gering. Um auf Sporenzahlen zwischen 100 und 300 zu kommen, mussten bis zu 12 Deckgläser von jeweils einer Probe angefertigt werden. Die detaillierte Bestimmung morphologischer Merkmale wurde bei 1000-facher Vergrößerung durchgeführt.

Für die Identifizierung des Einzugsgebietes muss in Betracht gezogen werden, dass die hier untersuchten Sporen- und Pollenproben der *Site U1356* und der *Site 1172* aus dem marinen Milieu stammen (siehe Kapitel 1.4). In dieser Studie wird deswegen angenommen, dass die terrestrischen Komponenten in den Sedimenten zum einen ihren Ursprung im *Wilkes Land margin* haben (*Site U1356*), sowie zum anderen aus Tasmanien stammen (*Site 1172*). Die Ablagerungen liefern somit Einblicke in die damalige Vegetation dieser Gebiete. Diese Annahme konnte durch weitere Hinweise bestätigt werden, die in Kapitel 2 und 3 (*Site U1356*) und in Kapitel 4 (*Site 1172*) ausführlich diskutiert werden.

Die vorliegende Arbeit hatte folgende Schwerpunkte, die mit Hilfe von Pollen- und Sporenanalysen an Sedimentgesteinen der *Site U1356* und *Site 1172* bearbeitet wurden: (1) die Rekonstruktion der klimatischen Bedingungen im terrestrischen Milieu (*Wilkes Land margin* und Tasmanien) für das Zeitintervall mittleres Paläozän bis mittleres Eozän; (2) die Untersuchung der Struktur, sowie der Diversität und der Zusammensetzung der Wälder, die im frühen Paläogen entlang von *Wilkes Land margin* und Tasmanien vorhanden waren; (3) die Rekonstruktion der Reaktion der Wälder in den südlichen Breiten auf die Dynamik des Klimas im frühen Paläogen; (4) die Ausarbeitung der Beziehung zwischen den ermittelten terrestrischen Palynomorphen-Daten und den publizierten Temperaturen des Oberflächenwassers des Ozeans, die an den gleichen Bohrkernen bestimmt wurden.

Die hier durchgeführte Rekonstruktion der klimatischen Bedingungen im terrestrischen Milieu der australisch-antarktischen Region beruht auf dem Aktualitätsprinzip (*nearest living relative*, NLR). Es wird angenommen, dass fossile Taxa die gleichen klimatischen Ansprüche hatten wie ihre heutigen nächsten lebenden Verwandten. Dieser Ansatz wurde auf die Pollen- und Sporendaten der Lokationen *Site U1356* und *Site 1172* angewendet, unter Einsatz der „bioklimatischen Analyse“. Basierend auf den botanischen Vorlieben, die die Taxa, für die der NRL bekannt ist, aufweisen, konnten daher folgende Klimaparameter bestimmt werden: die Jahresdurchschnittstemperatur (*mean annual temperature*, MAT), die Durchschnittstemperatur des kältesten Monats (*coldest month mean temperature*, CMMT), die Winterdurchschnittstemperatur (*mean winter temperature*, MWT), die Durchschnittstemperatur des wärmsten Monats (*warmest month mean temperature*,

WMMT), die Sommerdurchschnittstemperatur (*mean summer temperature*, MST) und der durchschnittliche Jahresniederschlag (*mean annual precipitation*, MAP). Alle Profile enthalten sowohl die höchsten, als auch die niedrigsten Werte für verschiedene Klimavariablen, die mit Hilfe jedes NRLs bestimmt wurden. Die bioklimatischen Analysen wurden angewendet, um die Zonen klimatischer Überschneidungen für die Mehrzahl der Taxa zu bestimmen.

In dieser Studie wurden qualitative und quantitative Analysen von fossilen Sporomorpha kombiniert. Es wurde sowohl die Struktur, als auch die Diversität der Vegetation derselben Region untersucht. Die Struktur der Vegetation sollte mittels des qualitativen Ansatzes rekonstruiert werden. Diese Ergebnisse basieren auf den ökologischen Anforderungen und den Lebensräumen heutiger eng verwandter Arten. Der quantitative Ansatz wurde gewählt, um beides, sowohl die Diversität, als auch die Struktur der Vegetation zu bestimmen. Dafür wurden Ordinationsverfahren (*Detrended Correspondence Analysis* und *Multidimensional Scaling*), Rarefizierung (*Rarefaction*) und Diversitätsindizes angewendet.

Die wesentliche Erkenntnis aus dieser Studie ist, dass temperierte und paratropische Wälder während des frühen Paläogens in den südlichen hohen Breiten wuchsen (zum einen am *Wilkes Land margin* bei $\sim 70^\circ\text{S}$, zum anderen in Tasmanien bei $\sim 65^\circ\text{S}$). Diese Aussage basiert auf den durchgeführten Rekonstruktionen paleoklimatischer Bedingungen und Vegetationsmuster.

Im Speziellen zeigen die Pollendaten des *Site* U1356, dass während des frühen Eozän (53.9 – 51.9) in der Antarktis ein hochdiverser Wald wuchs. Charakteristisch ist das Auftreten thermophiler Taxa, wie *Bombacoideae*, *Strasburgeria*, *Beauprea*, *Spathiphyllum*, *Anacolosa* und *Lygodium*. Heute sind diese Arten lediglich in den tropischen und subtropischen Breiten zu finden. Paläotemperaturen, die mittels des MBT/CBT-Proxies bestimmt wurden, geben, ebenso wie die Pollendaten, Hinweise darauf, dass nahezu tropische Temperaturen am *Wilkes Land margin* geherrscht haben, zumindest in den Küstenniederungen. Neben den tropisch/subtropischen Arten treten während des Eozäns zeitgleich Pflanzen auf, die heute auf temperierte Klimata beschränkt sind. Ein Beispiel ist *Nothofagus* (subgenus *Fuscospora* und *Nothofagus*). Dies weist darauf hin, dass die Wälder in dieser Region einen klimatischen Gradienten nachzeichneten, der von der Höhe über dem Meeresspiegel und/oder der Nähe zur Küstenlinie abhing. Die Vegetation am *Wilkes Land margin* war im frühen Eozän durch paratropische Wälder charakterisiert. Diese wurden aber im mittleren Eozän durch temperierte Wälder verdrängt, die eine geringere Diversität aufwiesen und von *Nothofagus* dominiert wurden. Der stetige Abkühlungstrend während dieses Zeitintervalls ist durch folgende Beobachtungen belegt: (1) das Vorkommen von „*Nothofagus*-Wäldern“; (2) das Fehlen von wärmeliebenden Pflanzen; (3) die Rekonstruktion von geringen Temperaturen, die zum einen auf MBT/CBT Paläothermometrie beruhen, zum anderen mit Hilfe von Pollenanalysen ermittelt wurden.

Die MAT-, MWT-, MST- und MAP-Daten für die *Site* U1356 wurden in dieser Studie sowohl für die Biome in den Niederungen (paratropische Bedingungen), als auch für die

Biome in den Hochländern (temperierte Bedingungen) bestimmt. Allerdings sind die Werte nicht für den gesamten antarktischen Kontinent repräsentativ. Dennoch spielen sie in den derzeit geführten Debatten über Klimawandel und Ökosysteme eine große Rolle. Zum einen wird diskutiert, ob es mit Hilfe von Klimamodellen überhaupt möglich ist, extreme Treibhausbedingungen zu rekonstruieren, zum anderen stellt sich die Frage, wie polare Ökosysteme auf ansteigende CO₂ Konzentrationen in der Atmosphäre reagieren.

Ein weiterer Aspekt dieser Arbeit war die qualitative und quantitative Charakterisierung der Wälder im Eozän am *Wilkes Land margin*. Diese basiert auf Pollen- und Sporengemeinschaften von *Site U1356*. Die Kombination der qualitativen und quantitativen Analysen zeigt, dass die Wälder im frühen Eozän am *Wilkes Land margin* sehr divers waren: die Zusammensetzung der Pflanzengemeinschaften ist typisch für die der heutigen Tropen; die Artenvielfalt entspricht der, die in den heutigen Wäldern auf Neukaledonien zu finden sind. Die Wälder des mittleren Eozäns waren durch *Nothofagus* dominiert. Ihre Biodiversität war gering, ähnlich wie die der heutigen *Nothofagus*-Wälder in Neuseeland. Die stratigraphische Verteilung ausgewählter Taxa ist in Appendix 1 dieser Arbeit zu finden; des Weiteren ist dort die Charakterisierung der Gruppen, die mit Hilfe taxonomischer Merkmale und Photos bestimmt wurden, dargestellt.

Die in dieser Studie ermittelten Sporomorphdaten und klimatischen Rekonstruktionen für *Site 1172* weisen darauf hin, dass vom mittleren Paläozän bis in das frühe Eozän drei verschiedene Vegetationstypen in Tasmanien auftraten. Das Vorkommen der verschiedenen Typen hing von den klimatischen Bedingungen während dieses Zeitintervalls ab. Während des mittleren bis späten Paläozäns wuchsen warm-temperierte Wälder auf Tasmanien, in denen Podocarpaceae und Araucariaceae dominierten. Am Übergang vom mittleren zum späten Paläozän (~59.5 to ~59.0 Ma) wurden diese Wälder vorübergehend durch Vegetationsstrukturen, die für ein kalt-temperiertes Klima charakteristisch sind, ersetzt. *Nothofagus* und Araucariaceae bestimmten die Wälder, frostsensitive Elemente wie Palmen (Arecaceae) und Palmfarne (Cycadales) fehlten. Im frühen Eozän und gekoppelt an das PETM wurde die im Paläozän vorherrschende Vegetation von paratropischen Regenwäldern ersetzt: anstelle von Gymnospermen, die für temperierte Klimata charakteristisch sind, traten im frühesten Eozän und während des PETM Mangroven (Nipapalme; *Nypa*) auf. Der Vergleich mit bisher veröffentlichten Pollen- und Sporen-Datensätzen aus der südwestpazifischen Region (einschließlich Südostaustralien und Neuseeland) unterstützt die Aussagekraft der präsentierten Daten aus Tasmanien. Er zeigt, dass während des frühen Eozäns in der ganzen Region im südwestlichen Pazifik temperierte Wälder von paratropischen Wäldern abgelöst wurden. Diese Neuaufstellung in der Zusammensetzung der Vegetation beinhaltet ein häufigeres Vorkommen von Farnen (überwiegend Cyatheaceae) und Angiospermen (unter anderem Proteaceae, Euphorbiaceae/Eumalvoideae, Casuarinaceae), die sich auf Kosten der Gymnospermen (hauptsächlich Podocarpiden) ausbreiteten. Die in dieser Studie gewonnenen Daten von *Site 1172* ermöglichen Rückschlüsse auf Klimabedingungen im terrestrischen Milieu. Bisher existieren Studien, in denen die marinen Ablagerungen desselben Kerns untersucht wurden.

Wesentliche publizierte Ergebnisse sind Temperaturrekonstruktionen für das Oberflächenwassers des Ozeans (*sea-surface temperature*; SST), die auf TEX₈₆-Messungen basieren. Während des Übergangs vom mittleren zum späten Paläozän (~59.5 bis ~59.0 Ma) wurde eine Abkühlung des Oberflächenwassers um ~3 °C ermittelt. Der Hinweis auf kältere Bedingungen, stimmt mit den hier gewonnenen Daten überein: frostsensitive Pflanzen (d. h. Palmen und Palmfarne) wurden in Tasmanien zunehmend verdrängt, des Weiteren entwickelten sich Wälder, die für kalt-temperierte Klimata typisch sind und von *Nothofagus* und Araucariaceae dominiert wurden. Dies weist darauf hin, dass zu dieser Zeit in dieser Region ein kälteres Klima herrschte (und vor allem harsche Winter auftraten, die durch starken und/oder häufige Frostperioden gekennzeichnet waren).

Die in dieser Arbeit ermittelten Niederschlagsrekonstruktionen für die Lokalität *ODP Site 1172* geben Hinweise, dass in Tasmanien die MAP-Werte vom mittleren Paläozän bis in das frühe Eozän bei ~180 cm/a weitgehend konstant waren. Für die Ostantarktis (*Site U1356*) wurde ein MAP-Mittelwert von ~132 cm/a für das frühe Eozän und 160 cm/a für das mittlere Eozän bestimmt. Die Niederschlagsrekonstruktionen beider Lokalitäten deuten darauf hin, dass während des frühen Paläogens die australisch-antarktischen Region durch starke Niederschläge (>100 cm/a) charakterisiert war. Die damaligen Bedingungen sind mit heutigen Zuständen in den Regenwäldern der südlichen Breiten vergleichbar.

Die hier dargestellten Ergebnisse ermöglichen die Rekonstruktion von Klimabedingungen im terrestrischen Milieu in der australisch-antarktischen Region im frühen Paläogen. Das Gesamtergebnis hilft schließlich, Klimamodelle zu prüfen und die Reaktion terrestrischer Ökosysteme der hohen Breiten auf die Klimadynamik im frühen Paläogen in den südlichen Breiten zu verstehen.

Um die klimatischen Bedingungen, die in den hohen Breiten im Paläogen herrschten, aufzuklären, wurden in der vorliegenden Arbeit terrestrische und marine Ergebnisse verglichen. Aus der Kombination von den hier ermittelten Sporomorphdaten mit publizierten SSTs, die auf TEX₈₆-Messungen an *Site 1172*, kann folgende Aussage gemacht werden: die Veränderungen in der Vegetation war eng mit der Temperaturentwicklung mariner und terrestrischer Gebiete der australisch-antarktischen Region gekoppelt. Des Weiteren wird deutlich, dass beide Kalibrierungsmethoden (d. h. TEX₈₆^H und TEX₈₆^L) eine einseitige Tendenz zur Rekonstruktion warmer Bedingungen zeigen, wenn sie auf Datensätze aus dem frühen Paläogen angewendet werden.

Appendices

Appendix 1 Taxonomy Site U1356

Selected sporomorph taxa are depicted on Plates I to VIII; an alphabetical list of all pictured taxa is provided below. For a full list of identified sporomorph taxa and their stratigraphic distribution in the Eocene of Site U1356 see Fig. 3.2. Slides and residues are stored in the collection of the Institute of Geosciences, Goethe University Frankfurt, Germany.

- Alisporites* spp. (Plate VIII, 1-2; reworked)
Anacolosidites luteoides Cookson and Pike, 1954 (Plate V, 10; botanical affinity: *Anacolosia* [Olacaceae])
Araucariacites australis Cookson, 1947 (Plate III, 4; Araucariaceae)
 ?*Arecipites* sp. A (Plate III, 9; Arecaceae?)
Arecipites spp. (Plate III, 7-8; Arecaceae)
Baculatisporites sp. (Plate II, 8; probably Osmundaceae)
Beaupreaidites sp. aff. *B. orbiculatus* Dettmann and Jarzen, 1988 (Plate VI, 11; *Beauprea* [Proteaceae])
Beaupreaidites sp. cf. *B. verrucosus* Cookson, 1950 (Plate VII, 8; *Beauprea* [Proteaceae])
Bluffopollis scabratus (Couper) Pocknall and Mildenhall, 1984 (Plate IV, 1-2; *Strasburgeria* [Strasburgeriaceae])
Bombacacidites sp. A (Plate IV, 5-6; Bombacoideae [Malvaceae])
Camarozonosporites ohaiensis (Couper) Dettmann and Playford, 1968 (Plate I, 12)
Cannanoropollis sp. (Plate VIII, 5; reworked)
Cicatricosisporites sp. (Plate VIII, 8; reworked)
Cingulatisporites sp. (Plate II, 1)
Classopollis sp. (Plate VIII, 6; reworked)
Crassoretitriteles sp. cf. *C. vanraadshooveni* (Germeraad) Hopping and Muller, 1968 (Plate II, 2; *Lygodium*)
Cyathidites sp. cf. *C. splendens* Harris, 1965 (Plate I, 7; Cyatheaceae, Adiantaceae)
Cyathidites australis Couper, 1953 (Plate I, 8; probably Cyatheaceae)
Cyathidites minor Couper, 1953 (Plate I, 9; probably Cyatheaceae)
Cycadopites sp. (Plate III, 10; Cycadophyta and other gymnosperms)
Dacrycarpites australiensis Cookson and Pike, 1953 (Plate II, 11; *Dacrycarpus dacrydioides* [Podocarpaceae])
Dacrydiumites sp. (Plate III, 3; *Dacrydium* [Podocarpaceae])
Dilwynites granulatus Harris, 1965 (Plate III, 5; *Wollemia* [Araucariaceae])
Dilwynites tuberculatus Harris, 1965 (Plate III, 6; *Wollemia* [Araucariaceae])
Ericipites sp. (Plate V, 6; Ericaceae)
Foveotriteles lacunosus Partridge, 1973 (Plate II, 3; *Huperzia* [Lycopodiaceae])
Gambierina edwardsii (Cookson and Pike) Harris, 1972 (Plate V, 8)
Gambierina rudata Partridge and Stover, 1973 (Plate V, 9)

- Gleicheniidites senonicus* Ross 1949 (Plate II, 4)
- Ischyosporites* sp. (Plate I, 10-11)
- Klukisporites* sp. (Plate VIII, 9; reworked)
- Laevigatosporites* sp. (Plate I, 4)
- Lycopodiumsporites* sp. (Plate VIII, 7; reworked)
- Malvacipollis subtilis* Stover in Stover and Partridge, 1973 (Plate V, 4-5; Euphorbiaceae, Malvaceae?)
- Margocolporites cribellatus* Srivastava, 1972 (Plate IV, 3-4)
- Microcachryidites antarcticus* Cookson, 1947 (Plate II, 10; *Microstrobos*, *Microcachrys tetragona* [Podocarpaceae])
- Myricipites harrisii* (Couper) Dutta and Sah, 1970 (Plate V, 2-3; Casuarinaceae, Myricaceae?)
- Myrtacidites* sp. (Plate III, 11; Myrtaceae)
- Myrtacidites tenuis* Harris, 1965 (Plate III, 12; Myrtaceae)
- Neoraistrickia truncata* (Cookson) Potonié 1956 (Plate VIII, 10; reworked)
- Nothofagidites asperus* (Cookson) Romero, 1973 (Plate IV, 9; *Nothofagus* subg. *Lophozonia*)
- Nothofagidites flemingii* complex *sensu* Macphail and Truswell, 2004 (Plate IV, 7; *Nothofagus* subg. *Nothofagus*)
- Nothofagidites lachlaniae* complex *sensu* Macphail and Truswell, 2004 (Plate IV, 8; *Nothofagus* subg. *Fuscospora*)
- Nothofagidites* sp. cf. *N. senectus* Dettmann and Playford, 1968 (Plate IV, 10; *Nothofagus*)
- Nothofagidites emarcidus* complex *sensu* Truswell and Macphail, 2009 (Plate IV, 11; *Nothofagus* subg. *Brassospora*?)
- Osmundacidites* sp. (Plate II, 7; Osmundaceae)
- Phyllocladidites mawsonii* Cookson, 1947 *ex* Couper, 1953 (Plate III, 1-2; *Lagarostrobos franklinii* [Podocarpaceae])
- Podocarpidites ellipticus* Cookson, 1947 (Plate II, 12; *Podocarpus* [Podocarpaceae])
- Polypodiisporites* sp. (Plate I, 3)
- Propylipollis* sp. cf. *P. annularis* Cookson, 1950 (Plate VI, 9; Proteaceae)
- Propylipollis* sp. cf. *P. reticulosabratus* Harris, 1965 (Plate VII, 12; Proteaceae)
- Propylipollis annularis* Cookson, 1950 (Plate VI, 7-8; *Xylomelum occidentale*, *Lambertia* [Proteaceae])
- Propylipollis reticulosabratus* Harris, 1965 (Plate VII, 10-11; *Gevuina/Hicksbeachia* type [Proteaceae])
- Propylipollis* sp. 3 (Plate VI, 4-5; Proteaceae)
- Proteacidites adenanthoides* Cookson, 1950 (Plate VIII, 9; *Adenanthos* ([Proteaceae])
- Proteacidites incurvatus* Cookson, 1950 (Plate VI, 3; Proteaceae)
- Proteacidites pachypolus* Cookson and Pike, 1954 (Plate VII, 6; Proteaceae)
- Proteacidites similis* Harris, 1965 (Plate VI, 12; Proteaceae)
- Proteacidites* sp. 2 (Plate VII, 1; Proteaceae)
- Proteacidites* sp. cf. *P. amolosexinus* Dettmann and Playford, 1968 (Plate VI, 7; Proteaceae)
- Proteacidites* sp. cf. *P. callosus* Cookson, 1950 (Plate VII, 5; Proteaceae)

- Proteacidites* sp. cf. *P. parvus* Cookson, 1950 (Plate VII, 2-3; *Belladena montana* type, Proteaceae)
- Proteacidites* sp. cf. *P. spiniferus* McIntyre, 1968 (Plate VII, 4; *Embothrium?* [Proteaceae])
- Proteacidites* sp. cf. *P. tuberculatus* Cookson, 1950 (Plate VI, 6; Proteaceae)
- Protohaploxypinus* spp. (Plate VII, 3-4; reworked)
- Punctatosporites* sp. (Plate I, 1-2)
- Rhoipites* sp. (Plate V, 7)
- ?*Scabramonoletes* sp. (Plate I, 5,6)
- Scabratrporites* sp. (Plate VI, 1-2)
- Spathiphyllum* type (Plate III, 13; *Spathiphyllum* [Araceae])
- Stereisporites* sp. (Plate II, 5; Sphagnaceae)
- Tetracolporites* sp. aff. *T. oamaruensis* Couper, 1953 (Plate V, 11)
- Tetracolporites* sp. (Plate IV, 12)
- Trichotomosulcites subgranulatus* Couper 1953 (Plate II, 9; Podocarpaceae)
- Tricolpites* sp. cf. *T. fissilis* Couper, 1960 (Plate V, 1)
- Triporopollenites* sp. cf. *T. ambiguus* Stover in Stover and Partridge, 1973 (Plate VI, 10)
- Tripunctisporis maastrichtiensis* (Krutzschn) Herngreen et al., 1986 (Plate II, 6; Sphagnaceae?)

Taxonomic Remarks

Pteridophyte and bryophyte spores

Genus *Cingulatisporites* Thomson in Thomson and Pflug, 1953 emend. Hiltman, 1967

Cingulatisporites sp. (Plate II, 1)

Dimensions: 41–52 μm (equatorial diameter; n = 5)

General description: amb subtriangular to circular, trilete mark distinct and reaching the equator, sporoderm scabrate to granulate, cingulate (cingulum 3–4 μm thick with spongy appearance).

Genus *Ischyosporites* Balme, 1957

Ischyosporites sp. (Plate I, 10-11)

Dimensions: 22–34 μm (equatorial diameter; n = 5)

General description: amb subtriangular, trilete, simple laesura reaching almost the equator, sporoderm 2 μm thick. In proximal view laevigate, in distal view foveolate to fossulate and surrounded by anastomosing ribs, foveolae and fossulae 2–3 μm wide.

Genus *Punctatosporites* Ibrahim 1933 emend. Alpern and Doubinger, 1973

Punctatosporites sp. (Plate I, 1-2)

Dimensions: 23–26 x 27–30 μm (width x length; n = 4)

General description: amb elliptical, monolete, laesura distinct and extending across $\frac{3}{4}$ of the length of the equatorial axis, sculpture granulate, granulae ~ 0.5 μm in diameter, sporoderm 1–2 μm thick.

Genus *Scabramonoletes* Ramanujam, 1966

?*Scabramonoletes* sp. (Plate I, 5)

Dimensions: 30–x 42–49 μm (width x length; n = 7)

General description: amb elliptical, laesura indistinct, sporoderm 2–2.5 μm thick, sculpture scabrate. The taxon is provisionally assigned to *Scabramonoletes* because the laesura is not visible in the examined specimens.

Angiosperm pollen

Genus *Arecipites* Wodehouse, 1933 emend. Nichols et al., 1973

Arecipites spp. (Plate III, 7,8)

Dimensions: 21–34 x 44–60 μm (width x length; n = 10)

General description: amb elliptical, monosulcate, sulcus long and tapered at the ends, exine 1 μm thick, tectate, columellae distinct in some specimens, sculpture scabrate to psilate. Specimens of *Arecipites* spp. at Site U1356 are comparable to *A. pseudotranquillus* and *A. punctatus* of Nichols et al. (1973). *Arecipites* is different from *Cycadopites* in that members of the former have a sulcus that is open at the ends and lack any structure within the exine (Nichols et al., 1973; Jansonius et al., 1998).

Botanical affinity: Areaceae

?*Arecipites* sp. A (Plate III, 9)

Dimensions: 29 x 54 μm (width x length; n = 1)

General description: amb elliptical, monosulcate, sulcus long, exine 1 μm thick, tectate?, sculpture verrucate (verrucae 0.5–1.5 μm wide and sparsely distributed), surface interverrucae scabrate. The taxon is provisionally assigned to *Arecipites* because the emendation of the genus by Nichols et al. (1973) does not include specimens with a verrucate sculpture.

Botanical affinity: Areaceae?

Genus *Bombacacidites* Couper, 1960 emend. Krutzsch, 1970

Bombacacidites sp. A (Plate IV, 5-6)

Dimensions: 35–50 μm (equatorial diameter; n = 8)

General description: *Bombacacidites* type, amb subcircular, brevitricolporate, costae 2–4 μm wide, exine 1–2 μm thick, semitectate, sculpture reticulate, lumina 1–2 μm wide. Some specimens of *Bombacacidites* sp. A are similar to *Intratripoporollenites notabilis* of Stover and Evans (1973). Although a detailed description of the apertures is not available, the illustration of *I. notabilis* in Stover and Evans (1973; Plate 3, Fig. 4) suggests the presence of a vestibulum (or fastigium, if the grain is brevitricolporate).

Botanical affinity: Bombacoideae

Genus *Margocolporites* Ramanujam ex Srivastava, 1969

Margocolporites cribellatus Srivastava, 1972 (Plate IV, 3-4)

Dimensions: 34–46 μm (equatorial diameter; $n = 5$)

General description: amb circular to subtriangular, tricolporate. Colpi long, broad at the equator, marginate and costate; margins produced by thinning of sexine, costae 2 μm wide, exine 2 μm thick, tectate, columellae distinct, sculpture micropitted to microreticulate, lumina ~ 0.5 μm wide, homobrochate.

Genus *Proteacidites* Cookson, 1950

Proteacidites sp. 2 (Plate VII, 1)

Dimensions: 48 μm (equatorial diameter; $n = 1$)

General description: amb triangular with straight sides, triporate, pores 10 μm wide, exine 2.5 μm thick, exine thinner towards the apertures, semitectate, columellae distinct, sculpture reticulate, lumina ~ 1 μm wide.

Genus *Propylipollis* Martin and Harris, 1975

Propylipollis sp. 3 (Plate VI, 4-5)

Dimensions: 42–46 μm (equatorial diameter; $n = 2$)

General description: amb triangular with straight sides, triporate, pores 4 μm wide. Exine 3 μm thick, thick endexine, columellae distinct, pores with postatrium, semitectate, sculpture microreticulate, lumina ~ 0.5 μm wide.

Genus *Scabratriporites* van der Hammen ex van Hoeken-Klinkenberg, 1964

Scabratriporites sp. (Plate VI, 1-2)

Dimensions: 28–45 μm (equatorial diameter; $n = 2$)

General description: amb triangular with convex sides, triporate, pores 5–7 μm wide, exine ~ 1 μm thick, tectate, columellae distinct, sculpture scabrate.

Spathiphyllum type *sensu* Hesse and Zetter, 2007 (Plate III, 13)

Dimensions: 64 x 24 μm (polar diameter x equatorial diameter; $n = 1$)

General description: prolate, polyplcate, narrow ribs, exine 1 μm thick, tectate, sculpture psilate, exposed endexine between the ribs.

Genus *Tetracolporites* Couper, 1953 emend. Pocknall and Mildenhall, 1984

Tetracolporites sp. aff. *T. oamaruensis* Couper, 1953 (Plate V, 11)

Dimensions: 24–32 μm (equatorial diameter; $n = 2$)

General description: amb circular, stephanocolporate (5 colpori), long colpi with protruding costae, costae ~ 0.5 μm wide, pores lalongate, exine 2–3 μm thick, columellae distinct,

semitectate, sculpture foveolate, foveolae 1 μm wide. *T. oamaruensis* is psilate to finely punctate and has a thicker exine.

Tetracolporites sp. (Plate IV, 12)

Dimensions: 32 μm (equatorial diameter; $n = 1$)

General description: amb rhombic, stephanocolporate (4 colpi), short colpi, colpi costate, costae 2 μm wide, exine 1 μm thick, tectate, sculpture psilate.

Plate I.

All specimens are from the Eocene of IODP Hole U1356. Scale bars equal 10 μm . Asterisk (*) indicates specimen previously pictured in Supplementary Information of Pross et al. (2012).

- 1.-2. *Punctatosporites* sp.; Sample 101R-1, 30–32 cm (949.1–949.12 mbsf), Slide 1, England-Finder coordinates O33; Sample 104R-4, 130–132 cm (983.32–983.34 mbsf), Slide 1, England-Finder coordinates Q22/1.
3. *Polypodiisporites* sp.; Sample 103R-1, 60–62 cm (968.6–968.62 mbsf), Slide 5, D3/4.
4. *Laevigatosporites* sp.; Sample 97R-CC, 8–11 cm (911.61–911.64 mbsf), Slide 4, V24/1.
- 5.-6. ?*Scabramonoletes* sp.; Sample 103R-4, 135–137 cm (973.85–973.87 mbsf), Slide 1, T20/2; Sample 96R-CC, 14–17 cm (900.74–900.77 mbsf), Slide 4, R8/2.
7. *Cyathidites* sp. cf. *C. splendens* Harris, 1965; Sample 103R-4, 135–137 cm (973.85–973.87 mbsf), Slide 4, G46.
- 8*. *Cyathidites australis* Couper, 1953; Sample 101R-2, 40–42 cm (950.7–950.72 mbsf), Slide 2, G10.
9. *Cyathidites minor* Couper, 1953; Sample 104R-4, 130–132 cm (983.32–983.34 mbsf), Slide 1, N24/3.
- 10.-11. *Ischyosporites* sp.; Sample 106R-2, 40–43 cm (998.56–998.59 mbsf), Slide 1, S25/3.
12. *Camarozonosporites ohaiensis* (Couper) Dettmann and Playford, 1968; Sample 96R-CC, 14–17 cm (900.74–900.77 mbsf), Slide 1, P20/3.

Plate II.

All specimens are from the Eocene of IODP Hole U1356. Scale bars equal 10 μm . Asterisk (*) indicates specimen previously pictured in Supplementary Information of Pross et al. (2012).

1. *Cingulatisporites* sp.; Sample 102R-1, 0–2 cm (958.4–958.42 mbsf), Slide 2, England-Finder coordinates L18/2.
- 2*. *Crassoretitriteles* sp. cf. *C. vanraadshooveni* (Germeraad) Hopping and Muller, 1968; Sample 102R-1, 60–62 cm (959–959.02 mbsf), Slide 2, W29/2.
3. *Foveotriteles lacunosus* Partridge, 1973; Sample 104R-5, 65–67 cm (984–984.02 mbsf), Slide 2, J31/4.
4. *Gleicheniidites senonicus* Ross 1949; Sample 101R-2, 40–42 cm (950.7–950.72 mbsf), Slide 1, W12/1.
5. *Stereisporites* sp.; Sample 102R-1, 0–2 cm (958.4–958.42 mbsf), Slide 1, J11/2.

6. *Tripunctisporis maastrichtiensis* (Krutzsch) Herngreen et al., 1986; Sample 101R-2, 40–42 cm (950.7–950.72 mbsf), Slide 1, F12/3.
7. *Osmundacidites* sp.; Sample 104R-3, 20–22 cm (980.75–980.77 mbsf), Slide 2, M6.
8. *Baculatisporites* sp.; Sample 105R-5, 100–102 cm (993.98–994 mbsf), Slide 1, V10/2.
9. *Trichotomosulcites subgranulatus* Couper 1953; Sample 103R-1, 0–2 cm (968–968.02 mbsf), Slide 7, V31.
10. *Microcachryidites antarcticus* Cookson, 1947; Sample 104R-3, 20–22 cm (980.75–980.77 mbsf), Slide 1, O15/1.
11. *Dacrycarpites australiensis* Cookson and Pike, 1953; Sample 99R-1, 122–125 cm (930.62–930.65 mbsf), Slide 6, C19/1.
12. *Podocarpidites ellipticus* Cookson, 1947; Sample 104R-3, 120–121 cm (981.75–981.76 mbsf), Slide 1, T25/3.

Plate III.

All specimens are from the Eocene of IODP Hole U1356. Scale bars equal 10 μ m. Asterisk (*) indicates specimen previously pictured in Supplementary Information of Pross et al. (2012).

- 1.-2. *Phyllocladidites mawsonii* Cookson, 1947 ex Couper, 1953; Sample 101R-2, 80–82 cm (951–951.12 mbsf), Slide 2, England-Finder coordinates E26/1; Sample 97R-CC, 8–11 cm (911.61–911.64 mbsf), Slide 5, W39/4.
3. *Dacrydiumites* sp.; Sample 103R-1, 20–22 cm (968.2–968.22 mbsf), Slide 2, V24/3.
- 4*. *Araucariacites australis* Cookson, 1947; Sample 102R-1, 0–2 cm (958.4–958.42 mbsf), Slide 2, S13.
5. *Dilwynites granulatus* Harris, 1965; Sample 103R-1, 20–22 cm (968.2–968.22 mbsf), Slide 1, Q31.
6. *Dilwynites tuberculatus* Harris 1965; Sample 100R-1, 10–13 cm (939.2–939.23 mbsf), Slide 3, E4.
- 7*.-8. *Arecipites* spp.; Sample 106R-1, 60–63 cm (997.4–997.43 mbsf), Slide 5, K16/4; Sample 103R-2, 70–72 cm (970.2–970.22 mbsf), Slide 2, E17/4.
9. ?*Arecipites* sp. A; Sample 105R-4, 139–141 cm (992.88–992.9 mbsf), Slide 1, N18/2.
10. *Cycadopites* sp.; Sample 101R-2, 120–121 cm (951.5–951.51 mbsf), Slide 4, P43/3.
11. *Myrtaceidites* sp.; Sample 99R-1, 2–5 cm (929.42–929.45 mbsf), Slide 3, M42/4.
12. *Myrtaceidites tenuis* Harris, 1965; Sample 102R-1, 60–62 cm (959.9–959.02 mbsf), Slide 1, N34/2.
13. *Spathiphyllum* type; Sample 105R-2, 70–72 cm (989.3–989.32 mbsf), Slide 4, D20/1.

Plate IV.

All specimens are from the Eocene of IODP Hole U1356. Scale bars equal 10 μ m. Asterisk (*) indicates specimen previously pictured in Supplementary Information of Pross et al. (2012).

- 1.-2*. *Bluffopollis scabratus* (Couper) Pocknall and Mildenhall, 1984; Sample 105R-4, 60–62 cm (992.09–992.11 mbsf), Slide 2, England-Finder coordinates H35; Sample 105R-6, 95–98 cm (994.95–994.98 mbsf), Slide 4, V22/4.

- 3.-4. *Margocolporites cribellatus* Srivastava, 1972; Sample 105R-3, 100–101 cm (991.11–991.12 mbsf), Slide 2, D29/3; Sample 105R-4, 60–62 cm (992.09–992.11 mbsf), Slide 2, S23.
- 5.-6. *Bombacacidites* sp. A; Sample 105R-5, 71–73 cm (993.69–993.71 mbsf), Slide 1, O31; Sample 101R-2, 120–121 cm (951.5–951.51 mbsf), Slide 1, E36/2.
7. *Nothofagidites flemingii* complex *sensu* Macphail and Truswell, 2004; Sample 98R-5, 0–3 cm (924.38–924.41 mbsf), Slide 5, N23/1.
8. *Nothofagidites lachlaniae* complex *sensu* Macphail and Truswell, 2004; Sample 103R-3, 60–62 cm (971.6–971.62 mbsf), Slide 2, M22/2.
9. *Nothofagidites asperus* (Cookson) Romero, 1973; Sample 99R-2, 40–43 cm (931.28–931.3 mbsf), Slide 3, H16/3.
10. *Nothofagidites* sp. cf. *N. senectus*, Dettmann and Playford, 1968; Sample 101R-1, 30–32 cm (949.1–949.12 mbsf), Slide 3, Q24.
11. *Nothofagidites emarcidus* complex *sensu* Truswell and Macphail, 2009; Sample 97R-CC, 8–11 cm (911.61–911.64 mbsf), Slide 4, Q14/2.
12. *Tetracolporites* sp.; Sample 104R-5, 95–97 cm (984.3–984.32 mbsf), Slide 5, D20/4.

Plate V.

All specimens are from the Eocene of IODP Hole U1356. Scale bars equal 10 μ m. Asterisk (*) indicates specimen previously pictured in Supplementary Information of Pross et al. (2012).

1. *Tricolpites* sp. cf. *T. fissilis* Couper, 1960; Sample 103R-4, 135–137 cm (973.85–973.87 mbsf), Slide 1, England-Finder coordinates S9.
- 2.-3*. *Myricipites harrisii* (Couper) Dutta and Sah, 1970; Sample 101R-2, 40–42 cm (950.7–950.72 mbsf), Slide 1, X23/2; Sample 101R-1, 110–112 cm (949.9–949.92 mbsf), Slide 2, S28/2.
- 4*.-5. *Malvacipollis subtilis* Stover in Stover and Partridge, 1973; Sample 99R-2, 40–42 cm (931.28–931.3 mbsf), Slide 3, M7; Sample 103R-4, 135–137 cm (973.85–973.87 mbsf), Slide 2, M15.
6. *Ericipites* sp.; Sample 99R-2, 120–123 cm (932.08–932.1 mbsf), Slide 4, V15/2.
7. *Rhoipites* sp.; Sample 101R-2, 80–82 cm (951.1–951.12 mbsf), Slide 1, V24/4.
- 8*. *Gambierina edwardsii* (Cookson and Pike) Harris, 1972; Sample 104R-5, 95–97 cm (984.3–984.32 mbsf), Slide 2, G12.
9. *Gambierina rudata* Partridge and Stover, 1973; Sample 104R-3, 120–121 cm (981.75–981.76 mbsf), Slide 1, F10/4.
- 10*. *Anacolosidites luteoides* Cookson and Pike, 1954; Sample 101R-2, 120–121 cm (951.5–951.51 mbsf), Slide 3, L6/3.
11. *Tetracolporites* sp. aff. *T. oamaruensis* Couper, 1953; Sample 103R-1, 40–42 cm (968.4–968.41 mbsf), Slide 1, F32/2.

Plate VI.

All specimens are from the Eocene of IODP Hole U1356. Scale bars equal 10 μ m.

- 1.-2. *Scabratrporites* sp.; Sample 105R-3, 0–2 cm (990.11–990.13 mbsf), Slide 5, England-Finder coordinates R43; Sample 106R-1, 40–43 cm (997.2–997.23 mbsf), Slide 2, L29/M29.

3. *Proteacidites incurvatus* Cookson, 1950; Sample 104R-3, 120–121 cm (981.75–981.76 mbsf), Slide 2, T10/2.
- 4.-5. *Propylipollis* sp. 3; Sample 105R-5, 10–13 cm (993.08–993.11 mbsf), Slide 7, M27/1; Sample 105R-2, 90–92 cm (989.5–989.52 mbsf), Slide 5, W18/4.
6. *Proteacidites* sp. cf. *P. tuberculatus* Cookson, 1950; Sample 106R-1, 60–63 cm (997.4–997.43 mbsf), Slide 12, O33/3.
- 7.-8. *Propylipollis annularis* (Cookson) Martin and Harris, 1975; Sample 102R-1, 60–62 cm (959–959.02 mbsf), Slide 1, L26/2; Sample 101R-1, 30–32 cm (949.1–949.12 mbsf), Slide 1, O23.
9. *Propylipollis* sp. cf. *P. annularis* (Cookson) Martin and Harris, 1975; Sample 101R-1, 110–112 cm (949.9–949.92 mbsf), Slide 2, F28/2.
10. *Tripoporollenites* sp. cf. *T. ambiguus*, Stover in Stover and Partridge, 1973; Sample 103R-1, 100–101 cm (969–969.01 mbsf), Slide 2, K38/4.
11. *Beaupreaidites* sp. aff. *B. orbiculatus* Dettmann and Jarzen, 1988; Sample 103R-1, 0–2 cm (968–968.02 mbsf), Slide 1, Q33.
12. *Proteacidites similis* Harris, 1965; Sample 99R-1, 42–45 cm (929.82–929.85 mbsf), Slide 5, Q48.

Plate VII.

All specimens are from the Eocene of IODP Hole U1356. Scale bars equal 10 μ m. Asterisk (*) indicates specimen previously pictured in Supplementary Information of Pross et al. (2012).

1. *Proteacidites* sp. 2; Sample 105R-4, 139–141 cm (992.88–992.9 mbsf), Slide 1, England-Finder coordinates V23/2.
- 2.-3. *Proteacidites* sp. cf. *P. parvus* Cookson, 1950; Sample 101R-2, 40–42 cm (950.7–950.72 mbsf), Slide 1, V24/2; Sample 102R-1, 0–2 cm (958.4–958.42 mbsf), Slide 2, G21.
4. *Proteacidites* sp. cf. *P. spiniferus* McIntyre, 1968; Sample 103R-1, 80–82 cm (968.8–968.82 mbsf), Slide 3, E43/3.
5. *Proteacidites* sp. cf. *P. callosus* Cookson, 1950; Sample 104R-5, 95–97 cm (984.3–984.32 mbsf), Slide 7, G32/4.
6. *Proteacidites pachypolus* Cookson and Pike, 1954; Sample 98R-1, 100–103 cm (920.8–920.83 mbsf), Slide 10, Q38/1.
7. *Proteacidites* sp. cf. *P. amolosexinus* Dettmann and Playford, 1968; Sample 97R-1, 8–11 cm (910.28–910.31 mbsf), Slide 6, L42.
8. *Beaupreaidites* sp. cf. *B. verrucosus* Cookson 1950; Sample 101R-2, 100–101 cm (951.3–951.31 mbsf), Slide 1, N29/4.
9. *Proteacidites adenanthoides* Cookson, 1950; Sample 103R-3, 110–112 cm (972.1–972.12 mbsf), Slide 5, C39.
- 10*.-11. *Propylipollis reticuloscabratus* (Harris) Martin and Harris 1975; Sample 104R-3, 20–22 cm (980.75–980.77 mbsf), Slide 1, V22/1; 103R-4, 135–137 cm (973.85–973.87 mbsf), Slide 2, W18/2.
12. *Propylipollis* sp. cf. *P. reticuloscabratus* (Harris) Martin and Harris 1975; Sample 102R-1, 0–2 cm (958.4–958.42 mbsf), Slide 1, L12/4.

Plate VIII.

All specimens are from the Eocene of IODP Hole U1356. Scale bars equal 10 μ m.

- 1-2. *Alisporites* spp.; Sample 101R-2, 40–42 cm (950.7–950.72 mbsf), Slide 1, England-Finder coordinates N23/2 [reworked]; Sample 103R-4, 135–137 cm (973.85–973.87 mbsf), Slide 2, S11/1 [reworked].
- 3.-4. *Protohaploxypinus* spp.; Sample 105R-4, 30–32 cm (991.79–991.81 mbsf), Slide 2, D17/3 [reworked]; Sample 104R-5, 95–97 cm (984.3–984.32 mbsf), Slide 1, U7/U8 [reworked].
5. *Cannanoropollis* sp.; Sample 102R-1, 0–2 cm (958.4–958.42 mbsf), Slide 1, U12 [reworked].
6. *Classopollis* sp.; Sample 104R-4, 100–101 cm (983.02–983.03 mbsf), Slide 1, O23/1 [reworked].
7. *Lycopodiumsporites* sp.; Sample 102R-1, 0–2 cm (958.4–958.42 mbsf), Slide 2, M8/4 [reworked].
8. *Cicatricosisporites* sp.; Sample 105R-1, 125–126 cm (988.45–988.46 mbsf), Slide 2, E9 [reworked].
9. *Klukisporites* sp.; Sample 102R-1, 0–2 cm (958.4–958.42 mbsf), Slide 1, N16/2.
10. *Neoraistrickia truncata* (Cookson) Potonié, 1956; Sample 105R-3, 0–2 cm (990.11–990.13 mbsf), Slide 5, W38 [reworked].

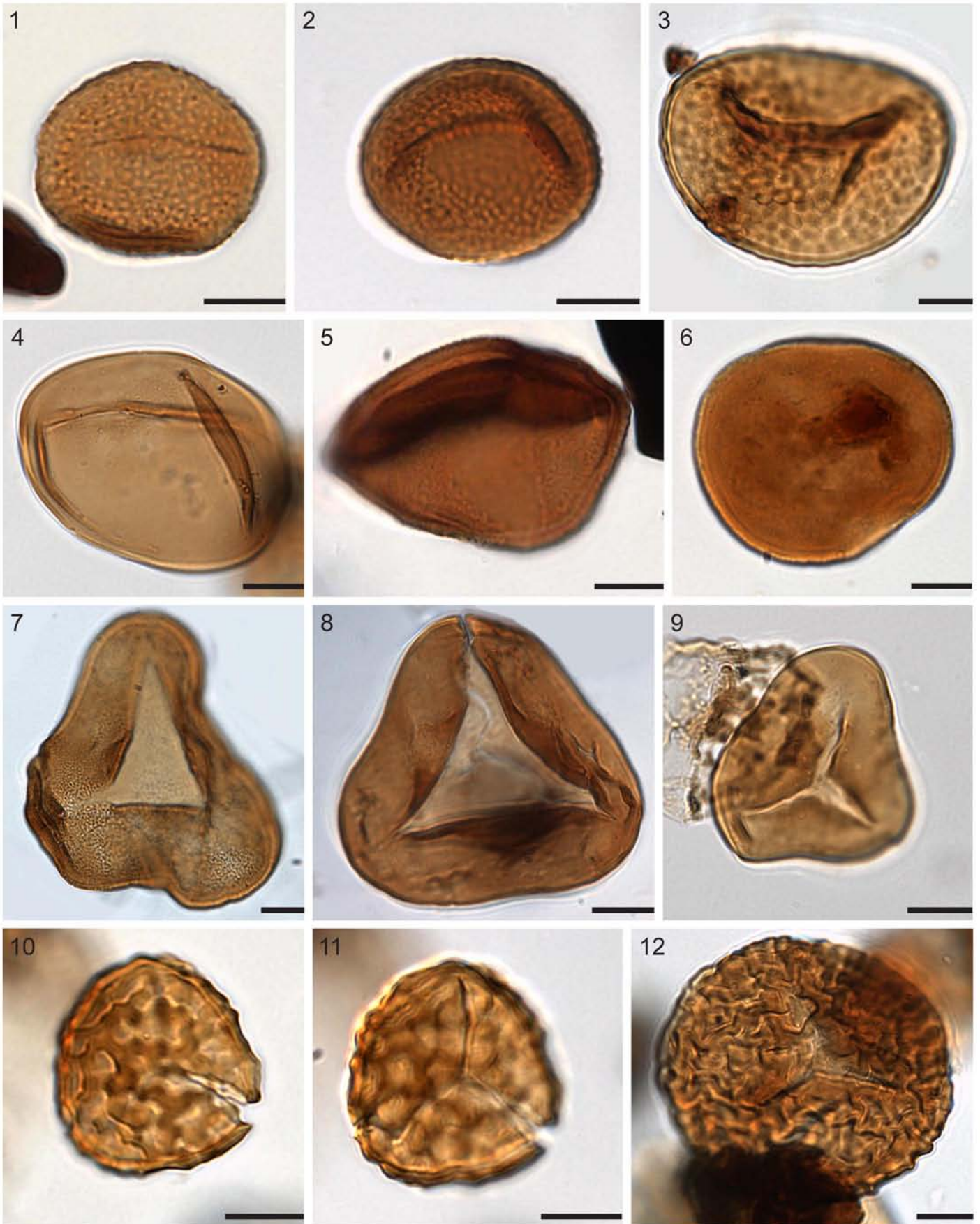


Plate I.

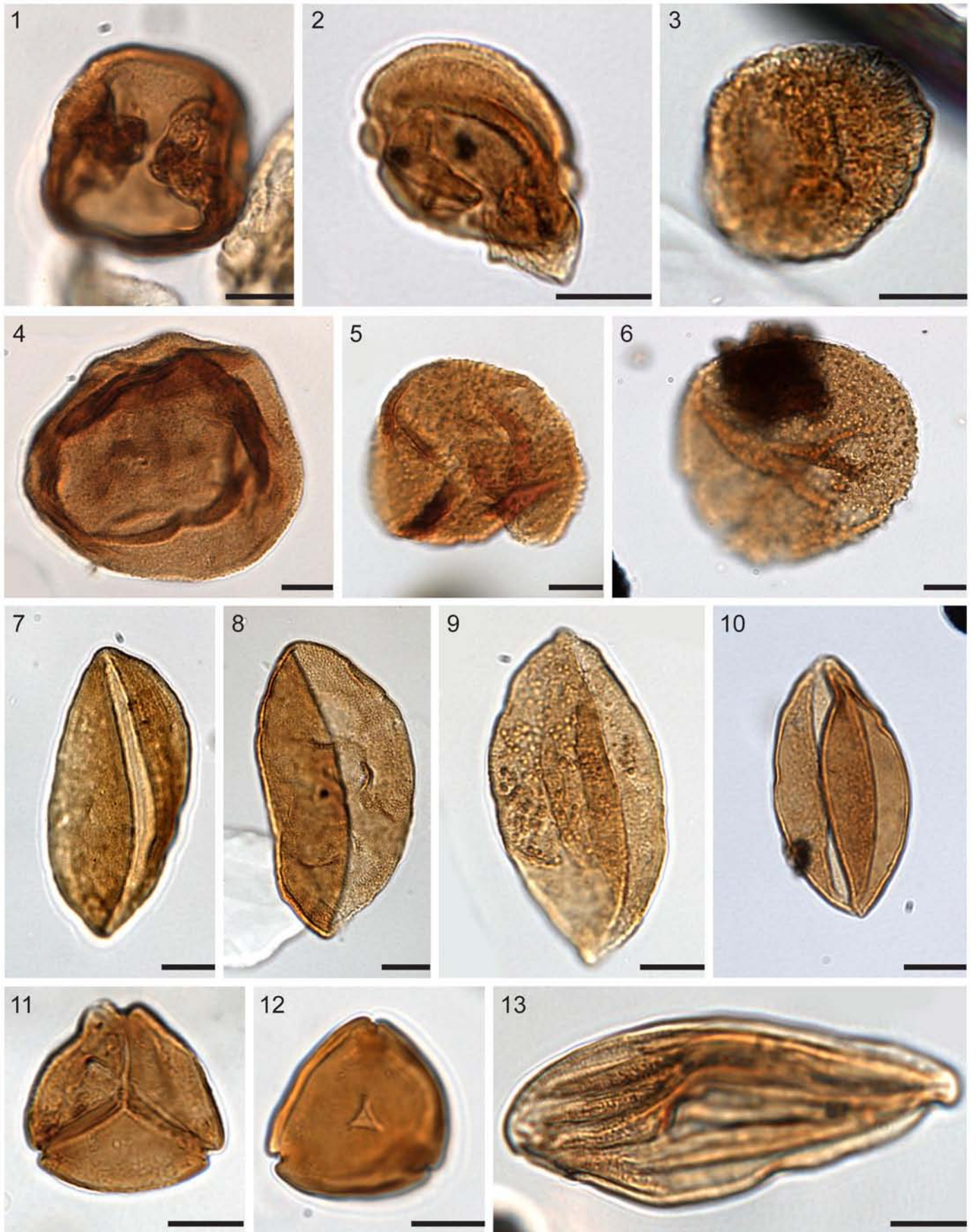


Plate III.

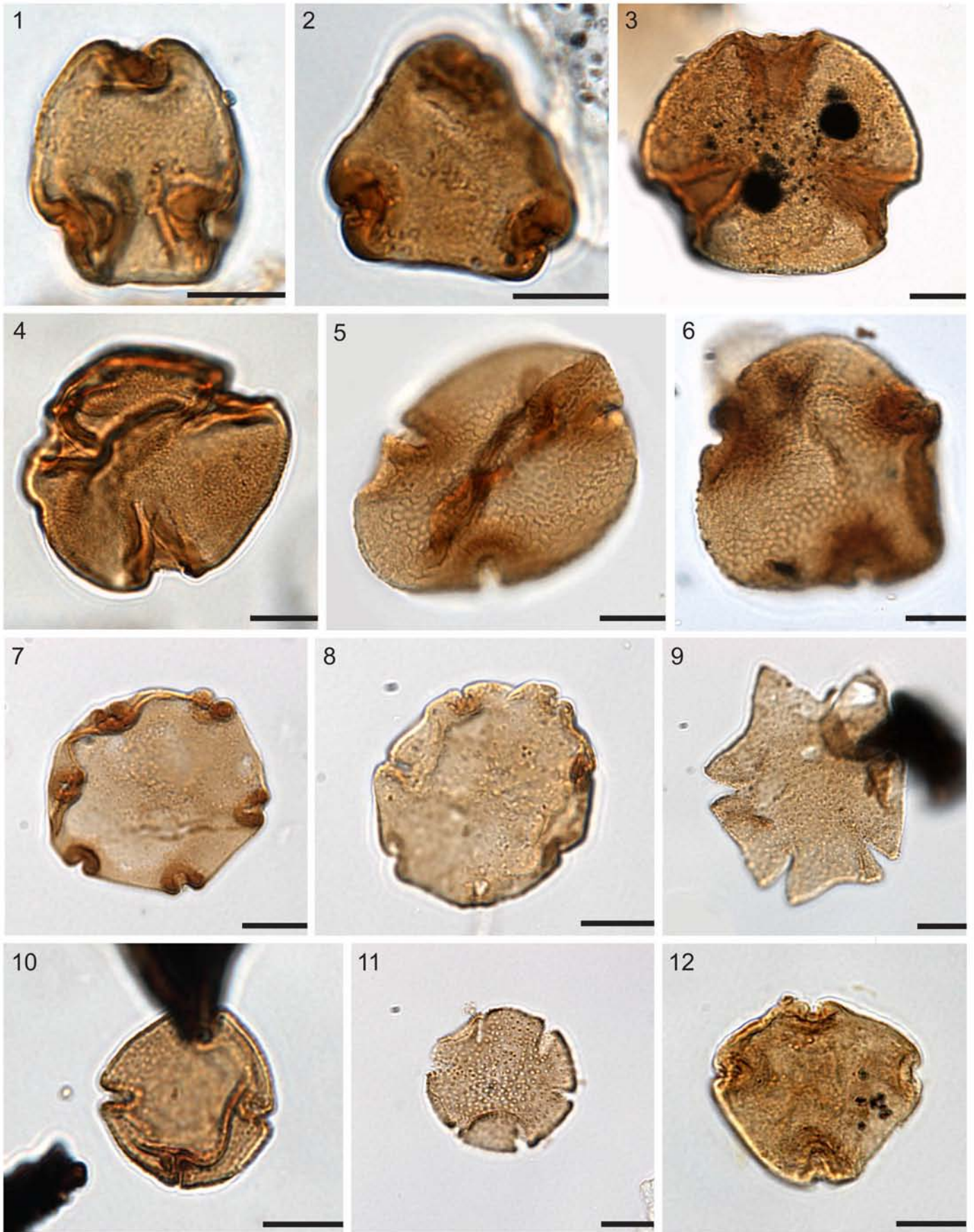


Plate IV.



Plate V.

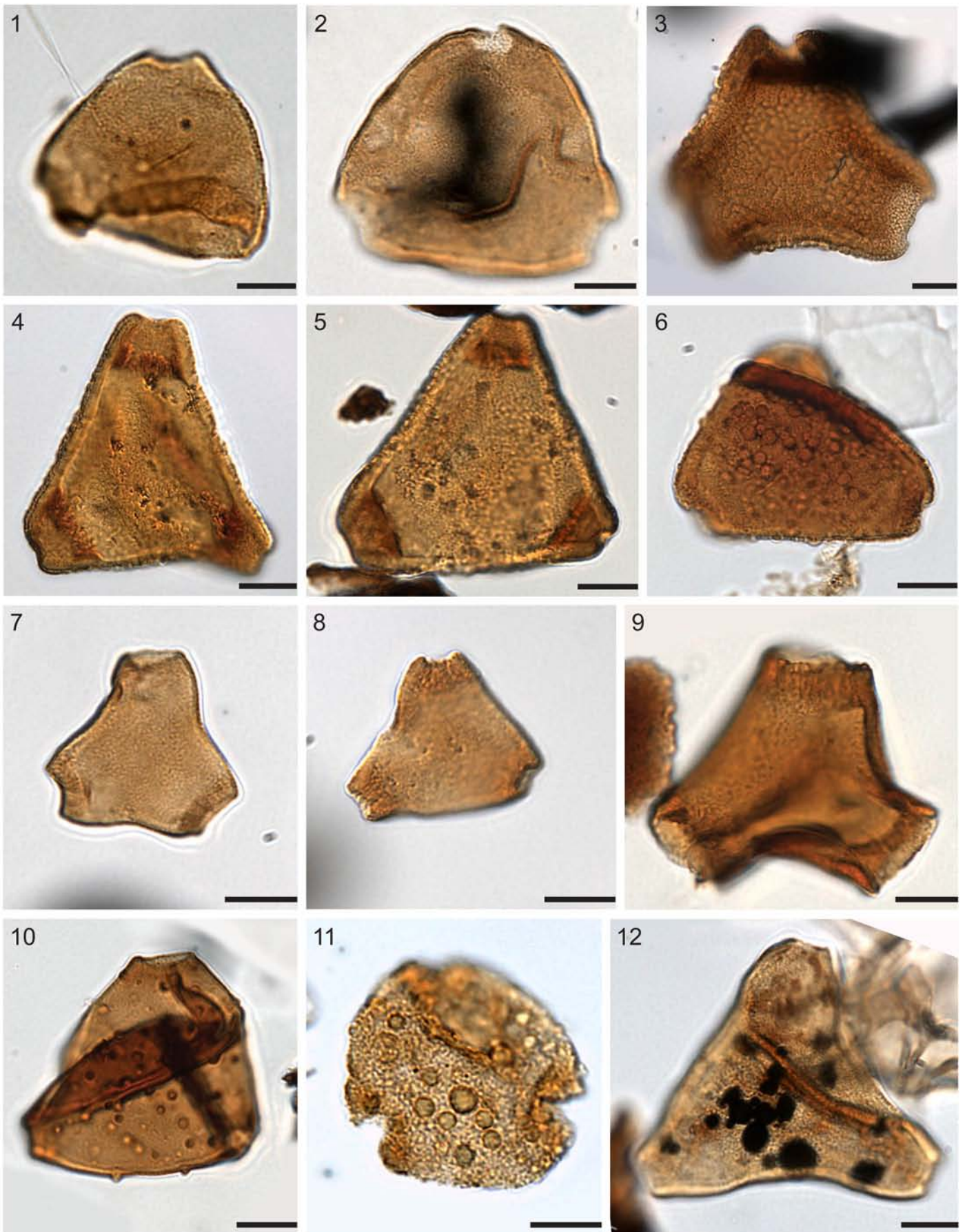


Plate VI.

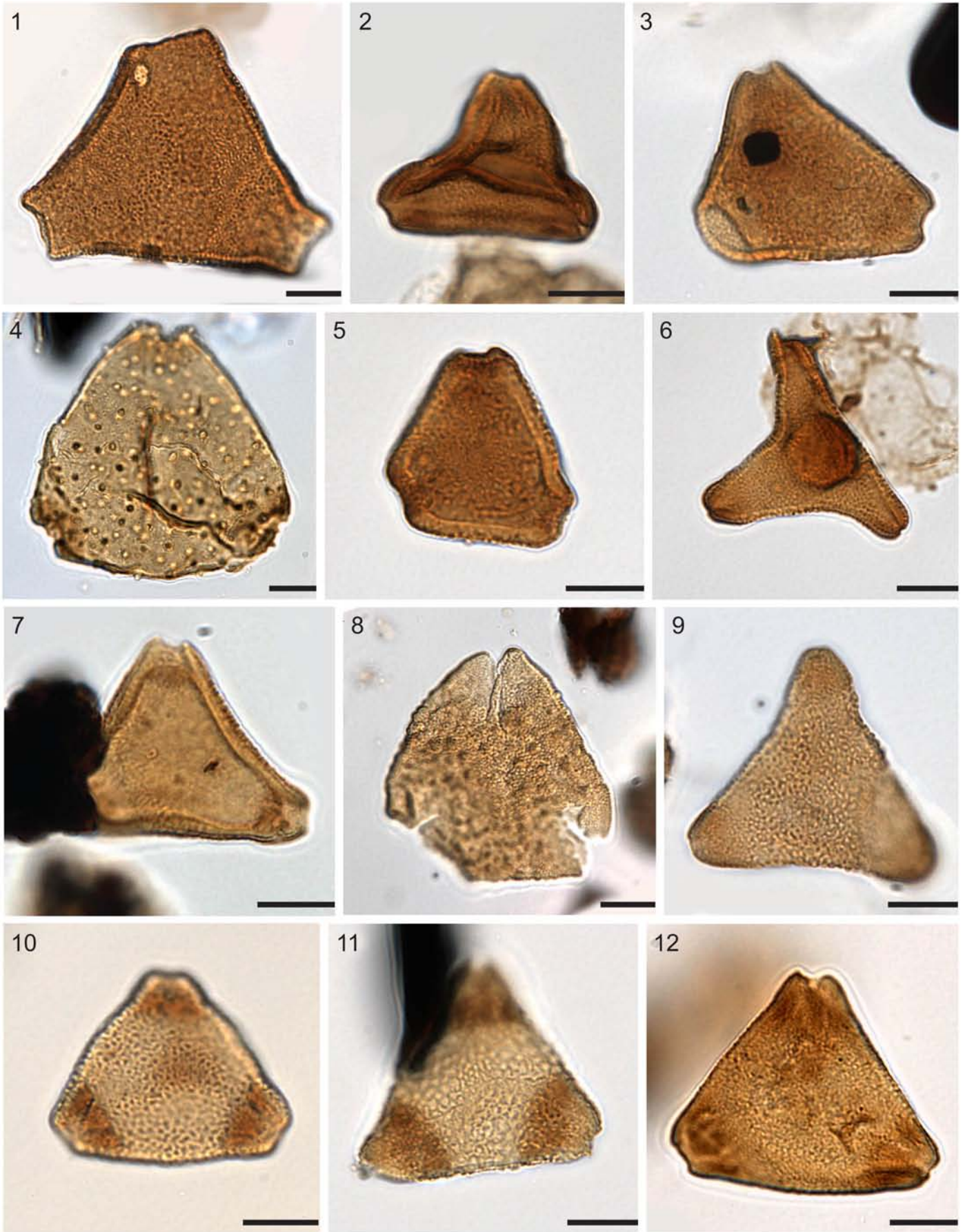


Plate VII.

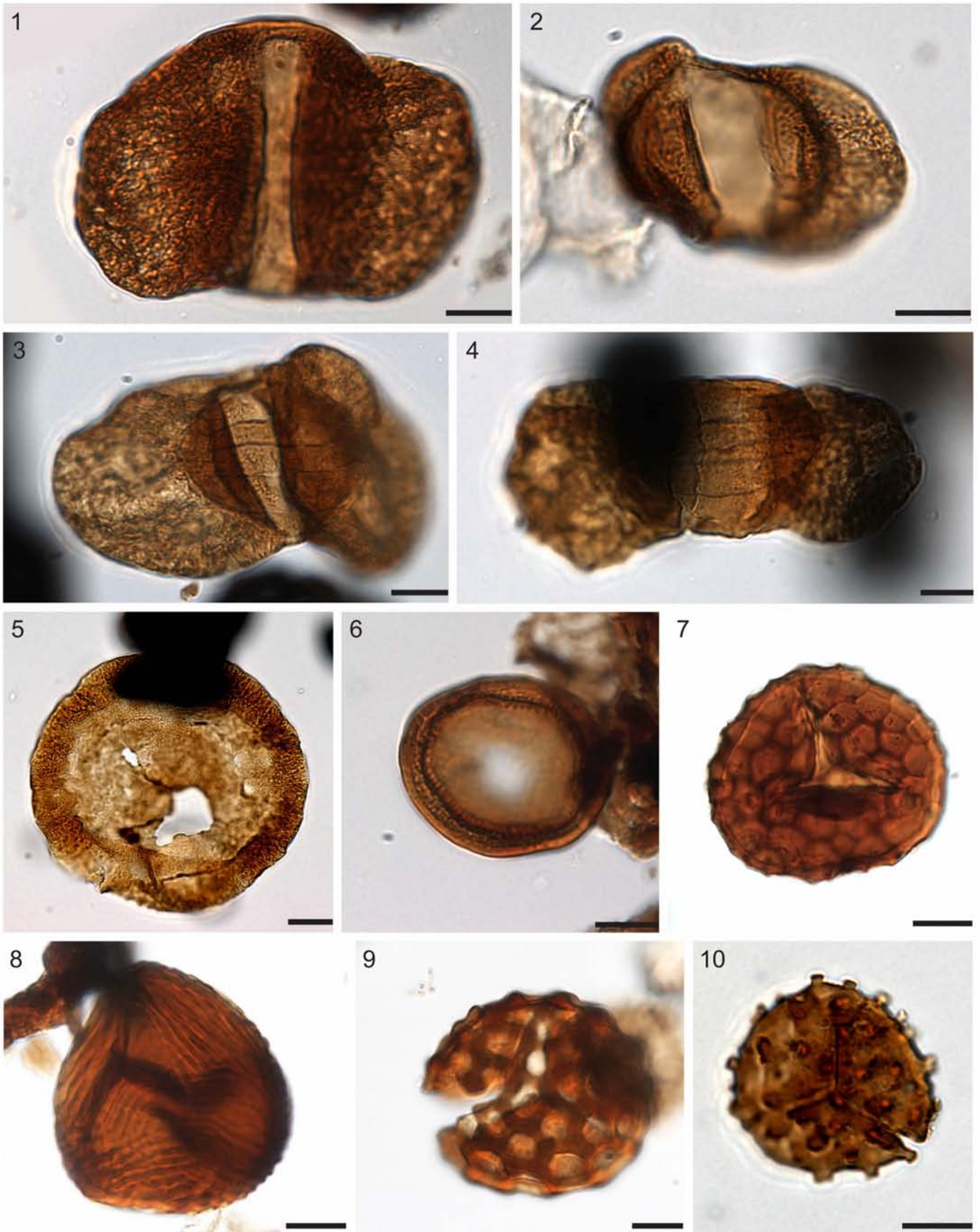


Plate VIII.

Appendix 2 Taxonomy Site 1172

Selected sporomorph taxa are depicted on Plates XI to XII; an alphabetical list of all pictured taxa is provided below. For a full list of identified sporomorph see supplementary tables of Chapter 4 (supplemdata1172.xlsx). For key sporomorph taxa studied at Site 1172 refer to Section 4.5.3. Slides and residues are stored in the collection of the Institute of Geosciences, Goethe University Frankfurt, Germany

- Baculatisporites* sp. (Plate X, 7; Osmundaceae)
Bacutriteles? sp.1 (Plate X, 8)
Banksieaidites arcuatus Stover in Stover and Partridge 1973 (Plate XII, 7)
Beaupreaidites cf. *diversiformis* Milne 1998 (Plate XII, 12; *Beauprea*)
Camarozonosporites cf. *Lycopodium cerniidites* (Ross) Brenner 1963 (Plate IX, 2)
Camarozonosporites sp.? (Plate IX, 7-8)
Cibotiumspora sp. (Plate X, 12)
Cyathidites sp. (Plate IX, 1)
Dicotetradites clavatus? Couper 1953 (Plate XI, 8)
Diporites sp. (Plate XII, 8)
Evansispora senonica Raine, 2008 (Plate IX, 11)
Forcipites sp. (Plate XIII, 5)
 Gemmate inaperturate pollen type (Plate XI, 7)
Granulatisporites sp. (Plate IX, 5-6)
Granulatisporites? sp. (Plate X, 11)
Ischyosporites? *crateris* Balme 1957 (Plate IX, 12)
Leptolepidites verrucatus Couper 1953 (Plate IX, 3)
Neoraistrickia cf. *truncate* (Cookson) Potonie 1956 (Plate XI, 2)
Nothofagidites sp.1 (Plate XI, 11; *Nothofagus*)
Nothofagidites sp. (Plate XI, 9-10; *Nothofagus*)
Ornamentifera sentosa Dettmann and Playford 1969 (Plate X, 9)
Peninsulapollis cf. *askiniae* Dettmann and Jarzen, 1988 (Plate XII, 10-11)
Peromonolites cf. *densus* Harris 1965 (Plate XI, 3)
Peromonolites densus Harris 1965 (Plate XI, 5)
Peromonolites sp. (Plate XI, 4)
Peromonolites? sp. (Plate XI, 6)
Perotriteles sp. (Plate XI, 1)
Proteacidites aff. *adenanthoides* Cookson 1950 (Plate XVI, 8; Proteaceae)
Proteacidites aff. *angulatus* Stover in Stover and Partridge 1973 (Plate XVII, 10; Proteaceae)
Proteacidites aff. *reflexus* Partridge in Stover and Partridge 1972 (Plate XVI, 10; Proteaceae)
Proteacidites aff. *similis* Harris 1965 (Plate XVI, 3-4; Proteaceae)
Proteacidites cf. *adenanthoides* Cookson 1950 (Plate XVI, 5-7; *Adenanthos?*)
Proteacidites cf. *asperatus* Dettmann 1963 (Plate XIV, 12; Proteaceae)
Proteacidites cf. *obscurus* Cookson 1950 (Plate XIII, 7-9; Proteaceae)
Proteacidites cf. *parvus* Cookson 1950 (Plate XIV, 7; *Bellendena montana*)
Proteacidites cf. *similis* Harris 1965 (Plate XV, 12; Proteaceae)
Proteacidites cf. *similis* Harris 1965 (Plate XVI, 1; Proteaceae)
Proteacidites concretus? Harris 1972 (Plate XV, 8-9; Proteaceae)
Proteacidites concretus? Harris 1972 (Plate XV, 6-7; Proteaceae)
Proteacidites concretus? Harris 1972 (Plate XV, 10; Proteaceae)

- Proteacidites scaboratus* Couper 1960 (Plate XV, 3-5; Proteaceae)
Proteacidites scaboratus? Couper 1960 (Plate XV, 1-2; Proteaceae)
Proteacidites similis? Harris 1965 (Plate XVI, 2; Proteaceae)
Proteacidites sp. (Plate XIV, 1-3; Proteaceae)
Proteacidites? sp. (Plate XIV, 4)
Proteacidites sp./*Cranwellipollis* sp. (Plate XIII, 1; Proteaceae)
Proteacidites sp.2 (Plate XVI, 12; Proteaceae)
Proteacidites sp.3 (Plate XVI, 11; Proteaceae)
Proteacidites sp.4 (Plate XVII, 4; Proteaceae)
Proteacidites? sp.5 (Plate XVII, 6-7)
Proteacidites sp.6 (Plate XV, 11; Proteaceae)
Proteacidites sp.7 (Plate XVII, 9; Proteaceae)
Proteacidites sp.9 (Plate XVII, 12; Proteaceae)
Proteacidites sp. 8 (Plate XIV, 5-6; Proteaceae)
Proteacidites sp.10 (Plate XIII, 11; Proteaceae)
Proteacidites sp.11 (Plate XIII, 10; Proteaceae)
Proteacidites sp.12 (Plate XVII, 11; Proteaceae)
Proteacidites sp.14 (Plate XVII, 5; Proteaceae)
Proteacidites sp.15 (Plate XVI, 9; Proteaceae)
Proteacidites subscabratus Couper 1960 (Plate XIII, 12; Proteaceae)
Proteacidites symphyonemoides/P. pseudomoides (Plate XIV, 8-11; *Symphyonema*, *Petrophile*)
Proteacidites tenuiexinus Stover in Stover and Partridge 1973 (Plate XVII, 1; Proteaceae)
Proteacidites tenuiexinus? Stover in Stover and Partridge 1973 (Plate XVII, 2-3; Proteaceae)
Psilatricolporites sp.2 (Plate XII, 6)
Retitricolpites sp.1 (Plate XIII, 2)
Retitricolporites sp.1 (Plate XII, 1)
Retitricolporites sp.2 (Plate XII, 2)
Retitricolporites sp.4 (Plate XII, 4)
Retitriletes cf. *rosewoodensis* (de Jersey) McKellar 1974 (Plate IX, 9-10)
Retitriletes sp. (Plate X, 3)
Retitriletes sp.2 (Plate X, 10)
Retitriletes sp.3 (Plate X, 5)
Retitriletes? *facetus* (Dettmann) Srivastava 1972 (Plate X, 6)
Retitricolporites sp.3 (Plate XII, 3)
Rubinella cf. *major* (Couper) Norris 1968 (Plate IX, 4)
Stereisporites regium (Drozastichich) Drugg 1967 (Plate X, 1-2; Sphagnaceae?)
Tetracolporites sp. (Plate XI, 12)
Tricolpites lilliei Couper 1953 (Plate XII, 9)
Tricolporites? *microreticulatus* Harris 1965 (Plate XII, 5)
Trilete spore undet. (Plate X, 4)
Triorites fragilis Couper 1953 (Plate XIII, 3-4)
Triorites sp./*Proteacidites* sp. Macphail 1990 (Plate XVII, 8)
Triporopollenites sp.1 (Plate XIII, 6)

Plate IX.

All specimens are from the Paleocene and Eocene of ODP Site 1172. Scale bars equal 10 μ m.

1. *Cyathidites* sp.; Sample 15R-4, 119–120 cm (601.26–601.27 rmbsf), Slide 1, England-Finder coordinates H20.
2. *Camarozonosporites* cf. *Lycopodium cerniidites* (Ross) Brenner 1963; Sample 15R-5, 99–100 cm (611.0–611.01 rmbsf), Slide 1, V18/2.
3. *Leptolepidites verrucatus* Couper 1953; Sample 19R-1, 40–42 cm (644.58–644.6 rmbsf), Slide 1, O23/2.
4. *Rubinella* cf. *major* (Couper) Norris 1968; Sample 14 R-3, 40–42 cm (599.74–599.76 rmbsf), Slide 1, G31/3.
- 5.-6. *Granulatisporites* sp.; Sample 15R-5, 79–80 cm (612.29–612.31 rmbsf), Slide 1, R27/1. Sample 16R-5, 20–22 cm (621.57–621.59 rmbsf), Slide 2, L21.
- 7.-8. *Camarozonosporites* sp.?; Sample 15R-5, 19-21 cm (611.7–611.72 rmbsf), Slide 1, U22. Sample 19R-1, 40-42 cm (644.58–644.6 rmbsf), Slide 2, L24/4.
- 9.-10. *Retitriletes* cf. *rosewoodensis* (de Jersey) McKellar 1974; Sample 16R-5, 20–22 cm (621.57–621.59 rmbsf), Slide 1, L20. Sample 15R-5, 110–112 cm (612.61–612.63 rmbsf), Slide 1, L19/4.
11. *Evansispora senonica* Raine, 2008; Sample 17R-7, 20–22 cm (634.17–634.19 rmbsf), Slide 1, E35.
12. *Ischyosporites?* *crateris* Balme 1957; Sample 15R-5, 40–41 cm (611.91–611.92 rmbsf), Slide 1, T27.

Plate X.

All specimens are from the Paleocene and Eocene of ODP Site 1172. Scale bars equal 10 μ m.

- 1.-2. *Stereisporites regium* (Drozastichich) Drugg 1967; Sample 20R-1, 40–42 cm (654.18–654.2 rmbsf), Slide 1, England-Finder coordinates V23/1. Sample 20R-5, 40–43 cm (660.18–660.21 rmbsf), Slide 1, J28/1.
3. *Retitriletes* sp.; Sample 14R-5, 40–42 cm (602.9–602.92 rmbsf), Slide 4, N15/2.
4. Trilete spore undet.; Sample 14R-3, 40–42 cm (599.74–599.76 rmbsf), Slide 3, N44/4.
5. *Retitriletes* sp.3; Sample 14R-2, 40–42 cm (598.24–598.26 rmbsf), Slide 1, B18.
6. *Retitriletes?* *facetus* (Dettmann) Srivastava 1972; Sample 15R-2, 40–42 cm (607.4–607.42 rmbsf), Slide 4, W49/2.
7. *Baculatisporites* sp.; Sample 16R-5, 20–22 cm (621.57–621.59 rmbsf), Slide 2, O36/2.
8. *Bacutriletes?* sp.1; Sample 18R-6, 40–42 cm (641.97–641.99 rmbsf), Slide 1, N22/3.
9. *Ornamentifera sentosa* Dettmann and Playford 1969; Sample 18R-1, 40–42 cm (634.98–635.0 rmbsf), Slide 1, Q30/3.
10. *Retitriletes* sp.2; Sample 16R-5, 20–22 cm (621.57–621.59 rmbsf), Slide 1, U32/4.
11. *Granulatisporites?* sp.; Sample 14R-6, 40–42 cm (604.44–604.46 rmbsf), Slide 3, 51/3.

12. *Cibotiumspora* sp.; Sample 17R-2, 70–72 cm (627.17–627.19 rmbsf), Slide 1, V36/1.

Plate XI.

All specimens are from the Paleocene and Eocene of ODP Site 1172. Scale bars equal 10 μ m.

1. *Perotriletes* sp.; 18R-1, 40–42 cm (634.98–635.0 rmbsf), Slide 1, England-Finder coordinates J17/2.
2. *Neoraistrickia* cf. *truncate* (Cookson) Potonie 1956; Sample 19R-3, 40–42 cm (647.57–647.59 rmbsf), Slide 1, G18/1.
3. *Peromonolites* cf. *densus* Harris 1965; Sample 15R-5, 19–21 cm (611.7–611.72 rmbsf), Slide 1, U21/4.
4. *Peromonolites* sp.; Sample 15R-5, 52–53 cm (612.02–612.03 rmbsf), Slide 1, T33.
5. *Peromonolites densus* Harris 1965; Sample 15R-5, 104–106 cm (612.55–612.57 rmbsf), Slide 1, V31/1.
6. *Peromonolites?* sp.; Sample 16R-1, 40–42 cm (615.77–615.79 rmbsf), Slide 1, N35/2.
7. Gemmate inaperturate pollen type; Sample 14R-4, 40–42 cm (601.26–601.28 rmbsf), Slide 1, L16/1.
8. *Dicotetradites clavatus?* Couper 1953; Sample 14R-4, 40–42 cm (601.26–601.28 rmbsf), Slide 2, S46/3.
- 9.-10. *Nothofagidites* sp.; Sample 17R-7, 20–22 cm (634.17–634.19 rmbsf), Slide 1, L19. Sample 16R-5, 20–22 cm (621.57–621.59 rmbsf), Slide 1, X29/2.
11. *Nothofagidites* sp.1; Sample 16R-3, 40–42 cm (618.77–618.79 rmbsf), Slide 2, R30/2.
12. *Tetracolporites* sp.; Sample 15R-5, 85–86 cm (612.36–612.37 rmbsf), Slide 10, V30.

Plate XII.

All specimens are from the Paleocene and Eocene of ODP Site 1172. Scale bars equal 10 μ m.

1. *Retitricolporites* sp.1; Sample 16R-5, 20–22 cm (621.57–621.59 rmbsf), Slide 1, England-Finder coordinates H31.
2. *Retitricolporites* sp.2; Sample 14R-3, 40–42 cm (599.74–599.76 rmbsf), Slide 4, J19/3.
3. *Retitricolporites* sp.3; Sample 15R-5, 52–53 cm (612.02–612.03 rmbsf), Slide 1, L29.
4. *Retitricolporites* sp.4; Sample 14R-3, 40–42 cm (599.74–599.76 rmbsf), Slide 1, K46.
5. *Tricolporites?* *microreticulatus* Harris 1965; Sample 15R-5, 0–2 cm (611.52–611.54 rmbsf), Slide 1, K33.
6. *Psilatricolporites* sp.2; Sample 15R-2, 40–42 cm (607.4–607.42 rmbsf), Slide 2, L42.
7. *Banksieaeidites arcuatus* Stover in Stover and Partridge 1973; Sample 15R-7, 40–42 cm (614.91–614.93 rmbsf), Slide 2, G15/4.

8. *Diporites* sp.; Sample 15R-6, 40–42 cm (613.41–613.43 rmbsf), Slide 2, G19/3.
9. *Tricolpites lilliei* Couper 1953; Sample 17R-5, 40–42 cm (631.37–631.39 rmbsf), Slide 1, U23/4.
- 10.-11. *Peninsulapollis* cf. *askiniae* Dettmann and Jarzen, 1988; Sample 14R-3, 40–42 cm (599.74–599.76 rmbsf), Slide 2, N24. Sample 17R-6, 40–42 cm (632.87–632.89 rmbsf), Slide 1, O22/1.
12. *Beaupreaidites* cf. *diversiformis* Milne 1998; Sample 15R-4, 40–42 cm (610.41–610.43 rmbsf), Slide 1, W19/2.

Plate XIII.

All specimens are from the Paleocene and Eocene of ODP Site 1172. Scale bars equal 10 μ m.

1. *Proteacidites* sp./*Cranwellipollis* sp.; Sample 14R-2, 40–42 cm (598.24–598.26 rmbsf), Slide 1, England-Finder coordinates B36/4.
2. *Retitricolpites* sp.1; Sample 15R-2, 40–42 cm (607.4–607.42 rmbsf), Slide 1, O18/4.
- 3.-4. *Triorites fragilis* Couper 1953; Sample 18R-6, 40–42 cm (641.97–641.99 rmbsf), Slide 2, J18/2. Sample 15R-5, 124–126 cm (612.75–612.76 rmbsf), Slide 1, K35/3.
5. *Forcipites* sp.; Sample 17 R-7, 20–22 cm (634.17–634.19 rmbsf), Slide 1, M23/2.
6. *Triporopollenites* sp.1; Sample 19R-1, 40–42 cm (644.58–644.6 rmbsf), Slide 1, G27/2.
- 7.8.-9. *Proteacidites* cf. *obscurus* Cookson 1950; Sample 19R-1, 40-42 cm (644.58–644.6 rmbsf), Slide 2, M22. Sample 17R-6, 40-42 cm (632.87–632.89 rmbsf), Slide 1, Q31/4. Sample 17R-5, 40-42 cm (631.37–631.39 rmbsf), Slide 2, H18.
10. *Proteacidites* sp.11; Sample 17R-7, 20–22 cm (634.17–634.19 rmbsf), Slide 1, K28/4.
11. *Proteacidites* sp.10; Sample 16R-1, 40–42 cm (615.77–615.79 rmbsf), Slide 1, U26/2.
12. *Proteacidites subscabratus* Couper 1960; Sample 20R-1, 40–42 cm (654.18–654.2 rmbsf), Slide 1, N28/4.

Plate XIV.

All specimens are from the Paleocene and Eocene of ODP Site 1172. Scale bars equal 10 μ m.

- 1.2.-3. *Proteacidites* sp.; Sample 20R-5, 40–43 cm (660.18–660.21 rmbsf), Slide 2, England-Finder coordinates W25/4. Sample 17R-7, 20–22 cm (634.17–634.19 rmbsf), Slide 2, M31/4. Sample 20R-5, 40–43 cm (660.18–660.21 rmbsf), Slide 2, V22/1.
4. *Proteacidites?* sp.; Sample 17R-4, 40–42 cm (629.87–629.89 rmbsf), Slide 1, Q20.
- 5.-6. *Proteacidites* sp. 8; Sample 15R-4, 146–147 cm (611.47–611.48 rmbsf), Slide 1, J27. Sample 20R-1, 40–42 cm (654.18–654.2 rmbsf), Slide 2, S32.
7. *Proteacidites* cf. *parvus* Cookson 1950; Sample 15R-5, 124–126 cm (612.75–612.77 rmbsf), Slide 1, W20/3.

- 8.-9. *Proteacidites symphyonemoides*/*P. pseudomoides*; Sample 17R-5, 40–42 cm (631.37–631.39 rmbsf), Slide 1, F35. Sample 17R-7, 20–22 cm (634.17–634.19 rmbsf), Slide 2, N32.
- 10.-11. *Proteacidites symphyonemoides*/*P. pseudomoides*; Sample 16R-3, 40–42 cm (618.77–618.79 rmbsf), Slide 1, O34/1. Sample 16R-5, 20–22 cm (621.57–621.59 rmbsf), Slide 1, L25/4.
12. *Proteacidites* cf. *asperatus* Dettmann 1963; Sample 15R-4, 69–70 cm (610.71–610.72 rmbsf), Slide 1, R23/3.

Plate XV.

All specimens are from the Paleocene and Eocene of ODP Site 1172. Scale bars equal 10 μ m.

- 1.-2. *Proteacidites scaboratus*? Couper 1960; Sample 14R-4, 40–42 cm (601.26–601.28 rmbsf), Slide 2, England-Finder coordinates G11. Sample 14R-3, 40–42 cm (599.74–599.76 rmbsf), Slide 3, K47/4.
- 3.4.-5 *Proteacidites scaboratus* Couper 1960; Sample 15R-5, 85–86 cm (612.36–612.37 rmbsf), Slide 1, V30. Sample 14R-2, 40–42 cm (598.24–598.26 rmbsf), Slide 2, J49/1. Sample 14R-6, 40–42 cm (604.44–604.46 rmbsf), Slide 3, K40/1.
- 6.-7. *Proteacidites concretus*? Harris 1972; Sample 14R-4, 40–42 cm (601.26–601.28 rmbsf), Slide 4, R14/4. Sample 16R-3, 40–42 cm (618.77–618.79 rmbsf), Slide 1, W28/4.
- 8.-9. *Proteacidites concretus*? Harris 1972; Sample 14 R-5, 40–42 cm (602.9–602.92 rmbsf), Slide 4, X33/2. Sample 14 R-2, 40–42 cm (598.24–598.26 rmbsf), Slide 1, B33/2.
10. *Proteacidites concretus*? Harris 1972; Sample 14R-6, 40–42 cm (604.44–604.46 rmbsf), Slide 2, U22/1.
11. *Proteacidites* sp.6; Sample 14R-2, 40–42 cm (598.24–598.26 rmbsf), Slide 1, O53/3.
12. *Proteacidites* cf. *similis* Harris 1965; Sample 14R-4, 40–42 cm (601.26–601.28 rmbsf), Slide 1, P20/4.

Plate XVI.

All specimens are from the Paleocene and Eocene of ODP Site 1172. Scale bars equal 10 μ m.

1. *Proteacidites* cf. *similis* Harris 1965; Sample 14R-6, 40–42 cm (604.44–604.46 rmbsf), Slide 4, England-Finder coordinates F40/4.
2. *Proteacidites similis*? Harris 1965; Sample 15R-2, 40-42 cm (607.4–607.42 rmbsf), Slide 2, P33.
- 3.-4. *Proteacidites* aff. *similis* Harris 1965; Sample 18R-6, 40–42 cm (641.97–641.99 rmbsf), Slide 1, E29 /1. Sample 15 R-5, 44–45 cm (611.95–611.96 rmbsf), Slide 1, S34/1.
- 5.-6. *Proteacidites* cf. *adenanthoides* Cookson 1950; Sample 15R-4, 69–70 cm (610.71–610.72 rmbsf), Slide 1, N18/4. Sample 15R-5, 104–106 cm (612.55–612.57 rmbsf), Slide 1, Y25/2.
7. *Proteacidites* cf. *adenanthoides* Cookson 1950; Sample 20R-5, 40–43 cm (660.18–660.2 rmbsf), Slide 2, E16/1.

8. *Proteacidites* aff. *adenanthoides* Cookson 1950; Sample 17R-7, 20–22 cm (634.17–634.19 rmbsf), Slide 1, J32.
9. *Proteacidites* sp.15; Sample 15R-5, 139–141 cm (612.9–612.92 rmbsf), Slide 1, D19/1.
10. *Proteacidites* aff. *reflexus* Partridge in Stover and Partridge 1972; Sample 15R-5, 59–60 cm (612.1–612.11 rmbsf), Slide 1, O16.
11. *Proteacidites* sp.3; Sample 14R-2, 40–42 cm (598.24–598.26 rmbsf), Slide 1, B41/1.
12. *Proteacidites* sp.2; Sample 15R-1, 40–42 cm (605.9–605.92 rmbsf), Slide 4, L23/1.

Plate XVII.

All specimens are from the Paleocene and Eocene of ODP Site 1172. Scale bars equal 10 μ m.

1. *Proteacidites tenuixinus* Stover in Stover and Partridge 1973; Sample 15R-5, 114–115 cm (612.65–612.66 rmbsf), Slide 1, England-Finder coordinates E16/2.
- 2.-3. *Proteacidites tenuixinus?* Stover in Stover and Partridge 1973; Sample 14R-6, 40–42 cm (604.44–604.46 rmbsf), Slide 3, Q15/2. Sample 14R-5, 40–42 cm (602.9–602.92 rmbsf), Slide 1, K23.
4. *Proteacidites* sp.4; Sample 17 R-6, 40–42 cm (632.87–632.89 rmbsf), Slide 3, Q36/4.
5. *Proteacidites* sp.14; Sample 15R-4, 135–137 cm (611.36–611.38 rmbsf), Slide 1, T20.
- 6.-7. *Proteacidites?* sp.5; Sample 15R-5, 120–121 cm (612.71–612.72 rmbsf), Slide 1, R27/4. Sample 16R-4, 40–42 cm (620.27–620.29 rmbsf), Slide 2, U22/1.
8. *Triorites* sp./*Proteacidites* sp. Macphail 1990; Sample 14R-6, 40–42 cm (604.44–604.46 rmbsf), Slide 4, U21/1.
9. *Proteacidites* sp.7; Sample 16R-5, 20–22 cm (621.57–621.59 rmbsf), Slide 1, U33/1.
10. *Proteacidites* aff. *angulatus* Stover in Stover and Partridge 1973; Sample 15R-5, 139–141 cm (612.9–612.92 rmbsf), Slide 1, D33/4.
11. *Proteacidites* sp.12; Sample 15R-1, 40–42 cm (605.9–605.92 rmbsf), Slide 3, J41/1.
12. *Proteacidites* sp.9; Sample 16R-5, 20–22 cm (621.57–621.59 rmbsf), Slide 2, U33/4.

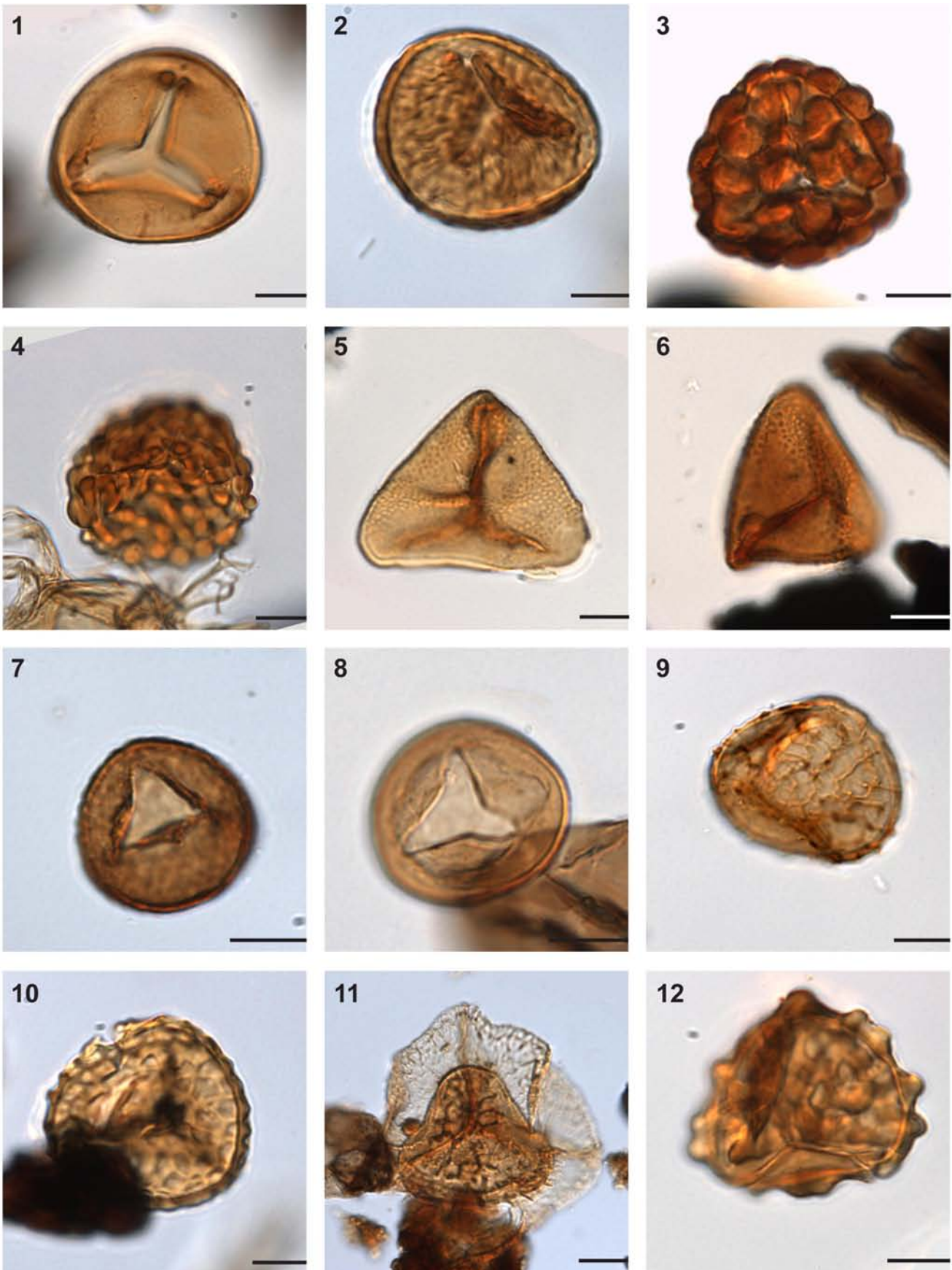


Plate IX.

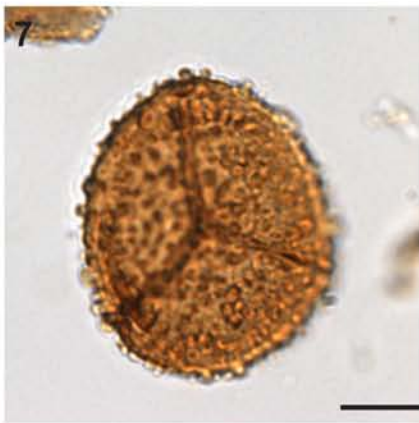
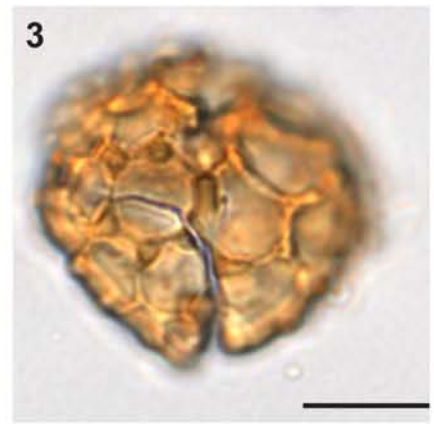
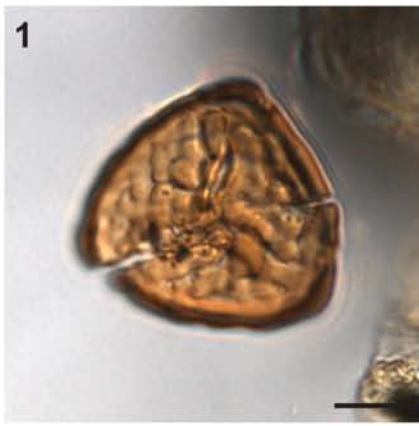


Plate X.

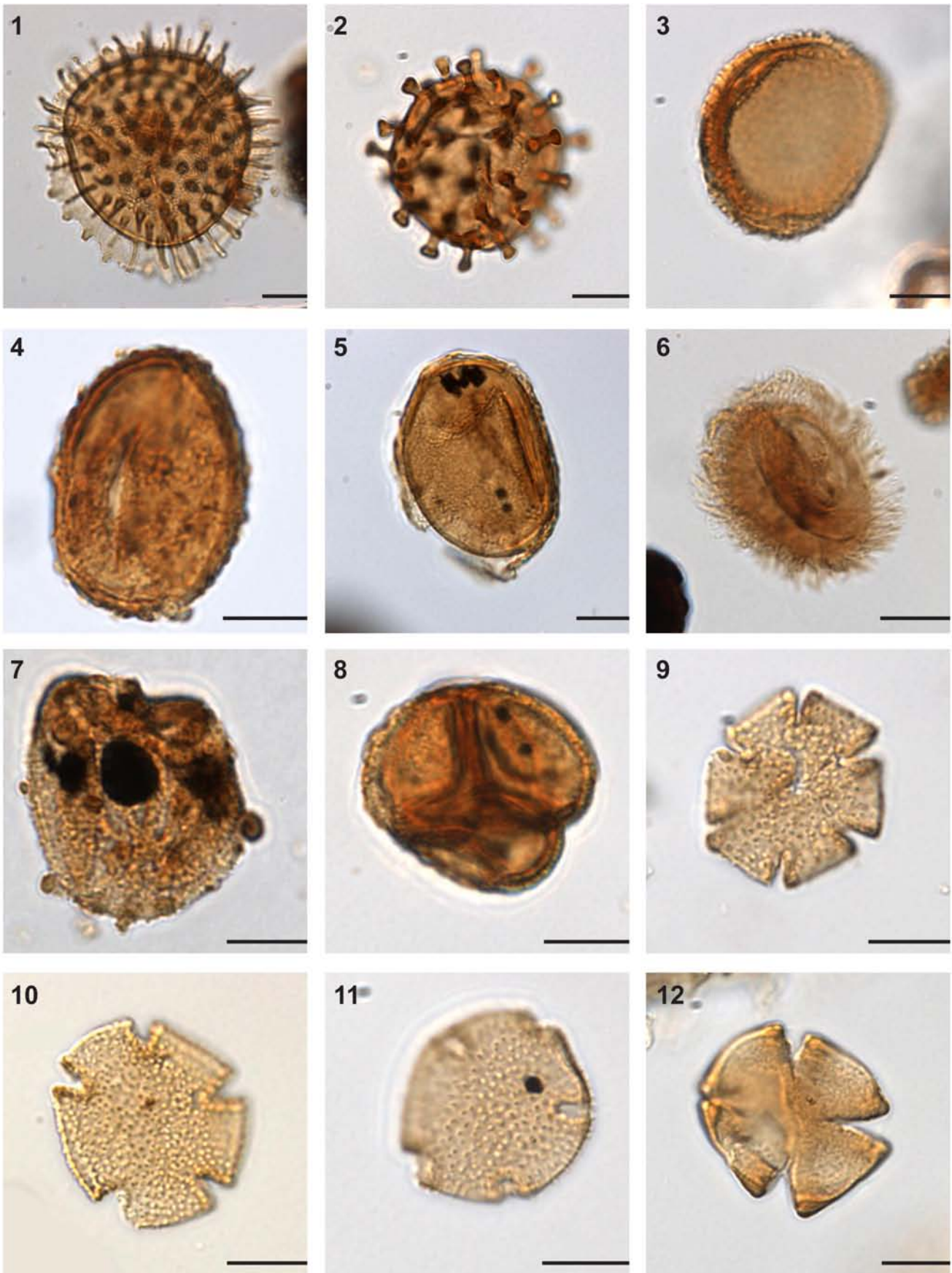


Plate XI.

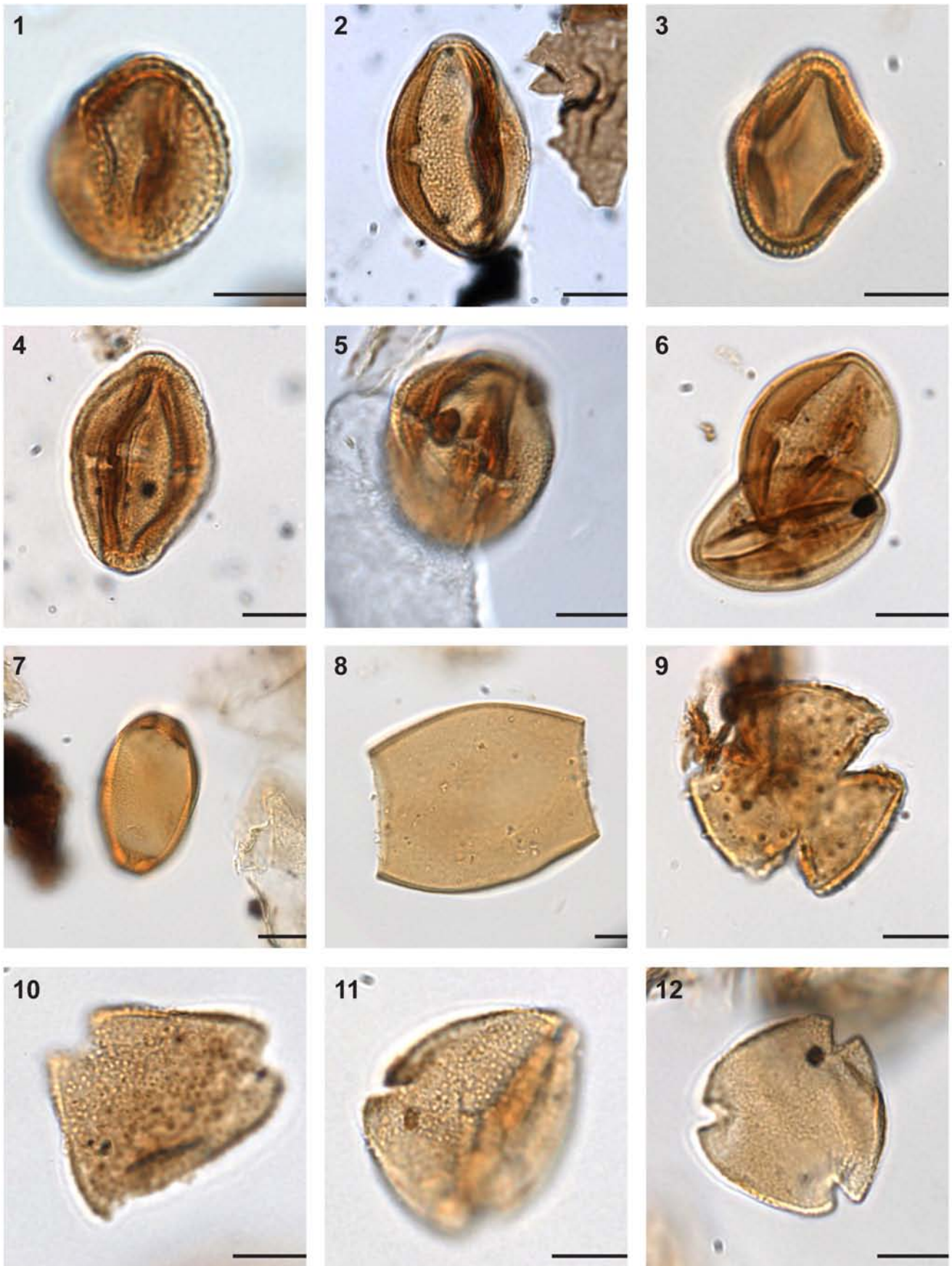


Plate XII.

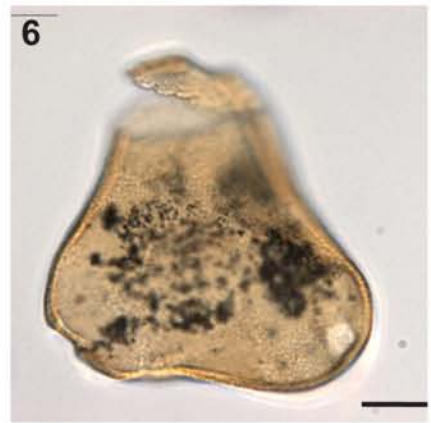
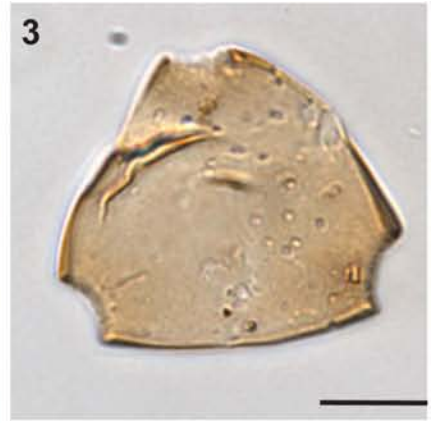
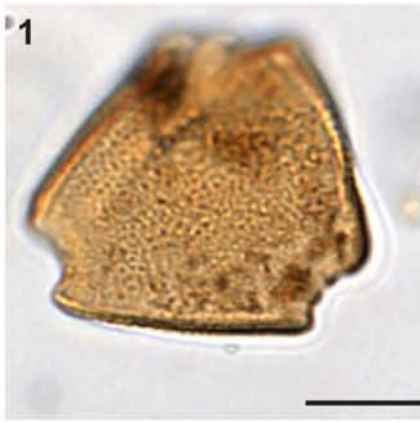


Plate XIII.

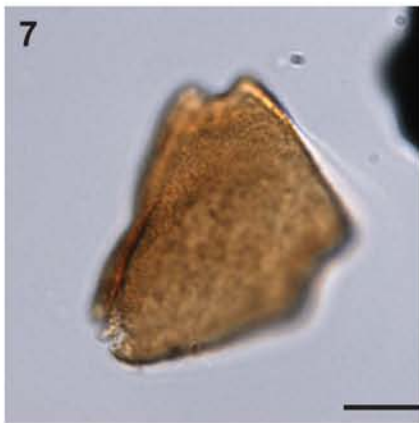


Plate XIV.

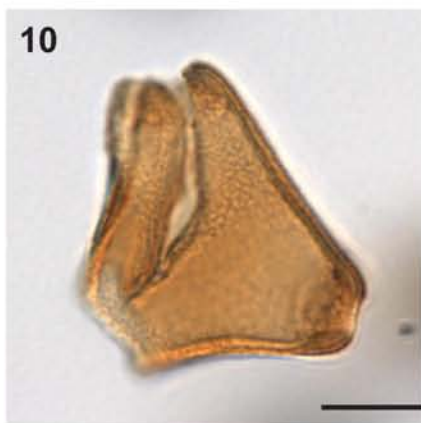
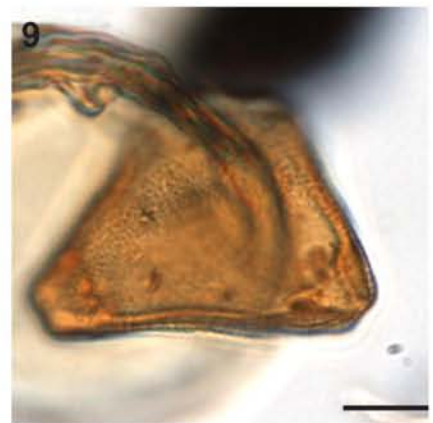
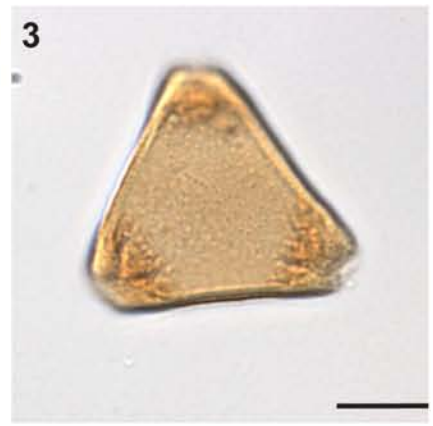


Plate XV.

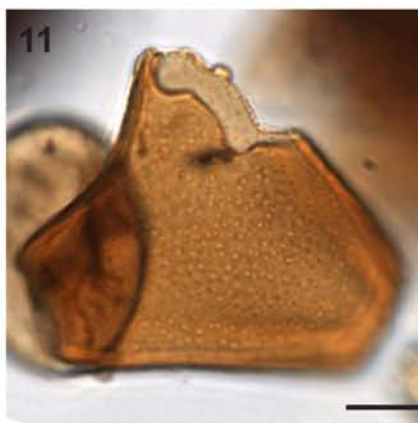
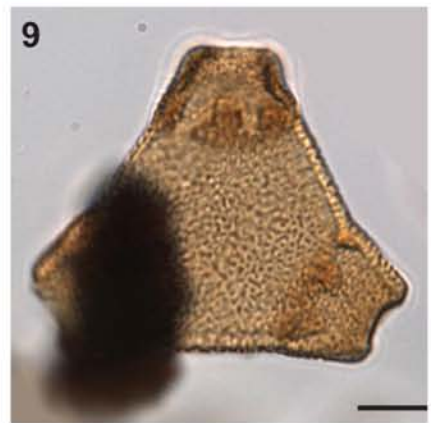
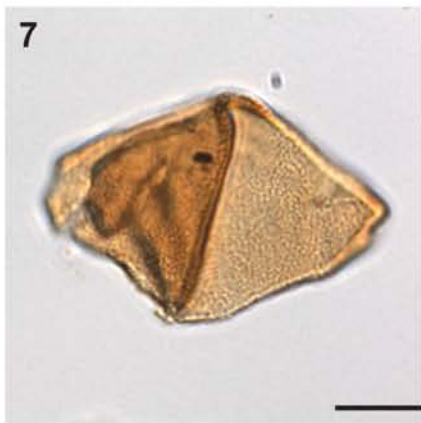
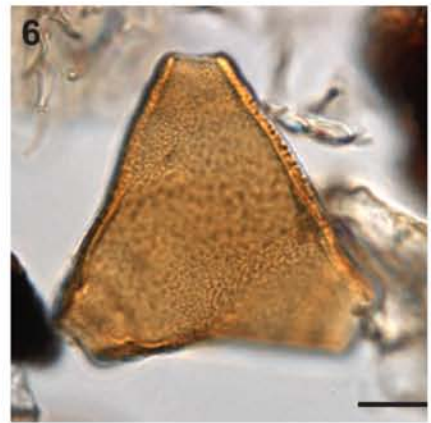
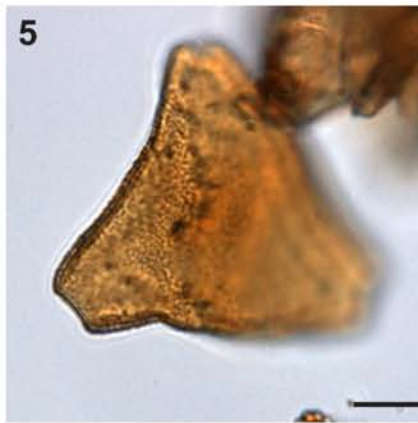
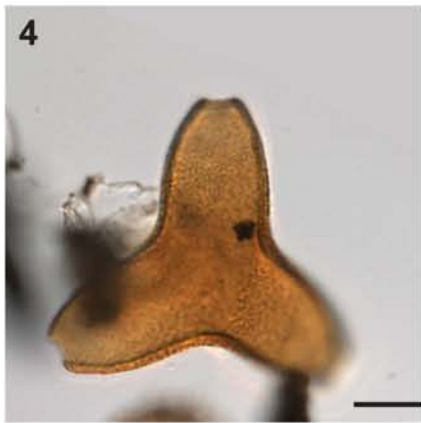
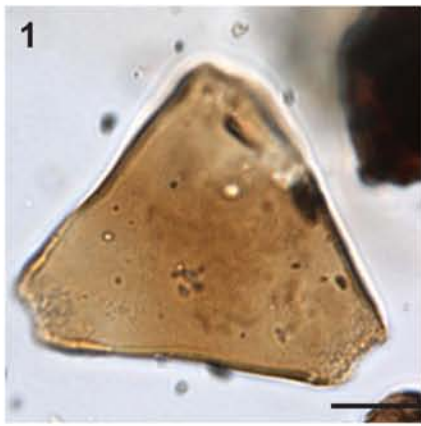


Plate XVI.

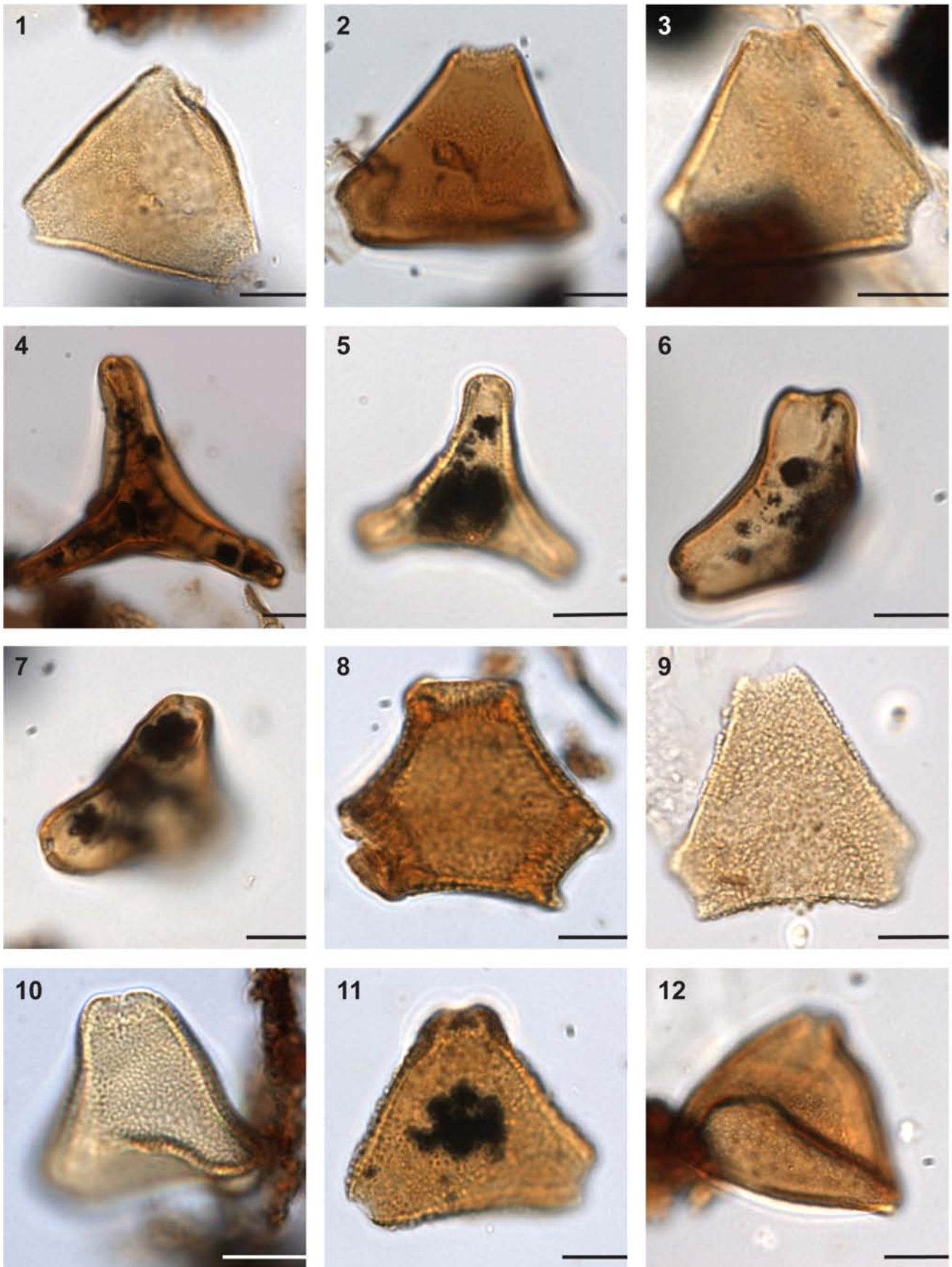


Plate XVII.

Declaration of contribution

Chapter 2

Title: Persistent near-tropical warmth on the Antarctic continent during the early Eocene epoch.

Published in Nature 488, 73-77.

Authors: Jörg Pross, Lineth Contreras, Peter K. Bijl, David R. Greenwood, Steven M. Bohaty, Stefan Schouten, James A. Bendle, Ursula Röhl, Lisa Tauxe, J. Ian Raine, Claire E. Huck, Tina van de Flierdt, Stewart S.R. Jamieson, Catherine E. Stickley, Bas van de Schootbrugge, Carlota Escutia, Henk Brinkhuis and IODP Expedition 318 Scientists.

Contribution

Sample preparation:

L.C. prepared part (20%) of the palynological samples for Site U1356.

Data evaluation:

L.C. performed 100% of the palynological analyses with guidance of I.R. and J.P.

L.C. made the paleoclimatic estimates (contribution: 30%) together with D.G.

L.C. implemented 100% of the statistical analyses related to the sporomorph data with guidance of Sabine Gollner.

Discussion and interpretation:

L.C. contributed (50%) of the interpretation and discussion of the terrestrial palynological data and statistical analyses. The paleoclimatic implications of these data presented in the manuscript were discussed and interpreted mainly by J.P.

Manuscript writing:

L.C. wrote part (5%) of the manuscript (sections 2.4.7 and 2.4.3.1; subsection: Statistical evaluation of sporomorph assemblages) with input of J.P.

L.C. made 100% of the graphics and tables related to the sporomorph data (Figs. 2.2, 2.3, Suppl. Figs., S2.2, S2.3, S2.4, S2.5, S2.7 and Suppl. Table S2.1) with guidance of J.P.

L.C. inserted with Endnote 100% of the references.

L.C. contributed (5%) to address the comments made by the reviewers by providing extra data (Fig. 1, Fig. 2 and Table 2 of the rebuttal letter).

Chapter 3

Title: Early to Middle Eocene vegetation dynamics at the Wilkes Land Margin (Antarctica).

Published in Review of Palaeobotany and Palynology 197, 119-142.

Authors: Lineth Contreras, Jörg Pross, Peter K. Bijl, Andreas Koutsodendris, J. Ian Raine, Bas van de Schootbrugge, Henk Brinkhuis.

Contribution

Sample preparation:

Same samples and raw data used in Chapter 2 (see above).

Data evaluation:

L.C. performed 100% of the analyses presented.

Discussion and interpretation:

L.C. interpreted and discussed 70% of the obtained data.

Manuscript writing.

L.C. wrote the manuscript (contribution: 50%) with J.P. and A.K.

L.C. wrote 90% of the Appendix with input of J.I.R. and J.P.

L.C. wrote the response to the reviewers (contribution: 50%) with J.P.

Chapter 4

Title: Terrestrial climate dynamics in the Tasmanian sector of the Southwest Pacific Ocean during the Paleocene-Eocene deduced from a marine pollen record (ODP Site 1172, East Tasman Plateau).

Published in Climate of the Past 10, 1401-1420.

Authors: Lineth Contreras, Jörg Pross, Peter K. Bijl, Robert B. O'Hara, J. Ian Raine, Appy Sluijs, Henk Brinkhuis.

Contribution

Sample preparation:

All samples were supplied by P.K.B and A.S.

Data evaluation:

L.C. performed 100% of the terrestrial palynological analyses with guidance of I.R.

L.C. made 100% of the paleoclimatic estimates.

L.C. implemented part (50%) of the numerical analyses (Rarefaction and DCA) presented in the manuscript. State space model (see Section 4.2.4), weighted averages and propagated errors were performed by R.B.O.

Discussion and interpretation:

L.C. interpreted and discussed 80% of the obtained data.

Manuscript writing:

L.C. wrote 70% of the paper with guidance and input of J.P.

P.K.B. and A.S. also contributed to improving the manuscript.

L.C. wrote 70% of the response to the reviewers with input of J.P., P.K.B and R.B.O.

Lineth Carolina Contreras Arias

Curriculum Vitae

I. Present educational level and institutions

- PhD student. Institute of Geosciences, University of Frankfurt (Germany), 2010 – 2014 (advisors: Jörg Pross, Heidelberg University; Bas van de Schootbrugge, Henk Brinkhuis, Utrecht University).
- Msc in Earth Sciences. Universidad EAFIT. Colombia, 2006 – 2007. Project: Effects of the Paleocene/Eocene Thermal Maximum on Neotropical Vegetation (advisors: Carlos Jaramillo, Smithsonian Tropical Research Institute; José Ignacio Martínez, Universidad EAFIT).
- BSc in Geology. Universidad Nacional de Colombia, 2000 – 2005. Project: High-resolution palynological analysis of the Fúquene Cores 9 and 10 (advisor: Juan Carlos Berrío, University of Amsterdam).

II. Job experience and internships

- Palynologist at Instituto Colombiano del Petróleo, Piedecuesta (Santander). Main duties included: (i) Palynological analysis of Upper Cretaceous - Cenozoic sequences from different basins of Colombia; (ii) Integration of biostratigraphy, stratigraphy, log analysis and seismic interpretation for solving stratigraphic and structural problems; (iii) On-site biostratigraphic control of exploratory wells providing casing location and geosteering recommendations. June 2008 – April 2010.
- Internship at Smithsonian Tropical Research Institute. Panamá. Main duties included: (i) Palynological analysis of Paleocene-Eocene sections of Northern South America; (ii) Statistical analysis of palynological data using R software; (iii) Fieldtrip assistance. June 2007 – June 2008.
- Palynology of MIS 11. Funza core, Colombia. Amsterdam University - Universidad Nacional de Colombia. July 2005 – January 2006.
- Fúquene project member. Palynology of of the Fúquene Cores 9 and 10. Amsterdam University - Universidad Nacional de Colombia. August 2004 – January 2006.

III. Publications

- **Contreras, L.**, Pross, J., Bijl, P.K., O'Hara R.B., Raine, J.I., Sluijs, A. Brinkhuis, H. 2014. Southern high-latitude terrestrial climate change during the Paleocene-Eocene derived from a marine pollen record (ODP Site 1172, East Tasman Plateau). *Climate of the Past* 10, 1401-1420.
- **Contreras, L.**, Pross, J., Bijl, P.K., Raine, J.I., Koutsodendris, A., van de Schootbrugge, B., Brinkhuis, H. 2013. Early to Middle Eocene vegetation dynamics at the Wilkes Land margin (Antarctica). *Review of Palaeobotany and Palynology*, 197, 119-142.

- Pross, J., **Contreras, L.**, Bijl, P., Greenwood D., Bendle, J., Tauxe L., Schouten, S., Röhl, U., Bohaty, S., Raine I., Huck, C., van de Flierdt, T., Jamieson, S., Stickley, C., van de Schootbrugge, B., Brinkhuis, H. 2012. Persistent near-tropical warmth on the Antarctic continent during the Early Eocene epoch. *Nature*, 488, 73-77.
- Jaramillo, C., Ochoa, D., **Contreras, L.**, Pagani, M, and other 26 authors. 2010. Effects of rapid global warming at the Paleocene-Eocene Boundary on Neotropical Vegetation. *Science*, 330, 957-960.
- Groot, M., Bogota, G., Lourens, L., Hooghiemstra, H., Vriend, M., Berrio, J., Tuenter, E., Van der Plicht, B., Van Geel, M., Ziegler, M., Weber, S., Betancourt, A., **Contreras, L.**, and other 12 authors. 2010. Rapid shifts in South American montane climates driven by pCO₂ and ice volume changes over the last two glacial cycles. *Climate of the Past*, 7, 299-316.

IV. Relevant abstracts presented in conferences

- **Contreras, L.**, Pross, J., Bijl, P.K., Röhl, U., Bohaty, S.M., Tauxe, L., Schouten, S., van de Schootbrugge, B., Koutsodendris, A., Brinkhuis, H., IODP Expedition 318 Science Party. 2013. Paleocene to Eocene climate and vegetation dynamics in the high southern latitudes: Insights from IODP Site U1356 and ODP Site 1172. Freiberg, Germany.
- **Contreras, L.**, Pross, J., Bijl, P.K., Röhl, U., Bohaty, S.M., Tauxe, L., Stickley, C.E., Schouten, S., Brinkhuis, H., IODP Expedition 318 Science Party. 2012. Early Eocene vegetation and climate on Antarctica: insights from IODP U1356. IODP/CDP Kolloquium. Kiel, Germany.
- **Contreras, L.**, Pross, J., Bendle, J., Schouten, S., Bijl, P., Röhl, U., Tauxe, L., Stickley, C., Bohaty, S., Brinkhuis, H., Escutia, C., Klaus, A., IODP Expedition 318 Science Party. 2011. Early Eocene Antarctic terrestrial ecosystem dynamics; a view from the Wilkes Land margin. EGU General Assembly, Vienna, Austria.
- **Contreras, L.**, Pross, J., Bendle, J., Schouten, S., Bijl, P., Röhl, U., Tauxe, L., Stickley, C., Bohaty, S., Brinkhuis, H., Escutia, C., Klaus, A., IODP Expedition 318 Science Party. 2011. Antarctic vegetation and climate dynamics during the Eocene: new data from the Wilkes Land margin. *Climate and Biota of the Early Paleogene*, Salzburg, Austria.
- **Contreras, L.**, Rodriguez, G., Rueda, M., Bedoya, G., Santos, C., De la Parra, F. 2010. Palynological events from Maastrichtian to Eocene in the Middle Magdalena Valley Basin, Colombia. AAPG Annual Conference. Search and Discovery Article #50336. New Orleans.
- **Contreras, L.**, Rodriguez, G., Carvajal, H., Rueda, M., Jaramillo, C., Vladimir, T., 2009. Paleocene Eocene transition in northern South America: from previous palynological barren interval to new calibrated biostratigraphic events. *Geological problems solving with microfossils II*. University of Houston, Houston, Texas.

- **Contreras, L.,** Ochoa, D., Jaramillo, C., Mora, G., 2007. Floristic changes in the neotropics at the PETM. AASP 40th Annual Meeting. Panamá.

V. Relevant courses

- Molecular Organic biogeochemistry. Royal Netherlands Institute for Sea Research. Texel, September 26 – October 1. 2010.
- Sequence stratigraphy. Ph.D. Germán Bayona. Universidad EAFIT- Smithsonian Tropical Research Institute. Bogotá (Colombia) March – June 2007.
- Sedimentological description and stratigraphy of cores from Northern Colombia. Ph.D. Flavia Fiorini, M.Sc Andrés Reyes, Ph.D, German Bayona. Instituto Colombiano del Petróleo and Smithsonian Tropical Research Institute. Bucaramanga (Colombia). February 19 – 21, 2007.
- Dynamics and Evolution of Cenozoic Climate, Urbino Summer School in Paleoclimatology. James Zachos, Gerry Dickens, Gabriel Bowen, Henk Brinkhuis, and others. Urbino University. Italy. July 19 – August 2, 2006.
- R Basic Statistics, Richard Condit. Smithsonian Tropical Research Institute. Panamá. December 4 – 7, 2006.

VI. Awards

- Distinguished oral presentation. Climate and Biota of the Early Paleogene. Salzburg. Austria. 2011.
- Scholarship to attend Summer school in Paleoclimatology. Urbino – Italy. 2006.
- Banco de la República Grant. “Fundación para la Promoción de la Investigación y la Tecnología”. Project: “Cambios Florísticos en respuesta a calentamientos extremos: el caso del PETM”. \$ 8.700. January 2007.
- Scholarship for Master studies and internship. Instituto Colombiano del Petróleo – Smithsonian Tropical Research Institute. January 2006 – June 2007.